THE OPTIMAL IMPLEMENTATION OF ON-LINE OPTIMIZATION FOR CHEMICAL AND REFINERY PROCESSES

VOL. I

A Dissertation

Submitted to the Graduate Faculty of the
Louisiana State University and
Agriculture and Mechanical College
in partial fulfillment of the
requirements for the degree of
Doctor of Philosophy

in

The Department of Chemical Engineering

by
Xueyu Chen
B.S., South China University of Technology, 1984
M.S., University of Mississippi, 1993

May 1998

ACKNOWLEDGMENTS

The author wishes to express her appreciation and gratitude to Professor Ralph W. Pike for giving her the opportunity to participate in this research work. His guidance and assistance are deeply appreciated. The examining committee members, Professors Armando B. Corripio, F. Carl Knopf, John R. Collier, and Jerry L. Householder are recognized for their efforts in reviewing and evaluating this research.

The cooperation of engineers and managers of the IMC Agrico Company and Monsanto Enviro-Chem System, Inc. was invaluable in this research, and the assistance of Mr. Thomas A. Hertwig of IMC Agrico and Dr. Daniel R. Schneider of Monsanto are especially acknowledged for providing the detailed information and data for the sulfuric acid process. In addition, the assistance of Mr. Tai Lee, Ms. Gayathri Srinivasan, Mr. Huitao Liu and Miss Qing Chen in Visual Basic programming for the Interactive On-Line Optimization System was invaluable.

The financial support for this research by Louisiana Mining and Mineral Resources Research Institute, the Gulf Coast Hazardous Research Center, and the Environment Protection Agency is gratefully acknowledged. Also, the Department of Chemical Engineering at Louisiana State University is recognized for its assistance and support.

Finally, the author would like to acknowledge the support and encouragement of friends and families during her post graduate study.

TABLE OF CONTENTS

LIST OF TABLES

LIST OF FIGURES

ABSTRACT

On-line optimization is an effective approach for process operation and economic improvement and source reduction in chemical and refinery processes. On-line optimization involves three steps of work as: data validation, parameter estimation, and economic optimization. This research evaluated statistical algorithms for gross error detection, data reconciliation, and parameter estimation, and developed an open-form steady state process model for the Monsanto designed sulfuric acid process of IMC Agrico Company. The plant model was used to demonstrate improved economics and reduced emissions from on-line optimization and to test the methodology of on-line optimization. Also, a modified compensation strategy was proposed to improve the misrectification of data reconciliation algorithms and it was compared with measurement test method. In addition, two ways to conduct on-line optimization were studied. One required two separated optimization problems to update parameters, and the other combined data validation and parameter estimation into one optimization problem. Two-step estimation demonstrated a better performance in estimation accuracy than one-step estimation for sulfuric acid process, while one-step estimation required less computation time.

The measurement test method, Tjoa-Biegler' contaminated Gaussian distribution method, and robust method were evaluated theoretically and numerically to compare the performance of these methods. Results from these evaluation were used to recommend the best way to conduct on-line optimization. The optimal procedure is to conduct combined gross error detection and data reconciliation to detect and rectify gross errors in plant data from DCS using Tjoa-Biegler's method or robust method. This step generates a set of measurements containing only random

errors which is used for simultaneous data reconciliation and parameter estimation using the least squares method (the normal distribution). Updated parameters are used in the plant model for economic optimization that generates optimal set points for DCS.

Applying this procedure to the Monsanto sulfuric acid plant had an increased profit of 3% over current operating condition and an emission reduction of 10% which is consistent with other reported applications. Also, this optimal procedure to conduct on-line optimization has been incorporated into an interactive on-line optimization program which used a window interface developed with Visual Basic and GAMS to solve the nonlinear optimization problems. This program is to be available through the EPA Technology Tool Program.

CHAPTER I INTRODUCTION

The objective of this research is to investigate the optimal implementation of on-line optimization for industrial plants. This includes the establishment of a framework for on-line optimization, the construction and validation of plant models, the evaluation of algorithms for conducting gross error detection, data reconciliation, parameter estimation and economic optimization, and the comparison of the available program languages. The results of this research should help determine the optimal way to perform on-line optimization.

This chapter introduces the structure of on-line optimization and describes the relations of the components in on-line optimization. It provides an overview of the detailed descriptions to be presented in subsequent chapters.

A. An Overview of On-Line Optimization

On-line optimization adjusts the operation of a plant based on product scheduling and production control to maximize the plant's profit. It provides the means for continuously driving a process toward its optimum operating point. In most industrial processes, the optimal operating point constantly moves in response to changing market demands for products, fluctuating costs of raw materials, products and utilities, and changing equipment efficiencies and capacities. In addition, ambient conditions, variations in feed quality and availability, and changes in equipment configuration are additional constraints that can alter the location of the optimal operation point. The time frame over which these various changes can occur ranges from minutes to months. The competitive economic environment requires timely response to these changing factors. This means

that the optimization must be done on-line to have the plant operate continually under the best conditions.

With the availability of distributed control systems (DCS) for process control and data acquisition as well as the application of multivariable controllers, large scale application of on-line optimization has become feasible. DCS provides current plant operating data (plant measurements) for updating the parameters in plant models to avoid the plant-model mismatch. Multivariable controllers ensure the control ability to quickly and accurately response to new optimal setpoints. Moreover, the decline in cost of computer hardware and software and the increase in the cost of energy and pollution prevention have stimulated manufacturers to improve and optimize their processes, which has boosted the development of on-line optimization.

There have been several industrial applications of on-line optimization reported recently in refineries and chemical plants, and the improvements in plant operations and economics ranged from a 5% to 20 % increase in profit (e.g., Lauks, et al., 1992; Van Wijk and Pope, 1992; Hardin, et al., 1995; Mudt, et al., 1995; and Kelly, et al, 1996). Also, on-line optimization applications have been developing commercially by advanced control and modeling technology companies. Some of the advanced control companies and their packages include: Setpoints, Inc.-"OPTCOM", Treiber Controls, Inc.-"OPS", Profimatics, Inc.-"On-Opt", and Dynamic Matrix Control (DMC) Corporation-"CLRTO". Modeling technology companies market capabilities based on their flowsheeting programs and graphical interface, and some of these are Simulation Science, Inc.-"ROM", ChemShare, Inc.-"Mirror Model" and Aspen Technology-"RT-Opt".

On-line optimization is the next growth area for improving the performance of chemical plants and petroleum refineries. The advanced control and modeling technology companies are

forming partnerships that capitalize on their individual capabilities. Recently, Aspen Technology has merged with Setpoint, Inc. and DMC Corporation. Simulation Science, Inc. and Shell Development Company have entered into a cooperative agreement; and Profimatics has been acquired by Honeywell (Basta, 1996). These changes were caused by an industry demanding for the integration of on-line optimization and advanced control. These companies' objectives include conducting on-line optimization projects for clients and making a profit. They do not share details of methodology to maintain a competitive advantage.

The main benefit from on-line optimization is improving the economic performance in terms of increasing the plant's profit and reducing pollutant emissions, which is the immediate benefit called on-line benefit. A number of other benefits are summarized in Figure 1.1 after Bayles at Conoco (1996) and Kleinshrodt, et al., (1995). The detail operation information generated from on-line optimization provides a better understanding of the processes; and thus, this can be used to debottleneck the process and to improve operating difficulties. Also, abnormal measurement information obtained from gross error detection can help instrument and process engineers to trouble shoot the plant instrument errors. The parameter data estimated from parameter estimation is very useful for process engineers to evaluate the equipment conditions and to identify the bottlenecks and problem sources. Furthermore, the detail process simulation from on-line optimization can be used for process monitoring and serves as a training tool for new operators to obtain the first hand operating experience. In Figure 1.1, a number of applications are summarized for both on-line and off-line uses that employ the same rigorous process model which was developed for on-line optimization. Also, this rigorous process model can be used for process

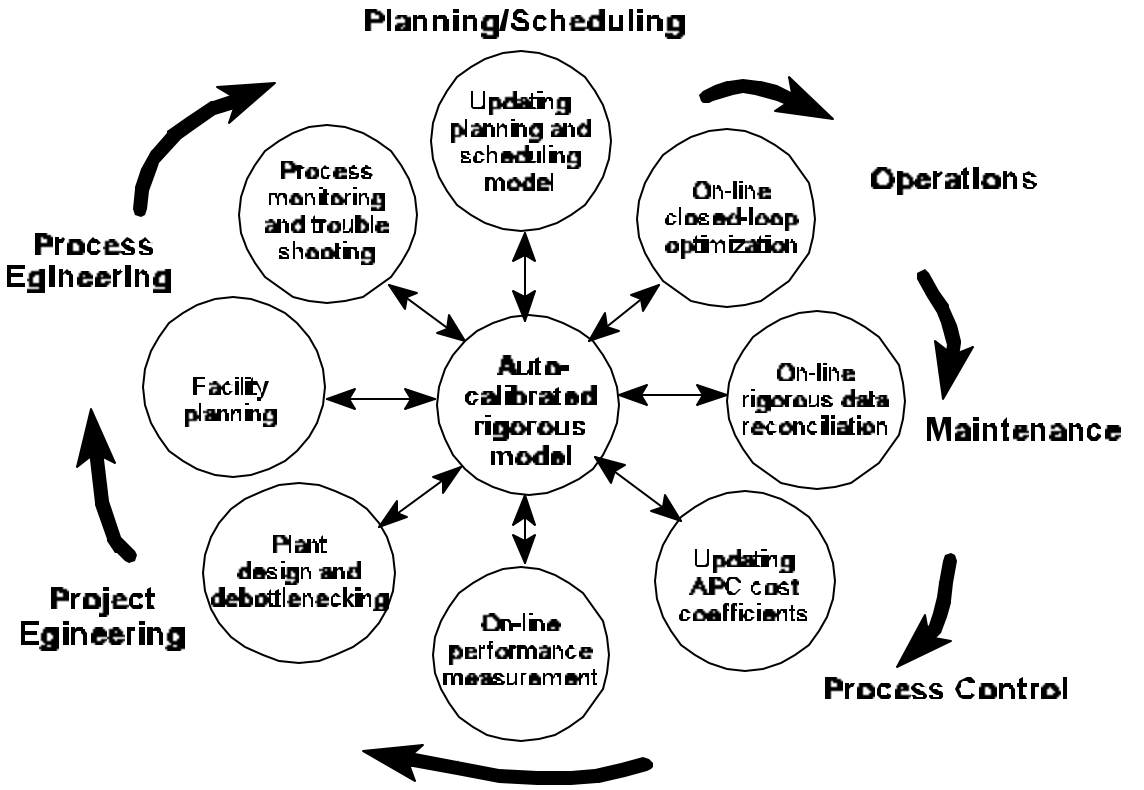

Figure 1.1 Lifecycle Modeling of a Process for Various Applications after Bayles (1996)

maintenance, advanced process control, process design and facility planning, and process monitoring.

In Figure 1.2, a general description of the time and plant scales of optimization is given for processes and plants. As shown on this diagram, maximizing the corporate profit from multiple plants requires the allocation of raw materials to meet the demand for products. This is an optimal production scheduling and control problem; typically, there are thousand of variables for which the optimal values need to be determined. Linear programming is the

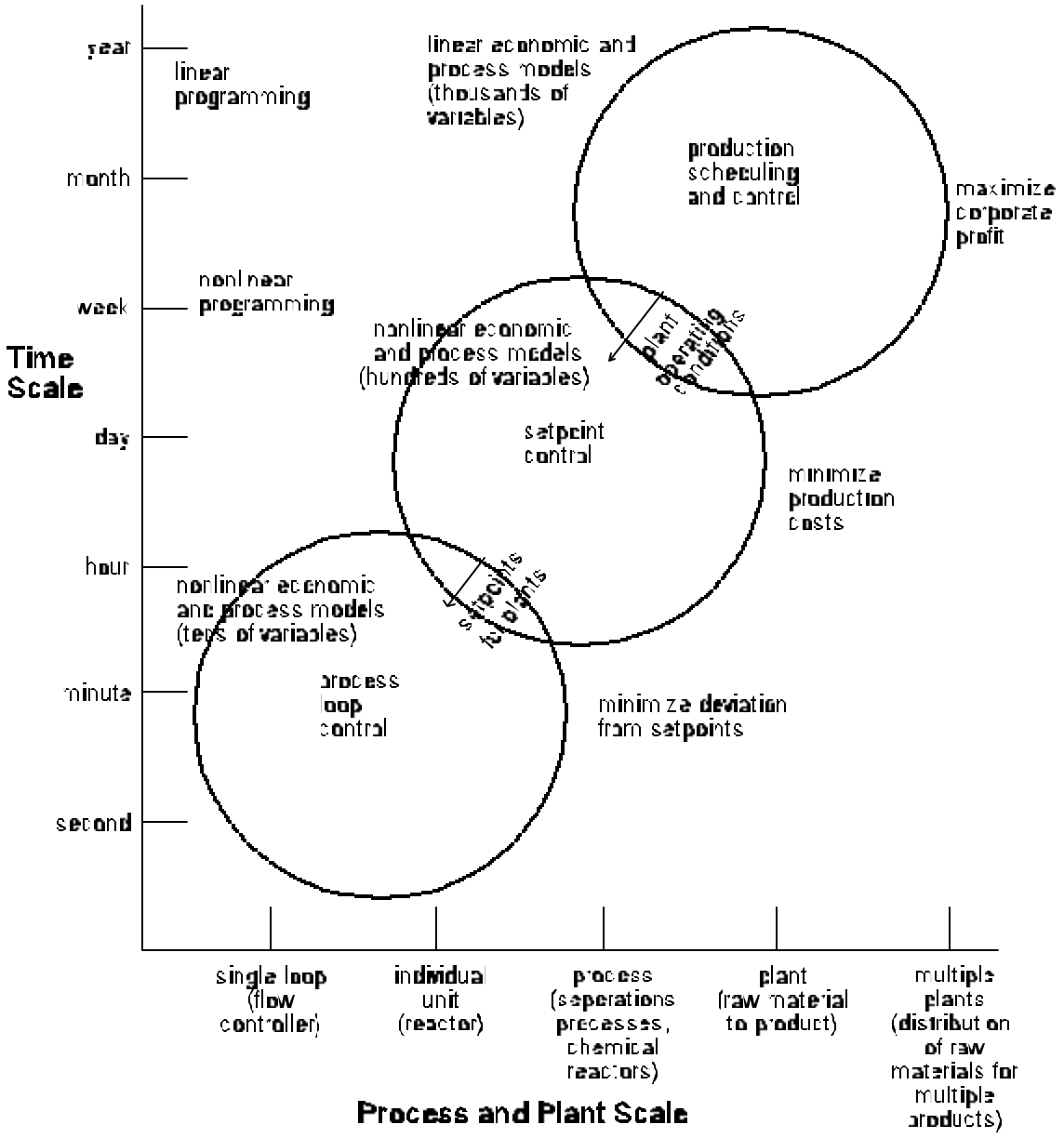

Figure 1.2 Diagram of Plant and Time Scales Encountered in Process Optimization, after Koninckx, et al., (1988)

optimization method usually used for problems at this level. In general, the frequency for this type of optimization is weekly or monthly. The results from the plant scheduling optimization assign the best production rates for the plants.

On the single plant scale, the task of optimization is to find the optimal operation set points for the plant that satisfy the assignment from optimal plant scheduling and minimize the production cost. This type of optimization usually involves nonlinear plant and economic model and has a size about hundreds or thousands of variables and constraints. It updates the parameters in plant models to eliminate the plant-model mismatch. Also, it provides information for identifying the sources of abnormal operations, such as detecting leaking equipment or malfunctioning instruments.

For single loop or individual unit optimization, the task is to optimize decision variables, such as, reactor temperature and resident time at the existing catalyst activity or reflux ratios on distillation columns. This type of optimization involves nonlinear plant model with a size of tens of variables and constraints.

B. Structure of On-Line Optimization

In Figure 1.3, the structure of on-line optimization is shown along with the components which work together to maximize the profit from the operation of the plant. The key components of on-line optimization include the plant and economic models, gross error detection, data reconciliation and parameter estimation. Also, an efficient optimization algorithm is used to solve the three nonlinear optimization problems shown in Figure 1.3. Referring to Figure 1.3, plant data

is sampled from the distributed control system, and gross errors are removed from the data. Then the data is reconciled to be consistent with

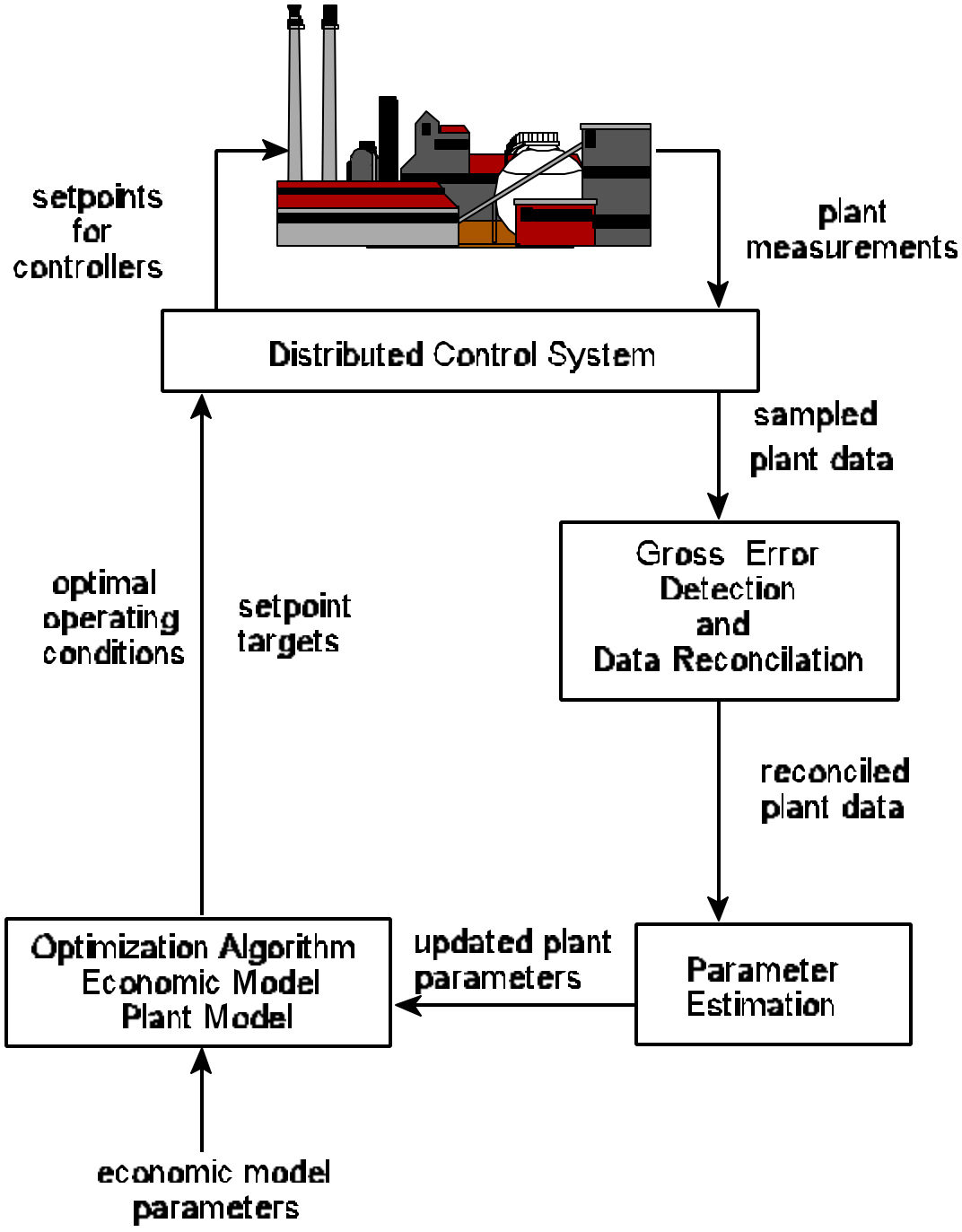

Figure 1.3 Structure of On-Line Optimization

material and energy balances of the process. This data is then used to update the parameters in the plant model to ensure the plant model predicts the operation of the plant. The updated plant model is used with the profit function (economic model) to generate the best operating conditions for the plant. Then these are sent to the plant distributed control system as set points for the controllers. Also, a coordinator program is used to supervise and control on-line optimization, the frequency that it is repeated and the interaction with plant operators.

For a steady state plant model, Figure 1.4 describes the implementation procedure of on-line optimization system modified from Kelly, et al., (1996). First, the selected key measurements are examined to test if the process is at steady state. If not, testing of the process is continuing until the process reaches steady state. When the process is at steady state, the plant measurements are extracted from DCS and are processed through the data validation step to remove or rectify the gross errors in the measurements. The measurements include temperatures, pressures, flow rates, compositions, for example. Then the validated plant data can be used to estimate the parameters in the plant model at parameter estimation step. These parameters are usually unmeasurable and time-varying constants, such as catalyst activity, heat exchanger fouling factors, and tray efficiencies of distillation columns. They reflect the equipment conditions that change with time and are relative independent of plant operation conditions. Estimating these parameters on-line has the plant simulation model match the plant operation at the current operating conditions.

The parameters in the economic model include sale prices and demand for products, costs and availability of raw materials, utility cost, etc., which are determined by conditions that are separated from process operations and are also subject to change. These parameters

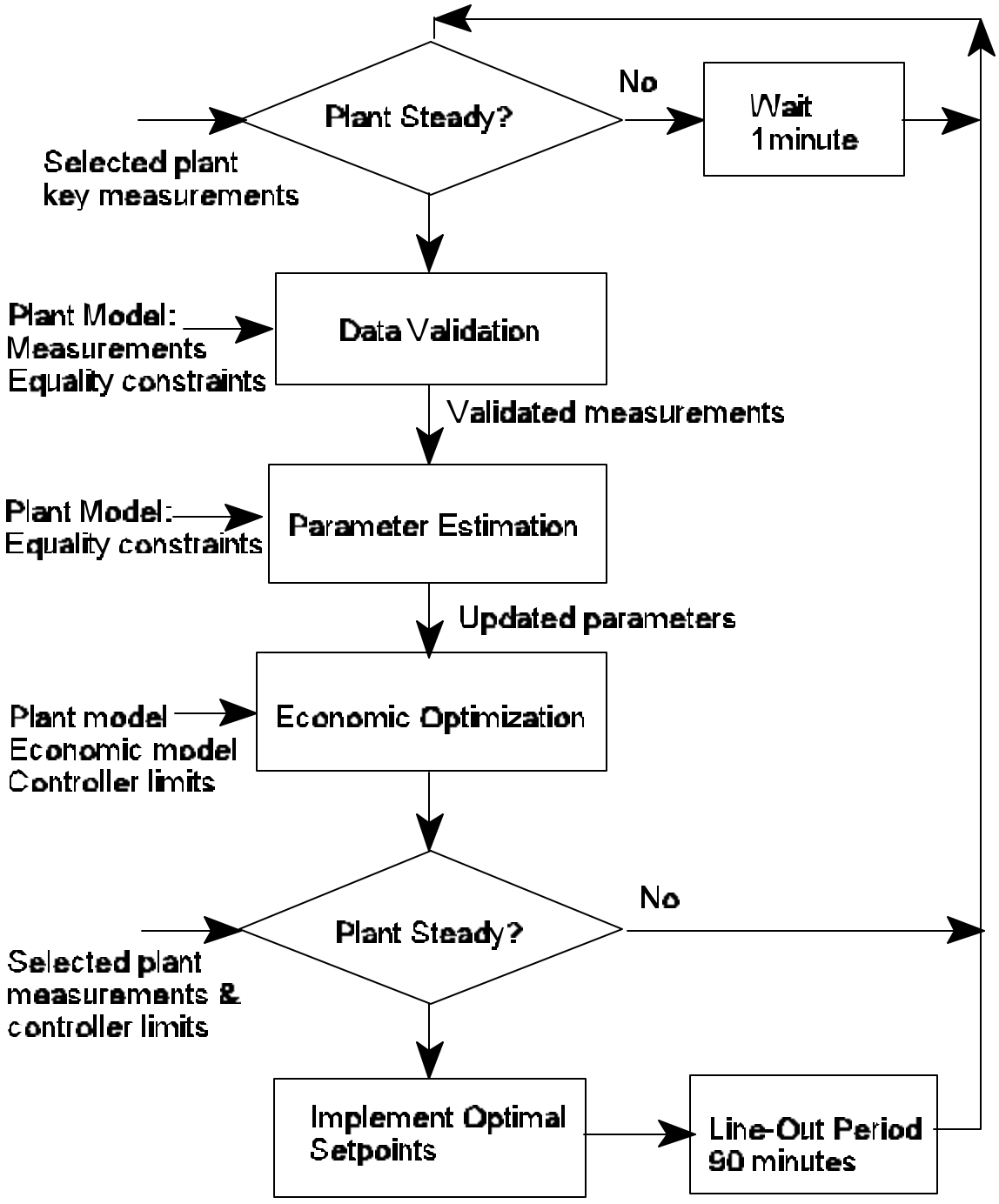

Figure 1.4 Implementation Procedure of On-Line Optimization
after Kelly, et al., 1996

have to be adjusted to have an accurate description of the profit. Finally, current economic model incorporated with the updated and precise plant model is used to determine the best operating conditions (e.g. temperatures, pressures, and flow rates) for distributed control system to operate the plant. These optimal operating conditions maximize the profit and satisfy the plant model.

After the optimal set points are obtained from economic optimization, the operating state must be examined again to ensure the process still remain in the same steady state as the plant data was taken to update the plant parameters previously. If not, the optimal set points is discarded and the procedure is restarted again. If the process remain the same, then the optimal operation set points are sent to the regulatory control system to implement.

As shown in Figure 1.4, on-line optimization system involves solving three nonlinear optimization problems represented by three boxes: data validation, parameter estimation, and economic optimization. These three nonlinear optimization problems share the same plant model as constraints and can be solved by the same optimization algorithm. A precise and robust plant model is essential for on-line optimization. It serves as the constraints for data validation, parameter estimation and economic optimizations. Therefore, a plant model must be formulated and validated before the on-line optimization implementation. The plant model is written based on the conservation laws, chemical kinetics and thermodynamic relations.

In order to perform on-line optimization for a plant as described above, both computer hardware and software are required. First, the plant must have an automated control system to sample the plant operating conditions. Also, all of the key components for optimization need to be programmed in a computer language and run on the plant computer system. In addition, a

coordinator program is needed to coordinate the sequence of executions of each step in Figure 1.4. This program also manipulates the plant sample data from the distributed control system and returns the optimal set-points to the distributed control system.

C. Execution of On-Line Optimization

The execution frequency of optimization is the time between conducting optimizations of the process, and it has to be determined for each of the units in the process. It depends on the settling time, i.e., the time required for the units in the process to move from one set of steady-state operating condition to another. The settling time can be estimated from the time constant determined by process step testing. The time period between two on-line optimization execution must be longer than the settling time to ensure that the units have returned to steady state operations before the optimization is conducted again. This is illustrated in Figure 1.5, after Darby and White (1988). The figure shows an execution frequency for optimization that was satisfactory for one process may be too rapid for another process which has a longer settling time. In Figure 1.5a, the process has returned to steady-state operations and held that position until the next optimization. However, in Figure 1.5b, the process did not have enough time to return to steady-state operations before the optimization altered the operating conditions; the process would not return to steady state operations if such optimization continued. The settling time for an ethylene plant is four hours according to Darby and White (1988), and this time for sulfuric acid contact process is twelve hour according Hertwig (1997).

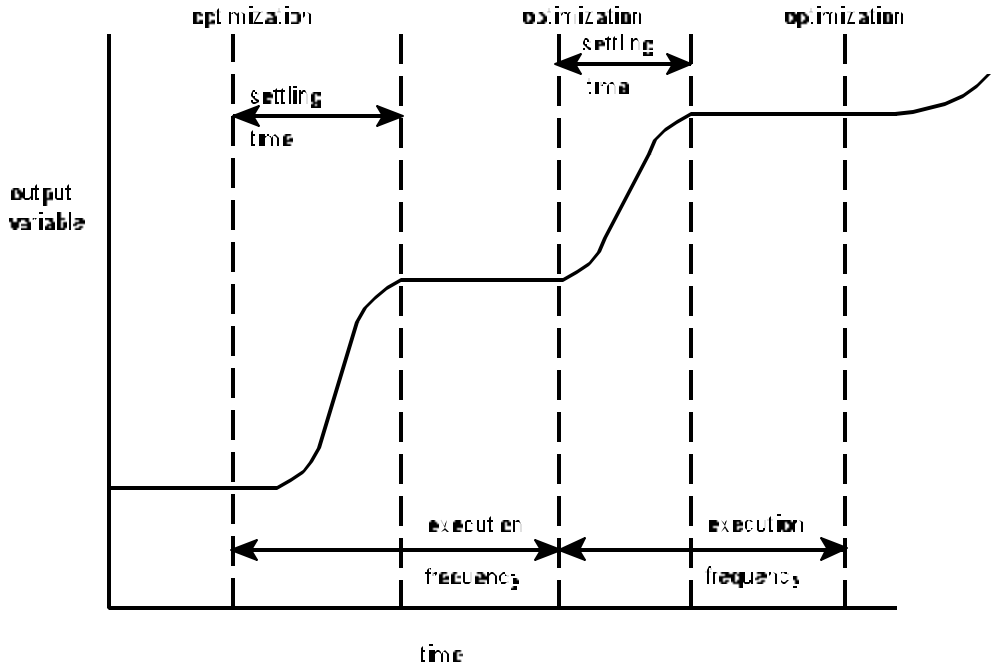

a. Time between optimizations is longer than settling time

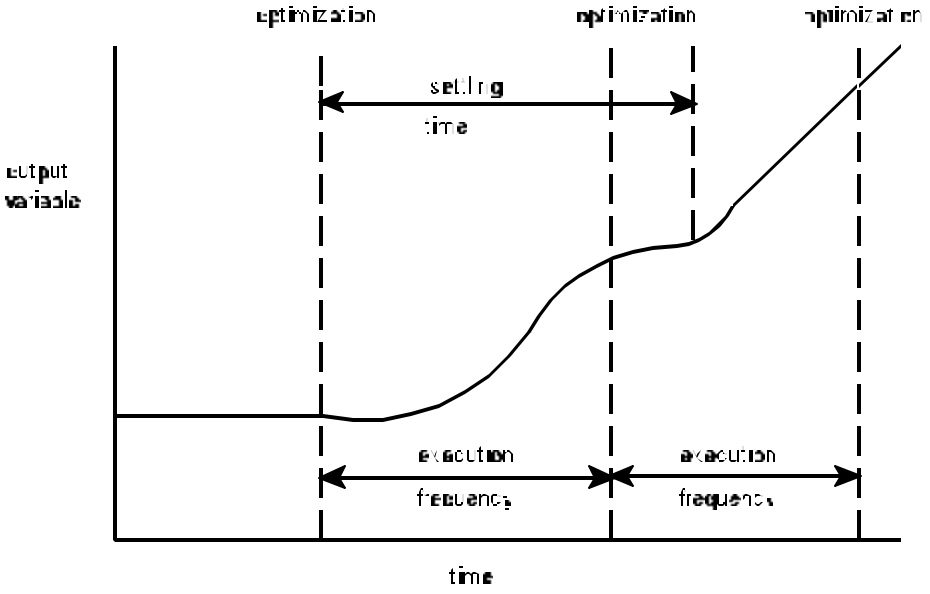

b. Time between optimizations is less than settling time

Figure 1.5 Comparison of Time between Optimization and Process Settling Time, after Darby and White (1988)

D. Summary

The rapid development in computer hardware and software as well automation technology in the last ten years has made it possible to consider on-line optimization of chemical plants. On-line optimization improves the economic and environmental performances of chemical plants and refinery processes without requiring substantial capital investment, and it is a growth area for modeling technology and advanced control companies.

On-line optimization takes advantage of the fact that chemical plants operate at steady state with transient periods that are relatively short compared to steady state operations. Consequently, steady-state process models are used to describe the plants. The idea of on-line optimization is to reconcile data samppled from distributed control system to update parameters in the plant model to have plant-model matching. Then the current plant and economic models are used to conduct economic optimization and to generate a set of optimal set points that achieve the maximum profit. On-line optimization is repeated as the internal conditions (plant parameters and plant configuration) and/or external conditions (economic parameters) change.

In the following sections, the current status for the methodology of on-line optimization will be reviewed. This will provide the basis for developing the best way to implement on-line optimization in this research. In the subsequent section, the detail methodology of on-line optimization will be investigated and evaluated. Based on the evaluation results, the best procedure to implement on-line optimization will be proposed. Also, an actual sulfuric acid plant from IMC Agrico Company in Louisiana will be used to evaluate the efficiency and accuracy of the algorithms and to investigate the best way to implement on-line optimization.

CHAPTER II LITERATURE REVIEW

In this chapter, industrial applications of on-line optimization will be summarized first. The key elements of on-line optimization will then be outlined, and the current status of the methodology for on-line optimization will be reviewed. Based on this information, the procedure for implementing on-line optimization will be proposed and applied to actual plants.

A. Industrial Applications of On-Line Optimization

Boston, et al., (1993) gave a wide review for computer simulation and optimization as well as advanced control in chemical process industries (CPI). He described the new computing power for process optimization and control that leads to higher product qualities and better processes, which are cleaner, safer, more efficient, and less costly. Also, it results in speedier response to changes in economics, regulatory, and technological conditions, as well as market demands. As Parkinson and Fonhy (1995) reported, the global market for distributed control system (DCS) is about $6 billion with the U.S. accounting for about $1.5 billion now, and it is growing by over 20% per year in some Asian countries and by 5% per year in the U.S. The wide installation of DCS in chemical plants and refinery processes provides the necessary measurements of processes for on-line optimization. The new optimization tools are pushing the plant performances to a level that was not felt possible before.

There have been several industrial applications of on-line optimization reported recently in refineries and chemical plants. They reported improvements in plant operations and economics in a range of 3% to 20%. However, details of methodology used is sketchy because proprietary processes are being used.

Lauks, et al., (1992) reviewed the industrial applications of on-line optimization reported in the literature from 1983 to 1991 and cited nine applications for five ethylene plants, a refinery, a gas plant, a crude unit and a power station. These results showed a profitability increase of 3% or $4M/year. Also, intangible profits from a better understanding of the plant behavior were significant. In addition, they gave results for the OMV Deutschland GmbH complex including a refinery unit, an ethylene plant and downstream treating units in Burghausen, Germany. An equation oriented flowsheeting program was used for the process model having more than 5,000 linear and nonlinear equations which led to an optimization problem with 106 constraints and 37 decision variables. Data reconciliation involved 450 points, and there were about 300 tuning parameters. The program was run on a DG-AVIION 4200 Unix system with a total computation time of 60 minutes. Optimization results were summarized in a setpoint report and manually implemented by plant operators on a TDC 2000 system. The improvement in profitability has been between 1-3% depending on price structure, and it has provided better insight to operation of the plant.

Scott, et al., (1995 and 1994) reported that Texaco Refining and Marketing Inc. (TRMI) has implemented ROM from Simulation Sciences Inc. on a four unit complex. This on-line optimization package provides integrated modeling of reaction units, optimization across multiple units, validation of laboratory and plant data, higher quality control, and a large amount of operating information. It was expected that the benefits from this project would exceed $1 million annually. Also, this can be used as a versatile tool for troubleshooting, planning, and training of the processes.

Zhang (1993) had conducted a case study of on-line optimization for Monsanto designed sulfuric acid plant from IMC Agrico Company at Convent, Louisiana. The economic optimization achieved 17% increase in plant profit and 25% reduction in sulfur dioxide emission. The same sulfuric acid plant will be used in this research to test the methodology of on-line optimization.

Krist, et al., (1994) described the development and implementation of a generic system for on-line optimization (SOLO) in a benzene plant of Dow Benelux N.V. SOLO contains generic modules and plant specific modules. The generic modules are used for data-retrieved, data analysis, data reconciliation and decision mechanism; and the plant specific modules are used for parameter estimation and final optimization. This optimization increased the plant's margin by an average of 4%.

Fatora, et al., (1992) reported that the use of closed-loop real-time optimization and dynamic matrix control technology has achieved significant economic benefits in an olefin plant. The pay-back period for the total project was less than one year. In addition, benefits of this on-line optimization system were that it pushed the unit to the most profitable constraints based on current economics and operating objectives. This increased the plant capacity, reduced energy requirement, and improved product qualities.

Van Wijk and Pope (1992) described on-line optimization of the catalytic cracking complex at Shell's Stanlow refinery in the UK. The on-line optimization system received process and economic data from the refinery supervisory control system and performed optimizations on a three hour cycle providing targets to the process controllers. The process and economic models were nonlinear, and a reduced gradient algorithm was used for the optimization. Data

reconciliation was performed on several hundred points, and rotating equipment efficiencies and heat transfer coefficients were two of the parameters updated in the process model. Benefits of on-line optimization were a 10% average increase in feed rate, a 9% increase in catalyst circulation rate which resulted in a 9% increase in gasoline production.

OEMV, an Austrian company, had successfully installed an on-line control and optimization system in the fluid catalytic cracking units (FCCU) in 1987 (Rhemann, et al., 1989). The advanced control and optimization project schedule was included in an overall project providing a new digital instrument control system (DCS) for FCCU, gas plant and treating units, consolidated in one common control area. The new DCS was installed and commissioned without a plant shutdown during normal plant operations. The improved control from advanced control and on-line optimization translated into a large reduction in the standard deviation of control variables. The advanced control and on-line optimization gave a 4.3% increase in the maximum operating feed rate for FCCU. Also, the controls showed both a high flexibility at varying unit constraints and a high reliability in daily operating.

Sourander, et al., (1984) described the on-line optimization of an ethylene plant using refinery heavy feedstocks. The plant produced 200,000 tpa of ethylene using nine cracking furnaces which had a computer control system with set point supervisory controls of analog controllers. Gas chromatographs using dedicated microcomputers sampled feed and product streams, and analyses were sent to the main process computer. Seven different feedstocks and three different recycle streams were sent to the nine heaters at varying rates to meet production demand for seven products. The economic model was based on gross margin, and linear

programming was used to maximize gross margin subject to market demand, feed availability and the plant constraints (material and energy balances and process unit capacities). The on-line optimization cycle was executed every four hours. Error detection was very important, especially for the heater effluent, and a bad analyses not detected and included in the model updating caused errors to be carried through to the control system. The results of using on-line optimization were reported to be increased furnace run times of 30%, efficiencies of 3%, capacities of 4% and increased ethylene yields of 2%.

Saha, et al., (1990) of Amoco Production Company reported results for the on-line optimization of a 240 MMscfd gas-processing plant in Evanston, Wyoming using the ChemShare ProCAM system which has data reconciliation and a proprietary process modeling system using a simultaneous solution technique. More than 550 data points were taken from the plant's distributed control system (DCS) and reconciled for optimization using a plant model with 170 pieces of equipment and detailed economic model. The optimization analysis determined the best operating conditions for 40 process variables which were reported to the plant operator for implementing via the DCS. Preliminary estimates were approximately $9,000 per day for an increased pretax profit and 50% higher than this for a high ethane recovery mode.

Moore and Corripio (1991) reported on the on-line optimization of distillation columns in series which used dynamic programming with steepest descent and a simple model for product recovery for two and three distillation columns in series. Applied to a two and three column train at Dow Chemical Company's Louisiana Division, the control system performed successfully to reduce operating costs beyond what was anticipated.

Bailey, et al., (1993) reported on the on-line optimization of a hydrocracker fractionation plant using MINOS as optimizer. The full plant model contains 2891 variables with 10 degree of freedom. Detailed methodologies including modeling and numerical techniques were outlined. They showed that the important factors for implementing the model-based optimizer were scaling, starting points, sparsity patterns and thermodynamic approximations. The on-line optimization system gave an 3% increase in profit.

Gott, Roubidoux and Heersink(1991) described an on-line optimization system for the Conoco's Billings refinery fluid catalytic cracking (FCC) units using Profimatics Inc. FCC-SIMOPT package. The on-line optimizer generates both optimal control targets as well as the optimal operating strategy for the advanced FCC constraint control. The on-line optimization was divided into five phases: 1) process data monitoring, 2) program scheduling, 3) data reconciliation, 4) model update, 5) optimization. The results are sent to the advanced control system. They concluded that this system increased the profit and provided better insight into the operation of the FCC units.

Simulation Sciences Inc. uses the flowsheet simulator PRO/II and data reconciliation package DATACON as the main engines in their On-line Rigorous Model (ROM) (Mullick, 1993). ROM was applied to a refinery crude unit for on-line planning, scheduling and optimization. They concluded that ROM provide a rapid and robust model of the current plant operations and is a valuable tool to improve profitability and operations through case studies and optimization.

ChemPlant technology has developed a data reconciliation program, RECON, to reconcile process measurements (Madron, 1997). RECON is a PC oriented software for mass and heat balancing. Problems are defined interactively in the graphical user interface. Also, RECON can be used for balancing in the stage of process design.

Strand (1989) described on-line optimization of a mechanical pulping systems in his dissertation. Detailed process modeling of the pulping system and data reconciliation based on a simple linear models were discussed. Sequential Linear Programming (SLP) was used to optimize the pulping system operations by maintaining the pulp quality while minimizing the energy consumption. When this system was applied in the pulping system, 6% reduction in energy consumption and 0.5T/hr production rate increase was achieved.

Mahalec (1993) of Aspen Technology Inc. examined the on-line, closed loop optimization of continuously operating plants from a viewpoint of software requirements. The open form of model equations was considered to be a basic requirement for a successful long-term implementation of the closed-loop optimization. This open form equation-oriented structure was demonstrated to provide user friendliness and enable the plant engineers to maintain the on-line optimizer more easily.

Leung and Pang (1990) of Simulation Sciences Inc. described their company's codes for data reconciliation and gross error detection. The package DATACON uses the measurement test (MT) and provides a friendly user interface (Simsci, Inc., 1991). It accesses PROII's component library for thermodynamic data and reconciles the raw data with both process

material and energy balances. This DATACON package is widely used in their company's on-line monitoring and optimization system.

Canfield and Nair (1992) of ChemShare, Inc. described their company's codes for data reconciliation and gross error detection using complete and rigorous process models with least square methods. The ChemShare's package was implemented on-line at Amoco Production Company's Painter Complex NGL Recovery/Nitrogen Rejection Unit which had a total of 170 pieces of equipment including distillation columns, multi-stream plate fin heat exchangers, a heat pump and a propane refrigeration system. Initially, ten percent of a total of 550 measurements were found to have gross errors by the program. The subsequent analysis of the instruments in the plant verified that all of the flagged instruments were indeed faulty. In most cases the instruments require recalibration. In one case, an incorrect flow rate was caused by the orifice plates being installed backwards. Also, they showed that reconciliation with a complete and rigorous process model was superior to reconciliation with only material and energy balances.

May and Payne (1992) of Monsanto described automating plant-tested techniques derived directly from the operator experience. All of the techniques outlined in their paper are engineering common sense, have been already field-tested and proven manually by years of experience among operators, engineers and mechanics. They point out that this kind of operator-interactive computer program is more valuable when provision is made for updates and modifications as experience with the system grows.

Hardin, et al., (1995) of Conoco and AspenTech reported that a rigorous crude unit optimizer has been implemented at Conoco's Lake Charles, Louisiana refinery. The benefits

were a profit increase in $0.03 when a BBL crude was processed and better understanding of the plants.

Kelly at DMCC and Fatora and Davenport at Lyondell Petrochemical Co. has applied a closed loop real-time optimization system to a large scale ethylene plant (Kelly, et al., 1996). Their results indicated a project payback period of less than 9 months. In addition to the economic improvement, the optimization system improved the understanding of process operations and the analysis of the equipment performance. Also, Edwards and Masaki of Setpoint (1994) reported that an average project payback ratio over ten years period can exceed ten to one from on-line optimization for a typical refinery with 130 MBPD capacity.

There have been a number of papers and presentations that proposed various ways to conduct on-line optimization (Darby and White, 1988; Macchietto and Stuart, 1989; Lojek and Whitehead, 1989; Chen and Joseph, 1987; Fisher, et al., 1990; Pierucci and Rovaglio, 1991; and Koninckx, et al., 1988). Many of the authors are with companies that provide process control and flowsheeting services to the chemical and refining industry.

In summary, on-line optimization significantly improved profitability, plant operation, and emission reduction; and it provided better understanding of processes. Typically, profitability was increased by 5 to 10% with comparable improvements in plant operations. Also, it was reported that a more thorough understanding of the plant performance was very valuable but is difficult to quantify economically.

B. Key Elements of On-Line Optimization

The objective of on-line optimization is to determine optimal process setpoints based on plant's current operating and economic conditions. As shown in Figure 1.3, the key elements of on-line optimization are:

- Gross Error Detection
- Data Reconciliation
- Parameter Estimation
- Economic Model (Profit Function)
- Plant Model (Process Simulation)
- Optimization Algorithm

A procedure for implementing on-line optimization is illustrated in Figure 1.4. It involves the detection of steady state, data validation, parameter estimation, and economic optimization sequential as discussed previously.

The relationship between these key elements is outlined in Figure 2.1. From Figure 2.1, both plant model and optimization algorithms are required in the three steps of on-line optimization. On-line optimization involves solving three nonlinear optimization problems: economic optimization, parameter estimation, and data validation. The plant model serves as the constraint equations in these three nonlinear optimization problems and the optimization algorithm is used to solve the nonlinear optimization problems. For economic optimization, the plant model is used with economic model to maximize the plant profit and provide the optimal setpoints for the distributed control system to operate. For parameter estimation, parameters in the plant model are estimated by optimizing an objective function,

Figure 2.1 Relationship between Key Elements of On-Line Optimization

such as minimizing the sum of squares of measurement errors, subject to the constraints in the plant model. For data validation, the errors in plant measurements are rectified by optimizing a joint probability distribution function subject to plant model, and a test statistic is used to detect the gross errors in the measurements.

Data reconciliation is conducted in combined gross error detection and data reconciliation and simultaneous data reconciliation and parameter estimation. In combined gross error detection and data reconciliation, data reconciliation is required to reconciled process data and to estimate the measurement errors for gross error identification. In simultaneous data reconciliation and parameter estimation, data reconciliation is required to estimate process parameters and process variables. These two data reconciliation optimization problems use the same plant model, and the only difference is that the process parameters are constants in combined gross error detection and data reconciliation and are variables in simultaneous data reconciliation and parameter estimation. Data reconciliation in combined gross error detection and data reconciliation step should use current values of the process parameters for the plant model, but current parameters come from the subsequent parameter estimation step. Consequently, it is necessary to use previous values of process parameters for combined gross error detection and data reconciliation. Hence, updated values of the parameters strongly dependent on previous (old) values of the parameters if all reconciled measurements are used for estimating the parameters.

Some authors (Almasy and Sztano, 1975; Mah, et al., 1976) suggested separated procedure for gross error identification (such as global or nodal test), data reconciliation, and parameter estimate. The others proposed combined gross error detection with data reconciliation

(such as measurement test) or combined parameter estimation with data reconciliation. Seber and Wild (1989) described a robust method that has an ability of automatically rejecting the extreme observations (with gross errors). This method improves the performance of data validation and will be a potentially powerful method for combining parameter estimate with data validation.

The following paragraphs present a review of the literature giving the status of these key elements. First, the methodology for data reconciliation, gross error detection, combined gross error detection and data reconciliation, parameter estimation, and simultaneous data reconciliation and parameter estimation will be reviewed sequentially. Then the status of economic optimization, plant model formulation, and optimization algorithms will be described.

B-1. Data Reconciliation

Results of research on data reconciliation have been reported for both steady state and dynamic process. They were reviewed and evaluated in detail through 1988 by Mah (1990) for steady state processes. Generally, raw process data is subject to two types of errors, random and gross errors. Random errors come from the randomness of measurements and are commonly assumed to be independently and normally distributed with zero mean. Gross errors are caused by non-random event such as process leaks, biases in instrument measuring or malfunction of instrument measuring, and so on. Data reconciliation is a procedure to adjust or reconcile process data and to obtain more accurate values for the sampled data by requiring the reconciled data consistent with material and energy balances, for example. The data

reconciliation problem can be formulated as a constrained optimization problem, e.g., least squares estimation problem if the measurements contains only random errors.

The vector of measurement errors **e** is defined as:

$$\mathbf{e} = \mathbf{y} - \mathbf{x} \tag{2-1}$$

where vector **y** represents measured process variables with sampled values and vector **x** denotes the true values of the measured variables. The basic idea to reconcile the process data using a statistical method is to find a set of reconciled data $\hat{\mathbf{x}} = \mathbf{y} + \mathbf{a}$ that maximizes the joint distribution function (objective function) and satisfies the constraints.

If all measurements are subject to only random errors with known normal distributions, the normal distribution function for the individual measurement error is:

$$p_i \quad \frac{1}{\sqrt{2\pi}\sigma_i}\exp\left[\frac{1}{2}\left(\frac{e_i}{\sigma_i}\right)^2\right] \tag{2-2}$$

where σ_i is the standard deviation of a measurement error, e_i. The measurement error e_i has the same meaning as in Eq. 2-1. If the measurement errors are independent of each other, then the joint distribution for all measurement errors (or likelihood function) is the product of distributions for individual measurement error, i.e.,

$$P \quad \prod_{i=1}^{n} p_i \quad \frac{1}{(2\pi)^{n/2}|\Sigma|^{1/2}}\exp\left[(\mathbf{e}^T\Sigma^{-1}\mathbf{e})/2\right] \tag{2-3}$$

where Σ is the known variance matrix of measurement errors **e**, $\Sigma = \{\sigma^2_{ij}\}$.

The measurement errors are estimated by maximizing the joint probability density function in Eq. 2-3 or minimizing sum squares of standardized measurement errors, $\mathbf{e}^T\boldsymbol{\Sigma}^{-1}\mathbf{e}$, subject to a set of constraints that describe the relationship among the variables, i.e., the process model. This is the well known least squares method, and it is expressed as:

$$\begin{aligned} &\underset{\mathbf{x}}{\textit{Minimize}}: && \mathbf{e}^T\boldsymbol{\Sigma}^{-1}\mathbf{e} = (\mathbf{y}-\mathbf{x})^T\boldsymbol{\Sigma}^{-1}(\mathbf{y}-\mathbf{x}) \\ &\textit{Subject to}: && \mathbf{f}(\mathbf{x}) = 0. \end{aligned} \tag{2-4}$$

Eq. 2-4 is a nonlinear optimization problem of data reconciliation. Solving Eq. 2-4 gives the reconciled values of process variables and the estimated measurement errors.

If the constraints are linear, and they can be written as:

$$\mathbf{Ax} = 0 \tag{2-5}$$

then, the optimization problem of Eq. 2-4 has an analytical solution (Mah and Tamhane, 1982), which is:

$$\tilde{\mathbf{x}} = \mathbf{y} - \boldsymbol{\Sigma}\mathbf{A}^T(\mathbf{A}\boldsymbol{\Sigma}\mathbf{A}^T)^{-1}\mathbf{Ay} \tag{2-6}$$

and the vector of measurement adjustments is:

$$\mathbf{a} = \tilde{\mathbf{x}} - \mathbf{y} = -\boldsymbol{\Sigma}\mathbf{A}^T(\mathbf{A}\boldsymbol{\Sigma}\mathbf{A}^T)^{-1}\mathbf{Ay} \tag{2-7}$$

This linear data reconciliation problem can be extended to include component material balances, energy flow treated as additional components, stoichiometric constraints and elemental balances (Mah, 1990). In component material balances, there are products of composition and total flow rate in the constraint equations, and these balance equations are bilinear. In the energy equation, species enthalpies are not measurable and are usually expressed as a nonlinear function of the measured variables (temperature and species mass flow rate). Hence, the energy balance

equations are nonlinear. When constraints are nonlinear, the optimization problem must be solved by nonlinear programming techniques.

The solution of data reconciliation given in Eq. 2-6 is for the case that constraints are linear and all variables in the constraints are measured. Crowe, et al., (1983) proposed a projection matrix technique to decompose the data reconciliation problem that has linear constraints and unmeasured variables into the solution of two subproblems. First, the unmeasured variables in constraints are removed by multiplying a matrix (projection matrix) and the variables in constraints are all measured, then the solution of this subproblem is obtained by Eq. 2-6. Then the solution of the unmeasured variables can be determined through the original constraints (before multiplying the projection matrix) and the reconciled values of the measured variables.

Crowe (1986) extended the projection matrix technique to the case of nonlinear constraints using an iterative algorithm. First, the initial values are assigned to measured variables with the measurements and to unmeasured variables with guessed values, and the nonlinear constraints are linearized at the initialized point. Then, the data reconciliation problem with linearized constraints can be solved by projection matrix technique discussed Crowe, et al., (1983). The solution of this data reconciliation is used as the initial point to linearize the nonlinear constraints. This procedure iteratively updated the values of variables until convergence is achieved.

Pai and Fisher (1988) surveyed Crowe's iterative methods (Crowe, 1986) and proposed an application of Broyden's method to update derivatives from the matrix of last iteration. This

modified scheme has the simplicity of the constant-direction approach and retains the efficiency of the repeated computation of the Jacobian matrix. The method solved the nonlinear least squares objective function subject to nonlinear material and energy balance constraints and had rapid convergence to a solution.

Ramamurthi and Bequette (1990) recommended the nonlinear program techniques, successive quadratic programming and the generalized reduced gradient method, to solve the nonlinear data reconciliation problem. Based on the results from several test problems including the one from Pai and Fisher (1988). They showed that the iterative linearization can not handle the nonlinear constraints well and resulted in significant bias, when measurement errors are large and constraints are highly nonlinear. The reason is the approximation from Taylor expansion results in larger errors when constraints are highly nonlinear or measured variables have measurements far from the true values (larger errors). Also, the nonlinear program techniques can explicitly include the bounds of variables and allow the unmeasured variables in constraints.

Sanchez, et al., (1992) described the successful application of a plant data reconciliation program PLADAT which first classified the measured and unmeasured variables to reduce the problem size and then used successive quadratic programming for the constrained nonlinear least squares problem. This program was applied to an ethylene plant with 150 process streams and 45 units with an unspecified gross error detection procedure prior to data reconciliation. They showed that the norms of the residuals errors of the balance equations have been reduced by two order of magnitude.

Meyer, et al., (1993) presented data reconciliation on multicomponent network process, with or without chemical reactions. The basic rules to classify the measured variables into redundant and non-redundant and the unmeasured variables into observable and unobservable were proposed for formulating the linear process model. Special numerical methods were designed to obtain a matrix structure enabling the solution of large-scale systems. The proposed algorithms were tested in three industrial examples and successfully reconciled a set of data representing 34 streams and 11 components of a distillation process.

In summary, the constrained least squares method was widely used to reconcile the process data by assuming that the measurement errors are normally distributed. Data reconciliation is a nonlinear optimization problem that can be solved by the successive linear programming (successive linearization of nonlinear equations) or nonlinear programming techniques, such as successive quadratic programming or the generalized reduced gradient method. The nonlinear program techniques have been reported to successfully solve this nonlinear programming problem, and they are more robust than successive linearization as reported by Ramamurthi and Bequette (1990). For the applications of on-line optimization, data reconciliation usually is conducted with gross error detection and/or parameter estimation. The nonlinear program techniques will be used to solve the nonlinear optimization problems in our research work.

B-2. Gross Error Detection

The results for gross error detection have been reviewed and evaluated in detail through 1988 by Mah (1990) and through 1993 by Crowe (1994). As mentioned previously, raw

process data is subject to two types of errors, random errors and gross errors. Gross errors are caused by non-random event such as process leaks, biases in instrument measurements, malfunction of instruments, inadequate accounting of departures from steady state operations and/or inaccurate process models. The random errors come from the randomness of measurements, and they are normally distributed.

Significant reduction in product variability can be made through advanced control. However, there is a limitation of understanding instrumentation errors. Sanders (1995) reported that nearly two-thirds of the process upsets, which were severe enough to result in the restriction and downgrading of the product, could be traced to instrument faults. On-line gross error detection is the method for identifying instruments that produce abnormal information.

Several approaches, such as time series screening, statistical methods, or neural network method, have been practiced or proposed for gross error detection. Time series screening has been practiced in industrial applications. People use so called horizontal time screening to check for the steady state data and use the vertical screening to filter out the outliers (gross errors) in sampled data. This method is simple and easy to conduct. However, it can not detect persistent gross errors which are typical in the sampled data of chemical processes. Instrument errors and process leaks usually results in persistent gross errors, and they can not be detected or eliminated by time series screening methods.

Hoskins, Kaliyur and Himmelblau (1991) and others (Venkatasubraamanian, et al., 1990; Ferrada, et al., 1989; Leonard and Kramer, 1990; Karuri, et al., 1992; Chen and Modarres, 1992; Martin, 1997; Keeler and Boe, 1997; Himmelblau and Karjala, 1996) showed that trained

artificial neural networks were effective for fault detection and diagnosis for a complex chemical plant. Neural networks consist of a number of simple, highly interconnected processing elements, and they process information obtained from dynamic responses to external inputs. These networks can be trained to learn associations between system faults and the vector of sensor measurements. They accommodated noise in process measurements; and therefore, effectively detect and identify system faults. However, it is computationally expensive, if thousands of sensors are to be used in training these networks. Also, the models used in neural networks are empirical and they do not use the fundamental laws of chemical engineering. There is no physical meaning for the model in neural networks and the parameters in this model.

The statistical approach has been proposed in the literature for gross error detection. It requires a detail plant model to relate the individual measurement and provides the resolution for adjusting the measurement values and detecting the gross errors. Also, the knowledge about the measurement error structure is required for adjusting the measurements, and it is the basis to verify the measurements. The statistical approach usually requires solving a complicated nonlinear optimization problem to estimate the measurement errors and reconcile measurement values. It is effective in detecting the persistent gross errors.

The statistical approach has been found to be the most effective method for detecting gross errors in measurements. Also, theoretical background using in statistical approach for gross error detection is consistent with one for parameter estimation. Gross error detection, parameter estimation, and economic optimization uses the same plant model, which is established based on the fundamental laws and knowledge of chemical engineering. The following gives the review on

gross error detection with statistical methods, and the combined gross error detection and data reconciliation methods will be reviewed in the following section.

The most commonly used method for detecting gross errors is statistical hypothesis testing which requires selecting a statistic for the test with a known distribution and performance characteristics. A gross error is declared if the computed test statistic exceeds a critical value which is selected from the table of distribution. If the value of the test statistic does not exceed the critical value, then the null hypothesis H_0 is accepted, and this means the measurement does not contain a gross error. If the value of the test statistic exceeds the critical value, then the alternative hypothesis H_1 is accepted and this means that the measurement contains a gross error. The test statistic may cause faulty decisions in classifying the measurements as normal measurements (no gross errors) or abnormal measurements (with gross errors). These are called type I or type II errors. If the null hypothesis is true for a measurement (i.e., a measurement does not contain gross error) and the test rejects the null hypothesis (i.e., the test misidentifies the measurement with gross error), then this is called a type I error. The number of type I errors indicates qualitatively the degree of the misrectification from data reconciliation of a algorithm. If the null hypothesis is not true for a measurement (i.e., a measurement contain gross error) and the test accepts the null hypothesis (i.e., the test misidentifies the measurement without gross error), then this is called a type II error. The number of type II error represents the number of gross errors that are not detected.

The statistical hypothesis tests include global test, nodal or constraint test, measurement test, generalized likelihood ratio (GLR) method, Akaike's Information criterion (AIC) method,

and unbiased estimation technique (UBET), and they have been described by a number of authors (Almasy and Sztano, 1975; Mah, et al., 1976; Willsky and Jones, 1974; Narasimhan and Mah, 1987 and 1988; Yamamura and coworkers, 1988; Rollins and Davis, 1992; Mah and Tamhane, 1982). If the covariance matrices of constraint residuals or measurement adjustments are not diagonal, the assumption that measurement errors are independent of each other is not satisfied, and this affects the power of the statistical tests. The methods of maximum power (MP) test (Tamhane, 1982) and principal component analysis (PCA) (Tong and Crowe, 1994 and 1995) were developed to overcome this weakness.

There are two typical approaches for detecting gross error using statistical methods. One is based on the distribution of constraint residuals; the other is based on the distribution of measurement adjustments. The constraint residual **r** is given by (Mah, 1990)

$$\mathbf{r} = \mathbf{A}\mathbf{y} - \mathbf{c} \tag{2-8}$$

where **A** is the coefficient matrix of constraint equations in Eq. 2-5 and **c** is a constant vector in the constraints. The vector of measurement adjustments **a** is given by

$$\mathbf{a} = \tilde{\mathbf{x}} - \mathbf{y} \tag{2-9}$$

Methods based on the constraint residual are represented by global test, nodal test, and GLR. These gross error detection methods do not require simultaneous data reconciliation. However, these methods require that the constraints are linear and that all variables must be measured (or the unmeasured variables must be removed from constraints by the projection matrix method before gross error detection). They are not applicable to on-line optimization for complicated and highly nonlinear chemical processes. Methods based on the vector of

measurement adjustments include measurement test method, Tjoa and Biegler's contaminated Gaussian distribution method and robust function method. These methods reconcile the process data first, and then they use the reconciled data to examine if a measurement contains a gross error. They are classified as combined gross error detection and data reconciliation methods. These methods can be applied to nonlinear constraints. Also, they allows unmeasured variables in the plant model, if nonlinear programming techniques are used to solve the data reconciliation problem. They have great flexibility in plant model formulation. The combined gross error detection and data reconciliation method will be reviewed later.

Global Test (GT): This method was developed by Almasy and Sztano (1975). Global test uses a chi-square distribution to detect the presence of gross errors. For a quantity χ^2 that is the sum of the squared differences between the observed values and their theoretical predictions, suitably weighted by the errors of measurements, i.e.,

$$\chi^2 \quad \sum_{i=1}^{n} \frac{[y_i - x_i]^2}{\sigma_i^2} \qquad (2\text{-}10)$$

This quantity χ^2 will follow the chi-square distribution, if the sampled data is independent and if $(y_i - x_i)/\sigma_i$ follows standard normal distribution (Barlow, 1989; Larsen and Marx, 1986). The chi-square distribution is given by (Barlow, 1989)

$$P(\chi^2; n) \quad \frac{2^{n/2}}{\Gamma(n/2)} \chi^{n-2} e^{-\chi^2/2} \qquad (2\text{-}11)$$

The distribution depends on the number of points in the sum, n. This number is called the number of degrees of freedom. The global test uses a test statistic that satisfies the requirement of chi-

square distribution, i.e. to find a random variable that follow a standard normal distributed and whose sample data is independent of each other under null hypothesis. If the null hypothesis is true (no gross errors in measurements), then the summation in Eq. 2-10 should follow a chi-squares distribution, and χ^2 will be smaller than the threshold (critical) value determined by chi-square distribution at the selected significant level. **If null hypothesis is not true (measurements contain gross errors), then the summation in Eq. 2-10 will not follow a chi-squares distribution, and χ^2 will exceed the** threshold (critical) value.

It is assumed that all measurements are subject to only random errors with known normal distributions under null hypothesis and that measurement errors are independent of each other. The constraint residuals defined in Eq. 2-8 are rewritten as:

$$\mathbf{r} = \mathbf{Ay} - \mathbf{c} = \mathbf{A}(\mathbf{e} + \mathbf{x}) - \mathbf{c} = \mathbf{Ae} + (\mathbf{Ax} - \mathbf{c}) = \mathbf{Ae} \tag{2-12}$$

Under null hypothesis, the expected values of **r** can be determined by the expected values of **e** and the coefficient matrix of constraints, i.e.,

$$E(\mathbf{r}) = E(\mathbf{Ae}) = \mathbf{A}E(\mathbf{e}) = 0 \tag{2-13}$$

and the covariance matrix of **r** is the expected values of the squared differences between the individual constraint residual and its mean, i.e.,

$$\begin{aligned} \mathrm{Cov}(\mathbf{r}) &= E[\{\mathbf{r}-E(\mathbf{r})\}\{\mathbf{r} - E(\mathbf{r})\}^T] = E[\{\mathbf{Ae}\}\{\mathbf{Ae}\}^T] \\ &= E[\mathbf{A}(\mathbf{e}\,\mathbf{e}^T)\mathbf{A}^T] = \mathbf{A}\,E[\mathbf{e}\,\mathbf{e}^T]\,\mathbf{A}^T = \mathbf{A\Sigma A}^T = \mathbf{H} \end{aligned} \tag{2-14}$$

where **H** is the covariance matrix of constraint residuals. The constraint residuals **r** follow a normal distribution with zero mean and covariance matrix **H** under null hypothesis (no gross

errors in measurements). Hence, the sum of squared r_i weighted by the variance will follow the chi-square distribution, if no gross errors are present in measurements.

The test statistic of global test is (Almasy and Sztano, 1975; Mah, 1990):

$$\mathbf{r}^T\mathbf{H}^{-1}\mathbf{r} \sim \chi_m^2 \text{ , if } H_0 \text{ is true.} \qquad (2\text{-}15)$$

Eq. 2-15 means that $\mathbf{r}^T\mathbf{H}^{-1}\mathbf{r}$ follows a chi-square distribution χ_m^2 with m degrees of freedom under null hypothesis, where m is the rank of **A**.

If the value of test statistic exceeds the critical value C, then at least one gross error exists in the constraint residuals. C is determined from chi-square distribution at selected α significant level. Significant level α is equal to 1 - selected confidential level, and it represents the probability of type I errors that are possibly committed by the test statistic, i.e.,

$$\alpha = P(\text{Type I error}) = P(\text{reject } H_0 \mid H_0 \text{ is true}) \qquad (2\text{-}16)$$

If a gross errors is detected, then it can be identified by trial deletion of one or more constraint residuals until the test statistic $\mathbf{r}^T\mathbf{H}^{-1}\mathbf{r}$ does not exceed the critical value C. The procedure is deleting one or more of the constraint residuals and recalculating the test statistic value until the test statistic does not exceed the critical value. Then the deleted residuals are suspected containing gross errors.

The merit of this method is that it does not require the data reconciliation, and **r** is easy to calculate. However, the global test only indicates the presence of gross errors, and it can not directly identify the source of gross errors. This method requires trial deletion of constraint residuals to detect gross errors. Also, it is restricted to the cases of linear constraints. The reason is that the distribution of the constraint residuals used in global test is derived from the

linear combination of measurement errors. If the constraints are not linear, the means and covariances of the constraint residuals can not be obtained as Eq. 2-13 and 2-14, and the constraint residuals may not follow the normal distributions.

Nodal/Constraint Test: This test has the same assumption as global test and the test is based on the constraint residuals **r**. As discussed in global test, the constraint residuals follow a normal distribution, if the measurement errors are normally distributed. Therefore, Mah, et al., (1976) proposed the constraint test method to detect gross errors. The test statistic of constraint test is:

$$|r_j|/\sqrt{H_{jj}} \sim N(0, 1), \text{ if } H_0 \text{ is true.} \qquad (2\text{-}17)$$

Eq. 2-17 means that the standardized constraint residual, $|r_j|/\sqrt{H_{jj}}$, follows a standard normal distribution N(0, 1) under null hypothesis, where H_{jj} is the variance of constraint residual j.

If the value of test statistic for constraint residual j exceeds the critical value C, then this constraint contains gross error. The critical value C is selected from the table of standard normal distribution function at the significant level β for individual constraint residual. The overall significant level for all constraint residuals (the overall probability of type I error) can be determined by the significant level for individual constraint residual β (the probability of type I error for individual constraint residual), if the constraint residuals are independent of each other.

Let Λ be the probability that the test statistic accepts the null hypothesis when null hypothesis is true for all constraint residuals, i.e.,

$$\Lambda = P(\text{accept } H_0 \mid H_0 \text{ is true; } \mathbf{r}) = 1 - P(\text{reject } H_0 \mid H_0 \text{ is true; } \mathbf{r}) = 1-\alpha \qquad (2\text{-}18)$$

and λ_j be the probability that the test statistic accepts the null hypothesis when null hypothesis is true for constraint residual j, i.e.,

$$\lambda_j = P(\text{accept } H_0 \mid H_0 \text{ is true; } r_j) = 1 - P(\text{reject } H_0 \mid H_0 \text{ is true; } r_j) = 1 - \beta_j \qquad (2\text{-}19)$$

If the constraint residuals are independent of each other, the joint probability Λ for all constraint residuals is equal to the product of the probability λ_j for individual constraint residual, i.e.,

$$\Lambda = \lambda_1 \lambda_2 \cdots \lambda_j \qquad (2\text{-}20)$$

or
$$(1-\alpha) = (1-\beta_1)((1-\beta_2) \cdots (1-\beta_m) \qquad (2\text{-}21)$$

If the individual significant levels are set to the same as β, then Eq.2-21 becomes:

$$(1-\alpha) = (1-\beta)^m \qquad (2\text{-}22)$$

Eq. 2-22 can be rewritten as:

$$\beta = 1 - (1-\alpha)^{1/m} \qquad (2\text{-}23)$$

Eq. 2-23 is used to determined the significant level for individual constraint residual β. It is determined by overall significant level α and the dimension of constraint residuals m. It must be noted that Eq. 2-23 is true only when the constraint residuals are independent of each other, otherwise the individual significant level β can not be determined by Eq 2-23.

Although the constraint test can identify the constraint associated with gross errors, the same drawback as global test still remains. It can not locate the source that creates the nodal gross error, i.e., it can not indicate which measurement contains a gross error. Because the constraint that is identified having gross error is associated with a number of the measurements that are present in this constraint and with possible process leak in the unit for which this constraint equation describes. Also, multiple gross errors present in the same constraint may be

canceled each other, and they may not be detected. In addition, the applications of this method are limited to linear constraints.

Generalized Likelihood Ratio Test: This test was originally developed by Willsky and Jones (1974) to identify abrupt failures in dynamic system. Narasimhan and Mah (1987 and 1988) proposed a general framework for identifying different types of gross errors, caused by either measurement biases and/or process leaks, with the generalized likelihood ratio (GLR) test. This test requires a model that describes the effect of each type of gross errors. The measurement model with instrument bias is defined as:

$$\mathbf{y} = \mathbf{x} + \mathbf{e} + a\boldsymbol{\delta}_i \tag{2-24}$$

where $\mathbf{y}$ and $\mathbf{x}$ have the same meaning as in Eq 2-1, and $\mathbf{e}$ represents random errors. In Eq. 2-24, $\boldsymbol{\delta}_i$ is a unit vector with one in position i and zero elsewhere, and a is the unknown magnitude of a bias (gross error).

A leak occurring in a process unit will not affect the measurement model in Eq. 2-24, but it affects the constraint equations associated with the leak. The linear process model, $\mathbf{Ax} = 0$, can be rewritten as following equations with a leak.

$$\mathbf{Ax} - a\mathbf{m}_j = 0 \tag{2-25}$$

where $\mathbf{m}_j$ is a vector representing different constraints, and a in Eq. 2-25 is the unknown magnitude of leak in a constraint. With either measurement bias or a process leak, the constraint residual is defined as:

$$\mathbf{r} = \mathbf{A}\,(\,\mathbf{x} + \mathbf{e} + a\boldsymbol{\delta}_i) \tag{2-26}$$

or

$$\mathbf{r} = \mathbf{A}\,(\,\mathbf{x} + \mathbf{e}) - a\mathbf{m}_j \tag{2-27}$$

If no gross errors are present, then the mean and variances of constraint residuals will be the same as given in Eq. 2-13 and 2-14 discussed in global test section. Narasimhan and Mah proposed to test the null hypothesis H_0, $E(\mathbf{r}) = 0$ that assumes no gross errors are present, against the alternative hypothesis H_1, $E(\mathbf{r}) = a\mathbf{A}\boldsymbol{\delta}_i$ or $a\mathbf{m}_j$ that assumes one gross error is present in either measurement bias or process leak, by the likelihood ratio test. This test also estimates the unknown magnitude of gross error if a gross error is indicated,. The likelihood ratio test is given by (Mah, 1990):

$$\lambda \quad \text{supremum} \quad \frac{Pr(r|H_1)}{Pr(r|H_0)} \tag{2-28}$$

where $P(r|H_1)$ and $P(r|H_0)$ are the probability of constraint residuals under alternative and null hypothesis respectively. The supremum in Eq. 2-28 is computed over all possible values of the parameters (δ_i, m_j and a) present in the hypotheses.

If constraint residuals **r** are normally distributed, then the distribution function of $P(r|H_0)$ and $P(r|H_1)$ are written as:

$$P(r|H_0) \quad \prod_{i=1}^{n} p(r_i|H_0) \quad \frac{1}{(2\pi)^{n/2}|H|^{1/2}} \exp\left[\frac{r^T H^{-1} r}{2}\right] \tag{2-29}$$

and

$$P(r|H_1) \quad \prod_{i=1}^{n} p(r_i|H_1) \quad \frac{1}{(2\pi)^{n/2}|H|^{1/2}} \exp\left[\frac{(r - af_i)^T H^{-1} (r - af_i)}{2}\right] \tag{2-30}$$

Substituting Eq. 2-29 and 2-30 into Eq. 2-28 and taking a logarithm of Eq. 2-28 gives:

$$T \quad 2\ln\lambda \quad \underset{a f_i}{supremum}\left[r^T H^{-1} r \; (r - a f_i)^T H^{-1} (r - a f_i) \right] \qquad (2\text{-}31)$$

where

$$\mathbf{f}_i \in (\mathbf{A\delta}_i,\ i = 1, 2, .., n;\ \mathbf{m}_j,\ j = 1, 2, .., m) \qquad (2\text{-}32)$$

In Eq. 2-31, the possible outcome from either measurement error $\mathbf{A\delta}_i$ or process leak $\mathbf{m}_j$ is combined and represented by $\mathbf{f}_i$ as shown in Eq. 2-32.

The computation of T proceeds as follows. For any given vector $\mathbf{f}_i$, the estimated gross error magnitude a is determined by maximizing Eq. 2-31. The solution of the maximization of Eq. 2-31 for given vector $\mathbf{f}_i$ is:

$$a = (\mathbf{f}_i\ \mathbf{H}^{-1}\ \mathbf{f}_i)^{-1}\ (\mathbf{f}_i\ \mathbf{H}^{-1}\ \mathbf{r}) \qquad (2\text{-}33)$$

Substituting Eq. 2-33 into Eq. 2-31 gives test statistic T_i for each case $\mathbf{f}_i$ as:

$$T_i = (\mathbf{f}_i\ \mathbf{H}^{-1}\ \mathbf{r})^2 / (\mathbf{f}_i\ \mathbf{H}^{-1}\ \mathbf{f}_i) \qquad (2\text{-}34)$$

This calculation is performed for every possible vector $\mathbf{f}_i$ and the test statistic is therefore obtained as:

$$T = \text{supremum}\ T_i \qquad (2\text{-}35)$$

Let f^* be the vector that leads to the supremum in Eq. 2-35. The test statistic T is compared with a pre-specified threshold (critical values) C determined by the distribution function of T at the selected significant level α. If T exceeds C, then the measurement or constraint that corresponding to f^* is identified as having a gross error or a leak, and its magnitude is estimated

by Eq. 2-33 using $\mathbf{f}^*$ for $\mathbf{f}_i$. For each case of $\mathbf{f}_i$, T_i has a central chi-square distribution with one degree of freedom under null hypothesis H_0.

Generalized Likelihood Ratio Test for Multiple Gross Errors: It is assumed that only one gross error exists in either measurement model or constraint model for each application of generalized likelihood ratio test. For multiple gross error cases, the compensation strategy has been proposed to adjust the measurement or constraint that is declared containing gross error (Narasimhan and Mah, 1987). If a gross error is identified, the estimated magnitude of the error is used to compensate (adjust) the measurement or constraint associated with the detected gross error. And then the GLR test is repeated again until no gross error is detected.

The advantage of GLR test is that it can identify the gross error source as instrument error or process leak. However, its applications are still restrict to linear process constraint or approximate linear ones. The linearization of nonlinear constraints brings in great errors in approximation of nonlinear constraints and distribution when the process is highly nonlinear and gross errors are large. Also, the implementation of GLR for searching gross errors is not efficiency. It is not applicable for complicated and highly nonlinear process of on-line optimization.

Other Gross Error Detection Methods: Rollins and Davis (1992) proposed an unbiased estimation technique (UBET) for gross error detection which considers both bias measurement and process leaks. The conditions for this technique are restricted to normally distributed errors, steady state, and linear constraints. First, a global test is conducted to test for the presence of gross errors. Then, UBET is used to detect the number and location of gross errors by trial and

error search for the unbiased estimators, where two test statistics, F test and Bonferroni test, are used as the criteria for the identification of gross errors. Also, Rollins and Roelfs (1992) extended this approach to the case where constraints are bilinear.

Yamamura and coworkers (1988) presented a method for the detection of multiple gross errors in process data based on Akaike's information criterion (AIC). The AIC is defined as:

$$AIC = - 2L + 2p \tag{2-36}$$

where L is the logarithm of a likelihood function and p is the number of parameters (or the number of system errors) in the model. This criterion divides the measured variables into two types. One is only subject to the random error that is normally distributed with zero mean, i.e., $N(0, \sigma^2)$. The other is subject to random error plus gross error that is normally distributed with non-zero mean, i.e., $N(\mu, \sigma^2)$. The gross errors are identified by comparing the values of AIC function for all possible combination states. The combination state with minimum value of AIC is declared as the most probably faulty state; the gross errors presumed in this combination state will be identified as the gross errors. Each measurement has two possible outcomes, either no bias or with bias. For the system with n measurements, the number of possible faulty states is 2^n. Hence, this method will be computation expensive if n is large and constraints are nonlinear. To overcome this problem, the authors provided a branch-and-bound strategy for their algorithm and demonstrated its effectiveness in a hypothetical petroleum refinery system with 22 measurements and 13 linear constraints.

To improve the power of the statistical tests, Tamhane (1982) proposed the maximum power (MP) measurement test method. This method has the

greatest probability of correctly detecting a single gross error in measurements when only one gross error is present. The maximum power of the detection is achieved by using a linear transformation, i.e., the measurement error vector is transformed by multiplying a non-singular matrix, the inverse of the variance-covariance matrix of measurement errors,

$$\mathbf{d} = \mathbf{\Sigma}^{-1}\,\mathbf{e} \tag{2-37}$$

then this transformed measurement errors **d** will have the maximum power in detecting gross error with measurement test method. Mah and Tamhane (1982) have given an extensive discussion of the power of this test.

Crowe (1989) extended the concept of maximum power for gross error detection to the constraint test. In addition, Crowe (1992) extended MP test for gross errors to bilinear constraint cases. Crowe concluded that MP statistic for the original constraints is precisely the square root of the corresponding generalized likelihood ratio test of Narasimhan, Eq. 2-28.

Similar to the MP test, Tong and Crowe (1994 and 1995) introduced the principal component technique into the gross error detection based on the idea of Pearson and Hotelling on the principal component analysis (PCA). PCA is an effective tool in multivariate data analysis. In this technique, a set of correlated variables is transformed into a new set of uncorrelated variables, known as principal component (PC), through a orthonormal matrix constructed by the eigenvectors of the covariance matrix **H** for the projected constraint residuals, i.e.,

$$\mathbf{d} = \mathbf{W}^{T}\,\mathbf{r} \tag{2-38}$$

where **W** is constructed from the eigenvector of covariance matrix **H** of constraint residuals and satisfies

$$\mathbf{W} = \mathbf{U}\mathbf{\Lambda}^{-1/2} \tag{2-39}$$

where matrix $\mathbf{\Lambda}$ is diagonal, consisting of the eigenvalues of $\mathbf{H}$ on its diagonal and satisfies

$$\mathbf{\Lambda} = \mathbf{U}^{T}\mathbf{H}\,\mathbf{U}. \tag{2-40}$$

The matrix $\mathbf{U}$ consists of the orthonomalized eigenvectors of $\mathbf{H}$ so that

$$\mathbf{U}\mathbf{U}^{T} = I \tag{2-41}$$

Through this transformation, the new vector $\mathbf{d}$ becomes a new set of uncorrelated variables and is normally distributed, i.e., $\mathbf{d} \sim N(0, 1)$. Then the gross errors are detected by the nodal test method as discussed previously. This new test has been implemented in two examples and compared with univariate, maximum power, and chi-square tests. The authors concluded that PC test is sharper and has shown a capability of detecting gross errors of small magnitudes when the other tests fail.

The principal component method improves the power in detecting gross errors. However, the drawback on nodal test method still remains in principal component test method, i.e., the constraints must be linear and additional identification for the sources of constraint residual gross errors is required. Also, the errors in plant sampled data are related to the respective instruments and the measuring of different instruments is independent of each other. Therefore, the assumption that measurement errors for different measured variables are independent of each other is true for the sampled data from distributed control system. Then the variance-covariance matrix of errors should be diagonal, and the maximum power and principal component techniques are not necessary for improving the power of gross error detection algorithms for the process sampled data of on-line optimization.

Narasimhan and Mah (1989) described four statistical tests for gross error detection: global test, constraint test, measurement test and generalized likelihood ratio test. They also presented a procedure for transforming a general steady-state model into a form required by these tests.

Almasy and Uhrin (1993) proposed a new theoretical base for the identification of gross errors subject to linear constraints. Traditionally, gross errors are considered as non-random quantities caused by non-random events. Almasy and Uhrin presented a different opinion for the concept of gross errors. They viewed the gross errors as random variables for a broader time horizon. Based on this concept, they identified the measurement biases and process leaks as gross errors because of the random nature of these errors. However, both model mismatches and departure from steady state are not considered as gross errors because they are not random events. **Model mismatches cause deterministic errors,** and the departure from steady state **can be counted in a dynamic model.** They proposed two families of probability distributions, Gamma distribution and non-zero mean Gaussian distribution, for the residuals with gross errors. Also, the maximum likelihood estimation was **suggested** as a better approach for gross error detections.

In summary, the time series screening method has been practiced in industrial applications. It is simple and easy to conduct. However, it can not detect the persistent gross errors. The statistical approach is effective in detecting persistent gross errors in sampled data through other normal measurements. This approach identifies the gross error of a measurement by other normal measurements through the process constraints. It requires a detail and precise

plant model as constraints to integrate individual measurement together and the knowledge of the distribution pattern of errors as basis for adjusting the measurements. The gross error detection using statistical methods has been studied by university researchers with simple and small hypothesis plant models (Crowe, 1989 and 1992; Tamhane, 1982; Mah and Tamhane, 1982; and Narasimhan and Mah, 1987 and 1988)

The test statistic of the gross error detection methods reviewed above are constructed based on the assumption that the constraint residuals are normally distributed with known variance matrix. These methods are easy to implement and the gross error can be detected without reconciling the process data. However, the applications of these methods are limited to linear constraint cases and requires that all variables in the model must be measured. These methods are not applicable for an actual plant that is highly nonlinear and in which large portion of process variables are unmeasured. Also, gross errors are identified by the trial deletion of the suspected residuals and this is inefficient.

B-3. Combined Gross Error Detection and Data Reconciliation

There are several efficient methods to conduct combined gross error detection and data reconciliation. All these methods are based on the distribution function of measurement errors. The procedure of these methods is first reconciling all process data by maximizing the joint distribution function subject to process constraints. Then the gross errors are identified according to the estimated errors and a test statistic. These methods have less restrictions on the applications than the methods based on constraint residuals discussed above. They can be applied to a nonlinear plant model and allow unmeasured variables in the constraints of the plant

model. Also, gross errors can be directly identified by the test statistic without a trial deletion strategy. The following describes several combined gross error detection and data reconciliation methods and gives a review of their application.

Measurement Test Method: This method was first proposed by Mah and Tamhane (1982) to directly detect the sensor biases. It assumes that the measurement errors are independent of each other, and all measurements are normally distributed when no gross error is present. Then the joint distribution for all measurement errors (or likelihood function) is the product of the normal distributions for individual measurement error as given in Eq. 2-3, i.e.,

$$P \quad \prod_{i=1}^{n} p_i \quad \frac{1}{(2\pi)^{n/2}|\Sigma|^{1/2}} \exp\left[(\mathbf{e}^T\Sigma^{-1}\mathbf{e})/2\right] \tag{2-3}$$

where Σ is the known variance matrix of measurement errors $\mathbf{e}$.

The measurement errors are estimated by maximizing the joint probability density function or minimizing the sum squares of standardized measurement errors, $\mathbf{e}^T\Sigma^{-1}\mathbf{e}$, subject to a set of constraints that describe the relationship among the variables, i.e., the process model. This is the well known least squares method and it is expressed as:

$$\begin{aligned} &\underset{\mathbf{x}}{\textit{Minimize}}: && \mathbf{e}^T\Sigma^{-1}\mathbf{e} = (\mathbf{y}-\mathbf{x})^T\Sigma^{-1}(\mathbf{y}-\mathbf{x}) \\ &\textit{Subject to}: && \mathbf{f}(\mathbf{x}) = 0. \end{aligned} \tag{2-42}$$

Eq 2-42 is a nonlinear optimization problem of data reconciliation that is the same as Eq. 2-4 for data reconciliation. Solving Eq. 2-42 gives the reconciled values of process variables and the estimated measurement errors. These estimated measurement errors are used to determine if the measurements contain gross errors. If the constraints are linear, the optimization problem in Eq.

2-42 has an analytical solution as shown in Eq. 2-6 and 2-7 for the reconciled values and estimated measurement adjustments.

The test statistic of measurement test method is:

$$\epsilon_i = |e_i/\sigma_i| \sim N(0,1), \text{ if } H_0 \text{ is true.} \quad (2\text{-}43)$$

Eq. 2-43 means that the standardized measurement error, ϵ_i, follows a standard normal distribution N(0,1) under null hypothesis.

If the estimated standardized error i ($\epsilon_i = |e_i/\sigma_i|$) does not exceed the critical value C, then measurement i does not contain a gross error. Otherwise, the measurement contains a gross error. The critical value C is selected from the table of standard normal distribution function based on the selected significant level β for individual measurement. The significant level for individual measurement β is calculated by Eq. 2-23 from a given overall significant level α. The m in Eq 2-23 is the number of distinct values of $|e_i|/\sigma_i$ for all measurement errors.

Measurement test method is able to identify the sources of gross errors, but it requires data reconciliation first to determine the measurement errors. These estimated measurement errors are the basis for the gross error identification. Compared with the global test and nodal test, measurement test not only has the advantage in directly identifying the sources of gross errors, but also it is not restricted to the linear constraint case. It allows unmeasured process variables in the model if a nonlinear programming technique (optimization algorithm) is used to solve the data reconciliation problem of measurement test method. However, the measurement test method still can not overcome the main deficit of traditional methods for gross error detection, which assumes that the errors are normally distributed. This distribution function can

not describe the distribution behavior of gross errors, and bias estimations are obtained when gross errors exist, especially for very large gross errors.

For independent measurements, the variance-covariance matrix of measurement errors is diagonal, and the least squares function in Eq. 2-42 can be rewritten as following linear function using a first order Taylor expansion:

$$e^T\Sigma^{-1}e \quad \sum_i \frac{e_i^2}{\sigma_i^2} \quad \sum_i \frac{2e_i^0}{\sigma_i^2}(e_i - e_i^0) \qquad (2\text{-}44)$$
$$w_1(e_1 - e_1^0)\, w_2(e_2 - e_2^0) \cdots w_n(e_n - e_n^0)$$

where $w_i = 2e_i^0/\sigma_i^2$ is the weight coefficient of a measurement error e_i in the objective function of Eq. 2-42 evaluated at the last feasible point e_i^0. As shown in Eq. 2-44, the least squares function is approximated as the sum of the products of weight coefficient w_i and Δe_i, $\Delta e_i = e_i - e^0_i$, for all measurements. Eq. 2-42 for measurement test method is a minimization optimization problem. When the optimization algorithm search for a optimal solution of Eq. 2-42, it looks for a set of e_i's values that satisfy the constraints in Eq. 2-42 and have smaller weight coefficients for each measurement error e_i. This means a measurement having a larger coefficient will have more significant effect on the minimization than one having a smaller weight coefficient. The weight coefficient of a measurement in least squares function is proportional to the measurement error size of the measurement as shown in Eq. 2-44, i.e., a measurement with a larger error has a larger weight coefficient in the least squares function. This means that a measurement with a larger error has more significant effect on the minimization of measurement test method than one with a smaller

error, and this results in biased estimation when measurements with gross errors are used in data reconciliation. This biased estimation from measurement test method has been pointed out by Mah (1990) and Crowe (1994). When a set of process data is subject to constrained least-squares reconciliation, a high penalty that is the weight coefficient in Eq. 2-44 is imposed on making any single large correction to the measurement with a larger gross error.

The presence of gross errors invalidates the statistical basis of reconciliation procedures. Therefore, they must be detected or corrected. This weakness of measurement test method motivated a number of researchers to develop the strategies to overcome the bias estimation and improve the performance of measurement test method.

The strategies to improve the misrectification of measurement test method are represented by iterative elimination methods (Ripps, 1965; Nogita, 1972; Serth and Heenan, 1986), series compensation method (Narasimhan and Mah, 1987), and modified iterative elimination methods (Serth and Heenan, 1986 and 1987; Rosenberg, et al., 1987). These strategies improve the detection of multiple gross errors, and they avoid the misrectification caused by the presence of large gross errors. However, the methods are inefficient. They require the reconstruction of constraints in plant model, and this results in frequent modification of the optimization programs during search for the gross errors. This brings in difficulties for their use in the automatic implementation of on-line optimization.

Serth and Heenan (1986) performed a detailed comparison of seven algorithms for combined gross error detection and data reconciliation in a steam-metering system. They found that the modified iterative measurement test (MIMT) method was superior to the others in terms of power to detect gross errors, power to reduce random errors and computational efficiency. The MIMT algorithm detected 80% of the gross errors and achieved a total error reduction over 60% for a steam-metering process in a methanol synthesis unit. Iterative elimination and bounds on the variables are the strategies used in this MIMT method. This MIMT algorithm represents probably the best data screening algorithm for linear equality process models among the traditional gross error detection methods. However, the implementation is still inefficient compared with Tjoa-Biegler's contaminated Gaussian distribution method and robust function methods which will be reviewed later.

The following will illustrate the algorithms of measurement test (MT), iterative measurement test (IMT), and modified iterative measurement test (MIMT) described in Serth and Heenan's paper (Serth and Heenan, 1986).

The implement procedure of measurement test (MT) method is:

Step 1 Compute reconciled values $\tilde{\mathbf{x}}$ and measurement adjustments **a** for the full system using Eq. 2-6 and Eq. 2-7.

Step 2 Compute standardized measurement adjustments for each measurement, $\epsilon_i = a_i / \sigma_i$.

Step 3 Compare each ϵ_i with the critical value of test statistic, C, selected from the table of standard normal distribution at the selected significant level β. If $|\epsilon_i| > C$, then denote measurement i as a suspected measurement containing systematic errors and add the suspected measurements to set S. If $|\epsilon_i| < C$ for all measurements, then go to Step 7.

Step 4 If the set S is empty, proceed to step 7. Otherwise, remove measurements contained in S from the system by nodal aggregation. This process eliminates some of the constraints and variables and yields a new system with reduced number of constraints and variables, and the original constraints (**Ax** = 0) are reduced as **Bd** =0. In the reduced constraints, **d** represents the variable vector as **x** excluding the variables that are eliminated by the nodal aggregation, and **B** represents the constraint coefficient matrix as **A** excluding the rows and columns that are corresponding to the eliminated constraints and variables from the nodal aggregation. Also, the measurement vector **y** is reduced to vector **w** that excludes the eliminated measurements from nodal aggregation, and let T denote the set of measurements contained in **w**. In addition, the variance and covariance matrix of

measurement errors $\mathbf{\Sigma}$ is reduced to matrix **P** that excludes the variances and covariances of the eliminated measurements.

Step 5 Repeat Step 1 to compute the estimated values of process variables and measurement adjustments by Eq. 2-6 and 2-7 with **A**, **y**, and $\mathbf{\Sigma}$ replaced by **B**, **w**, and **P**, respectively.

Step 6 Compute corrected values of variables in S by solving $\mathbf{Ax} = 0$ with the variables in set T specified with the estimated values from step 5 and the variables in set R specified with the original measured values. R is a set of variables that were eliminated during the nodal aggregation and whose measured data does not contain gross error, i.e., $R = U - (S \cup T)$, where U is the set of all variables in the system. Then go back to Step 2.

Step 7 If the set S is empty, then all measurements do not contain gross error, and the estimated values of process variables in step 1 by Eq. 2-6 are the reconciled values of all process variables. Otherwise, the set of reconciled values is obtained from the values computed in step 6 for the variables containing gross errors in set S, the reconciled values computed in step 5 for the variables in set T, and the original measured values for the variables in set R.

As noted by Mah and Tamhane (1982), Serth and Heenan (1986), and Chen and Pike (1996), Eq. 2-23 that is used to determine the individual significant level β proposed by Mah and Tamhane (1982) is too conservative. The critical value for the test statistic in Eq. 2-43 is determined by the individual significant level β and the normal distribution function. For example, if 0.05 overall significant level (95% confidential level) is used and the number of measurements is 43, then the significant level for individual measurement β is

$$\beta = 1 - (1-\alpha)^{1/m} = 1-(1-0.05)^{1/43} = 0.0012.$$

At the $\beta/2=0.006$ point, the critical value C is determined from the standard normal distribution with accumulated probability at 0.994, and the value is 3.2. This means that only the standardized measurement adjustment larger than 3.2 will be identified as having gross error. This is very easy to commit type II error when the magnitude of gross errors are less than 5 times the standard deviation. Also, the measurement test method tends to spread the gross errors over all measurements, thereby creating large residuals corresponding to good measurements. When these residuals fail the test for gross errors, the corresponding measurements are erroneously identified as containing gross errors, which results in a large number of type I errors. Therefore, an iterative elimination strategy was proposed to improve this problem by Ripps (1965), Nogita (1972), and Serth and Heenan (1986 and 1987) and is incorporated with measurement test method. It is called iterative or series measurement test (IMT).

The procedure of iterative measurement test (IMT) is:

Step 1 Compute reconciled vector $\hat{\mathbf{x}}$ and measurement adjustments vector **a** as in MT.

Step 2 Calculate the standardized measurement adjustments $\boldsymbol{\epsilon}$ as MT.

Step 3 Compare each ϵ_i with the critical value C of test statistic as in MT. If $|\epsilon_i| \leq C$ for all measurement, go to step 6. Otherwise, select the measurement corresponding to the largest value of $|\epsilon_i|$ and add it to set S as suspected measurement that contains a gross error. If two or more measurements have the same maximum values of $|\epsilon_i|$, select the one with lower index.

Step 4 If set S is empty, proceed to Step 6. Otherwise, remove the measurements contained in S from system by nodal aggregation to obtain a lower dimension of system with constraint coefficient matrix **B**, measurement vector **w**, and covariance matrix **P** as MT (**B**, **w**, and **P** have the same meaning as given in MT). Let T denote the measurements contained in **w**. Repeat Step 1 to compute $\tilde{\mathbf{x}}$ and **a** with **A**, **y**, and $\boldsymbol{\Sigma}$ replaced by **B**, **w**, and **P**, respectively.

Step 5 Compute corrected values for measurements in set S by solving equations $\mathbf{Ax} = 0$ with the variables in set T specified with the reconciled values from step 4 and the variables in set R specified with the original measured values. R is a set of variables that were eliminated during the nodal aggregation and whose measured data does not contain gross error, i.e., $R = U - (S \cup T)$, where U is the set of all variables in the system. Then, go back to Step 2.

Step 6 If the set S is empty, then all measurements do not contain gross error, and the estimated values of process variables in step 1 by Eq. 2-6 are the reconciled values of all process variables. Otherwise, the set of reconciled values is obtained from the computed values **in step 5 for the variables containing gross errors in set S, the reconciled values computed in step 4 for the variables in set T, and the original measured values for the variables in set R.**

The IMT described here is slightly different from series elimination strategy proposed by Ripps (1965). In IMT method, only the measurement corresponding to the largest standardized

measurement error is deleted at each application of MT, and it is automatically identified as containing a gross error. The least squares calculation is thus made only once at each application of MT. In Ripps' series elimination strategy, each suspect measurement is deleted and least squares calculation is repeated each time. If more than one gross error is present, the entire procedure must be repeated with combination of two, three, etc., measurements until a combination is found that results in the remaining data satisfying the test statistic of MT.

IMT significantly reduces the type I errors committed by measurement test. However, the drawback that the set of reconciled flow rates may contain negative values or absurdly large values remains. This situation generally indicates the failure of the algorithm to correctly identify the gross errors in the data. To avoid this problem, a modified iterative strategy was proposed and incorporated in measurement test. It is so called modified iterative measurement test (MIMT).

The MIMT is essential the same as IMT. The only different is that it adds one more step to check if all reconciled data satisfies the pre-specified bounds after IMT implementation. If one or more of reconciled data does not satisfy the bounds, it returns to step 3 of IMT and delete the last entry in set S and replaces it with the measurement corresponding to next largest value of $|\epsilon_i|$. Then the procedure continues as in IMT. The bounds checking is a safeguard to ensure that the reconciliation from least squares does not conflict with the process simulation rules.

The procedure of modified iterative measurement test (MIMT) is:

Step 1 Compute reconciled vector $\hat{\mathbf{x}}$ and measurement adjustment vector $\mathbf{a}$ as in MT.

Step 2 Calculate the standardized measurement errors $\boldsymbol{\epsilon}$ as MT.

Step 3 Compare each ϵ_i with the critical value C of test statistic as in MT. If $|\epsilon_i| \leq C$ for all measurement, go to step 7. Otherwise, select the measurement corresponding to the largest value of $|\epsilon_i|$ and add it to set S as suspected measurement that contains a gross error. If two or more measurements have the same maximum values of $|\epsilon_i|$, select the one with lower index.

Step 4 If set S is empty, proceed to Step 7. Otherwise, remove the measurements contained in S from system by nodal aggregation to obtain a lower dimension of system with constraint coefficient matrix **B**, measurement vector **w**, and covariance matrix **P** as MT (**B**, **w**, and **P** have the same meaning as given in MT). Let T denote the measurements contained in **w**. Repeat Step 1 to compute $\hat{\mathbf{x}}$ and **a** with **A**, **y**, and $\boldsymbol{\Sigma}$ replaced by **B**, **w**, and **P**, respectively.

Step 5 Compute corrected values for measurements in set S by solving equations $\mathbf{Ax} = 0$ with the variables in set T specified with the reconciled values from step 4 and the variables in set R specified with the original measured values. R is a set of variables that were eliminated during the nodal aggregation and whose measured data does not contain gross error, i.e., $R = U - (S \cup T)$, where U is the set of all variables in the system.

Step 6 Check the reconciled values of process variables with the pre-specified bounds. If one or more of reconciled data does not satisfy the bounds, then discard the reconciled data and return to step 3, delete the last entry in set S, and replace it with the measurement corresponding to next largest value of $|\epsilon_i|$. If no bound violation is found, go back to Step 2.

Step 7 If the set S is empty, then all measurements do not contain gross error, and the estimated values of process variables in step 1 by Eq. 2-6 are the reconciled values of all process variables. Otherwise, the set of reconciled values is obtained from the computed values **in step 5 for the variables containing gross errors in set S, the reconciled values computed in step 4 for the variables in set T, and the original measured values for the variables in set R.**

In a subsequent study, Serth and Heenan (1987) extended their linear data screening techniques to the nonlinear case. They linearized the nonlinear constraints and used similar strategies as the linear MIMT algorithm to reconcile the linearized constrained data. However, the successive linearization of the nonlinear constraint equations had to be used to determine the reconciled data and estimated measurement errors by Eq. 2-6 and 2-7. They tested the algorithm in a metallurgical grinding circuit problem and concluded that the overall performance of this algorithm on the nonlinear system was comparable to that exhibited on a linear system of approximately the same size. The algorithm correctly detected about 80% of all systematic errors in the data and achieved an average reduction in total error of more than 60%. However, this algorithm for nonlinear problems is computational inefficient. It requires numerous linearization of the nonlinear equations for each deletion of suspected measurement to search for the gross errors.

Kim, et al., (1997) have conducted the MIMT (modified iterative measurement test) with a simple CSTR example and compared the result using the nonlinear program techniques with one

using a successive linearization method applied by original MIMT's author, Serth and Heenan (1986). They found the nonlinear programming techniques has more advantage in explicitly handling the nonlinear constraints and bounds. These techniques gave a more accurate result than successive linearization did when the constraints are highly nonlinear and the measurement errors are larger. Also, the nonlinear programming techniques allow unmeasured variables in constraints equations, but the successive linearization method used by Serth and Heenan was not able to incorporate the unmeasured variables explicitly. The unmeasured variables must be removed before data reconciliation.

Kao, Tamhane, and Mah (1990) evaluated the effect of serially or chronologically correlated measurements on the gross error detection. Their simulation results indicated that the measurement test (MT) based on the independence assumption was extreme sensitive to the presence of correlation among measurements. Two algorithms have been outlined in their paper. The first involves suitably adjusting the variance of the test statistics, and the second involves filtering out the correlations and then applying the desired test based on the independence assumption. They concluded that both of these two methods were robust, effective and simple to use. **If the sample data is correlated each other, the independence assumption used in the gross error detection techniques is improper. However, each measurement error is associated with the individual instrument, and the measuring of different instruments is independent of each other. Therefore,**

the independence assumption is true for the measurements from distributed control system.

In summary, the measurement test method requires data reconciliation to estimate the measurement errors. This method can directly locate the sources of gross errors and explicitly handle nonlinear constraints and unmeasured variables of the plant model if an nonlinear programming technique is used to solve the data reconciliation optimization problem. However, the normal distribution used in measurement test method can not describe the distribution behavior of gross errors, and the presence of gross errors invalidates the statistical basis for data reconciliation. Thus, this results in bias estimation and a large number of type I errors. To avoid this problem, series elimination, iterative elimination, modified iterative elimination strategies have been proposed to improve the performance of measurement test method. These strategies significantly reduce the number of type I errors committed by measurement test method. However, they require the reconstruction of constraints and the reclassification of measured and unmeasured variables during searching for gross errors. This is difficult to incorporate in a general computer program. Also, the method of solution used in MT, MIT, and MIMT can not explicitly deal with the unmeasured variables and bounds, and the successive linearization of nonlinear equation results in lower solution accuracy when the plant model is highly nonlinear and errors are larger. The nonlinear program techniques, such as generalized reduced gradient and successive quadratic programming should be used to solve this nonlinear data reconciliation problem (Ramamurthi and Bequette, 1990). In addition, the test statistic of measurement test proposed

by Mah and Tamhane (1982) is too conservative. It is very easy to commit type II error when the magnitude of gross errors is small.

Contaminated Gaussian Distribution Method: This method was developed by Tjoa and Biegler (1991) for combined gross error detection and data reconciliation. They proposed using a two modes (random and gross errors) Gaussian distribution. A measurement can have either a random or a gross error. The two possible outcomes are: G = {Gross error occurred} with prior probability η and R = {Random error occurred} with prior probability $1-\eta$. Therefore, the distribution function of measurement error i is:

$$P(y_i \mid x_i) = (1-\eta)P(y_i \mid x_i, R) + \eta\, P(y_i \mid x_i, G) \qquad (2\text{-}45)$$

where $P(y_i \mid x_i, R)$ is the probability distribution function for the random error and $P(y_i \mid x_i, G)$ is the probability distribution function for the gross error.

It is assumed that the random error is normally distributed with a zero mean and known variance σ^2, then the distribution of a random error is:

$$P(y \mid x, R) \quad \frac{1}{\sqrt{2\pi}\sigma} e^{\frac{(y-x)^2}{2\sigma^2}} \qquad (2\text{-}46)$$

Also, it is assumed that the gross error is subject to a normal distribution which has a zero mean and a larger variance $(b\sigma)^2$, $(b >> 1)$. Therefore, the distribution function for a gross error can be expressed as:

$$P(y \mid x, G) \quad \frac{1}{\sqrt{2\pi}b\sigma} e^{\frac{(y-x)^2}{2b^2\sigma^2}} \qquad (2\text{-}47)$$

If the measurement errors are independent of each other, then the likelihood function for all measurements is the product of the distribution functions for individual measurements, i.e.,

$$P(\mathbf{y}|\mathbf{x}) = \prod_i P(y_i \mid x_i) = \prod_i \{ (1-\eta)P(y_i \mid x_i, R) + \eta\, P(y_i \mid x_i, G)\} \qquad (2\text{-}48)$$

Tjoa-Biegler called Eq. 2-48 a contaminated Gaussian distribution, and it was used to reconcile the values of process variables by maximizing the likelihood function (joint distribution function of measurement errors) in Eq. 2-48 or minimizing the negative logarithm of the likelihood function subject to the constraints in plant model, i.e.,

$$\underset{\mathbf{x}}{\text{Minimize:}} \quad \sum_i \left\{ \ln\left[(1-\eta) e^{-\frac{(y_i - x_i)^2}{2\sigma_i^2}} + \frac{\eta}{b} e^{-\frac{(y_i - x_i)^2}{2b^2\sigma_i^2}} \right] - \ln\sqrt{2\pi}\sigma_i \right\} \qquad (2\text{-}49)$$

$$\text{Subject to:} \quad \mathbf{f}(\mathbf{x}) = 0$$
$$\mathbf{x}^L \le \mathbf{x} \le \mathbf{x}^U$$

where $\mathbf{f}(\mathbf{x}) = 0$ is the process equality constraints of plant model. $\mathbf{x}^L \le \mathbf{x} \le \mathbf{x}^U$ is the bounds for the process variables. Eq. 2-49 is a nonlinear data reconciliation optimization problem and it can be solved by nonlinear programming techniques. Solving Eq. 2-49 gives the reconciled data for all process variables, which maximizes the joint probability $P(\mathbf{y} \mid \mathbf{x})$ and satisfies the process constraints.

After data reconciliation, each measurement is examined with a test statistic to see if it contains a gross error. The test statistic for gross error detection is:

$$\text{If} \qquad \eta P(y_i|x_i, G) \ge (1-\eta)P(y_i|x_i, R) \qquad (2\text{-}50)$$

or if

$$\left|\epsilon_i\right| \left| \frac{y_i - x_i}{\sigma_i} \right| > \sqrt{\frac{2b^2}{b^2 - 1} \ln\left[\frac{b(1-\eta)}{\eta}\right]} \qquad (2\text{-}51)$$

then measurement i contains gross error. Otherwise, no gross error is present in this measurement.

The procedure to conduct contaminated Gaussian distribution method is:

1. Solve Eq. 2-49 to determined the reconciled values for measured variables and unmeasured variables, and then the measurement adjustments, $\mathbf{a} = \tilde{\mathbf{x}} - \mathbf{y}$, are determined by the measurements $\mathbf{y}$ and reconciled data $\tilde{\mathbf{x}}$.
2. Examine the standardized measurement adjustment ϵ_i, $\epsilon_i = a_i / \sigma_i$, using the criterion given Eq. 2-51 to determine if a measurement contains a gross error. If a measurement contains a gross error, then its value is replaced with the reconciled data. A new set of measurements is constructed using the reconciled data to replace the measurements containing gross errors along with the original measurements that contain only random errors. This new set of measurements contains only random errors, and it is used in simultaneous data reconciliation and parameter estimation to update plant parameters for on-line optimization.

The authors applied this algorithm to two simple examples. One was a simple model having eight variables and six constraints given by Pai and Fisher (1988). The other one was a simple hypothesis heat exchanger process model having 16 measured variables, 14 unmeasured variables, and 17 constraints. The results showed that the method gave unbiased estimates and it is effective in identifying gross errors. Also, the authors exploited the properties of this function and designed a better approximation of the Hessian matrix rather than using a general BFGS

update formula to yield a better convergence of successive quadratic programming (SQP) for solving this optimization problem.

The contaminated Gaussian distribution describes the distribution pattern of both random and gross errors. The logarithm of joint distribution (objective function in Eq. 2-49) is the sum of the logarithm of the contaminated Gaussian distribution for each measurement. This means that the individual contaminated Gaussian distribution function for each measurement has a contribution on the joint distribution function (objective function). Due to the characteristic of contaminated Gaussian distribution, the individual contaminated Gaussian distribution for a measurement with a larger error has a smaller contribution on the joint distribution than one for a measurement with a smaller error. This can be seen by weight coefficients of measurements in the linearized joint distribution, which is described in the following.

The objective function in Eq. 2-49 can be approximated as a linear function using a first order Taylor expansion, i.e., $P = \sum w_i [(y_i - x_i)-(y_i - x_i)^0] = \sum w_i (\epsilon_i - \epsilon_i^0)$, where w_i is the weight coefficient of measurement y_i on the joint distribution function (objective function in Eq. 2-49) evaluated at the last feasible point x_i^0 or ϵ_i^0. This coefficient is the derivative of the joint contaminated Gaussian distribution function with respect to the variable x_i as shown as in following,

$$w_i \frac{\frac{(y_i - x_i)}{\sigma^2}\left\{(1-\eta)e^{\frac{(y_i-x_i)^2}{2\sigma^2}\left(1-\frac{1}{b^2}\right)} \frac{\eta}{b^3}\right\}\Big|_{x_i, x_i^0}}{(1-\eta)e^{\frac{(y_i-x_i)^2}{2\sigma^2}\left(1-\frac{1}{b^2}\right)} \frac{\eta}{b}} \frac{\frac{\epsilon_i}{\sigma}\left\{(1-\eta)e^{\frac{\epsilon_i^2}{2}\left(1-\frac{1}{b^2}\right)} \frac{\eta}{b^3}\right\}\Big|_{\epsilon_i, \epsilon_i^0}}{(1-\eta)e^{\frac{\epsilon_i^2}{2}\left(1-\frac{1}{b^2}\right)} \frac{\eta}{b}} \quad (2\text{-}52)$$

where the weight coefficient is a function of the standardized measurement error, $\epsilon_i = (y_i - x_i)/\sigma_i$. For smaller error, e.g., $\epsilon_i < 2$, the exponential term in the Eq. 2-52 is much larger than the second term η/b^3 (or η/b), The weight function can be simplified as:

$$w_i \propto (y_i - x_i)/\sigma_i^2 = \epsilon_i/\sigma_i \quad (2\text{-}53a)$$

For larger error, e.g., $\epsilon_i > 4$, the exponential term in the equation is much smaller than the second term η/b^3 (or η/b). The weight function can be simplified as:

$$w_i \propto (y_i - x_i)/(b\sigma_i)^2 = \epsilon_i/(\sigma_i\, b^2) \quad (2\text{-}53b)$$

Therefore, the weight coefficient w_i in Eq. 5-52 can be approximated as:

$$w_i \begin{cases} \epsilon_i/\sigma_i & \text{for } \epsilon_i < 2 \\ \epsilon_i/(\sigma_i b^2) & \text{for } \epsilon_i > 4 \end{cases} \quad (2\text{-}54)$$

Comparison of weight coefficient functions for small (random) errors in Eq. 2-53a and for large (gross) errors in Eq. 2-53b shows that the weight coefficient for measurements with gross errors is reduced b^2 times compared with those with random errors. The shows that the measurement with a smaller error has a larger contribution on the linearized objective function (joint distribution function) than one with a larger error, and it has more significant effect on the minimization of Eq. 2-49 than a measurement with a larger error.

Since the measurements with larger errors has a very weak effect on the minimization, the reconciled data will depend on the measurements without gross errors. Therefore, it is said that contaminated Gaussian distribution method has an ability to reduce the effect of measurements with gross errors on the reconciled data and give an unbiased estimation for reconciled data.

In contaminated Gaussian distribution, b is a tuning parameter to shape the distribution. Increasing b will reduce the effect of a gross error on the estimation and increase the robustness of this approach. However, it will decrease the asymptotic efficiency to the normality. In the practical applications, b is usually chosen as 10-20, and the weight coefficient for a measurement with a gross error is 100-400 times smaller than one with a random error. The prior probability of a gross error, η, is another parameter in contaminated Gaussian distribution. If no prior information about the errors available, then the equal prior probability, i.e., $\eta = 0.5$, is recommended.

The contaminated Gaussian distribution method is more effective than measurement test method. It incorporates the distribution pattern for both random and gross errors, and it is able to rectify both random and gross errors in measruements. This method can directly locate the

gross errors and gives an unbiased estimation for all reconciled data. It can be used for the combined gross detection and data reconciliation, and it will be extended to simultaneous gross error detection, data reconciliation, and parameter estimation of on-line optimization in this research.

Bayesian Method: Albuquerque and Biegler (1995) and Johnston and Kramer (1995) extended the contaminated Gaussian distribution method using Bayesian theorem and incorporated the contaminated distribution in the posterior density function. Bayesian theorem gives (Bretthorst, 1989 and Barlow, 1989):

$$P(\mathbf{x} \mid \mathbf{y}) = P(\mathbf{y} \mid \mathbf{x})\, P(\mathbf{x})/P(\mathbf{y}) \tag{2-55}$$

where $P(\mathbf{x} \mid \mathbf{y})$ is the probability that variables have the true values under given measurements, and it is called a posterior density function. In Eq. 2-55, $P(\mathbf{y}|\mathbf{x})$ is the probability of the measurements $\mathbf{y}$ under condition that variables have true values $\mathbf{x}$, and it is often referred as a likelihood function. $P(\mathbf{x})$ is the prior probability of $\mathbf{x}$, and $P(\mathbf{y})$ is the prior probability of measurements $\mathbf{y}$.

The prior probability of measurements $P(\mathbf{y})$ is a uniform distribution function dependent on the measure range of instruments. It is the normalized constant and independent of $\mathbf{x}$. It does not affect the optimization. Therefore, it can be excluded from the optimization (Johnston and Kramer, 1995).

The prior probability of true values of variables $\mathbf{x}$, $P(\mathbf{x})$, can be constructed by the principle of maximum entropy based on the prior qualitative knowledge about the process variables. Detail methodology about maximum entropy was given by Shannon (1948). Also,

Johnston and Kramer (1995) have proposed a probability bootstrapping technique to estimate the parameters in the prior probability function P(**x**) using the historical plant data. However, the accuracy of the P(**x**) obtained by this method depends on the accuracy of the information and data used. A blunder in the information or data would mislead the construction of P(**x**); and therefore, it results in inaccurate estimation of data reconciliation.

On-line optimization will move the set points from time to time based on the production schedule and market demand. The operating behavior from previous knowledge or historical plant data may not agree with the current plant operations. If the historical data about the plant operation is used to construct the prior probability P(**x**), it will possibly mislead the construction of P(**x**) and will affect the accuracy of the estimation of data reconciliation. It is believed that an equal prior probability for P(**x**) will give an more accurate estimation for data reconciliation, if the character of the process operation is not accurately known.

If an uniform distribution (equal prior probability) is used for P(**x**), then the posterior function is proportional to likelihood function, and the Bayesian method reduces to maximum likelihood method. Maximizing posterior density function is equivalent to maximizing the likelihood function. If information about the true values of process variables is known and if it is incorporated in the posterior density function, then Bayesian method can not only predict the true values of the variables, but also it can predict the range of their variations.

The likelihood function can be constructed by the normal distribution, contaminated Gaussian distribution or another that describes the distribution behavior of measurement errors. To describe the error structure of measurements more precisely, Johnston and Kramer (1995)

proposed a multiple mode distribution for measurement errors. For individual measurement i, the distribution function is the linear combination of probability functions of all possible error modes weighted by the respective prior probabilities, i.e.,

$$P(y_i \mid x_i) = \sum_k P(y_i \mid x_i, m_k) P(m_k) \tag{2-56}$$

where $P(m_k)$ represents the prior probability of error mode m_k. The error modes m_k can be normal, biased, and/or failed. The most common used distribution function for random errors is a normal distribution with zero mean. However, the distribution function for gross errors will be different dependent on the nature of the errors. For the instrument biased error, the distribution function will be a normal distribution with a unknown mean representing the bias. The failed modes can be characterized as the failure to a fixed value (modeled as a delta function) and as a failure to a random value (modeled as an uniform distribution). Also, the leaking mode can be modeled as a uniform function determined by the possible range of the leak.

Including all possible error modes in the distribution function would provide the complete information about the measurement errors. However, adding all possible measurement error modes to the distribution function will significantly increase the difficulty of solving the optimization problems. Also, the prior probabilities for different types of errors are usually not available. It is better to construct a general distribution function which combines all the information about the possible gross error modes, such as, the two mode contaminated Gaussian distribution function proposed by Tjoa and Biegler (1991) to describe the distribution for both random and gross errors.

Johnston and Kramer (1995) applied the Bayesian method to two examples. One is a flow system from Mah (1987) that had three nodes and five streams and the other one was a simple hypothetical heat exchanger network from Tjoa and Biegler (1991). The simulation results from these two examples showed that the performance of the contaminated Gaussian distribution was better than traditional least squares method. The contaminated Gaussian distribution method can automatically reject the contribution of measurements containing gross errors to the data reconciliation and give unbiased estimation. Also, the authors briefly described the influence function and showed the influence functions for least square, contaminated Gaussian distribution, and Lorentzian distribution that is a robust function from Huber (1981). However, no application with Lorentzian function was conducted in their work.

The advantage of this Bayesian method over the likelihood function method is that it also includes the distribution function of the true values of variables in the objective function (posterior density function). Therefore, Bayesian method not only can predict the true values of process variables, and it also can predict their variations. However, the accuracy of the estimation of data reconciliation is strongly depends on the accuracy of the prior distribution P(**x**) if it is incorporated. It is very difficult to construct prior probability P(**x**) because the distribution function depends on many aspects of information about the process. It is suggested to use an equal prior probability for P(**x**), if this probability is not known.

Robust Function Methods: These methods were developed originally to find a robust estimate of location (mean) and scale (variance) for univariate data (one variable with n repeated sample data) (Huber, 1972 and 1981; Seber, 1984; and Hampel 1973). When analyzing

experimental data, one usually faces two difficulties (Seber, 1984). First, various studies suggested that likely 0.1-10% of observations (or even more) would be "dubious" (containing gross errors) from wrong measurements or any other sources of blunders. Second, sampled data is rarely normally distributed and tend to have distributions that are normal in the middle, but have longer tails than the normal distribution on the two sides. Robust estimation was developed to overcome these two difficulties, i.e., gross errors (outliers) in the data and the distribution function for the data deviating from the normal distribution.

The basic idea of robust estimation is to build a robust distribution function ρ. This robust distribution is asymptotic to a normal distribution or a pre-defined distribution function that describes the distribution pattern of measurement errors under some ideal assumptions. The robust function is to be insensitive to the presence of gross errors in sampled data when this function is used to conduct data reconciliation, and it still maintains a high efficiency (lower dispersion) that indicates the accuracy of estimation (Huber, 1972; Seber, 1984).

Several useful classes of robust estimators have been developed, and these are the adaptive estimator, L-estimator (linear function of order statistics), M-estimator (analogues of maximum likelihood estimator), R-estimator (rank test estimator), and others. The most important class applicable to on-line optimization is M-estimator.

The well known maximum likelihood estimator (MLE) or M-estimator finds the values of $\mathbf{x}$ (estimated values) by maximizing $\prod_i P(y_i, x_i)$, or minimizing $- \ln [\prod_i P(y_i, x_i)] = -\sum [\rho(y_i, x_i)]$ equivalently, where $\rho = \ln P(y_i, x_i)$,

$$\begin{aligned} &\text{Minimize:} && -\sum_{i} [\ \rho(y_i, x_i)\ ] \\ &\mathbf{x} && \\ &\text{Subject to:} && \mathbf{f}(\mathbf{x}) = 0 \\ & && \mathbf{x}^{L} \le \mathbf{x} \le \mathbf{x}^{U} \end{aligned} \tag{2-57}$$

The distribution function ρ is called the distribution of observations (measurements) or robust function which will be given in the following. Usually, a robust function is expressed as a logarithm of probability function, then the joint distribution function in the objective function becomes the summation format that is mathematically simpler than the product format.

The basic concept for M-estimator is the same as the traditional likelihood estimation using the contaminated Gaussian distribution or normal distribution. The only difference is that the distribution function used in robust estimation is the asymptotic function of likelihood probability function. For the case that the data will most likely follows a normal distribution with a small percentage of extreme points (or gross errors), it is suggested that the distribution function $\rho(y_i, x_i)$ should be asymptotic to the ideal normal distribution. The shape of the distribution should be normal in the middle, but have longer and flatter tails on its two sides.

Two robust functions have been proposed in literature (Johnston and Kramer, 1995; Huber, 1981; and Albuquerque and Biegler, 1995) for mean estimation, and they are applicable for rectifying gross errors in process sampled data. Johnston and Kramer (1995) proposed the Lorentzian distribution, which was originally presented by Huber (1981), for reconciling process variables. The Lorentzian distribution is:

$$\rho(\epsilon_i) \quad \frac{1}{1 \quad \frac{1}{2}\epsilon_i^2} \tag{2-58}$$

where ϵ_i is the standardized measurement error including both random and gross errors, i.e., $\epsilon_i = (y_i - x_i)/\sigma_i$. This robust function was briefly mentioned in Johnston and Kramer's paper (1995) for data regression, but the authors did not give any applications of gross error detection and data reconciliation.

Albuquerque and Biegler (1995 and 1996) proposed Fair function for estimating the process variables as following:

$$\rho(\epsilon_i, c) \quad c^2\left[\frac{|\epsilon_i|}{c} \quad \log\left(1 \quad \frac{|\epsilon_i|}{c}\right)\right] \qquad (2\text{-}59)$$

where ϵ_i is the standardized measurement error and c is a tuning parameter. The change in parameter c change the shape of distribution, and the efficiency (or estimation accuracy) of this distribution is determined by this parameter. It was pointed out that Fair function is convex and has continuous first and second derivatives (Albuquerque and Biegler, 1995).

Also, the authors described the exploratory statistics method for identifying the gross errors based on the estimated measurement residuals (errors). They proposed a technique, boxplot where the center of the box is the median and the sides are the quartiles, to identify the gross errors based on the order statistics. The outliers are spotted by computing the order statistics (median and quartiles) and their distances from these. The interquartile-range d_F is defined as:

$$d_F = F_u - F_l \qquad (2\text{-}60)$$

where F_u and F_l are the third and first quartiles, respectively. The outlier cutoffs were defined as $F_l - \gamma d_F$ and $F_u + \gamma d_F$, where γ was usually set to 1/3. The measurements outside the cutoffs

were considered outliers. The gross errors can be identified by boxplot method with packages like MINITAB (Ryan, et al., 1985) or xlispstat (Tierney, 1990). However, the criterion set by Albuquerque and Biegler seems to cause more type I errors (i.e., a measurement does not contain gross error, but the test misidentifies the measurement with gross error). Qualitatively, approximate one sixth of data is found containing gross errors using the test proposed for boxplot method, no matter how good or how bad the data set is.

In addition, Albuquerque and Biegler (1996) introduced the concept of an influence function for the distribution. They compared influence functions for contaminated Gaussian distribution and Fair function. Also, they discussed the variable classification for the dynamic process model.

The Fair function was applied to a dynamic process of two connected tanks that has five measured variables and two parameters and compared with the algorithm of contaminated Gaussian distribution (Albuquerque and Biegler, 1995 and 1996). They concluded that Fair function not only is less sensitive to the presence of gross error, but it is mathematically simple and easy to use.

Albuquerque and Biegler (1996) used a simple heat exchanger network (Tjoa and Biegler, 1991; and Swartz, 1989) to demonstrate the effectiveness of the simultaneous gross error detection approach by comparing the results of both the contaminated Gaussian distribution and Fair function with the serial gross error detection test (measurement test). They showed that there were no significant difference between contaminated Gaussian distribution and iterative measurement test (IMT) method. They concluded that robust approach had a number of

advantages, including better numeric characteristics and less biased estimates. Also, this approach had the interesting property (because Fair function is convex) of yielding global solution for nonlinear programs with lower constraint curvature.

In the steady-state heat exchanger example problem, Albuquerque and Biegler (1996) compared the results of the least squares method, the contaminated Gaussian distribution method, and a robust function method (Fair function). The tabulated results showed the reconciled data of variables from the least squares method with run 1 and run 2, the contaminated Gaussian distribution method, and Fair function method. In the least squares method, run 1 showed the data reconciliation result which did not exclude a measurement with a gross error, and run 2 showed the data reconciliation result which excluded a measurement with a gross error. The result from the contaminated Gaussian distribution was closer to one of run 2, which were the reconciled results using least squares method after the gross error was removed, than Fair function did. This indicated that the estimation from contaminated Gaussian distribution was more accurate than one from Fair function. The least squares method gives the highest estimation accuracy if gross errors in measurements were correctly removed before the data reconciliation. The true values of process variables was not available for comparison, and therefore, the results of run 2 for least squares method should be used as comparison, but not the reconciled residuals (the difference between reconciled data and measurements) as the authors did.

When comparing the performance of algorithms, both the influence function and efficiency of a distribution are important criteria to evaluate the algorithms. The influence function

(IF)represents how sensitive an algorithms is to the presence of gross errors, and it is proportional to the derivative of the distribution, i.e.,

$$IF \propto \partial\rho/\partial x \tag{2-61}$$

The efficiency of a distribution function indicates the estimation accuracy from data reconciliation and it is given by the shape of the distribution, i.e., a sharper distribution has higher efficiency and higher estimation accuracy, and a flatter distribution has lower efficiency and lower estimation accuracy. It is favorable to have a algorithm that has the combination of smaller or even zero influence function for larger errors and high efficiency. It will be shown that the contaminated Gaussian distribution has a better combination of influence function and efficiency than Fair function and normal distribution (measurement test) next chapter.

In summary, robust statistical methods were developed to overcome difficulties with the data that contains gross errors and that does not follow the ideal normal distribution. Robust approach uses an objective function that is insensitive to the deviation of the data from the ideal normal distribution due to its mathematical structure (Albuquerque and Biegler, 1996; and Huber, 1980). These methods tend to look at the bulk of the data and ignore atypical values. Robust methods have the advantages of having a very simple mathematical form and of having very convenient properties for optimization. However, the efficiency (accuracy) of robust functions will be slightly lost because they have a flatter shape that gives larger variation in estimation. In addition, the boxplot and dotplot methods from exploratory statistics (Albuquerque and Biegler, 1996) can be used to identify the gross errors in sampled data. However, the criterion set by Albuquerque and Biegler seems to cause more type I errors (i.e., a measurement does not

contain gross error, but the test misidentifies the measurement with gross error). Qualitatively, approximate one sixth of data is identified containing gross errors no matter how good or how bad the data set was, according to the test they proposed for boxplot method. Also, caution is needed in that these methods were original proposed for the same type of data. However, the data sampled from DCS includes different types of data, such as temperature, flow rate, pressure, and composition, which have very different numerical values. This may cause a problem in using order statistics method which is the basis of boxplot and dotplot method, although using standardized measurement errors in these methods gives a better scale of the errors.

Summary of Methods for Gross Error Detection: Only combined gross error detection and data reconciliation methods are practical to detect and rectify gross errors in on-line optimization applications. These methods apply to models that are highly nonlinear and in which a large portion of process variables are unmeasured or unmeasurable. Measurement test (MT, IMT, MIMT) methods, contaminated Gaussian distribution method, and robust function method were able to detect and rectify gross errors in data from distributed control system for on-line optimization.

Since the normal distribution used in the measurement test method is not able to describe the distribution behavior of a gross error, the measurement test method is very sensitive to the presence of gross errors in measurements. The presence of gross errors invalidates the statistical basis for the data reconciliation and results in biased estimation. To avoid this problem, series elimination, iterative elimination, modified iterative elimination strategies have been proposed in literature to improve the performance of measurement test. These strategies significantly improve

the error rectification and gross error detection. However, they require the reconstruction of constraints and the reclassification of measured and unmeasured variables which are caused by nodal aggregation during searching for gross errors. This is very inefficient. Also, the method of solution used in MT, MIT, and MIMT can not explicitly handle the unmeasured variables and bounds, and the successive linearization of nonlinear equation results in lower solution accuracy when the plant model is highly nonlinear and errors are larger. In addition, the test statistic of measurement test proposed by Mah and Tamhane (1982) is too conservative. It is very easy to commit type II error when the magnitude of gross errors is small.

The contaminated Gaussian distribution algorithms incorporated the distribution pattern for both random and gross errors, and it can automatically reject the contribution of measurements containing gross errors by giving a much smaller weight factors to such measurements. It can directly locate the gross error sources and gives an unbiased estimation for all reconciled data. The characteristic of this distribution demonstrates the properties of a robust function, i.e., it is not sensitive to the presence of gross errors, and it gives unbiased estimation even the measurements contain both random and gross errors. Also, the shape of contaminated Gaussian distribution is sharper than those of robust functions. This distribution function has higher efficiency than robust functions. However, this distribution function still has the nature of the normal distribution. When the gross error goes to extremely large (e.g., infinite), the performance of the contaminated Gaussian distribution decreases and still results in biased estimation. This will be shown in the theoretical evaluation of distribution functions next chapter.

Robust statistical methods were developed to overcome difficulties with the data that contains gross errors and that does not follow the ideal normal distribution. Robust statistical methods use an objective function that is insensitive to the presence of gross errors in sampled data. These methods tend to look at the bulk of the data and ignore atypical values. Robust methods have the advantages of having a very simple mathematical form and of having very convenient properties for optimization. However, the efficiency (accuracy) of estimation from these methods will be slightly lost because robust functions have a flatter shape that gives larger variation in the estimation. Also, the test to detect gross error of robust methods is not as straight forward as the contaminated Gaussian distribution or other likelihood function does, although the boxplot and dotplot methods from exploratory statistics (Albuquerque and Biegler, 1996) may be used to identify the gross errors of sampled data. Moreover, the criterion set by Albuquerque and Biegler (1996) seems to cause more type I errors as discussed previously.

In closing, measurement test method has been widely studied by both university and industrial researchers. However, its biased nature on the estimation and the inefficient implementation from the iterative procedures result in a limitation of its applications to large scale on-line optimization problems. The new approaches, contaminated Gaussian distribution and robust functions, have been proposed for the detection of gross errors. However, they have not been studied with real, large scale nonlinear plant models. Based on the nature of the distributions and the ability of ignoring the contribution of gross errors on the estimation, they are seen as the appropriate algorithms for conducting combined gross error detection and data reconciliation and for simultaneous gross error detection, data reconciliation, and parameter estimation with large

scale plant models in on-line optimization. They will be tested and evaluated as part of this research.

B-4. Parameter Estimation

There are two types of models for parameter estimation according to Britt and Luecke (1973). One type is the explicit model, in which measurements are divided into two sets of measured variables, independent variables and dependent variables. In this type of model, independent variables are measured with a much greater accuracy than dependent variables. The dependent variables can be expressed as an explicit function of independent variables and the parameters. For this type of model, parameters can be estimated by minimizing the sum of squared errors of dependent variables (least squares method) or maximizing the likelihood function, a probability distribution function of the measurement errors of dependent variables (maximum likelihood method). This is a unconstrained optimization problem, and linear regression method is one of examples for this type of estimation.

The other type of model is implicit or error-in-variables model. There are errors in all measurements and the variables can not be partitioned into dependent and independent variables as in the explicit model. The constraints of process models are implicit. Therefore, the optimization problem of parameter estimation must be formulated as constrained optimization problem which will be discussed in the following section. The error-in-variables models represent the general case of process simulations for on-line optimization. Hence, only the parameter estimation methods that are applicable to this type of process model can be used for the

parameter estimation of on-line optimization. The methods for error-in-variables model will be reviewed in the next section.

Stewart, Caracotsios, and Sorensen (1992) gave a review of the literature for parameter estimation, and they proposed the Bayesian method for the parameter estimation with explicit model using n repeated experimental data. The explicit model is expressed as:

$$y_{ui} = f_i(\mathbf{x}_u, \boldsymbol{\theta}) + e_{ui}, \ (u = 1, 2, .., n; \ i = 1, 2, .., m) \tag{2-62}$$

where y_{ui} represents the multiple response data array, i.e., $\mathbf{y} = \{y_{ui}\}$. $\mathbf{x}_u$ represents the vector for independent variables that have accurate sampled data. $\boldsymbol{\theta}$ is the vector of the parameters to be estimated. u from 1 to n denotes the independent events (the repeated experiments) and i from 1 to m represents the dimension of dependent variables **y**. The function **f** describes the relationship between the dependent variables **y** and independent variables **x** and parameters $\boldsymbol{\theta}$. e_{ui} is the error of dependent variable y_{ui} and it is assumed that e_{ui} is normally distributed with mean as zero and unknown covariance matrix $\boldsymbol{\Sigma}$. Therefore, the parameters and unknown covariance matrix can be estimated by maximizing the posterior density function (Stewart, Caracotsios, and Sorensen, 1992), i.e.,

$$\text{Maximum: } p(\boldsymbol{\theta}, \boldsymbol{\Sigma} \mid \mathbf{y}) \propto |\boldsymbol{\Sigma}|^{-(n + m + 1)/2} \exp\{-\text{tr}[\boldsymbol{\Sigma}^{-1}\mathbf{v}(\boldsymbol{\theta})]\} \tag{2-63}$$

The elements of matrix $v(\boldsymbol{\theta})$ in Eq. 2-63 is determined by:

$$v_{ij}(\boldsymbol{\theta}) = \sum_{u=1}^{n} [y_{ui} - f_i(\mathbf{x}_u, \boldsymbol{\theta})][y_{uj} - f_j(\mathbf{x}_u, \boldsymbol{\theta})] \tag{2-64}$$

The authors concluded that Bayesian and likelihood approaches were superior to weighted least squares and to the use of a pre-specified error covariance matrix. The advantage

of their approach is giving the estimation of the error structure from a multiresponse data set, along with the parameter vector of a predictive model based on Bayesian theorem. The optimization problem of parameter estimation in Eq. 2-63 is formulated for the traditional parameter estimation with repeated experimental data. It can not be directly applied to the parameter estimation of on-line optimization. However, its methodology can be used for the parameter estimation of on-line optimization by modifying the problem formulation into constrained optimization problem using error-in-variables models.

Biegler, et al., (1986) presented the results of an industrial nonlinear parameter estimation problem from Dow Chemical Company. The model consists of six ordinary differential equations and four algebraic equations (DAE) with nine parameters. This is stiff differential/algebraic model with error structure unspecified and the starting guess leads to a nontrivial optimization problem. This problem was attempted by eleven researchers yielding five acceptable solutions. They compared the five solutions along with a failed solution in terms of accuracy and efficiency. Finally, they arrived at the conclusions that good problem formulation, proper scaling and reasonable initial guess were the guideline for tackling dynamic parameter estimation problems.

Rhinehart and Riggs (1991) presented a new technique for parameter estimation by two simple methods, one for dynamic equations and one for steady-state models. The one for steady-state models used Newton's method with a relaxation coefficient, a one-step ahead filtered process/model mismatch, and it used the modeled output/parameter sensitivity to calculate an incremental adjustment to the model parameter at each sampling interval. The relaxation coefficient is incorporated in the Newton's linearization to improve convergence for highly

nonlinear process model. They concluded that these methods are effective and simple both conceptually and implementationally and can be easily extended to multivariable case.

Pinto, et. al., (1991) reformulated the general approach to parameter estimation in terms of the relative uncertainties in the model parameters. This new formulation took relative uncertainties in model parameters into consideration and lead to new sequential experimental design criteria. Their numerical examples showed that the relative β-trace design criterion was the best criterion for sequential experimental design.

The other applications for parameter estimation are for the optimal design of sequential experiments. Dovi, Reverberi, and Maga (1993) described this application for both explicit and implicit models and developed the theoretical formula to determine the optimal conditions for next experiment.

A new branch of parameter estimation is the quality control parameter design which originated from the work of the Japanese quality expert G. Taguchi in 1980. Parameter estimation methodology is an off-line quality control method for identifying design settings that make the product performance less sensitive to the effects of manufacturing and environmental variations.

Maria and Muntean (1987) described an application of kinetic parameter identification for the methanol conversion to olefin. The complex kinetic model contained 33 reactions and 16 chemical species. The reaction rate constants were estimated by minimizing the weighted sum of squares of the errors for the product concentrations subject to a set of dynamic constraints. The minimization used the combinative DP-SP-RRA (derivatives discretization procedure-a cubic

spline approximation procedure-ridge regression analysis) and IP-SP-RRA **(integral transformation procedure-a cubic spline approximation procedure-ridge regression analysis)** strategy and a multimodel NLSQ techniques was used to refine the parameter values for the reduced model.

Based on the technique of Dunn and Bertsekas in optimal control problems, Albuquerque and Biegler (1993) developed a decomposition algorithm for on-line estimation with nonlinear dynamic constraints, a set of ODE. In this approach, the differential equations were discretized as algebraic constraints and a SQP method was used to solve this optimization problem. The authors proposed a strategy to solve the QP subproblem efficiently by taking advantage of the problem structure. Compared with the other methods, this algorithm performed well for both linear and nonlinear cases in both efficiency and robustness.

Krishnan, et al., (1992) proposed a serial of techniques to locate the key parameters that contributes a significant effect to the profit optimization and to filter out the unrelated plant measurements for reducing the size of the optimization problems. The authors described a two-step parameter estimation scheme that was specially designed for on-line optimization. The first step involved determining key model parameters. The second step was finding the best set of measurements to estimate these parameters. The key model parameters are determined through perturbing individually by an amount depending on the estimation accuracy of parameters. If perturbing a parameter significantly changes the optimal objective function and/or alters the active constraint set at the calculated optimum, then this parameter is regarded as a key parameter.

After the key parameters are determined, the necessary measurements for estimating these parameters are selected through testing the accessibility of measurements to parameters and the observability of the parameters. The simulated results using the William-Otto (simulated) plant showed that the scheme was robust in the presence of measurement noise and uncertainties in non-key parameters. The methods proposed here is related to the methodology of plant model formulation, and they will be incorporated in the strategy to formulate the plant simulation model of our research work.

In subsequent research (Krishnan, et al., 1993), they applied this robust parameter estimation technique to part of an operational zinc refinery. They showed that the proposed technique could be applied to an complex process where a highly detailed process model was not available. The methods involved developing a simple plant model with only steady-state mass balance and simple shrinking core kinetic model. They determined the key parameters and a set of measurements, and minimized the nonlinear least square estimator. They concluded that the simple process model adequately represented the plant performances and was suitable for on-line applications.

Diwekar and Rubin (1993) presented a methodological approach to the parametric design of chemical processes which used the ASPEN simulator and was based on the stochastic modeling capability. They also analyzed different sampling techniques and compared the stochastic optimization techniques of Latin Hypercube sampling and traditional Monte Carlo Sampling.

In summary, above is a brief review of the traditional parameter estimation. These methods require an explicit process model and the parameter estimation problem is formulated as unconstrained optimization problem using repeated sampled data. The methods proposed above can not be directly used in the parameter estimation of on-line optimization. The process models of on-line optimization are complicated, highly nonlinear and all measurements in the model are subject to errors. They can not be formulated as an explicit model. In addition to the parameters, there can be a large number of unmeasured variables in the process models. Consequently, an error-in-variables model must be used. Some of the methodology discussed above, such as least squares method, maximum likelihood method, and Bayesian method, can be modified and used to conduct the simultaneous data reconciliation and parameter estimation of on-line optimization using the error-in-variables model as constraints. The following will review the results for simultaneous data reconciliation and parameter estimation.

B-5. Simultaneous Data Reconciliation and Parameter Estimation

On-line optimization requires that the model of a plant matches the performance of the plant. This is referred to as plant-model matching. Plant-model mismatch can be caused by either inaccuracies in the models, e.g., imprecise simplification, blunders in equations, and uncertain plant parameters which are unmeasurable and time-varying. The familiar examples of time-varying plant parameters are catalyst deactivation and heat exchanger fouling which cause change in the effectiveness factor of catalyst and in heat transfer coefficients from the new plant. Also, inaccurate parameters used in the process model for economic optimization will result in non-optimal operating conditions. In order to have the model match the plant operations,

updating the process parameters is essential for on-line optimization. In addition, the process models of on-line optimization are complicated and highly nonlinear, and only error-in-variables models can be used to describe the process.

Deming (1943) originally formulated the general problem of parameter estimation by taking into account the errors in all measured variables. Britt and Luecke (1973) presented general methodology for the parameter estimation of error-in-variables model. This type of parameter estimation is a constrained optimization problem. In error-in-variables model, vector **y** represents the measured process variables with measurement values, and **x** represents the true values of these variables. All of the variables have errors and the relation of **y** and **x** is the same as the measurement error model given in Eq. 2-1, i.e.,

$$\mathbf{y} = \mathbf{x} + \mathbf{e} \tag{2-1}$$

The error vector **e** has a zero mean and positive definite covariance matrix $\mathbf{\Sigma}$.

The general methodology of parameter estimation with error-in-variables model has a structure similar to the data reconciliation and it is a simultaneous data reconciliation and parameter estimation optimization problem. The only difference is that the parameters in plant model are considered as variables along with the variables in simultaneous data reconciliation and parameter estimation rather than being constants in data reconciliation. Both process variables and parameters are simultaneously estimated through minimization of the sum squares of measurement errors if the least squares method is used.

The general mathematical formulation of parameter estimation using maximum likelihood method for normally distributed measurement errors is (Britt and Luecke, 1973):

$$\underset{\mathbf{x},\,\boldsymbol{\theta}}{\textit{Maximize}}: \quad L(\mathbf{x}, \boldsymbol{\theta}) = (2\pi)^{-n/2} \, |\boldsymbol{\Sigma}|^{-½} \exp\{-½(\mathbf{y} - \mathbf{x})^T \boldsymbol{\Sigma}^{-1}(\mathbf{y} - \mathbf{x})\} \tag{2-65}$$

$$\textit{Subject to}: \quad \mathbf{f}(\mathbf{x}, \boldsymbol{\theta}) = 0$$

where $\boldsymbol{\theta}$ represents a set of parameters in plant model, and they are estimated with the variables $\mathbf{x}$ by solving this optimization problem. The equality constraints $\mathbf{f}(\mathbf{x}, \boldsymbol{\theta})$ are the plant simulation equations and denote the implicit relationship among the process variables and parameters. Solving Eq. 2-65 finds the values of $\mathbf{x}$ and $\boldsymbol{\theta}$ that maximize the likelihood function $L(\mathbf{x}, \boldsymbol{\theta})$ and satisfy the process constraints. Taking a negative logarithm of the likelihood function converts the maximization of the likelihood function to the minimization of the sum of squared measurement errors, i.e., maximum likelihood method is converted to least squares method if the likelihood function is a normal distribution function. Therefore, Eq. 2-65 can be rewritten as (Britt and Luecke, 1973; and Ramamurthi et al. 1993):

$$\underset{\mathbf{x},\,\boldsymbol{\theta}}{\textit{Minimize}}: \quad (\mathbf{y} - \mathbf{x})^T \boldsymbol{\Sigma}^{-1}(\mathbf{y} - \mathbf{x}) = \mathbf{e}^T \boldsymbol{\Sigma}^{-1} \mathbf{e} \tag{2-66}$$

$$\textit{Subject to}: \quad \mathbf{f}(\mathbf{x}, \boldsymbol{\theta}) = 0$$

The values for both the parameters and reconciled process variables are obtained simultaneously by solving the optimization problem of Eq. 2-65 or 2-66. This is a simultaneous data reconciliation and parameter estimation optimization problem.

Britt and Luecke (1973) described the use of Lagrange multiplier method to solve the optimization problem of Eq. 2-66. The constraints are implicit nonlinear equation, and there is no analytical solution for Eq. 2-66. The authors developed an iterative linearization technique to solve this nonlinear problem. They linearized the nonlinear constraints using Taylor expansion at the point that was the solution of the last linearization, then iteratively searched for the optimal

solution. They reported difficulties in converging to the optimum in some test problems. They concluded that their algorithm provided a feasible approach to the general parameter estimation problems.

The methodology of parameter estimation proposed by Deming (1943) and Britt and Luecke (1973) is the basic structure of parameter estimation in on-line optimization. The improvement over this structure is to provide a better distribution function that more accurately describes the error structure of measurements and better optimization algorithms to solve the problem, such as the generized reduced gradient or successive quadratic programming.

MacDonald and Howat (1988) reported the results of two procedures for parameter estimation. One is a statistically rigorous simultaneous data reconciliation and parameter estimation, and it simultaneously reconciled the data to satisfy the constraints and estimate the process parameters. The other is a faster, non-rigorous sequential procedure. It first reconciled data to satisfy the material and energy balances and then estimates the process parameters. The authors applied these two procedures to estimate the tray efficiency of a flash unit. It was concluded that the simultaneous procedure gave a better estimation. The sequential procedure was computationally faster.

Kim, Liebman and Edgar (1990) used a two-stage and a nested nonlinear algorithm which decoupled parameter estimation and data reconciliation to reduce the problem size. The two-stage method solved two NLP sub-problem iteratively, and the nested method

nested reconciliation problem into parameter estimation problem. Both of these two methods used NLP to overcome the drawbacks of successive linearization solution. When these methods were compared with the simultaneous algorithm and successive linear algorithm, they found that the two-stage algorithm succeeded in finding optimal parameter estimates for all test problems in an efficient manner while other methods failed on one or more of the problems.

Ramamurthi, et. al. (1993) proposed a successively linearized horizon-based strategy for the estimation of parameter and dynamic data reconciliation. They also proposed a two-level strategy to decouple the estimation of process input from the estimation of the process outputs and parameters. The new algorithm resulted in a significant reduction in computational time compared with NLP based methods. The proposed algorithm demonstrated effective and efficient performance for both open-loop and closed loop applications on a continuous stirred tank reactor (CSTR).

The profiling method, which is a technique based on the signed-squared root of likelihood function, was proposed by Albuquerque, et al. (1997) for error-in-variable measurement problems. This method produces

improved confidence interval on the estimated parameters. The authors adopt a Bayesian approach and apply Laplace's method to integrate out the incidental parameters (or control input variables). The authors concluded that estimation of and nonlinear inference about process parameters can be obtained fairly inexpensively by applying profiling and Laplace's approximation. Also, this approach leads to an efficient and effective analysis tool for process modeling, data reconciliation, and on-line optimization.

In summary, the errors-in-variables model represents the general case of chemical plant models used for simultaneous data reconciliation and parameter estimation in on-line optimization. The least squares method has been used for the simultaneous data reconciliation and parameter estimations. Most of reported applications assumed that measurement errors are normally distributed and they used the least squares method to conduct the simultaneous data reconciliation and parameter estimation. Other methods, such as contaminated Gaussian distribution and robust functions, are considered as potential methods for plant parameter estimation. They will be used to conduct simultaneous data reconciliation and parameter estimation in this research.

For on-line optimization using errors-in-variables model, parameter estimation is conducted with data reconciliation simultaneously. In order to reduce the optimization size and improve the convergency and efficiency of solutions, some decomposed strategies have been proposed to solve the simultaneous parameter estimation and data reconciliation optimization problems when the scale of models is large and highly nonlinear.

B-6. Economic Model

The economic model represents the net profit from plant operations which is to be maximized along with satisfying the material and energy balances for the plant and meeting the demand for product with the available raw materials. The net profit is the difference between the sale of products and by-products and the total production cost which includes manufacturing costs and general expenses. The manufacturing costs include direct production costs, fixed charges and plant overhead costs, administrative expenses and distribution and marketing expenses. Included in direct production costs are raw materials, labor, power, utilities, maintenance, laboratory charges, and royalties, among others. Fixed charges include depreciation, taxes, insurance and financing. Plant overhead costs include safety, general plant and payroll overhead, control laboratories and storage. Administrative expenses include executives salaries, clerical wages, engineering and legal costs and communications. Distribution and marketing expenses include sales expenses, shipping advertising and technical sales services. Also included in total product costs are research and development and gross-earnings expenses (Peter and Timmerhaus, 1991).

To develop the mathematical expression for the economic model, the sale prices are obtained as projections from the marketing department as a function of plant production rate, availability of product from competitors and time, among others. Manufacturing costs are estimated from historical data, and depend on the condition, severity of operation, and time between turn-around, in addition to other factors. General expenses are usually treated as fixed on an annual basis, for convenience.

In summary, standard methods can be used to develop the economic model with the appropriate data available. Thus depending on the need, the economic model can be very elaborate or a simple value-added equation. Economic optimization in on-line optimization is to determine the optimal operation condition for the plant. This optimization generates the optimal set points for controllers in the distributed control system.

B-7. Plant Model

A precise and robust plant model is essential for on-line optimization. It serves as the constraints for gross error detection, data reconciliation, parameter estimation and economic optimization. Therefore, a plant model must be established and validated before using it for on-line optimization. The plant model is written based on conservation laws, kinetic and thermodynamic models, and any other engineering knowledge. It is generally expected that rigorous models based on fundamentals would represent the plant better than a simple one based on empirical results. However, a rigorous model may have the disadvantage of requiring significantly longer computation time. On the other hand, a simple model may not provide an

accurate enough representation of the plant behavior and the optimization based on this type of model may result in non-optimal or physically infeasible set points (Krishnan et al, 1992).

Open Form Equation Based Versus Close Form Modular Process Model: Chemical and refinery processes can be simulated as different formats of simulation models. One is called open form equation based process model; the other is the traditional closed form sequential modular model. The open form models are written as a set of algebraic and/or differential equations, such as,

$$f_i\left(\frac{dx}{dt}, x, t\right) = 0, \; i = 1, 2, \ldots, m \qquad (2\text{-}67)$$

for dynamic processes or $f(\mathbf{x}) = 0$ for steady state processes. In Eq. 2-67, all of the variables are determined by a simultaneous solution of the equations. For example, the energy balance equations for a heat exchanger can be written as:

heat balance on cold side: $Q - F_c C_{pc} (T_{c2} - T_{c1}) = 0$ (2-68)
heat balance on hot side: $Q - F_h C_{ph} (T_{h1} - T_{h2}) = 0$
heat transferred: $Q - UA[((T_{h1}-T_{c2}) - (T_{h2} - T_{c1}))/\ln((T_{h1} - T_{c2})/(T_{h2} - T_{c1}))] = 0$

These three equations can simultaneously determine any three unknown variables (e.g., T_{c2}, T_{h2} and Q)in the equations using a simultaneous solution method. The optimization problems with open form models can be solved simultaneously and efficiently by optimization modeling packages, such as GAMS or AMPL, which have a number of solvers built-in.

The closed form plant model follows traditional design methods, using the information at input streams of a unit to determine the values of the output variables. The changes at an up-stream location can affect variables at down-stream locations, but the changes at a down-stream

location can not affect the determination of process variables at up-stream locations. The solution for this type of model is sequential. Therefore, optimization problems with closed form models can only be solved with iterative methods to search for the optimal solution. This requires nested convergence schemes for unit operations within flowsheets. This can be seen by the simulation for the determination of the output temperatures T_{c2} and T_{h2} and heat transferred Q for a heat exchanger. The energy balance equations for a heat exchanger are:

heat balance on cold side: $Q = F_c C_{pc} (T_{c2} - T_{c1})$ (2-69)
heat balance on hot side: $Q = F_h C_{ph} (T_{h1} - T_{h2})$
heat transferred: $Q = UA [((T_{h1} - T_{c2}) - (T_{h2} - T_{c1}))/ \ln((T_{h1} - T_{c2}) / (T_{h2} - T_{c1}))]$

To determine T_{c2}, T_{h2} and Q, the sequential flowsheet simulation package (closed form sequential modular) requires coding a convergence scheme to solve these equations iteratively for T_{c2}, T_{h2} and Q (Fatora and Ayala, 1992). The reason is that logarithm mean temperature difference is highly nonlinear and these three variables can not be explicitly determined by other known variables. These complex convergence schemes lack robustness in the presence of changing real time process data, and they consume excessive amounts of computer time.

There has been a debate about the use of open form equation based process models versus traditional closed form sequential modular models for on-line optimization since the mid 1980's (Hardin, et al., 1995). The debate centered around the relative speed of the open form solution versus the relative robustness of closed form model development. The open form plant model has a great advantage in terms of computation efficiency and robust solvers, and this is not available for the closed form plant models. The difficulty in developing open form plant models will be solved by the development of process modeling software that creates a model

development environment similar to sequential modeling. The process modeling software will automatically translate the graphic input information from users to an equation-based model with graphical, object-oriented environments for configurating, executing and maintaining the on-line optimization applications. Also, the open form plant models are easily modified to account for process changes since the convergence scheme is separated from the process model. Eventually, the use of open form models becomes the accepted state of art (Hardin, et al., 1995). However, the discontinuity in the constraints of process models, e.g., the thermodynamic properties are expressed by different regression functions for different ranges, still challenges researchers in solving optimization problems with open form process models.

Plant optimization with closed form process models can be solved by process flowsheeting programs. Process flowsheeting programs were designed to relieve the burden deriving process models and writing computer programs. They use a simulation language which connects unit modules. Flowsheeting programs available now are large, elaborate and can be used for complicated design problems. They use well-established numerical methods to solve process model equations which include rigorous unit operation model and sophisticated thermodynamic model equations. Also, they can contain detailed costing programs and a built-in optimization algorithm for optimal design. These programs run on PC's, workstations, and mainframes. There are several the commercial codes such as ASPEN, DESIGN II, PRO II and HYSIM that are widely used in chemical process industries.

The optimization problems with open form equation based process model can be solved by optimization-modeling languages such as GAMS (General Algebraic Modeling System) and

AMPL (A Modeling Language for Mathematical Programming). GAMS and AMPL were developed to make the formulation and solution of large scale mathematical programming problems more straightforward and comprehensible to the users. GAMS has been used successfully with large economic models of industrial sectors by the World Bank (Brook, Kendrick, and Meeraus, 1988), and AMPL was developed AT&T Bell Laboratories for telecommunication applications (Fourrer, Gay, and Kernigan, 1993). However, applications to chemical plants have been limited and confined to relatively small problems. They are equation based programming languages, and the programs are similar to the mathematical formulation of process models. Also, a number of solvers for solving linear, nonlinear, and mixed integer linear/nonlinear optimization problems are provided as options for users to choose. A disadvantage is that detail unit modules of processes (process constraint equations) are not available and must be provided by users.

In summary, both open form equation based and close form sequential modular process models have been used for simulating and optimizing processes. Flowsheeting simulation programs can develop close form sequential models for users to simulate and optimize a process. However, there is no process modeling software available for developing the open form process model. An open form model must be developed by users writing in a mathematical programming language, and this model can be solved by optimization modeling packages. Flowsheeting programs offer a quick and efficient way to develop plant simulations, but require significant amounts of computer time. The optimization modeling languages require the same effort as required to develop the individual process models in Fortran without having to incorporate

optimization algorithms. Optimization modeling languages are able to simultaneously and efficiently solve the optimization problem. They require much less computation time and provide more reliable solution.

Steady State Model Versus Dynamic Model: A chemical process can be simulated by either a steady state or dynamic model. Chemical plants operate at steady state with transient periods that are relatively short compared to steady state operations. A steady-state representation of a process is generally used for continuous operations in chemical plants and petroleum refineries. Steady state models are used to simulate the plants in on-line optimization applications. However, during the starting up of a continuing process or for a batch process, it is necessary to use the dynamic models to simulate the process.

The steady state process models are represented by a set of algebraic equations. The equations do not vary with time. The algebraic equations in steady state models are established based on conservation laws and other engineering knowledge. Dynamic process models are represented by a set of ordinary differential equations that describe dependency of process variables on time. The differential equations in dynamic models are based on conservation laws, i.e., the accumulation of mass, momentum, and energy, which is the time varying term, is equal to the input plus generation minus the output of the mass, momentum, and energy (Albuquerque and Biegler, 1995; and Robertson and Lee, 1996). Usually, each differential equation in the dynamic model is discretized to obtain a set of algebraic equations with an appropriate time step. Albuquerque and Biegler (1995) proposed to discretize the differential equations using standard Implicit Runge-Kutta method (IRK).

Observability and Redundancy: A process model used as constraints for data reconciliation of on-line optimization must satisfy the observability in unmeasured variables and redundancy in measured variables (measurements). The observability in unmeasured variables ensures the unique solution for unmeasured variables from data reconciliation. The redundancy in measured variables (measurements) is necessary for reconciling process data and rectifying measurement errors. Observability is defined by Crowe (1989) as:

> "An unmeasured quantity at steady state is observable if and only if it can be uniquely determined from a fixed set of values, corresponding to the measured variables, which are consistent with all of the given constraints. Any unmeasured quantity which is not so determinable is unobservable."

And redundancy is defined by Crowe (1989) as:

> "A measured quantity is redundant if and only if it would be observable if that quantity was not measured. Otherwise, the measured quantity is non-redundant."

Kretsovalis and Mah (1988) and Crowe (1989) has given detail review on the methodology for classifying the observability of unmeasured variables and the redundancy of the measured variables for steady state process models. For a single component process network (mass balance only), a simple graph-theorety procedure has been derived for observability and redundancy examination by Mah, et al., (1976). A more general treatment using projection matrices was developed by Crowe, et al., (1983) for a network with linear constraints. For single component mass and energy networks (mass and energy balances) without chemical reactions, a examination method has been developed by Stanley and Mah (1981). For

multicomponent networks, Kretsovalis and Mah (1987) presented two new examination algorithms which made use of graph-theorety properties and the solvability of subsets of constraint equations. These algorithms do not require that the stream compositions be either measured with respect to all components or not measured at all. However, the reactions and energy balances are not considered in these algorithms. To have a more general framework for identifying the observability of unmeasured variables and redundancy of measured variables, Kretsovalis and Mah (1988) presented a treatment for a general process network, allowing for overall and component mass balance, energy balances, reactions, heat exchanges and stream splitting. This method uses the graph-theoretic properties and solvability similar to their previous work.

For a process model that includes a numbers of linear algebraic equations, $\mathbf{f}(\mathbf{x}, \mathbf{z}) = 0$, it is rearranged as following for examining the observability and redundancy:

$$\mathbf{Ax} + \mathbf{Bz} = 0 \tag{2-70}$$

where **A** and **B** are the coefficient matrices corresponding to measured variables **x** and unmeasured variables **z** in linear constraints. In Eq. 2-70, the measured variables are considered as known variables (constants) using the measurements as their values. Then, Eq. 2-70 is rearranged as:

$$\mathbf{Bz} = \mathbf{-Ax} = \mathbf{S} \tag{2-71}$$

where **Ax** in the right hand side is a constant vector **S**. If equations **Bz** = **S** have a unique solution for variables **z**, then the plant model satisfies the observability on unmeasured variables.

Otherwise, the values of the unmeasured process variables determined from the constraints in the plant model have no meaning.

Crowe (1989) presented a direct method for identifying the observability of unmeasured variables and the redundancy of measured variables for linear mass balances with chemical reactions. To examine the observability and redundancy of a linear plant model, the linear constraints are rearranged as Eq. 2-71. According to the definition of the observability given by Crowe, the following lemma provides the test for classifying the observability of unmeasured variables.

Lemma (Crowe, 1989):If there exists a nonzero vector **t** such that **Bt** = 0, then each unmeasured variables corresponding to a nonzero element of **t** is unobservable.

Proof of lemma: Suppose there is a solution **z** = **z**1 that satisfies equations in Eq. 2-71, i.e., **Bz**1 = **S**. If **t** ≠ 0 and if **Bt** = 0, then the vector (**z**1 + ν**t**) also satisfies those equations in Eq. 2-71 for any scalar ν, i.e.,

$$\mathbf{B}(\mathbf{z}1 + \nu\mathbf{t}) = \mathbf{B}\mathbf{z}1 + \nu\mathbf{B}\mathbf{t} = \mathbf{S}, \text{ where } \mathbf{B}\mathbf{z}1 = \mathbf{S} \text{ and } \mathbf{B}\mathbf{t} = 0 \qquad (2\text{-}72)$$

This means that these equations have multiple solutions **z** = **z**1 + ν**t** where ν is an arbitrate scalar with any value. Therefore, the equations do not have a unique solution for unmeasured variables **z** and each variable corresponding to a nonzero element of **t** is unobservable.

Krishnan, et al., (1992 and 1993) proposed a structural analysis method to examine the observability of unmeasured variables by checking the rank of the structural parameter observability matrix. They proposed a structural analysis method to examine the required

measurements for estimation. For a steady-state linearized system, the constraint equations is rearranged as:

$$\mathbf{Ax} + \mathbf{Bu} + \mathbf{E\theta} = 0 \tag{2-73}$$

where **A**, **B** and **E** are matrices corresponding to the state variables **x**, input variables **u**, and parameters **θ** respectively. Input variables **u** are the variables in the input streams of a unit. State variables are the variables in Eq. 2-73 excluding input variables **u** and parameters **θ**. Also, measured variables **y** are expressed as linear functions of state variables of system, i.e.,

$$\mathbf{y} = \mathbf{Cx} \tag{2-74}$$

Two steps are required to determine the observability of parameters in a process model. First, the measurements in the model must be examined to determine if they are accessible to the parameters. A measurement is said to be accessible to a parameter if it contains some information about the parameter, that is, if changes in the parameter are the cause of changes in the measurement (Krishnan, et al., 1992). If a measurement is not accessible to the parameter, it can be excluded from the set of necessary measurements. In the examination of accessibility, input variables **u** are considered as unknown parameters for all of the units except the first unit in the plant flowsheet and the output variables are considered as measured variables for all of the units except the last unit. The necessary measurements for entire plant are examined unit by unit through an extended structural matrix S_{mod} for each unit. The extended structural matrix S_{mod} is defined as:

$$S_{mod} \quad \begin{bmatrix} A & E & B \\ C & 0 & 0 \end{bmatrix}^T \tag{2-75}$$

where **A, B, E** and **C** are the same matrices as defined in Eq. 2-73 and 2-74.

The second step is to test the observability of parameter using the structural parameter observability matrix $S_{pob.}$ The structural parameter observability matrix is defined as:

$$S_{pob} \begin{bmatrix} A & E \\ C & 0 \end{bmatrix}^T \qquad (2\text{-}76)$$

where the matrices **A**, **E**, and **C** have the same meaning as in Eq. 2-73 and 2-74. A system is said to be structurally parameter observable, if and only if, its measurements are accessible to all the parameters and the structural parameter observability matrix S_{pob} has full generic rank (Krishnan et al., 1992). A structural matrix is said to have generic rank if a unique column variable can be associated with each row. The detail methodology of this structural analysis is discussed in Krishnan et al.'s paper (1992). The determination of generic rank of the structural matrix is referenced on Johnston et al.'s (1984) algorithm. The method proposed to determine the observability of parameters in a process model will be incorporated in this research for developing the process model of the sulfuric acid plant.

In summary, observability of unmeasured variables and parameters is necessary for having a unique solution of these unmeasured variables and parameters from data reconciliation. Having some degree of redundancy in process measurements is necessary for rectifying the measurement errors. Several methods have been proposed to examine the observability and redundancy for steady state process models. However, these methods are limited to certain type of simple linear process model and are not general enough for implementation. Also, there are no reports in literature on how many degrees of redundancy in measured variables are required to have an accurate data reconciliation result. Based on the methods proposed by Crowe

(1989) and Krishnan, et al., (1992 and 1993), a general method to examined the observability and redundancy of a plant model will be proposed and used to formulate the simulation model of the sulfuric acid process.

Summary: A precise and robust plant simulation is necessary to describe the processes for on-line optimization. It gives the relationship among the process variables and serve as constraints for the optimization problems. The plant models can be written as either open form equation based or close form sequential modular. The close form plant model has been used in process design and optimization for many years, and it is easily developed with flowsheeting programs. However, the computation for solving a optimization problem with this type of models is time consuming. The optimization problem with an open form equation based plant model can be solved simultaneously and efficiently by current optimization programs. However, the development and modification of the open form models is not as straight forward as one of closed form. It requires the user to provide the detail information about the constraint equations. Simulation software is being developed, and this will provide a process model development environment similar to the ones available now for sequential modeling to automatically translate the graphic input information to an equation based model, e.g., Aspen Tech's RT-OPT and Simulation Science's ROMEO. Open form equation based models are required for on-line optimization.

A chemical process can be simulated by either steady state or dynamic models. Chemical plants usually operate for extended period at steady state with transient periods that are

relatively short compared to steady state operations. Therefore, the steady state process models can be used for on-line optimization.

The plant model for on-line optimization must satisfies the requirement of observability to ensure that the model has unique solution and redundancy to provide resolution for error rectification. Methods for examining the observability and redundancy has been proposed by several authors for steady state models. However, they are limited to the simple linear plant model and not general enough for implementation.

B-8. Steady State Detection and Data Exchange

Steady State Detection: As shown in Figure 1.4, it is necessary to make sure the process is operating at steady state before the plant data is taken from distributed control system for conducting on-line optimization. Steady state plant data is required for steady state process models.

The time series horizontal screening method has been used in industry to detect the steady state. In this method, the measured values for key process variables are observed for a time period. If the measured values remain in a stable range with tolerant random noises, then the process is said operating at steady state.

Data Exchange: An important step between DCS and on-line optimization is data exchange. Before conducting on-line optimization, the plant data is retrieved from distributed control system and input into on-line optimization system by a coordinator program. The general practice in managing data in a distributed control system is with a data historian program. Data from this database can be extracted and used in a spreadsheet program for example. A

coordinator program is used to extract the sampled data that is required by on-line optimization system and to generate a data file in a format required by on-line optimization system. Then this data file will be used by the optimization programs for gross error detection, data reconciliation, and parameter estimation.

As shown in Figure 1.4, after on-line optimization executes economic optimization and generate a set of optimal set point, the coordinator program will generate a report file which includes the optimal set points. These optimal set points can be sent directly to distributed control system or they can be viewed by operators for the use of DCS.

B-9. Optimization Algorithms

There is general agreement in the literature (Pike, 1986 and Biegler, 1992) that the three best optimization algorithms for solving nonlinear programming problems are successive linear programming, successive quadratic programming and the generalized reduced gradient methods. Successive linear programming linearlizes the objective function and constraints around a feasible starting point and solves a sequence of linear programming problems to arrive at a local optimum. Successive quadratic programming uses a quadratic approximation to the objective function and a linear approximation to the constraints and solves a sequence of quadratic programming problems to arrive at a local optimum. Quadratic programming uses the Kuhn-Tucker conditions to convert the quadratic programming problem to a set of linear equations which can be solved by linear programming. Thus, successive quadratic programming solves a sequence of linear programming problems. To avoid evaluating the Hessian matrix of second partial derivatives of the objective function, a quasi-Newton update formula such as BFGS is used which only requires

gradient values. The generalized reduced gradient also linearlizes the objective function and constraint equations about a starting point, and it manipulates these equations to form a reduced gradient line to provide a direction to perform a series of line searches to arrive at a local optimum. All of the methods use the same information, values of the first partial derivatives of the objective function and constraints; but each use this information in a different way (Pike, 1986).

Biegler (1992) discussed embellishments for these algorithms and their further applications in data validation and parameter estimation which are nonlinear programming problems. He exploited the structure of process optimization problems to propose general decomposition method to deal with large, nonlinear models with few degrees of freedom, and tailored quasi-Newton strategy for least-square structure of the optimization problem, and more. These extensions of the successive quadratic programming (SQP) algorithms yield more reliable and efficient performance than the general purpose SQP algorithm.

GAMS (General Algebraic Modeling System) was developed at the World Bank to solve large and complex mathematical programming models and uses a programming language that makes concise algebraic statements of the models that is easily read by both the modeler and the computer (Brook et al., 1988). This was done to expand the application of mathematical programming in policy analysis and decision making. GAMS includes a number of mathematic programming solvers for linear programming (LP), mixed integer linear programming (MILP), nonlinear programming (NLP), discontinuous nonlinear programming (DNLP), and mixed integer non-linear programming (MINLP). Its NLP solvers have been tested in a wide variety of

problems and have been proven to be robust and reliable. They are well suited for the nonlinear programming problem for data reconciliation.

GAMS includes a number of important and widely used nonlinear programming codes such as MINOS, NPSOL and CONOPT. MINOS, developed at Stanford University, implements generalized reduced gradient method which is more effective for problems with constraint equations that have sparse matrices. NPSOL, also developed at Stanford University, uses successive quadratic programming and is more effective for problems with constraint equations that give dense matrices. CONOPT, developed by Drud (1985,1992), uses the general reduced gradient algorithm and is well suited for models with very nonlinear constraints and models with very few degree of freedom. These codes were developed to facilitate the formulation and solution of the optimization problem.

The modeling language AMPL (A Modeling Language for Mathematical Programming) appeared in 1993 and was developed at AT & T Laboratory for communication applications (Fourer, et al., 1993). AMPL has language structure similar to GAMS. In addition, it has separate model and data files and can function interactively. AMPL includes the solver MINOS, XA, and OSL with other to be available.

In summary, GAMS and AMPL offer attractive new tools for solving nonlinear programming problems. They map the mathematical optimization problems to the rigorous programs required by optimization solvers and provide flexibility in writing source codes for process models. Therefore, the user does not have to write the process and economic models

in a higher level language like Fortran and link to a solver like MINOS. They release the users from the work of programming.

B-10. Variance and Covariance Matrix Estimation

As described in the sections on gross error detection, data reconciliation, and parameter estimation previously, all algorithms require information for the variance and covariance of measurement errors to scale the errors. The most commonly used statistical technique for covariance matrix estimation is the direct method, i.e., the variance/covariance is determined by:

$$\sigma_{ij}^2 \quad covar(y_i, y_j) \quad \frac{1}{n\ 1}\sum_{k\,1}^{n}(y_{ik} y_i)(y_{jk} y_j) \tag{2-77}$$

with the mean determined by:

$$y_i \quad \frac{1}{n}\sum_{k\,1}^{n} y_{ik} \tag{2-78}$$

where n is the number of samples. The covariance matrix of measurement errors is $\mathbf{\Sigma} = [\sigma_{ij}^2]$. The covariance matrix of constraint residuals **H** is determined by Eq. 2-14 for linear constraints as discussed previously, i.e.,

$$\mathbf{H} = \mathbf{A}\,\mathbf{\Sigma}\,\mathbf{A}^T \tag{2-14}$$

Eq. 2-77 and 2-78 represent the unbiased maximum likelihood estimators for variances and means if the sample data is independent of each other and no gross errors are present in the samples. This method requires the n samples must be taken from the same steady state point of the process, otherwise the direct method may give incorrect estimates. Also, the presence of gross error in sampled data violates the statistical basis that only random errors are present.

Almasy and Mah (1984) and Keller, et al., (1992) made use of the covariance matrix of the constraint residuals to eliminate the dependency between sample data (or the influence of unsteady state behavior of the process during sampling period) through an indirect method. The indirect method estimates the variance of measurement errors by minimizing the sum of the squared differences between the variances **H** of constraint residuals calculated directly from sampled data and the estimated constraint residual variances $\mathbf{A\Sigma^*A}^T$, i.e.,

$$\text{Minimize:} \qquad (\mathbf{H} - \mathbf{A\Sigma^*A}^T)^T(\mathbf{H} - \mathbf{A\Sigma^*A}^T) \tag{2-79}$$

where the variances of constraint residual **H** are determined by Eq 2-14 using the direct method in Eq. 2-77 to determine $\mathbf{\Sigma}$. Minimizing Eq. 2-79 estimates the variances and covariances of measurement errors, $\mathbf{\Sigma^*}$.

The authors compared simulation results, and they suggested that this indirect method for variance-covariance estimation should be used in practical applications. This indirect method can reduce the influence of unsteady state behavior of the process on the estimation. However, this method is still sensitive to the presence of gross errors in the sample data. Consequently, a few outlying sample data will cause an incorrect estimation of the covariance matrix, and it is not robust. Also, this method is only applicable to process models with linear constraints.

Chen, et al., (1997) proposed a robust indirect method to estimate the variance-covariance matrix based on an M-estimator proposed by Huber (1964). The basic idea of M-estimator is to assign weights to each sample data vector based on its own Mahalanobis distance so that the influence of a given point decreases as it becomes less and less characteristic. This approach uses an iterative method to calculate the variance and covariance matrix of constraint

residuals. After the variance and covariance matrix of constraint residuals is determined, it uses the indirect method to estimate the variance and covariance matrix of measurement errors. This algorithm is described as follows.

Consider a n dimensional process sample data vector at a time k $\mathbf{y}_k$:

$$\mathbf{y}_k = \mathbf{x}_k + \mathbf{e}_k \tag{2-80}$$

where $\mathbf{y}_k = \{y_{k1}, y_{k2}, ..., y_{kn})$, for k = 1, 2, ..., s standing for repeated sample data. $\mathbf{x}_k$ is the process variables at time k and $\mathbf{e}_k$ is the vector of measurement errors at time k. Process variables $\mathbf{x}_k$ satisfies constraints in the process model, i.e.,

$$\mathbf{A}\mathbf{x}_k = 0 \tag{2-81}$$

where **A** is the coefficient matrix of constraints in the process model. The constraint residual $\mathbf{r}_k$ is determined by:

$$\mathbf{r}_k = \mathbf{A}\mathbf{y}_k = \mathbf{A}\mathbf{x}_k + \mathbf{A}\mathbf{e}_k = \mathbf{A}\mathbf{e}_k \tag{2-82}$$

Assuming that $\mathbf{e}_k$ is normally distributed with zero mean and positive definite covariance matrix $\mathbf{\Sigma}$ as discussed in gross error detection section, the mean vector and covariance matrix of constraint residuals are:

$$E(\mathbf{r}_k) = E(\mathbf{A}\mathbf{e}_k) = \mathbf{A}E(\mathbf{e}_k) = 0 \tag{2-83}$$

and $$\mathbf{H} = \text{cov}(\mathbf{r}_k) = E(\mathbf{r}_k\, \mathbf{r}_k^T) = E(\mathbf{A}\, \mathbf{e}_k\mathbf{e}_k^T\mathbf{A}^T) = \mathbf{A}E(\mathbf{e}_k\mathbf{e}_k^T)\mathbf{A}^T = \mathbf{A}\mathbf{\Sigma}\mathbf{A}^T \tag{2-84}$$

where $\mathbf{H} = (h_{ij})_{m\times m}$, i = 1, 2, ..., m and j = 1, 2, ..., m. Using the Kronecker product of matrices and *vec*(*o*) operator (Almasy and Mah, 1984), the covariance matrix **H** can be rewritten as:

$$vec(\mathbf{H}) = (\mathbf{A}\otimes\mathbf{A})vec(\mathbf{\Sigma}) \tag{2-85}$$

The indirect method uses Eq. 2-85 to estimate covariance matrix of measurement errors **Σ**. This procedure requires the value of the covariance matrix **H** which can be calculated from the residuals using the balance equations.

The procedure of the robust covariance estimation is described in following:

Step 1 Calculate the residuals **r** by:

$$\mathbf{r}_k = \mathbf{A}\mathbf{y}_k, \text{ for } k = 1, 2, ..., s \tag{2-86}$$

where, $\mathbf{r}_k = [r_{k1}, r_{k2}, ..., r_{km}]^T$. s is the number of sample data sets and m is the dimension (number) of constraint residuals.

Step 2 Calculate the weight functions u1 and u2 for each data set by:

$$u1(d) \begin{cases} 1 & d < k \\ k/d & d \geq k \end{cases} \tag{2-87}$$

and $$u2(d) = [u1(d)]^2 / 6 \tag{2-88}$$

where $$6 = G(k^2/2, 1.5) + 2k^2 [1-\phi(k)] \tag{2-89}$$

In Eq. 2-89, $\phi(k)$ is a multivariate normal cumulative distribution; and G(x,f) is a Gamma distribution with f degree of freedom. In Eq. 2-87, k is a constant specified by the user to take into account of the loss in efficiency to Gaussian distribution for the exchange of resistance to gross errors. d_k is the Mahalanobis distance for a sample data set from the current estimate of mean (location) **m*** and it is determined by:

$$d_k^2 = (\mathbf{r}_k - \mathbf{m}^*)^T \mathbf{H}^{*-1} (\mathbf{r}_k - \mathbf{m}^*) \tag{2-90}$$

where **H*** is the current estimate of the covariance matrix, and **m*** is the current estimate of mean. Both **H*** and **m*** are initialized by:

$$\mathbf{m}^* = \underset{k}{\text{median}}\,(r_{kj});\ k = 1, 2, ..., s;\ j = 1, 2, ..., m. \tag{2-91}$$

and $$\mathbf{H}^* = \text{diag}(t_1^2, t_2^2, ..., t_m^2) \tag{2-92}$$

where $$t_j = \underset{k}{\text{median}}\,(|r_{kj} - m_j|)/0.6745 \tag{2-93}$$

After weight factors for each set of data are determined, mean **m** and variance/ covariance matrix **H** are updated by the following functions:

$$\mathbf{m} \quad \mathbf{m} \quad \frac{\sum_i u1(d_i)(r_i \ \mathbf{m})}{\sum_i u1(d_i)} \tag{2-94}$$

and $$\mathbf{H} \quad \frac{1}{n}\sum_i u2(d_i^2)(r_i \ \mathbf{m})(r_i \ \mathbf{m})^T \tag{2-95}$$

After the means **m** and covariances **H** are updated, the new weight factors u1 and u2 are calculated based on the current values of **m** and **H**. Then the means and variances are calculated by Eq. 2-94 and 2-95 using the new weight factors. This iterative process continues until the maximum difference of elements of **H** between two successive iterations are smaller than a pre-specified threshold value (authors use 10^{-6} as the threshold value).

Step 3 Calculate the maximum likelihood estimator of $vec(\mathbf{\Sigma})$ by

$$vec(\mathbf{\Sigma}) = (\mathbf{G}^T\mathbf{G})^{-1}\mathbf{G}^T vec(\mathbf{H}) \tag{2-96}$$

where $vec(\mathbf{H}) = (h_{11}, h_{12}, ..., h_{1m}, h_{21}, h_{22}, .., h_{2m}, ..., h_{m1}, h_{m2}, ..., h_{mm})^T$ is determined from Step 2. The matrix **G** is determined by the coefficient matrix of linear constraints, i.e.,

$$G \begin{bmatrix} a_{11}A_1 & a_{12}A_2 & \cdots & a_{1i}A_i & a_{1q}A_q & \cdots & a_{1k}A_k \\ a_{21}A_1 & a_{22}A_2 & \cdots & a_{2i}A_i & a_{2q}A_q & \cdots & a_{2k}A_k \\ & & & & \cdots\cdots & & \\ a_{m1}A_1 & a_{m2}A_2 & \cdots & a_{mi}A_i & a_{mq}A_q & \cdots & a_{mk}A_k \end{bmatrix} \qquad (2\text{-}97)$$

where a_{ij} is the elements of coefficient matrix **A** and $\mathbf{A}_j$ is the jth column of matrix **A**, i.e., $\mathbf{A} = (\mathbf{A}_1, \mathbf{A}_2, ..., \mathbf{A}_d)$. Then the robust covariance $\boldsymbol{\Sigma}$ can be obtained by reshaping $vec(\boldsymbol{\Sigma})$ as following:

$$\boldsymbol{\Sigma} = vec^{-1}(vec(\boldsymbol{\Sigma})) \qquad (2\text{-}98)$$

where $vec(\boldsymbol{\Sigma}) = (\sigma_{11}^2, \sigma_{12}^2, ..., \sigma_{1m}^2, \sigma_{21}^2, \sigma_{22}^2, ..., \sigma_{2m}^2, ..., \sigma_{m1}^2, \sigma_{m2}^2, ..., \sigma_{mm}^2)$.

Above is the procedure to estimate the variance and covariance matrix of measurement errors using robust indirect method. This method assigns different weight factors to the sampled data according to its distance of the sample data to the current estimate values of means **m***. It eliminates the effect of sample data containing gross errors by a iterative procedure described in Step 2 and determines the covariance matrix of constraint residuals based on the normal (good) sample data. Then, the variance and covariance matrix of measurement errors is determined by the indirect method proposed by Keller, et al., (1992). This robust method is able to eliminate the influence of unsteady state behavior of the process and is insensitive to the sample data containing gross errors. However, this method is still limited to linear process constraints. This method has not been able to apply to on-line optimization applications that have a highly nonlinear and complicated process and a large number of unmeasured variables.

In summary, there are three methods to estimate the variance and covariance matrix of measurement errors for the algorithms required known variance/covariance information. The direct method can give unbiased estimation if the repeated sample data is taken from a steady state process and no gross errors are present in the sample data. This method directly determined the variance/covariance matrix of measurement errors using sample data for measured variables, and it is applicable for any process and easy to compute. However, in the real process operation, the process conditions are continuously undergoing changes. Also, some of sample data may contains gross errors. The indirect method proposed by Keller, et al. (1992), is to overcome the influence of unsteady state behavior of the process. However, this method is still sensitive to the presence of gross errors in the sample data, and its applications are limited to linear constraints with all variables measured. The robust indirect method proposed by Chen, et al. (1997) improves the robustness of indirect method by assigning different weight factors to the sample data set according to the distance of the sample data to the current estimated means to calculate the mean and covariance matrix of constraint residuals. This robust indirect method is not sensitive to the presence of gross errors in sample data and is able to eliminate the influence of unsteady state behavior of the process. However, it still limited to linear constraints with all variables measured as the indirect method.

In addition to the above theoretical approach to determine the variance/covariance matrix, the time series screening methods are used to detect steady state and to filter out outlier in sample data. Although these methods can not detect the persistent gross errors, it is a practical and effective way to detect steady state and to eliminate the instantaneous outlier. For

complicated and highly nonlinear process data, it is proposed to apply the time series screening methods to pre-process sample data, and then the variance/covariance matrix of measurement errors can be determined by direct method using the pre-processed sample data.

C. Dynamic On-Line Optimization

For the dynamic on-line optimization, the methodology is similar to the steady state on-line optimization. The difference between these two approaches is the process model. The steady state process models are represented by a set of algebraic equations. The equations do not vary with time. The algebraic equations in steady state models are established based on conservation laws and other engineering knowledge. Dynamic process models are represented by a set of ordinary differential equations that describe dependency of process variables on time. The differential equations in dynamic models are based on conservation laws, i.e., the accumulation of mass, momentum, and energy, which is the time varying term, is equal to the input plus generation minus the output of the mass, momentum, and energy (Albuquerque and Biegler, 1995; and Robertson and Lee, 1996).

The optimization problem with a dynamic process model is expressed as (Albuquerque and Biegler, 1995) :

$$\begin{aligned} &\text{Maximize:} && P(\mathbf{x}, \mathbf{y}) && (2\text{-}99)\\ &\text{Subject to:} && \mathbf{f}\left(\frac{d\mathbf{x}}{dt}, \mathbf{x}, t\right) = 0 \\ & && \mathbf{x}(t_1) = \mathbf{x}_1 \end{aligned}$$

where $\mathbf{f}$ represent a set of differential and algebraic equations for a dynamic process and $\mathbf{x}(t_1) = \mathbf{x}_1$ is the initial conditions. To solve this optimization problem, the differential equations in the

dynamic model are discretized and converted into a set of algebraic equations with an appropriate time step. Then this optimization problem with discretized algebraic equations can be solved by the optimization language, such as GAMS and AMPL. Albuquerque and Biegler (1995) proposed to discretize the differential equations using standard Implicit Runge-Kutta method (IRK).

Liebman, et al., (1992) described a new method for general nonlinear dynamic data reconciliation that used nonlinear programming techniques to minimize a weighted least-squares objective function in a moving time window. The dynamic process models are usually ordinary differential equations as shown in the constraints of Eq. 2-99 and they are discretized into algebraic equations by collocation techniques. A large sparsity successive quadratic programming (LSSQP) which was well-suited for solving large sparse NLPs was developed to perform optimization over a window width each time. The optimization is repeated until current time is reached. They showed that the method was insensitive to the level of measurement noise when applied to processes operating in strongly nonlinear regions where the Kalman filter approach is not applicable. Also, a procedure was developed to treat the systematic errors in the data. They also indicated that the main disadvantage of the approach was the computational burden for solving the required accurate dynamic process model.

The Dynamic Matrix Control Corporation used rigorous equation-based models and dynamic control technology in their closed-loop real time optimization systems (Culter and Ayala, 1993). The optimization system utilized global spline collocation to solve process differential and algebraic equations (DAE) simultaneously using a tailored successive quadratic programming

methods. Both on-line and plant laboratory measurements are used to update the model parameters. This system was applied in GE Plastics's two Bisphenol-A plants (Lowery, et al., 1993). This system resulted in a two percent increase in production and improved product quality with higher product yield.

D. Summary of the Status of On-Line Optimization

On-line optimization involves several steps. They are combined gross error detection and data reconciliation to eliminate or rectify gross errors in plant data, simultaneous data reconciliation and parameter estimation to updated plant model to ensure that model matches the plant operations, and economic optimization to generate a set of optimal setpoints for the distributed control system.

Gross errors can be detected by time series screening methods or statistical methods. Time series screening methods are simple and have been practiced in industrial applications. However, they can not detect persistent gross errors such as instrument bias or malfunctioning and process leaks. Statistical methods are more complicated and require a detailed plant model to relate the individual measurements. Persistent gross errors can be rectified using other good measurements through statistical methods and the process model. It has been proved that the statistical approach is an effective way to detect the gross errors in plant data.

Statistical methods have been widely studied. However, most studies are based on the assumption that measurement errors are normally distributed, and they were applied to a simple small hypothetical process. Only the least squares or measurement test method has been reported to have been applied to real chemical and refinery processes. The normal distribution

used by this method results in biased estimation when gross errors are present. Therefore, developing new effective statistical methods for gross error detection is very important. The contaminated Gaussian distribution and robust functions have been proposed to detect the gross errors. The estimation from these methods are insensitive to the presence of gross errors. Therefore, these methods result in unbiased estimation even thought gross errors are present in measurements.

Chemical processes are complicated, and large portion of process variables are unmeasured, only errors-in-variables models are suitable for describing the chemical processes. Therefore, the methods for conducting gross error detection and parameter estimation, which are applicable to on-line optimization, requires simultaneous data reconciliation.

The least squares, likelihood function, and Bayesian methods have been proposed for traditional parameter estimation, and they can be modified and used for parameter estimation in on-line optimization. The methodology of parameter estimation for large scale on-line optimization applications is still under developed. It is possible to combine gross error detection with parameter estimation if the algorithm used to reconcile process variables and estimate parameters is not sensitive to the presence of gross errors.

The objective of economic optimization in on-line optimization is to generate a set of optimal set points that maximize the plant profit, which can include minimizing pollutant emission and energy consumption, and maximizing product quality. This can be achieved by solving the economic optimization problem which is to optimize the economic model subject to process

model. Depending on the need, the economic model can be very elaborate or a simple value-added equation.

A precise plant model is necessary to simulate the process for on-line optimization. It serves as constraints for data validation and parameter estimation to relate individual measurement together for error rectification and for economic optimization to determine the best operation conditions of the plant. Chemical processes can be simulated by an open form equation based model or a closed form sequential modular model. The open form model has the advantage of computation speed and solution robustness. The close form model can be easily developed using flowsheeting programs. However, solving a optimization problem with a close form model as constraints requires iterative methods to search for optimal solution. It is time consuming and may be difficult to converge. The development of simulation software will provide a convenient graphical user interface environment similar to sequential modular simulation for developing open form equation based models. Open form models are required for simulating processes in on-line optimization. Also, to ensure the results of the research are meaningful to industrial plants, an actual process is required rather than a mathematical simulation of a hypothetical process, e.g. the William-Otto plant (Krishnan, 1992).

Several optimization algorithms, such as SLP, SQP, GRG, have been developed for solving the nonlinear optimization problems with open form models. Each is effective for solving certain type of problems. The SQP and GRG algorithms have been widely used in industrial practice and are accepted as standard algorithms for solving nonlinear optimization problems.

To ease engineers's effort in solving optimization problems, optimization modeling languages, such as GAMS and AMPL, were developed to alleviate many of the difficulties associated with the development and solution of large, complex mathematical programming models and to allow direct formulation and solution on a computer. They have problem formulation in a language similar to the mathematical statement of the optimization problems. Also, there are a number of solvers included in the languages for users to choose, and changing the solver (optimization algorithm) will not require modifications to the program.

Based on the review above, the work will be conducted on this research project will be described as follows. The objective of this project is to investigate the best way to implement on-line optimization. This work involves the development and evaluation of process simulation model for typical chemical plants and the investigation and evaluation of the methodology for on-line optimization. Also, an interactive on-line optimization program will be developed to alleviate the effort of engineers to apply on-line optimization which is based on the results from this research project.

Plant model: An actual plant, the sulfuric acid contact process from IMC Agrico Chemical Company's plant in Convent, Louisiana, is used in this on-line optimization research for comparing the efficiency and accuracy of the algorithms and investigating the best way to implement on-line optimization.

A open form steady state process model will be established based on the previous research by Lowery (1966), Crowe (1971), Doering (1976), Richard (1987), and Zhang (1993), for the sulfuric acid plant. This process incorporates nearly all types of process units

found in chemical plants such as packed bed catalytic chemical reactors, absorption towers and heat exchanger networks, among other.

Through contacts with the Agrico Chemical Company's engineers, actual plant designed data and plant operating data were obtained on the IMC Agrico Chemical Company's Uncle Sam E-train plant in Convent, Louisiana. The data will be used to study the best way to conduct on-line optimization. This plant, designed by Enviro-Chem System Division of Monsanto, began operation in March, 1992. It is automated with the Bailey INFI 90 Distributed Control System (DCS). It converts at least 99.7% raw sulfur feed into acid product and extracts the energy produced in the exothermic reactions in an efficient manner to produce steam as a by-product. It represents the state-of-art contact sulfuric acid technology.

The flow rate and temperature measurements play an important role in controlling and monitoring the process. Also, a rigorous kinetic model is important to describe the reaction rates and conversion of sulfur dioxide to sulfur trioxide. It is necessary to include material and energy balances as well as kinetic model of SO_2 reaction in the sulfuric acid plant model. This results in a nonlinear steady-state plant model.

The work in plant model formulation chapter will include establishing process simulation model for the Monsanto's designed sulfuric acid contact process, evaluating how precise the process model represents the processes, examining the observability and redundancy of the plant

model, and comparing the performance of different types of measurements and constraints on data validation and parameter estimation. Based on the evaluation results, the general rules to formulate the process simulation model will be proposed for better formulating process models.

Combined Gross Error Detection and Data Reconciliation: Based on the complex characteristics of chemical process, i.e., the constraints are highly nonlinear and large portion of process variables are unmeasured, only the statistical methods based on the distribution function of measurement errors are applicable for gross error detection of on-line optimization. These methods include measurement test method, contaminated Gaussian distribution method, and robust function method. The performance of these algorithms will be evaluated theoretically based on the influence function and relative efficiency and numerically based on gross error detection rate, number of type I errors, and error reductions after data reconciliation. Also, a modified compensation strategy will be proposed to avoid the misrectification by data reconciliation algorithms (distributions) due to the presence of larger gross errors.

As discussed previously, the data reconciliation results from the combined gross error detection and data reconciliation and the simultaneous data reconciliation and parameter estimation are interactive. Data reconciliation associated with gross error detection and with parameter estimation uses the same plant model. Data reconciliation in gross error detection step uses previous values of process parameters in the process model when reconciling the process data. This results in the reconciled data is consistent with the old (previous) values of parameters. If the whole set of reconciled values for measured variables is used for estimating the parameters, the parameters will have the same values as the previous and they are not able to be updated.

Therefore, a strategy to generate a set of pre-processed data from the combined gross error detection and data reconciliation (data validation) for the simultaneous data reconciliation and parameter estimation will be proposed to avoid the interaction between data validation and parameter estimation.

Simultaneous Data Reconciliation and Parameter Estimation: Normal distribution (least squares method), contaminated Gaussian distribution and robust function can be used to conduct combined gross error detection, data reconciliation, and parameter estimation. Two strategies will be used to conduct parameter estimation, and their performance will be compared. One is called two step estimation. Step one is to detect and rectify gross errors in measurements using the contaminated Gaussian distribution, and this step generates a set of pre-processed measurements based on the proposed strategy. Step two estimates the parameters using the least squares method with the measurements generated from step one. The other one is called one step estimation that conducts gross error detection, data reconciliation, and parameter estimation simultaneously using contaminated Gaussian distribution algorithm or robust functions.

Economic Optimization: After the algorithms for conducting gross error detection and parameter estimation are evaluated. The final plant economic optimization is performed subject to the current plant model and external economic conditions. The mathematical modeling software, GAMS, will be used to solve the optimization problems in on-line optimization. This will determine the best operating conditions for the current plant operation.

Interactive On-Line Optimization System: An interactive on-line optimization program will be developed to alleviate engineer's effort in applying the on-line optimization. It will incorporate

the best structure of on-line optimization developed in this research and provide a graphical users interface (GUI) environment for engineer to enter the process information and to solve the on-line optimization problems for values of the optimal set points for DCS. The capability of this program will be demonstrated with the sulfuric acid process from IMC Agrico Company.

In the subsequent chapters, the methodology for on-line optimization used in the research will be discussed and a detail process model for the sulfuric acid contact plant from IMC Agrico Company will be established and validated. Then, this large scale process model will be used to conduct the numerical evaluations for the proposed methodology of on-line optimization system, and the results will be provided.

CHAPTER III THE METHODOLOGY OF ON-LINE OPTIMIZATION

A. Introduction

The on-line optimization for chemical processes includes three important steps: combined gross error detection and data reconciliation, simultaneous data reconciliation and parameter estimation, and plant economic optimization. In combined gross error detection and data reconciliation, a set of accurate plant measurements are generated from plant's distributed control system (DCS). This set of data is used for estimating the parameters in plant models; and parameter estimation is necessary to have the plant model match the current performance of the plant. Then, the plant economic optimization is conducted to optimize the economic model using this current plant model as constraints.

Each optimization problem in on-line optimization has a similar mathematical statement as following:

Optimize: **Objective function**
Subject to: **Constraints from plant model**

where the objective function is an joint distribution function for data validation or parameter estimation and a profit function (economic model) for plant economic optimization. The constraint equations describe the relationship among variables and parameters in the process, and they are material and energy balances, chemical reaction rates, thermodynamic equilibrium relations, and others.

Chemical plants operate at steady state with a relatively short transient periods and steady state plant models can be used to describe the relationship among process variables and

parameters of the plants. These plant models are complicated and highly nonlinear, and all measurements are subject to either random or gross errors. Therefore, the error-in-variables formulation is required for the plant model of on-line optimization.

B. The Implementation Procedures for On-Line Optimization

As discussed in previous chapter, gross error detection and parameter estimation are coupled with data reconciliation for complicated and highly nonlinear processes. Therefore, there are two ways to conduct on-line optimization as shown in Figure 3.1. In one procedure, three nonlinear optimization problems are solved sequentially as shown in Figure 3.1.a. These three optimization problems are combined gross error detection and data reconciliation, simultaneous data reconciliation and parameter estimation, and plant economic optimization represented by three boxes. In combined gross error detection and data reconciliation, gross errors in the plant

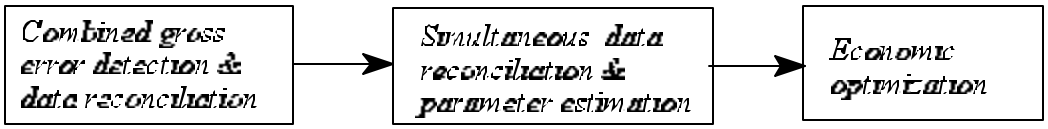

a. Three Optimization Problems

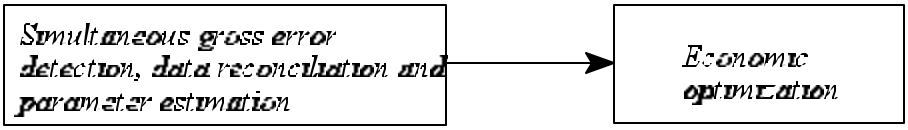

b. Two Optimization Problems

Figure 3.1 The Procedure of On-Line Optimization Implementation

data are eliminated or rectified, and a set of reconstructed measurements is generated based on the result of data reconciliation and gross error detection. In simultaneous data reconciliation and parameter estimation, parameters in a plant model are estimated using the reconstructed measurements from combined gross error and data reconciliation. These updated values of parameters are used in the plant model for economic optimization. Plant economic optimization generates a set of optimal set points for plant DCS based on the updated plant model and economic conditions.

As mentioned previously, there are an interaction between data reconciliation associated with gross error detection and with parameter estimation. Data reconciliation associated with gross error detection requires updated parameters in the plant model. However, before the gross errors detection, only the parameter values from the previous optimization cycle are available. Consequentially, the previous parameters in last cycle of on-line optimization are used in the plant model for conducting gross error detection and data reconciliation. Data reconciliation in this step will force the all reconciled process variables to satisfy the plant model with old plant parameter data. If reconciled data for all measurements is used in simultaneous data reconciliation and parameter estimation, then the parameters will not be updated because the reconciled data was obtained using the old plant parameters. Therefore, using all of the reconciled measurements from gross error detection and data reconciliation in parameter estimation step will give the same estimation as the old values for parameters.

Therefore, a strategy is proposed to avoid this dilemma. It is to detect and rectify the measurements containing gross errors using the plant model with the parameter values from

previous on-line optimization cycle in gross error detection and data reconciliation. Then a new set of measurements is constructed using the reconciled data to replace the measurements containing gross errors along with the original measurements that contain only random errors. This new set of measurements is supposed only containing random errors, and it can be used to conduct simultaneous data reconciliation and parameter estimation using least squares method with error-in-variables formulation.

The other procedure is that on-line optimization involves solving two nonlinear optimization problems as shown in Figure 3.1.b. In this procedure, gross error detection, data reconciliation, and parameter estimation are conducted simultaneously to rectify gross errors, reconcile process variables, and estimate plant parameters using one algorithm. Then, economic optimization is conducted using the updated plant and economic models.

Simultaneous gross error detection, data reconciliation, and parameter estimation procedure may be a better way to conduct on-line optimization, if the algorithm is not sensitive to the presence of gross errors, and if that both parameters and measurements with gross errors are converted to unmeasured variables in the one data reconciliation optimization problem does not affect the observability and redundancy of the plant model. This procedure eliminates the interaction of data reconciliation associated with gross error detection and with parameter estimation. No one has reported an application using this simultaneous procedure yet. As discussed in literature review, least squares method is not able to accurately reconcile process data that contains gross errors, and it can not be used for this simultaneous procedure. The contaminated Gaussian distribution and robust functions are insensitive to the presence of gross

errors when reconciling process data. The methods based on these distribution functions can be used to conduct the simultaneous gross error detection, data reconciliation, and parameter estimation, and this will be investigated and evaluated as part of this research work.

In summary, two possible procedures for on-line optimization have been proposed, and they will be investigated using a large scale real chemical plants. One procedure uses combined gross error detection and data reconciliation algorithms to pre-process the plant data, i.e., identify measurements with gross errors and replace them with reconciled data for these measurements. Then this set of pre-processed plant data with only random errors is used to conduct simultaneous data reconciliation and parameter estimation. This strategy will avoid the effect of using old plant parameters in the plant model for combined gross error detection and data reconciliation on updating parameters in simultaneous data reconciliation and parameter estimation. The other is a simultaneous gross error detection, data reconciliation, and parameter estimation procedure using the algorithms that have an ability to rectify data containing both random and gross errors.

The following section will discuss and evaluate the methodology for gross error detection, data reconciliation, parameter estimation, and plant economic optimization. Also, the statistical background information which is cited in main text is given in Appendix B.

C. Methodology of On-Line Optimization

In general, an optimization problem is to optimize an objective function subject to a set of linear/nonlinear constraints. In on-line optimization applications, the objective function is an joint probability function for data reconciliation and parameter estimation or a profit function

(economic model) for plant economic optimization. The constraints are a set of linear and nonlinear equations that describe the relationship among the process variables and parameters, which is called process model or simulation. The general mathematical statement for the optimization problems of on-line optimization is:

$$\begin{aligned} &\textit{Optimize}: && P(\mathbf{y}, \mathbf{x}) \\ &\textit{Subject to}: && \mathbf{f}(\mathbf{x}, \mathbf{z}, \boldsymbol{\theta}) = 0 \\ & && \mathbf{g}(\mathbf{x}, \mathbf{z}, \boldsymbol{\theta}) \le 0 \\ & && \mathbf{x}^L \le \mathbf{x} \le \mathbf{x}^U, \mathbf{z}^L \le \mathbf{z} \le \mathbf{z}^U \end{aligned} \tag{3-1}$$

Eq. 3-1 is to optimize the objective function P subject to a process model that includes the equality constraints **f**, inequality constraints **g**, and bounds on the variables. In Eq. 3-1, the vector **y** represents a set of measurements sampled from distributed control system for measured variables and vector **x** denotes the true values of the same measured variables as **y**. The vector **z** represents a set of unmeasured process variables that include all process variables except the measured ones in plant model, and $\boldsymbol{\theta}$ is the vector of process parameters. The equality constraints **f** describe the relationship among the process variables and parameters, such as mass and energy balances, chemical reaction rate equations, heat transfer equation, and others. The inequality constraints **g** represents the demand of products, the availability of raw materials, the limitation on the capacity of equipment, the allowable operating conditions, and the restrictions on waste and pollutant emission. In addition, $\mathbf{x}^L \le \mathbf{x} \le \mathbf{x}^U$ and $\mathbf{z}^L \le \mathbf{z} \le \mathbf{z}^U$ give upper and lower bounds on process variables.

The relation between measurements **y** and the true data **x** for measured variables is defined by a measurement model given in Eq. 2-1, i.e.,

$$\mathbf{y} = \mathbf{x} + \mathbf{e} \tag{2-1}$$

where the vectors **e** represents the measurement errors that could be random or gross errors.

The following will discuss and theoretically evaluate the applicable algorithms for combined gross error detection and data reconciliation, simultaneous data reconciliation and parameter estimation , and plant economic optimization.

C-1. Algorithms for Combined Gross Error Detection and Data Reconciliation

The process data from distributed control system is subject to two types of errors, random error and gross error, and the gross error must be detected and rectified before the data is used to estimate plant parameters. As discussed in Chapter II, only combined gross error detection and data reconciliation algorithms can be used to detect and rectify the gross errors in measurements for on-line optimization. These algorithms are measurement test method using a normal distribution, Tjoa-Biegler's method using a contaminated Gaussian distribution, and robust statistical method using robust functions. The methodology of these algorithms will be given, and their theoretical performance will be evaluated in the following section.

Measurement Test Method: This method assumes all measurements are subject to only random errors with known normal distributions under null hypothesis and the measurement errors are independent of each other. Then the distribution function for measurement error i under null hypothesis is:

$$P_i \quad \frac{1}{\sqrt{2\pi}\sigma_i} \exp\left[\frac{1}{2}\left(\frac{e_i}{\sigma_i}\right)^2\right] \tag{3-2}$$

where e_i is the measurement error as described in Eq. 2-1 and σ_i is the standard deviation of the measurement error. The joint distribution for all measurement errors is the product of the distributions for individual measurement error given in Eq. 3-2, i.e.,

$$P \quad \prod_{i=1}^{n} p_i \quad \frac{1}{(2\pi)^{n/2}|\Sigma|^{1/2}} \exp\left[(e^T \Sigma^{-1} e)/2\right] \tag{3-3}$$

where $\mathbf{\Sigma}$ is the diagonal matrix of the known variances σ_i^2 of measurement errors $\mathbf{e}$.

The measurement errors are estimated by maximizing the joint probability density function P or minimizing the sum squares of standardized measurement errors, $\mathbf{e}^T\mathbf{\Sigma}^{-1}\mathbf{e}$, subject to a set of constraints which represent the relationship among the variables. This is the well known least squares method and it is expressed as:

$$\begin{aligned} &\underset{\mathbf{x},\,\mathbf{z}}{\textit{Minimize}}: && \mathbf{e}^T\mathbf{\Sigma}^{-1}\mathbf{e} = (\mathbf{y}-\mathbf{x})^T\Sigma^{-1}(\mathbf{y}-\mathbf{x}) \\ &\textit{Subject to}: && \mathbf{f}(\mathbf{x}, \mathbf{z}, \boldsymbol{\theta}) = 0 \\ & && \mathbf{x}^L \le \mathbf{x} \le \mathbf{x}^U,\ \mathbf{z}^L \le \mathbf{z} \le \mathbf{z}^U. \end{aligned} \tag{3-4}$$

where $\mathbf{x}$, $\mathbf{y}$, $\mathbf{z}$, and $\boldsymbol{\theta}$ have the same meaning as described in Eq. 3-1 previously. In Eq. 3-4, $\mathbf{x}$ and $\mathbf{z}$ are variables to be determined by the optimization. $\boldsymbol{\theta}$ is a constant vector of parameters ans $\mathbf{y}$ is a constant vector of measurements. Solving Eq. 3-4 will estimate the values for the measured variables $\mathbf{x}$ and unmeasured variables $\mathbf{z}$. Then, the measurement errors can be determined by $\mathbf{e} = \mathbf{y} - \mathbf{x}$.

After data reconciliation, each measurement error is examined to see if it contains a gross error by a test statistic. The test statistic of measurement test method is:

$$|\epsilon_i| = |e_i|/\sigma_i \sim N(0, 1) \quad (3\text{-}5)$$

Eq. 3-5 means that the standardized measurement error, $\epsilon_i = e_i/\sigma_i$, follows a standard normal distribution N(0, 1) if the measurement does not contain gross error.

If the value of test statistic, $|e_i|/\sigma_i$, exceeds the critical value C, then this measurement contains a gross error. Otherwise, there is no gross error in this measurement. The critical value C is selected from the table of standard normal distribution function at the significant level β for individual measurement. If the overall significant level is specified as 0.05 (e.g., 95% confidential interval), $\alpha = 0.05$, and 43 measurements are used, then the significant level for individual measurement is:

$$\beta = 1 - (1-\alpha)^{1/m} = 1-(1-0.05)^{1/43} = 0.0012.$$

At the $\beta/2$=0.006 point, the critical value C is determined from the standard normal distribution with accumulated probability at 0.994, and the value is 3.2, i.e., C = 3.2.

The optimization problem of measurement test method in Eq. 3-4 is programmed in GAMS language, and the program is given in Table F-13 of Appendix F and in GAMS source code disk with file name as: meastest.gms..

The Contaminated Gaussian Distribution: Biegler, et al., (Tjoa and Biegler, 1991; Albuquerque and Biegler, 1995) proposed a contaminated Gaussian distribution function to describe the measurement errors. A measurement is subject to either random or gross error. The two possible outcomes are: G = {Gross error occurred} with prior probability η and R = {Random error occurred} with prior probability $1-\eta$. Therefore, the distribution of a measurement error is:

$$P(y_i \mid x_i) = (1-\eta)P(y_i \mid x_i, R) + \eta\, P(y_i \mid x_i, G) \tag{3-6}$$

where $P(y_i \mid x_i, R)$ is the probability distribution of a random error and $P(y_i \mid x_i, G)$ is the probability distribution of a gross error.

It is assumed that the random errors are normally distributed with a zero mean and a known variance σ_i^2. The distribution function for a random error is:

$$P(y_i|x_i, R) \quad \frac{1}{\sqrt{2\pi}\sigma_i} e^{\frac{(y_i - x_i)^2}{2\sigma_i^2}} \tag{3-7}$$

Also, it is assumed that the gross errors are subject to a contaminated normal distribution which has a zero mean and larger variance $(b\sigma)^2$, $(b >> 1)$. Therefore, the distribution function for a gross error is:

$$P(y_i|x_i, G) \quad \frac{1}{\sqrt{2\pi}b\sigma_i} e^{\frac{(y_i - x_i)^2}{2b^2\sigma_i^2}} \tag{3-8}$$

If the measurement errors are independent of each other, then the likelihood function for all measurements is the product of the distributions for individual measurement, i.e.,

$$P(y|x) \quad \prod_i P(y_i|x_i) \quad \prod_i \frac{1}{\sqrt{2\pi}\sigma_i} \left\{ (1-\eta) e^{\frac{(y_i - x_i)^2}{2\sigma_i^2}} \quad \frac{\eta}{b} e^{\frac{(y_i - x_i)^2}{2b^2\sigma_i^2}} \right\} \tag{3-9}$$

The measurement errors are estimated by maximizing the joint probability density function (likelihood function) in Eq. 3-9 or minimizing the negative logarithm of Eq. 3-9. The optimization

$$\rho \quad \sum \left\{ \ln \left[(1-\eta) e^{\frac{(y_i - x_i)^2}{2\sigma_i^2}} \quad \frac{\eta}{b} e^{\frac{(y_i - x_i)^2}{2b^2\sigma_i^2}} \right] \ln \sqrt{2\pi}\sigma_i \right\} \tag{3-10}$$

problem for combined gross error detection and data reconciliation using the contaminated Gaussian distribution can be stated as:

Minimize:
$\mathbf{x}, \mathbf{z}$

Subject to: $\mathbf{f}(\mathbf{x}, \mathbf{z}, \boldsymbol{\theta}) = 0$
$\mathbf{x}^L \le \mathbf{x} \le \mathbf{x}^U, \mathbf{z}^L \le \mathbf{z} \le \mathbf{z}^U$

This optimization problem is comparable to Eq. 3-4 for the least squares (measurement test) method. Solving Eq. 3-10 determines the values of measured and unmeasured variables (**x** and **z**). These values maximize the joint likelihood function P(**y** | **x**) (or minimize the negative logarithm of the joint likelihood function) and satisfy the process constraints. Then, the measurement errors are determined by **e** = **y** - **x**.

After data reconciliation, each measurement is examined with a test statistic to see if it contains a gross error. The test statistic for gross error detection is:

If
$$|\epsilon_i| \quad \left|\frac{y_i - x_i}{\sigma_i}\right| > \sqrt{\frac{2b^2}{b^2 - 1}\ln\left[\frac{b(1-\eta)}{\eta}\right]} \qquad (3\text{-}11)$$

then measurement i contains gross error. Otherwise, no gross error is present in this measurement. In the GAMS program, DataVali.gms, two parameters in Eq. 3-11 are specified as: η =0.5 and b = 10. Therefore, the test statistic for contaminated Gaussian distribution of Tjoa-Biegler's method is: if $|\epsilon_i| > 2.157$, then measurement i contains a gross error.

As discussed in the review of contaminated Gaussian distribution method of Chapter II, contaminated Gaussian distribution method is composed of the distribution functions for random

and gross errors. The reconciled data from contaminated Gaussian distribution method is not sensitive to the presence of gross errors, and this method gives an unbiased estimation for the reconciled data. This can be seen by weight coefficients of measurements in the linearized joint distribution as discussed in contaminated Gaussian distribution method of Chapter II.

The objective function in Eq. 3-10 (or Eq. 2-49) can be approximated as a linear function using a first order Taylor expansion, i.e., $\rho = \sum w_i [(y_i - x_i)-(y_i - x_i)^0] = \sum w_i (\epsilon_i - \epsilon_i^0)$, where w_i is the weight coefficient of measurement y_i on the joint distribution function (objective function in Eq. 3-10) evaluated at the last feasible point x_i^0 or ϵ_i^0, and it is the partial derivatives of the joint contaminated Gaussian distribution function with respect to the variable x_i as given in Eq. 2-52, i.e.,

$$w_i = \left. \frac{\frac{(y_i - x_i)}{\sigma^2}\left\{(1-\eta)e^{\frac{(y_i-x_i)^2}{2\sigma^2}\left(1-\frac{1}{b^2}\right)} + \frac{\eta}{b^3}\right\}}{(1-\eta)e^{\frac{(y_i-x_i)^2}{2\sigma^2}\left(1-\frac{1}{b^2}\right)} + \frac{\eta}{b}} \right|_{x_i, x_i^0} \quad \left. \frac{\frac{\epsilon_i}{\sigma}\left\{(1-\eta)e^{\frac{\epsilon_i^2}{2}\left(1-\frac{1}{b^2}\right)} + \frac{\eta}{b^3}\right\}}{(1-\eta)e^{\frac{\epsilon_i^2}{2}\left(1-\frac{1}{b^2}\right)} + \frac{\eta}{b}} \right|_{\epsilon_i, \epsilon_i^0} \tag{2-52}$$

For smaller error, e.g., $\epsilon_i < 2$, the exponential term in the Eq. 2-52 is much larger than the second term η/b^3 (or η/b), The weight function can be simplified as $w_i \propto (y_i-x_i)/\sigma_i^2 = \epsilon_i/\sigma_i$. For larger error, e.g., $\epsilon_i > 4$, the exponential term in the equation is much smaller than the second term η/b^3

(or η/b). The weight function can be simplified as $w_i \propto (y_i - x_i)/(b\sigma_i)^2 = \epsilon_i/(\sigma_i\, b^2)$. Therefore, Eq. 2-52 can be approximated as given in Eq. 2-54:

$$w_i \begin{cases} \epsilon_i/\sigma_i & \text{for } \epsilon_i < 2 \\ \epsilon_i/(\sigma_i b^2) & \text{for } \epsilon_i > 4 \end{cases} \qquad (2\text{-}54)$$

From the weight coefficient function in Eq. 2-54 and the linearized objective function, it is seen that the measurement with a smaller error has a large weight coefficient (i.e., $w_i = \epsilon_i/\sigma_i$) in the linearized objective function than the measurement with a larger error (i.e., $w_i = \epsilon_i/(\sigma_i\, b^2)$, where b>>1). This means the measurement with a larger error has a less effect on the minimization, and the objective function value is determined mainly by the measurements with small errors.

The procedure to conduct contaminated Gaussian distribution method is:

1. Solve Eq. 3-10 to determined the reconciled values for measured variables and unmeasured variables, and then the measurement adjustments, $\mathbf{a} = \tilde{\mathbf{x}} - \mathbf{y}$, are determined by the measurements $\mathbf{y}$ and reconciled data $\tilde{\mathbf{x}}$.
2. Examine the standardized measurement adjustment ϵ_i, $\epsilon_i = a_i / \sigma_i$, using the criterion given Eq. 3-11 to determine if a measurement contains a gross error. If a measurement contains a gross error, then its value is replaced with the reconciled data. A new set of measurements is constructed using the reconciled data to replace the measurements containing gross errors along with the original measurements that contain only random errors. This new set of measurements contains only random errors, and it is used in

simultaneous data reconciliation and parameter estimation to update plant parameters for on-line optimization.

The optimization problem of contaminated Gaussian distribution method in Eq. 3-10 is programmed in GAMS language, and the program is given in Table F-1 of Appendix F and in GAMS source code disk with file name as: datavali.gms.

Robust Statistical Methods: The basic idea of robust estimation is to build a robust distribution function ρ which is asymptotic to the normal distribution or any pre-assumed rigorous distribution function that describes the distribution pattern of measurement errors under some ideal assumptions. The estimator (mean or variance) determined by the robust distribution is insensitive to extreme observations and yet maintains a high efficiency (lower dispersion).

Two robust functions have been proposed in literature for mean estimation, and they are applicable for data reconciliation and gross error detection of on-line optimization. These robust functions are Lorentzian distribution proposed by Johnston and Kramer (1995), which was originally presented by Huber (1981), and Fair function proposed by Albuquerque and Biegler (1995).

Lorentzian distribution function of a measurement error is given as:

$$\rho(\epsilon_i) \quad \frac{1}{1 \quad \frac{1}{2}\epsilon_i^2} \tag{3-12}$$

where ϵ_i is the standardized measurement error, i.e., $\epsilon_i = e_i / \sigma_i = (y_i - x_i)/\sigma_i$. The robust function of measurement errors using Lorentzian distribution is the sum of the individual distribution, i.e,

$$\rho(\epsilon) \quad \sum_i \rho(\epsilon_i) \quad \sum_i \frac{1}{1 \quad \frac{1}{2}\epsilon_i^2} \tag{3-13}$$

The optimization problem for the combined gross error detection and data reconciliation using the Lorentzian distribution function is expressed as:

$$\begin{aligned} &\text{Maximize:} \quad \rho(\epsilon) \quad \sum_i \frac{1}{1 \quad \frac{1}{2}\epsilon_i^2} \\ &\quad \mathbf{x}, \mathbf{z} \\ &\text{Subject to:} \quad \mathbf{f}(\mathbf{x}, \mathbf{z}, \boldsymbol{\theta}) = 0 \\ &\qquad \mathbf{x}^L \le \mathbf{x} \le \mathbf{x}^U, \mathbf{z}^L \le \mathbf{z} \le \mathbf{z}^U \end{aligned} \tag{3-14}$$

Fair function for a measurement error is given as:

$$\rho(\epsilon_i) \quad c^2 \left[\frac{|\epsilon_i|}{c} \quad \log\left(1 \quad \frac{|\epsilon_i|}{c} \right) \right] \tag{3-15}$$

where ϵ_i is the standardized measurement error, i.e., $\epsilon_i = e_i / \sigma_i = (y_i - x_i)/\sigma_i$. The robust function of measurement errors using Fair function for individual measurement error is the sum of the individual distribution functions, i.e.,

$$\rho(\epsilon) \quad \sum_i \rho(\epsilon_i) \quad \sum_i c^2 \left[\frac{|\epsilon_i|}{c} \quad \log\left(1 \quad \frac{|\epsilon_i|}{c} \right) \right] \tag{3-16}$$

The optimization problem for the combined gross error detection and data reconciliation using Fair function is expressed as (Albuquerque and Biegler, 1995):

$$\begin{aligned} &\text{Minimize} \quad \rho(\epsilon) \quad \sum_i c^2 \left[\frac{|\epsilon_i|}{c} \quad \log\left(1 \quad \frac{|\epsilon_i|}{c} \right) \right] \\ &\quad \mathbf{x}, \mathbf{z} \\ &\text{Subject to:} \quad \mathbf{f}(\mathbf{x}, \mathbf{z}, \boldsymbol{\theta}) = 0 \end{aligned} \tag{3-17}$$

$$\mathbf{x}^L \le \mathbf{x} \le \mathbf{x}^U, \mathbf{z}^L \le \mathbf{z} \le \mathbf{z}^U$$

where c is a tuning parameter. This parameter reflects the relative efficiency of the estimator at this distribution. It was pointed out that Fair function is convex and has continuous first and second derivatives (Albuquerque and Biegler, 1995).

After solving the optimization problem in Eq. 3-14 or Eq. 3-17, the reconciled data for measured variables is determined, and the measurement adjustments can be determined by $\mathbf{a} = \mathbf{y} - \tilde{\mathbf{x}}$. Then , each measurement adjustment is examined to see if it contains a gross error by the test statistic.

The test statistic for robust method is established using a statistical hypothesis test procedure as measurement test method. If the standardized measurement adjustment, $|\epsilon_i| = |a_i|/\sigma_i$, does not exceed the critical value C, then measurement i does not contain a gross error. Otherwise, the measurement contains a gross error. The critical value C is determined by the robust function at the specified confidential interval or significant level β. For example, if 95% of confidential level is used, then the overall significant level α is 0.05 and the significant level for individual measurements β is calculated by Eq. 2-23 from the given overall significant level α and the number of measurements m. Then, the critical value C is the error size that has an accumulated probability value as $(1-\beta/2)$.

The procedure to conduct gross error detection and data reconciliation with robust method is the same as one for contaminated Gaussian distribution method, and it is:

1. Solve Eq. 3-14 or Eq. 3-17 to determined the reconciled values for measured variables and unmeasured variables, and then the measurement adjustments are determined by the measurements **y** and reconciled data $\tilde{\mathbf{x}}$.

2. Examine the standardized measurement adjustment ϵ_i, $\epsilon_i = a_i / \sigma_i$, to determine if a measurement contains a gross error. If the standardized measurement adjustment ϵ_i is larger than the critical value C, i.e., $|\epsilon_i| > C$, then measurement i contains a gross error. Otherwise, there is no gross error in measurement i. If a measurement contains a gross error, then its value is replaced with the reconciled data. A new set of measurements is constructed using the reconciled data to replace the measurements containing gross errors along with the original measurements that contain only random errors. This new set of measurements contains only random errors, and it is used in simultaneous data reconciliation and parameter estimation to update plant parameters for on-line optimization.

The optimization problem of robust method using Lorentzian distribution in Eq. 3-14 is programmed in GAMS language, and the program is given in Table F-14 of Appendix F and in GAMS source code disk with file name as: robust.gms.

In the following section, the theoretical performance of four distribution functions: normal distribution of measurement test method, contaminated Gaussian distribution of Tjoa-Biegler's method, Lorentzian distribution and Fair function of robust method, are evaluated based on the influence function and relative efficiency of the distributions. Then, the distributions that have

better theoretical performance will be tested with the sulfuric acid plant to numerically evaluate their performance.

Evaluation of Distribution Functions for Data Reconciliation and Gross Error Detection: Three important concepts in the theoretical evaluation of the robustness and precision of an estimator from a distribution function are the break-down point, relative efficiency, and influence function (Seber, 1984). In statistical estimation, estimator T is the mean or variance of the sample data, and T is estimated with samples of data. In data reconciliation of on-line optimization, T is the estimated values of reconciled variables from data reconciliation evaluated with plant data sampled from the distributed control system. Robustness of an estimator is unbiasedness (insensitivity) to the presence of gross errors in measurements. How sensitive an estimator to the presence of gross errors can be measured by the influence function of the distribution function that is used to verify the samples of data. Also, the precision (accuracy) of an estimator from a distribution is measured by the relative efficiency of the distribution. It is said that the estimator is precise if the variation (dispersion) of its distribution function is small (Larsen and Marx, 1986).

The break-down point can be thought of as giving the limiting fraction of gross errors that can be in a sample of data and a valid estimation of the estimator is still obtained using this data (Huber, 1981). For repeated samples, the break-down point is the fraction of gross errors in the data that can be tolerated and the estimator gives a meaningful value. It is the maximum allowable number of extreme observation for a given sample size n, and it represents the global reliability.

For constrained estimation using single set of process data in data reconciliation of on-line optimization, a validated estimation for the reconciled data also depends on the degree of

redundancy in the measurements. Exceeding either the degree of redundancy or the break-down point will cause the estimator to give an incorrect value. The degree of redundancy is the excessive number of measurements in addition to those that are required to determine the status of a process.

The relative efficiency of estimator T_1 with respect to estimator T_2 is defined as the ratio of the variances of distribution function P_1 for estimator T_1 and distribution P_2 for estimator T_2. Also, estimator T_1 is more efficient than T_2 if the variance of distribution P_1 for estimator T_1 is less than the variance of distribution P_2 for estimator T_2 (Larsen and Marx, 1986). This is intuitively viewed by the shape of the distribution functions. A distribution that is wider in shape will has a larger variance or standard deviation than one that is narrower in shape. This means that the former has a lower efficiency than the latter.

For the two distribution functions shown in Figure 3.2, the μ represents the true value of a variable. T_1 is the estimator of the variable from distribution P_1, and T_2 is the estimator of the

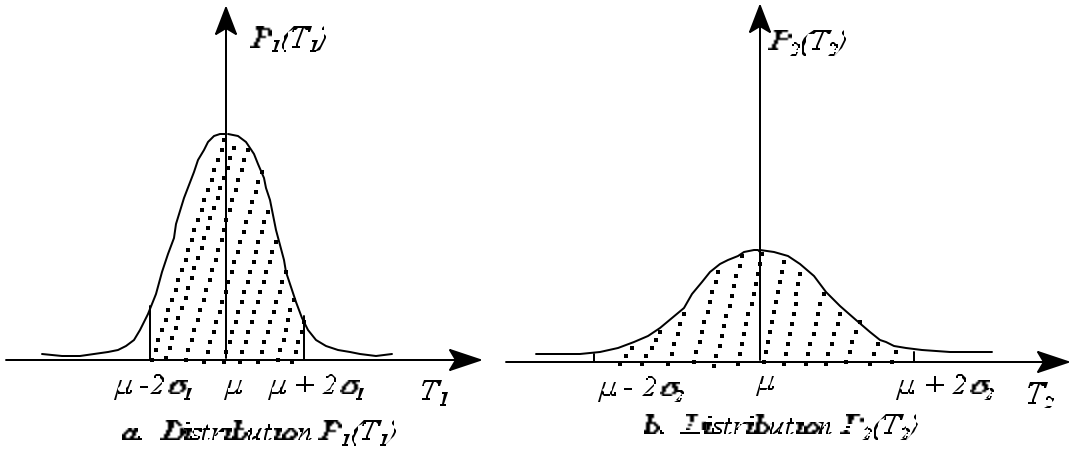

Figure 3.2 Comparison of Two Distributions with Different Dispersions
after Larsen and Marx, 1986

variable from distribution P_2. For a given distribution function, the estimator can have a value in the range from the true value minus two times standard deviation of the distribution function to the true value plus two times the standard deviation with a 95% confidential interval. If distribution function P_1 is used to describe the samples of data, the possible estimated range of the estimator is from $\mu - 2\sigma_1$ to $\mu + 2\sigma_1$ as shown in Figure 3.2.a. If distribution function P_2 is used to describe the samples of data, the possible estimated range of the estimator is from $\mu - 2\sigma_2$ to $\mu + 2\sigma_2$ as shown in Figure 3.2.b. From the comparison of Figure 3.2.a for distribution P_1 and Figure 3.2.b for distribution P_2, it is seen that the distribution function P_1 has a smaller standard deviation than the one for P_2. Therefore, the estimated value from distribution function P_1 is closer to the true than one from distribution function P_2. It is concluded that the estimated accuracy of the reconciled data is determined by the relative efficiency of the distribution function that is used by the algorithm to describe the samples of data. A distribution having a smaller variation has higher

relative efficiency than one having a larger variation, and therefore, the corresponding estimator has a higher estimation accuracy.

The influence function quantifies the influence of a measurement on the estimated value from data reconciliation. The influence function (IF) of estimator T at F is given by (Hampel, et. al., 1986):

$$IF(y; T, F) \quad \lim_{\Delta t \to 0} \frac{T[(1-\Delta t)F + \Delta t G] - T[F]}{\Delta t} \tag{3-18}$$

where T is an estimator that is evaluated with sampled data **y**. In statistical estimation, T is the mean or variance of the sample data, and T is estimated with samples of data. In data reconciliation of on-line optimization, T is the estimated values of reconciled variables from data reconciliation evaluated with data sampled from the distributed control system. F is the distribution function for the majority of measurement data and G represents the distribution function of an arbitrary observation y, which can be a normal or an extreme measurement. In Eq. 3-18, Δt is the portion of data having the character of distribution G counted in all observations.

Based on the definition of IF given in Eq. 3-18, the influence function for the mean estimator with n repeated observations is derived as following. For the estimation of mean x using repeated n observations y_i (i = 1, 2, .. , n), the estimated mean using a normal distribution (least squares method) is equal to the sample mean, i.e.,

$$x_n = \frac{1}{n} \sum_{i=1}^{n} y_i \tag{3-19}$$

where x_n represents the sample mean x that is estimated by n observations. If one additional observation (observation n+1) is included, then the mean estimated by n+1 observations, x_{n+1} is:

$$x_{n+1} = \frac{1}{n+1}\sum_{i=1}^{n+1} y_i = \frac{n}{n+1}x_n + \frac{1}{n+1}y_{n+1} \tag{3-20}$$

Substituting Eq. 3-19 and 3-20 into Eq. 3-18, with $T[(1-\Delta t)F + \Delta tG] = x_{n+1}$ and $T[F] = x_n$, and $\Delta t = 1$, gives the influence function of the mean estimator as:

$$IF = x_{n+1} - x_n = \frac{n}{n+1}x_n + \frac{1}{n+1}y_{n+1} - x_n = \frac{y_{n+1} - x_n}{n+1} \tag{3-21}$$

which represents the contribution from a good measurement or the bias effect from a bad observation on the estimation. The influence function is proportional to the difference between the observation y_{n+1} and the mean estimated by n observations, x_n, which is the measurement error.

Above is a simple example to show how to determine the influence function of an estimator from the definition of influence function. The influence function in Eq. 3-18 represents the effect of an arbitrary observation on the estimator T. For M-estimate, the influence function is defined as a function that is proportional to the derivative of a distribution function with respect to the measured variable, $(\partial\rho/\partial x)$ (Huber, 1981 and Hampel, et al., 1986), i.e.,

$$IF \propto \partial\rho/\partial x \tag{3-22}$$

The measurement test method uses a normal distribution for measurement error as given in Eq. 3-2. Taking a logarithm of the normal distribution gives:

$$\rho_i \quad \ln p_i \quad \frac{1}{2}\left(\frac{y_i \; x_i}{\sigma_i}\right)^2 \quad \ln(\sqrt{2\pi}\sigma_i) \tag{3-23}$$

Therefore, the influence function of the normal distribution (measurement test method) for measurement i is proportional to $\partial\rho_i/\partial x_i$, i.e.,

$$IF_{MT} \propto \frac{\partial \rho_i}{\partial x_i} \; \frac{y_i \; x_i}{\sigma_i^2} \; \frac{\epsilon_i}{\sigma_i} \tag{3-24}$$

where y_i denotes an arbitrary observation (measurement) and x_i is the true value of the measurement.

IF_{MT} in Eq. 3-24 is similar to one of sample mean estimation in Eq. 3-21. As shown in Eq. 3-24, the influence function of measurement test method for measurement i is proportional to the measurement error and is not bounded when the measurement error goes to infinity. This means that measurement test method is unable to bound the effect of gross errors on estimators. The presence of gross errors will result in biased estimation of reconciled variables from measurement test method, and the degree of bias is proportional to the magnitude of the gross error.

The contaminated Gaussian distribution is a superposition of a normal distribution with a variance (σ^2) representing a random error and a normal distribution with a larger variance $(b\sigma)^2$, (b >>1) representing a gross error. This is given by the following equation:

$$P(y|x) \quad \frac{1}{\sqrt{2\pi}\sigma}\left\{(1-\eta)e^{-\frac{(y-x)^2}{2\sigma^2}} \quad \frac{\eta}{b}e^{-\frac{(y-x)^2}{2b^2\sigma^2}}\right\} \tag{3-25}$$

where b is the ratio of standard deviation of gross errors to one of random errors. η is the prior probability of a gross error and 1-η is the prior probability of a random error. Eq. 3-25 is illustrated in Figure 3.3. From Figure 3.3, it can been seen that the shape of contaminated Gaussian distribution is close to standard normal distribution N(0,1) in the middle and has longer and flatter tail than the standard normal distribution N(0, 1) at the two sides. Intuitively, this distribution should be more robust than a single normal distribution in bounding the effect of gross errors on the estimator. This distribution function is able to reduce the degree of bias caused by large gross errors on the estimation of reconciled variables, which will be seen from its influence function.

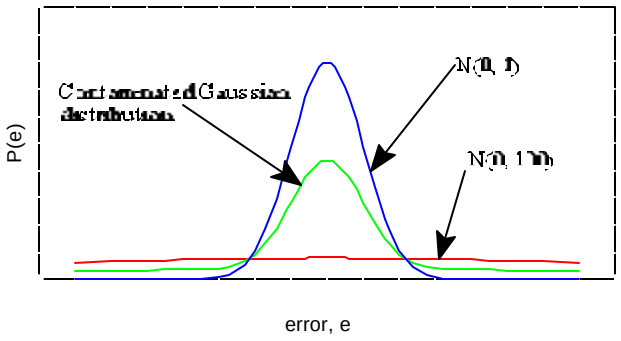

Figure 3.3 The Comparison of Contaminated Gaussian Distribution and Normal Distribution

Taking a logarithm of the contaminated Gaussian distribution in Eq. 3-25 gives:

$$\rho_i \quad \log[P(y_i|x_i)] \quad \log\left\{(1-\eta)e^{-\frac{(y_i-x_i)^2}{2\sigma_i^2}} \quad \frac{\eta}{b}e^{-\frac{(y_i-x_i)^2}{2b^2\sigma_i^2}}\right\} \log\sqrt{2\pi}\sigma_i \tag{3-26}$$

The influence function of the contaminated Gaussian distribution for measurement i is proportional to the derivative of ρ_i with respect to x_i, i.e.,

$$IF \propto \frac{\partial \rho_i}{\partial x_i} \propto \frac{\frac{(y_i - x_i)}{\sigma_i^2}\left\{(1-\eta)\, e^{\frac{(y_i - x_i)^2}{2\sigma_i^2}\left(1 - \frac{1}{b^2}\right)} \frac{\eta}{b^3}\right\}}{(1-\eta)\, e^{\frac{(y_i - x_i)^2}{2\sigma_i^2}\left(1 - \frac{1}{b^2}\right)} \frac{\eta}{b}} \quad \frac{\frac{\epsilon_i}{\sigma_i}\left\{(1-\eta)\, e^{\frac{\epsilon_i^2}{2}\left(1 - \frac{1}{b^2}\right)} \frac{\eta}{b^3}\right\}}{(1-\eta)\, e^{\frac{\epsilon_i^2}{2}\left(1 - \frac{1}{b^2}\right)} \frac{\eta}{b}} \tag{3-27}$$

Eq. 3-27 shows the influence function of the contaminated Gaussian distribution is a function of the standardized measurement error, $\epsilon_i = (y_i - x_i)/\sigma_i$. For smaller error e.g., $\epsilon_i < 2$, the exponential term in the Eq. 3-27 is much larger than the second term η/b^3 (or η/b) for $\eta = 0.5$ and $b = 10$. In this case, the influence function can be simplified to the one for normal distribution in Eq 3-25:

$$IF \quad \frac{y_i - x_i}{\sigma_i^2} \quad \frac{\epsilon_i}{\sigma_i} \tag{3-25}$$

The influence function of the contaminated Gaussian distribution for small errors ($\epsilon_i < 2$) is the same as one of the normal distribution for measurement test method. This contaminated distribution acts like a normal distribution for small measurement errors, i.e., the probability function of the random error dominates the contaminated Gaussian distribution. For a larger error, e.g., $\epsilon_i > 4$, the exponential term in the equation is much smaller than the second term η/b^3 (or η/b) for $\eta = 0.5$ and $b = 10$. The influence function can be simplified as:

$$IF \propto \frac{y_i - x_i}{(b\sigma_i)^2} \quad \frac{1}{b^2} \frac{\epsilon_i}{\sigma_i} \tag{3-28}$$

For a larger measurement error, the distribution function of the gross error dominates the contaminated Gaussian distribution. As shown in Eq. 3-28, the influence function of the contaminated distribution function is similar to one of the normal distribution with reduced magnitude of influence function value. The magnitude of influence function is reduced b^2 times compared with the influence function of the normal distribution for measurement test method in Eq. 3-24 when a measurement contains a gross error. For example, if a measurement has a gross error size at 10σ, the normal distribution function of measurement test method has an influence function value as 10; and the contaminated Gaussian distribution function has an influence function value as 0.025 for b=20.

The influence function of contaminated Gaussian distribution can be simplified as:

$$IF \begin{cases} \varepsilon_i/\sigma_i & for\ \varepsilon_i < 2 \\ \varepsilon_i/(\sigma_i b^2) & for\ \varepsilon_i > 4 \end{cases} \tag{3-29}$$

Eq. 3-29 shows that the influence function of the contaminated Gaussian distribution is still proportional to the error magnitude, although it has a much smaller value for a measurement with a larger (gross) error than a measurement with a smaller (random) error. Therefore, the contaminated Gaussian distribution function can not bound the effect of very large gross errors (e.g., a gross error larger than 50σ).

In contaminated Gaussian distribution, b is a tuning parameter to shape the distribution. Increasing b will reduce the effect of a gross error on the estimation and increase the robustness of this approach. However, it will decrease the relative efficiency to the normal distribution. In

the practical applications, b is usually chosen as 10-20; and therefore the effect of a gross error on the estimation reduces 100-400 times compared with measurement test method. Also, gross errors will rarely go to infinity but most are of moderate magnitude. For a moderate magnitude gross error (about 5σ to 20σ), the effect of the gross error is negligible using the contaminated Gaussian distribution. Therefore, it is concluded that the contaminated Gaussian distribution is robust for the estimation with the moderate magnitude of gross errors.

The Lorentzian distribution function is given in Eq. 3-11 previously, and the influence function is:

$$IF_{Lorentzian} \propto \frac{\partial p_i}{\partial \varepsilon_i} \quad \frac{\varepsilon_i}{\left(1 \quad \frac{1}{2}\varepsilon_i^2\right)^2} \tag{3-30}$$

As shown in Eq. 3-30, the influence function of Lorentzian distribution for measurement i is a function of the measurement error. The influence function increases with the increase of a error for small (normal) errors; and then it decreases and eventually approach zero with the increase of a error for large (gross) errors. As defined earlier, the value of the influence function represents the contribution of a measurement to the estimator. Lorentzian distribution has the advantage that it has a large value of influence function for measurements with small (random) errors and has a small or zero value of influence function for measurements with large (gross) errors. This means that Lorentzian distribution can ignore the contribution of the measurements with gross error even though these measurements are included in the data for data reconciliation.

The Fair function is given in Eq. 3-15 previously, and the influence function of the Fair function for measurement i is:

$$IF_{Fair} \propto \frac{\partial \rho_i}{\partial \epsilon_i} \propto c^2 \left(\frac{\frac{1}{c}}{1 + \frac{|\epsilon_i|}{c}} \right) \propto \frac{1}{\frac{1}{|\epsilon_i|} + \frac{1}{c}} \tag{3-31}$$

As shown in Eq. 3-31, the influence function is a function of the measurement error, i.e., with the increase of error, the influence function increases and finally approaches to a constant c. For the error smaller than c, the influence function has a similar dependency on error as one for normal distribution. For the error larger than c, the influence function increases slowly and approaches constant c when the error larger than 10 times of c. The effect of the gross error on the estimation is bounded on a value c when the error goes to infinite. The parameter c in Fair function determines the robustness and efficiency of the estimation. Smaller c value will be more robust but less efficiency. Fair function is able to bound the effect of very large gross errors.

The reconciled data (estimator) from a good distribution function is both robust (or insensitive) to the presence of gross error and has a high relative efficiency. The robustness of an estimator to larger (gross) errors is compared in Figure 3.4 by giving the influence function for normal distribution, contaminated Gaussian distribution, Lorentzian distribution, and Fair function as a function of error ϵ. This figure shows that the influence functions for four distributions have similar shapes for error less than 1σ-2σ. They increase with the increase of error size for measurements with small (random) errors. However, the shapes of the influence functions for these four distributions are different for large errors.

As discussed in contaminated Gaussian distribution method, the joint distribution function (the objective function) of the data reconciliation algorithm can be approximated as a linear function of measurement errors by the first order Taylor expansion, i.e., $P = \sum w_i (e_i - e_i^0)$. The weight coefficient w_i in the joint distribution function is the partial derivative of joint distribution function with respect to measurement error e_i evaluated at the last feasible point e_i^0, and it is the same as the influence function. Therefore, a joint distribution function (objective function of data reconciliation algorithm) can be rewritten as a linear function approximately, i.e.,

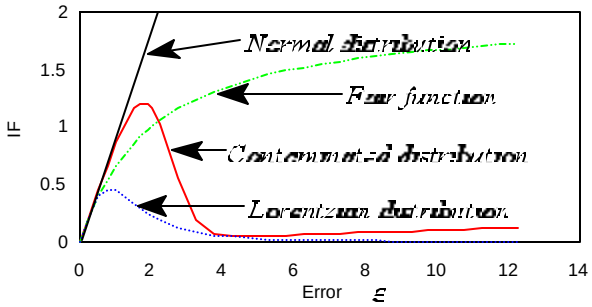

Figure 3.4 The Influent Functions of Distributions

$$P = \sum w_i e_i = \sum IF_i e_i \qquad (3\text{-}32)$$

As shown in Eq. 3-32, the objective function is equal to the sum of products of influence function and error of measurements. The influence function of a measurement in the joint distribution function is a weight of a measurement in the optimization objective (minimization), and it represents the contribution (or effect) of a measurement on the estimator. Therefore, it is optimal that a distribution function has a larger influence function value for measurements with small (random) errors and has a smaller (or zero) influence value for measurements with large (gross) errors. This means that measurements with small (random) errors contribute more on the estimation of reconciled data than those with large (gross) errors, and the estimation from this

type of distribution function is less sensitive to the presence of gross errors when measurements with both random and gross errors are used to reconcile process data.

The influence function for the normal distribution linearly increases with increasing error. This indicates that a measurement with a large error has a large contribution on the estimators based on the definition of influence function. This is inappropriate, and it gives biased estimation if measurements with gross errors are used in the data for data reconciliation. The shape of the influence function for Fair function is similar to the normal distribution, except that the increase of its influence function slows and finally stops with the increase of error size for larger (gross) errors. Compared with the normal distribution, it is less sensitive to the presence of larger gross errors and is able to bound the effect of extremely large gross errors. However, the shape of its influence function, i.e., a larger error has a larger value of influence function, indicates that a measurement with a large error contributes more on the estimation of reconciled variables (estimators) than one with a small error. This is not appropriate, and it gives biased estimation when measurements with gross errors are included in the data for data reconciliation.

For errors size from 2σ to 4σ, value of influence function for contaminated Gaussian distribution reduces with the increase of errors and reaches a lowest value at around 4σ. For error size larger than 4σ, its influence function increases linearly with the increase of an error with a much lower increase rate. As shown in Figure 3.4, the influence function of the contaminated Gaussian distribution has a much smaller value for measurements with gross errors ($\epsilon > 4$) than measurements with random errors ($\epsilon < 2$). The influence function for contaminated Gaussian distribution has a better pattern than the normal distribution and Fair function. However, for

extremely large gross errors, such as error larger than 50σ, the influence function for contaminated Gaussian distribution still demonstrates the unbounded nature as the normal distribution. The influence function of Lorentzian distribution function has the best pattern. It has a larger value for measurements with random (small) errors and it decreases with the increase of error size for errors larger than random errors and eventually goes to zero.

The relative efficiencies of four distributions (normal, contaminated Gaussian distribution, Fair function, and Lorentzian distribution) are compared in Figure 3.5. As shown in Figure 3.5, the normal distribution function has the smallest variation (variance) in all distributions. The normal distribution is a ideal distribution, and it usually is used to compare the efficiency of other distributions. Figure 3.5 shows that the variation (or variance) of the contaminated Gaussian distribution is the smallest in three distribution (contaminated Gaussian distribution, Lorentzian distribution, and Fair function). The contaminated Gaussian distribution has the highest relative efficiency to the normal distribution in three distributions based on the definition of relative efficiency. Therefore, it has higher accuracy of the estimation when measurement error is normal. The Fair function has the largest

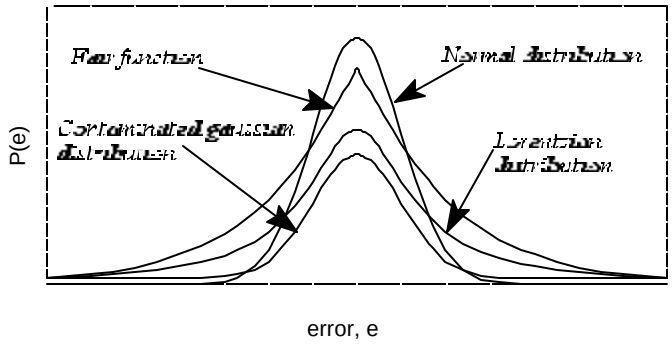

Figure 3.5 The Distributions of Measurement Error

variation (variance), hence it has the lowest efficiency compared with Lorentzian and contaminated Gaussian distributions. The relative efficiency for four distributions reduces in order: normal distribution, contaminated Gaussian distribution, Lorentzian distribution, and Fair function.

In summary, the evaluation of influence functions of distributions shows that normal distribution causes significant biased estimation if measurements with gross errors are used to reconcile data and the degree of bias increases unboundedly with the increase of errors. Therefore, a iterative elimination strategy is required to avoid the bias whenever a gross error is detected. Both contaminated Gaussian distribution and Lorentzian distribution have higher relative efficiency to the normality than Fair function and have a better influence function pattern than normal distribution and Fair function. The comparisons of influence function and relative efficiency concluded that both contaminated Gaussian and Lorentzian distributions have a better combination of influence function (gross error sensitivity) and relative efficiency (estimation accuracy), and therefore, they will have a better performance when reconciling data with both random and gross errors. The contaminated Gaussian distribution will have the best performance for measurements with moderate size of gross errors among four distribution; and Lorentzian will be more effective for extremely large gross errors or infinity gross errors.

The discussion above is based on the assumption that the measurement errors in plant data follow an approximate normal distribution with a few of extreme observations (i.e., containing gross errors). This assumption is close to the actual situation in chemical plants. However, if this is not the case, the distribution function of the measurement error must be redeveloped based on the true structure of the errors. In general, the performance of a

distribution for estimator strongly relies on the knowledge of the real error structure. With this knowledge, the distribution function of measurement errors can describe their behavior patterns, and the robustness and efficiency of the distribution for the estimator can be evaluated.

Modified Compensation Strategy: The theoretical evaluation above and numerical results in Chapter V showed that measurement test method results in seriously biased estimation when some of measurements contain gross errors. This has been reported in literature (**Mah, 1990; and Crowe, 1994**). Therefore, a strategy to eliminate the biased estimation from the presence of gross errors is necessary for measurement test. However, the strategies proposed in literature require the significant modification of the plant model, which is inefficient and difficult to implement. Also, the nodal aggregation to eliminate the measurements with gross errors in the iterative elimination strategies may not applicable for complex constraints.

From the numerical study of combined gross error detection and data reconciliation algorithms which is discussed in Chapter V, it was found that a larger gross error tends to cause the reconciliation algorithms to distribute the error to its neighboring measurements, and it is particularly serious for measurement test method that uses the normal distribution function. The presence of larger gross errors causes significant misrectification, and it can be observed by the increase number of type I errors. Therefore, a modified compensation strategy is proposed to avoid this misrectification based on the factors observed in the computations for the sulfuric acid plant:

1. After data reconciliation, a measurement containing a gross error is more likely to have larger rectification (measurement adjustment), which is the difference between the

measurement and the reconciled value, $a_i = \tilde{x}_I - y_i$, than measurements with random errors.

2. After data reconciliation, the error remaining in a variable is small and is in the range of random errors.

3. A measurement with a gross error only causes misrectification in its neighboring measurements (measurements in the same unit as this measurements and in the two adjacent units at its up and down streams); and two measurements with gross errors that are not located in the same unit or in two adjacent units in a process will not interact with each other.

The above three factors were found from the numerical study for combined gross error detection and data reconciliation as described in Chapter V. The numerical studies in Chapter V showed that the average relative gross error reductions were 84.3% for measurement test, 96.7% for Tjoa-Biegler's method, and 93.3% for Lorentzian. Therefore, it is appropriate to assume that the reconciled value of an abnormal measurement contains only random error after data reconciliation. For example, if a measurement has an error size at 20σ, the remaining error after data reconciliation is 3σ for measurement test, 0.6σ for Tjoa-Biegler's method, and 1.3σ for Lorentzian distribution function method. Also, it was observed that a measurement with a very large gross error may be detected with a gross error twice in the numerical study for modified compensation measurement test method. For instance, if a measurement with gross error size at 30σ, the error reduction for this measurement in the first data reconciliation is 80%, and the remaining error in this measurement is 6σ. At the second data reconciliation, this

measurement may have 70% error reduction, and the remaining error of the reconciled value for this measurement is 1.8σ which is in random error range. In addition, the numerical studies observed that if two measurements with two gross errors exist in two non-adjacent units, these two gross errors will not interact with each other. They are present as two single gross errors.

The modified compensation strategy can be incorporated with a combined gross error detection and data reconciliation algorithm to improve the misrectification of the algorithm. In this research, the modified compensation strategy is incorporated with measurement test method and was tested with multiple gross errors that is discussed in Chapter V. The procedure for modified compensation measurement test (MCMT) method is illustrated in the following:

Step 1 This step is to classify the neighboring measurements for each measured variable. For each measured variable, the measurements that are located in the same unit as this measured variable or are located in the two adjacent units at its up and down streams are classified as the neighboring measurements of this measured variable. A group of measurements consist of a measured variable and its neighboring measurements, and the measured variable is the core measurement of this group. If a process has 40 measured variables, there are 40 groups of measurements.

Step 2 Solve Eq. 3-4 to reconcile the process data and compute the measurements errors, **e**.

Step 3 Compare the standardized measurement error ϵ_i, $\epsilon_i = e_i / \sigma_i$,, with the critical values C based on the test statistic in Eq. 3-5. If $|\epsilon_i| > C$, then denote measurement i as one suspected of containing a gross error. All suspected measurement are included in set S.

Step 4 If set S is empty, then no gross error in measurements and proceed to step 5. Otherwise replace the measurement corresponding to the largest $|\epsilon_i|$ in set S with its reconciled data for each group. If only one measurement in a group is suspected of containing a gross error, then replace this measurement with the value from reconciled data and include it in set G. Set G includes the measurements that are identified with gross errors. If two or more measurements containing gross errors belong to the same group, then replace the measurement that has the largest value of $|\epsilon_i|$ in the group with its reconciled value and include it in set G. Then go back to step 2.

Step 5 Repeat step 2 to 4 until no suspected measurement is identified. Then the measured variables in set G are declared containing gross errors.

The above is the procedure for the modified compensation measurement test method. Step 1 for group classification should conduct before the computation. The classification result can be incorporated with the data reconciliation optimization problem and programmed in GAMS code to automatically construct a set of compensated measurements for next iterative data reconciliation. In this research, this modified compensation strategy is conducted manually with measurement test method. This modified compensation strategy can be incorporated with other gross error detection and data reconciliation algorithms to further improve the performance of the

algorithms. Their procedures are the same as MCMT, except that the distribution and test statistic for reconciling data and identifying gross errors are different for different algorithms.

C-2. Methodology of Simultaneous Data Reconciliation and Parameter Estimation

To conduct on-line parameter estimation, the important information that must be determined includes the determination of key parameters, the selection of necessary plant measurements, the construction of precise constraints among the process variables and parameters, and the investigation of the algorithms for parameter estimation. The general rules for the determination of key parameters and necessary measurements and the construction of constraints in process model will be discussed in plant model formulation section later. The distribution functions that are applicable to combined gross error detection and data reconciliation can be used for simultaneous data reconciliation and parameter estimation. These are the normal distribution for least squares method, the contaminated Gaussian distribution, and robust function as described and they were evaluated in previous section.

The general methodology of simultaneous data reconciliation and parameter estimation for the error-in-variables model has a structure similar to data reconciliation. The difference is that the parameters in plant model are considered as variables along with process variables in simultaneous data reconciliation and parameter estimation rather than being constants in data reconciliation. Both process variables and parameters are simultaneously estimated through the optimization of parameter estimation. The general mathematical statement for simultaneous data reconciliation and parameter estimation is written as:

$$\textit{Maximize}: \quad P(\mathbf{y}, \mathbf{x}) \tag{3-33}$$

$$\begin{aligned} & \mathbf{x}, \mathbf{z}, \boldsymbol{\theta} \\ \textit{Subject to}: \quad & \mathbf{f}(\mathbf{x}, \mathbf{z}, \boldsymbol{\theta}) = 0 \\ & \mathbf{x}^L \le \mathbf{x} \le \mathbf{x}^U, \mathbf{z}^L \le \mathbf{z} \le \mathbf{z}^U, \boldsymbol{\theta}^L \le \boldsymbol{\theta} \le \boldsymbol{\theta}^U \end{aligned}$$

where $P(\mathbf{y}, \mathbf{x})$ represents the joint probability density function **to be optimized. The equality constraints f denote the plant model which gives the relationship among the process variables and parameters.** $\mathbf{x}^L \le \mathbf{x} \le \mathbf{x}^U$, $\mathbf{z}^L \le \mathbf{z} \le \mathbf{z}^U$, and $\boldsymbol{\theta}^L \le \boldsymbol{\theta} \le \boldsymbol{\theta}^U$ represent the bounds on process variables ($\mathbf{x}$ and $\mathbf{z}$) and parameters $\boldsymbol{\theta}$. The constraints in Eq. 3-33 are the same for different algorithms of parameter estimation. However, the objective function can be based on different distribution functions. These distributions describe the error structure of measurements that are used to estimate the parameters and process variables. The normal distribution (least squares method), contaminated Gaussian distribution, and Lorentzian distribution, given by Eq. 3-3, 3-9, and 3-13 respectively, can be used as the objective function for simultaneous data reconciliation and parameter estimation.

If the distribution function only describes the random nature of measurement errors, e.g., normal distribution, then the measurements used to estimate the process parameters can only contains random errors. The plant data from DCS needs to be pre-processed through the combined gross error detection and data reconciliation step to eliminate or rectify the gross errors before it can be used for parameter estimation. This requires two steps to estimate the process parameters, and it will be described in the following. If the distribution function takes into account the distribution pattern for both random and gross errors in the measurements and it is able to rectify both random and gross errors, then the measurements used to estimate process

parameters can contain random and/or gross error, and the plant data sampled from DCS can be used directly for simultaneous data reconciliation and parameter estimation. This requires only one step to estimate process parameters. The contaminated Gaussian distribution and robust function have this type of the properties, and they will be used to conduct the combined data validation and parameter estimation. Then gross error detection, data reconciliation, and parameter estimation will be combined into one optimization problem.

Two-Step Estimation: As discussed previously, the normal distribution of the least squares method requires that the measurements used for parameter estimation contain only random errors. Therefore, a data pre-processing step is required to eliminate or rectify the gross errors before the parameter estimation. This requires two steps to estimate the plant parameters. Step one uses the contaminated Gaussian distribution to detect and rectify the measurements with gross errors and then constructs a new set of measurements that only contains random errors. Step two uses the least squares method to conduct simultaneous data reconciliation and parameter estimation with the new set of measurements.

Step one reconciles process data using a combined gross error detection and data reconciliation algorithm, contaminated Gaussian distribution, and identifies the gross errors based on reconciled data. The optimization problem for step one has the mathematical statement as:

$$\underset{x,\,z}{\textit{Maximize}}: \quad P(y|x) \quad \prod_i \frac{1}{\sqrt{2\pi}\sigma_i}\left\{(1-\eta)\,e^{-\frac{(y_i-x_i)^2}{2\sigma_i^2}} \quad \frac{\eta}{b}\,e^{-\frac{(y_i-x_i)^2}{2b^2\sigma_i^2}}\right\} \tag{3-34}$$

$$\textit{Subject to}: \quad \mathbf{f}(\mathbf{x}, \mathbf{z}, \boldsymbol{\theta}) = 0$$
$$\mathbf{x}^L \le \mathbf{x} \le \mathbf{x}^U,\ \mathbf{z}^L \le \mathbf{z} \le \mathbf{z}^U$$

where **y** is the plant measurements sampled from distributed control system for measured variables and **x** represents the true values of the measured variables. **z** denotes the unmeasured process variables. **θ** is the vector of process parameters, and they are constants in this step. Solving Eq. 3-34 reconciles all plant data and estimates the values of all process variables. This set of reconciled data will maximize the joint probability and satisfies the constraints. Based on the reconciled data, the gross errors in the measurements are identified by the test statistic and a new set of measurements is constructed. This new set of data is composed of reconciled data for measurements with gross errors and the original plant data for measurements without gross errors. Then this new set of measurements contains only random errors, and it is used in step two to estimate plant parameters.

Step two uses the least squares method to simultaneously reconcile process variables and estimate parameters with the new set of measurements generated in step one. The optimization problem for step two is stated as:

$$\begin{aligned} &\textit{Minimize}: \quad \underset{\mathbf{x},\,\mathbf{z},\,\boldsymbol{\theta}}{} \quad \mathbf{e}^{\mathrm{T}}\boldsymbol{\Sigma}^{-1}\mathbf{e} = (\mathbf{y}-\mathbf{x})^{\mathrm{T}}\Sigma^{-1}(\mathbf{y}-\mathbf{x}) \\ &\textit{Subject to}: \quad \mathbf{f}(\mathbf{x},\,\mathbf{z},\,\boldsymbol{\theta}) = 0 \\ &\qquad\qquad \mathbf{x}^{\mathrm{L}} \le \mathbf{x} \le \mathbf{x}^{\mathrm{U}},\ \mathbf{z}^{\mathrm{L}} \le \mathbf{z} \le \mathbf{z}^{\mathrm{U}},\ \boldsymbol{\theta}^{\mathrm{L}} \le \boldsymbol{\theta} \le \boldsymbol{\theta}^{\mathrm{U}} \end{aligned} \tag{3-35}$$

where **y** represents the measurements generated from step one for the measured variables. The process variables (**x** and **z**) and parameters (**θ**) are variables, and they will be determined simultaneously by solving this minimization problem.

The strategy to construct the measurements from step one (combined gross error detection and data reconciliation) of the two-step estimation avoids the modification of the

optimization program and the interaction between the two data reconciliation results associated with gross error detection in step one and with parameter estimation in step two. Although the elimination of measurements with gross error will completely avoid the effect of gross error on the estimation, it requires significant modification on the optimization program, such as the reconstruction of constraints and reclassification of measured and unmeasured variables. Also, it may causes the problem of unobservability. This is inefficient and not appropriate for the automatic implementation of on-line optimization. In addition, the gross errors of measurements are significantly reduced after data reconciliation using contaminated Gaussian distribution function. It is appropriate to assume that the reconciled data of measurements with gross errors contain only random errors and it can be used with other normal plant data to estimate process parameters. Therefore, the least squares method is suitable for the simultaneous data reconciliation and parameter estimation because it has the highest estimation accuracy when the measurements do not contain gross errors.

One-Step Estimation: In one-step estimation, the objective function uses a distribution function that takes into account the error pattern for both random and gross errors. This type of distribution function has an ability to ignore the contribution of gross errors on the estimation and to rectify the gross errors using good measurements through process constraints. Therefore, this type of distribution function can be used to estimate the process parameters and variables simultaneously using the plant data from DCS which may contains both random and gross errors. The objective function based on contaminated Gaussian distribution or Lorentzian distribution is this type, and it can be used for simultaneous gross error detection, data reconciliation, and

parameter estimation. Therefore, gross error detection, data reconciliation, and parameter estimation are combined into one nonlinear optimization problem, and this is called one-step parameter estimation method.

The general mathematical statement for one-step estimation using contaminated Gaussian distribution is written as:

$$\underset{x,\,z,\,\theta}{\textit{Maximize}}: \quad P(y|x) \quad \prod_i \frac{1}{\sqrt{2\pi}\sigma_i}\left\{(1-\eta)\,e^{-\frac{(y_i-x_i)^2}{2\sigma_i^2}} + \frac{\eta}{b}\,e^{-\frac{(y_i-x_i)^2}{2b^2\sigma_i^2}}\right\} \tag{3-36}$$

$$\textit{Subject to}: \quad \mathbf{f}(\mathbf{x}, \mathbf{z}, \boldsymbol{\theta}) = 0$$
$$\mathbf{x}^L \le \mathbf{x} \le \mathbf{x}^U,\ \mathbf{z}^L \le \mathbf{z} \le \mathbf{z}^U,\ \boldsymbol{\theta}^L \le \boldsymbol{\theta} \le \boldsymbol{\theta}^U$$

where **y** is the plant measurements from distributed control system for measured variables. Process variables (**x** and **z**) and parameters (**θ**) are variables, and they will be determined by solving the maximization problem. Solving Eq. 3-36 will simultaneously estimate the process variables and parameters. Then, each measurement will be examined by the test statistic based on the estimated measurement error to determine if it contains a gross error.

Summary: Two strategies are proposed to conduct parameter estimation: one-step estimation method and two-step estimation method. The two-step estimation includes step one that conducts combined gross error detection and data reconciliation to construct a new set of measurements for next step estimation and step two that conducts simultaneous data reconciliation and parameter estimation to estimate process parameters and variables. The one step estimation combines gross error detection, data reconciliation, and parameter estimation into one nonlinear optimization problem. In one-step estimation, the plant data from distributed

control system is directly used to conduct simultaneous data reconciliation and parameter estimation, then each measurement is examined to see if containing gross error based on the reconciled results.

C-3. Plant Economic Optimization

The objective of plant economic optimization is to generate a set of optimal operating setpoints for the distributed control system. This set of optimal setpoints will maximize the plant profit, satisfy the current constraints in plant model, and meet the requirement of market demanding and restriction on pollutant emission. This optimization can be achieved by maximizing the economic model subject to the process constraints. The general mathematical formulation for plant economic optimization is:

$$\begin{aligned} &\underset{\mathbf{x},\,\mathbf{z}}{\textit{Maximize}}: && P(\mathbf{x}) \\ &\textit{Subject to}: && \mathbf{f}(\mathbf{x}, \mathbf{z}, \boldsymbol{\theta}) = 0 \\ & && \mathbf{g}(\mathbf{x}, \mathbf{z}, \boldsymbol{\theta}) \le 0 \\ & && \mathbf{x}^L \le \mathbf{x} \le \mathbf{x}^U,\ \mathbf{z}^L \le \mathbf{z} \le \mathbf{z}^U \end{aligned} \tag{3-37}$$

where $P(\mathbf{x})$ represents the economic model (e.g., profit function). The equality constraints $\mathbf{f}$ are the same as those in data reconciliation. The inequality constraints $\mathbf{g}$ represent the additional restrictions for the economic optimization, such as the demand for the main products and by products, availability of raw materials, maximum and minimum capacities of the equipment, and restriction on the waste/pollutant emission. The bounds $\mathbf{x}^L \le \mathbf{x} \le \mathbf{x}^U$ and $\mathbf{z}^L \le \mathbf{z} \le \mathbf{z}^U$ represent the allowable minimum and maximum operating conditions for the process variables and product quality requirements.

The economic model in Eq. 3-37 can be different depending on the objectives of the optimization. The objectives can be to maximize plant profit, optimize plant configuration for energy conservation, minimize undesired by-products, minimize the waste/pollutant emission, or a combination of these objectives. If the objective is to maximize the plant profit, then a value-added profit function can be used as the objective function (Zhang, 1993), i.e.,

$$P(\mathbf{x}) = \text{Income from Sale of Products - Cost of Raw Materials - Operating and Maintenance Costs} \tag{3-38}$$

or it can be mathematically expressed as:

$$P(\mathbf{x}) = \mathbf{sx} - \mathbf{cx} \tag{3-39}$$

where **s** and **c** are constant vectors representing the sale prices of products and cost of the raw materials respectively. For vector **s**, the elements with respect to the variables of products are the sale prices of the corresponding products, and other elememts in **s** are zero. For vector **c**, the elements with respect to the variables of raw materials are the costs of the corresponding raw materials, and other elememts in **c** are zero. In this formulation, the operating and maintenance costs can be incorporated in the sale prices of the products or taken as constant.

Figure 3.6 gives one of the profit function used for sulfuric acid contact process of IMC Agrico plant. The IMC Agrico plant does not sell sulfuric acid on the open market because it is used in the production of phosphoric acid in an adjacent plant. Also, the costs for the labor, maintenance, and overhead are combined into operating cost, and these costs are included as an adjustment to the price charged to the phosphoric acid plant for the sulfuric acid product. As a results, the operating costs were considered as a fixed adjustment to the acid product price on

Profit Function:

$$f = s_{F64}F_{64} + s_{FS8}F_{S8} + s_{FS14}F_{S14} - c_{F50}F_{50} - c_{FS1}F_{S1} - c_{F65}F_{65}$$

Variable	Description	Sale and Cost Coefficients
F_{64}	Acid Product flow rate	\$21.6/long ton
F_{S8}	Low pressure steam flow rate	$\$1.55/10^3$ lb
F_{S14}	High pressure steam flow rate	$\$2.34/10^3$ lb
F_{50}	Raw sulfur flow rate	\$54/long ton
F_{S1}	Boiler feed water flow rate	$\$0.17/10^3$ lb
F_{51}	Dilution water flow rate	$\$0.05/10^3$ lb

Figure 3.6 Value Added Profit Function for the Contact Process

a per pound basis. This adjustment is included in the acid sale price list in Figure 3.6. The prices used for this study are provided by the IMC Agrico engineers. As shown in Figure 3.6, the profit function is equal to the total value of

products (sulfuric acid F_{64}, low pressure steam F_{S8}, and high pressure steam F_{S14}) subtracting the cost of raw materials (sulfur feed rate F_{50} , boiler feed water F_{S1} , and dilution water F_{51}).

The profit function incorporated with plant model as shown in Eq 3-43 is solved to determine the optimal values for all process variables. These optimal set point will maximize the plant profit, satisfy the constraints in process model and the restrictions on the product demand, raw material availability, equipment capacities, and pollutant emission.

As discussed by Richard (1987) and Zhang (1993), there are three important factors that can significantly affect the economic picture for sulfuric acid contact process. First is the cost for major raw material, sulfur feed. Thus, the conversion of sulfur into product is economically

important in this process. Higher conversion of sulfur to sulfuric acid will have higher profit. Secondly, the efficient extraction of the heats of combustion and chemical reaction by steam streams will increase the value of by product (steam) and the conversion rate of SO_2 to SO_3. Therefore, it benefits to the conversion of sulfur to sulfuric acid. Finally, environmental restrictions must be met. All these three factors interactively affect the final economic picture of the plant.

C-4. Formulation of Plant Models for On-Line Optimization

As discussed in the previous sections, all optimization problems require the plant model as constraints. The performance of these optimization problems strongly relies on both the objective function (the data reconciliation algorithm or profit function of the optimization problem) and the constraint equations of the optimization problem (the plant model to describe a process). A accurate plant model is necessary for on-line optimization.

C-4-1. Formulation of Constraints for Typical Chemical Process Units

The mathematical models to describe the relationship among variables may be classified in accordance with a number of aspects (Madron, 1992). For the models based exclusively on statistical evaluation of measured data, they are referred to as empirical or regression model. When building these types of models, no prior information about the physical and chemical attributes of the modeled object is used. The distribution model of measured data is a empirical or regression model. For the models that are built based on the laws of nature, they are called as mechanistic model since a certain mechanism is assumed. The process models used in on-line optimization are belong to the type of mechanistic model, and they are set up based on the

conservation laws as well as the knowledge on the physical and chemical attributes of the modeled object.

The information to build the mechanistic models can be divided into two groups. The laws of conservation (mass and energy) belong to the first group. In most cases, these law are valid strictly, and they can be used to verify the validity of other assumptions serving as the basis for modeling. The second group includes the other laws of nature, dependencies assessed empirically, and the like. The validity of this type of information is not the same as that of conservation laws; and it has some character of hypotheses. Typical examples are the models of chemical phase equilibrium, models of kinetics and stoichiometry of chemical reactions, chemical engineering correlations, etc.

A chemical plant includes tens to hundreds of process units, such as heat exchangers, reactors, distillation columns, absorption towers and others. For each unit, a number of constraints between input and output streams are imposed based on the conservation laws and the knowledge on the process. These constraints describe the relationship among the process variables and parameters and provide a link of all variables and parameters. They relate the individual measurements and provide the resolution for error rectification. The following gives a brief discussion of the constraint derivation for some typical chemical process units.

Heat Exchanger:

For a heat exchanger unit with multiple components in one side and single component in the other side, its flowsheet diagram and the constraints are shown in Figure 3.7. This unit includes two input streams (F1 and F3) and two output streams (F2 and F4). The heat is transferred from hot stream F3 to cold stream F1. The hot streams F3 and F4 have single component; and cold streams F1 and F2 have c components. The constraints for this unit are set up based on the conservation laws and the knowledge on the process.

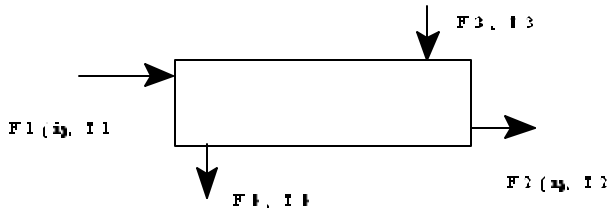

Constraints:

$$F1(i) - F2(i) = 0, \text{ for } i=1,2,..,c \quad (1)$$
$$F3 - F4 = 0 \quad (2)$$
$$(H1 + H3) - (H2 + H4 + Q_{loss}) = 0 \quad (3)$$
$$H3 - H4 - Q_{loss} - U A \Delta T_m = 0 \quad (4)$$
$$H1 = h1(F1(1), F1(2), .., F1(c), T1) \quad (5)$$
$$H2 = h1(F2(1), F2(2), .., F2(c), T2) \quad (6)$$
$$H3 = h2(F3, T3) \quad (7)$$
$$H4 = h2(F4, T4) \quad (8)$$
$$\Delta T_m = Tm(T1, T2, T3, T4) \quad (9)$$

*c - the number of components in stream F1 and F2

Figure 3.7 The Flowchart Diagram and Constraints of a Heat Exchanger

As shown in Figure 3.7, Eq. 1 is the species mass balances for cold streams, F1(i) and F2(i), where i =1, 2, .., c; and Eq. 2 is the mass balance for hot streams, F3 and F4, where F represents the mass flowrate. The total energy balance is shown in Eq. 3, where H represents the enthalpy of a stream and Q_{loss} denotes the heat loss from this unit. Eq. 4 represents the heat transfer equation that gives a restriction on the capacity of the heat exchanger, where U and A represent the heat transfer coefficient and area of the heat transfer, and ΔT_m is the mean

temperature difference between hot and cold streams. Eqs. 1 to 4 are established based on the mass and energy conservation laws. In addition to these four equations, Eq. 5 to 8 are the enthalpy equations to determine the energy of the streams, and they are empirical equations that are set up based on the physical and chemical properties of the species in the streams. Eq. 9 is an empirical function to determine the logarithm mean of temperature difference between hot and cold sides. These nine equations shown in Figure 3.7 simulate the operating behavior of the heat exchanger and provide link among the variables.

Reactors: The reactors are the key units of chemical plants. The performance of this type of units significantly affects plant operating in economic and environmental aspects. The formulation of constraints in this type of units are great important and complicated in regarding of the various types of reactors and the complex reaction kinetics. Unlike a heat exchanger whose constraints are similar regardless of types of equipment, there is a great variation in deriving the constraints for reactors.

There are three types of simple reactors for steady state processes: continued stirring tank reactor (CSTR), plug flow reactor (PFR), and fluidized bed reactor. For CSTR, the mass and energy balances are written as algebraic equations. While the mass and energy balances for PFR and fluidized bed reactor are differential equations that can be discretized into algebraic equations with the numerical methods.

The reactions can be classified into single reaction (the simplest case), parallel multiple reactions, series reactions, and combined parallel and series reactions. In addition, the reaction can have rate equations that have simple kinetics, such as the first, second, .., or nth order

reaction, or the complex reaction rate equations that have a very complicated kinetics and are complex and nonlinear.

In general, the reaction rate equation should be included in plant model. Including the reaction rate equation makes the variables in the reactor observable by the measurements at the up and down stream units. Also, it can reduce the number of necessary flow rate measurements. If the reaction rate is available, and it is determined by the measurable variables, e.g., component flow rate, temperature, and/or pressure, then the generation of species in mass balance equation can be determined by the reaction rate equation that are observable by the measurable variables. However, if the reaction rate equation is not available, then the generation of species in mass balance equation must be determined by the conversion of certain reactant. This conversion can not be considered as a parameter because the conversion of reactant is not a time varying constant as catalyst activity coefficient, and it changes with changes in operating conditions. Also, the conversion can not be determined by other measured variables as the reaction rate equation. Therefore, using conversion of a reactant in the mass balances for a reactor unit increases the unobservability of unmeasured variables in this unit.

Figure 3.8 shows the flowsheet diagram and the constrains for a PFR (sulfur dioxide convertor). This unit includes one input stream F1 and one output stream F2, and each stream has c components. As shown in Figure 3.8, Eq. 1 is the species mass balances for c components, and the reaction rate for component i, r(i), is determined by the basic reaction rate, $r = r(i)/s_i$, and the stoichiometric coefficient of the reaction for component i, s_i. Eq. 2 is the total energy balance. Both mass and energy balances are established based on conservation laws.

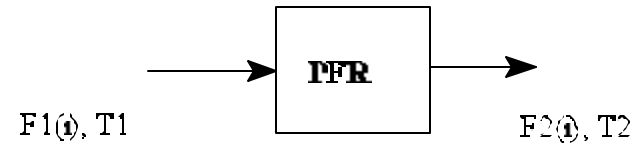

Constraints:

$$\frac{dF(i)}{dL} = r(i)\,A, \text{ for } i = 1, 2, .., n \quad (1)$$

$$\frac{dH}{dL} = r\,\Delta H_{rxn}\,A \quad (2)$$

$$H = H\,(F(1), F(2), .., F(n), T) \quad (3)$$

$$r = E_f\, r(F(1), F(2), .., F(n), T) \quad (4)$$

$$r(i) = r\,\varepsilon_i \quad (5)$$

Boundary Condition:

$$L=0,\ F(i) = F1(i), \text{ for } i = 1, 2, .., n,\ T = T1$$
$$L=L,\ F(i) = F2(i), \text{ for } i = 1, 2, .., n,\ T = T2$$

Figure 3.8 The Flowsheet Diagram and Constraints of a Plug Flow Reactor

Eq. 3 is the enthalpy equation to determine the energy of streams by flow rates and temperatures. Eq. 4 is the basic reaction rate for the reaction r, and the basic reaction rate is determined by kinetics of the reaction. The reaction rate for individual chemical species can be determined by the basic reaction rate r, and the stoichiometric coefficients as given in Eq. 5. In addition, A and L are the cross section area and the length of reactor. E_f is the reaction effectiveness factor, and it is a process parameter. Also, the boundary condition given in Figure 3.8 used to obtain the solution of the differential equations for the reactor.

Distillation and Absorption Columns: The distillation and absorption columns are the important units that can be found in most of chemical plants and refinery processes. They serve as feed preparation units for raw material going to reactor and as product purification units for streams from the reactor. Their performance plays an important role in energy saving, product quality, and environmental control.

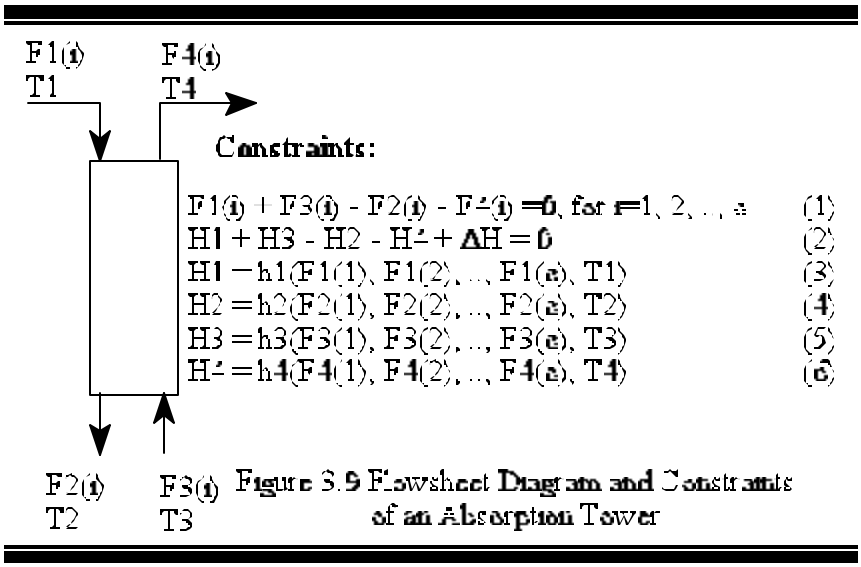

Figure 3.9 Flowsheet Diagram and Constraints of an Absorption Tower

The constraints for distillation and absorption columns are similar. They can be as simple as only including the mass and energy balances for the column, if no parameter need to be estimated. Or they can include more detail information, such as the tray-by-tray equilibrium relation between phases. Figure 3.9 shows the flowsheet diagram of an absorption column and the constraints that include species mass balances and the energy balance over the column. In Figure 3.9, Eq. 1 is the species mass balances for c components, and Eq. 2 is the overall energy balance where ΔH is the heat of absorption. Both Eq. 1 and 2 are based on conservation laws of mass and energy. Eq 3 through 6 are the enthalpy equation to determine the energy of the respect streams, and they are based on the physical and chemical properties of the species in the streams.

C-4-2. Classification of Variables and Determination of the Parameters

After the constraints in plant model are constructed, the variables in the model are divided into two groups of variables, measured variables and unmeasured variables. It is desired to have as many measured variables as possible. In general, more measurements will give a more

accurate estimation of the reconciled data. However, in an industrial process, some of measurable variables are not measured.

For a process, the measured variables are the variables that have measurements from the distributed controlled system (DCS) and the plant control laboratory. The remaining variables in the process model are unmeasured variables. Some additional measurements may be required after the examination of observability and redundancy which will be discussed in the following section. If some more redundant measurements are needed, then additional instruments must be added to provide additional measurements.

There are two types of parameters in the process model. One type is a permanent constant parameter, such as reaction activity energy, stoichiometry of chemical reactions, and the like. This type of parameters is constant all the time. They are constants in the process model and do not need to be estimated on-line. The other type of parameters is time-varying parameters, such as heat transfer coefficients, reaction effectiveness factors, tray efficiency, and the like. This type of parameters varies slowly with time, e.g., 25% change for a month. The values of this type of parameters are determined by the characteristics of the equipment and physical properties of materials but are not strongly relate to the operating condition. The presence of parameters in a plant model usually serves as the restrictions on the capacity of the equipment, and their values provide the information about equipment performance.

For a set of equations to describe a unit or a process, the quantities in the equations can be classified as variables (measured and unmeasured), parameters, and fixed constants as shown in Figure 3.10. The measured variables can be redundant or nonredundant, and the unmeasured

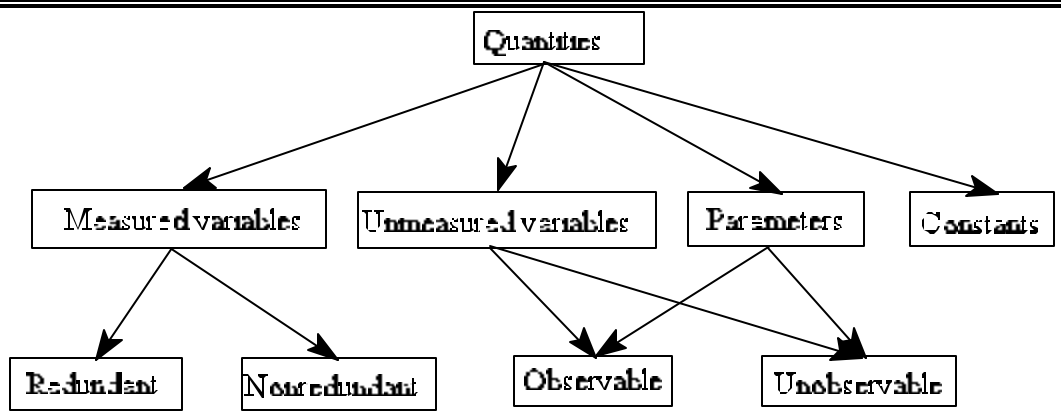

Figure 3.10 Classification of Quantities in Equations

variables and parameters can be observable or unobservable dependent on the numbers of measured variables, unmeasured variables, parameters, and equations. For the heat exchanger shown in Figure 3.7, the stream flow rates and temperatures are measured variables. The enthalpies are unmeasured variables. The overall heat transfer coefficient is process parameter, and it must be updated on-line to have the model match the plant performace. The heat exchanger area is a constant.

C-4-3. Examination of Observability and Redundancy

The plant model is used as constraints in data reconciliation to adjust the measurements for measured variables to satisfy the material and energy balances and to compute the values of unmeasured variables and parameters. In economic optimization, plant model is the constraints of the optimization problem to describe the process, and it is used to determine the set points for DCS. To conduct data reconciliation, redundant measurements are required to rectify the errors in measurements. Also, unmeasured variables and parameters must be observable to obtain a

unique solution. The following discusses the examination of observability and redundancy for a plant model.

The definition of observability is given by Crowe (1989) as:

> "An unmeasured quantity at steady state is observable if and only if it can be uniquely determined from a fixed set of values, corresponding to the measured variables, which are consistent with all of the given constraints. Any unmeasured quantity which is not so determinable is unobservable."

The definition of redundancy is given by Crowe (1989) as:

> "A measured quantity is redundant if and only if it would be observable if that quantity was not measured. Otherwise, the measured quantity is non-redundant."

The method to examine the observability and redundancy based on these definitions was given by Crowe (1989) using the coefficient matrices of constraint equations as discussed in Chapter II, and it is applicable to linear constraints.

In the following, the method to examine observability and redundancy is proposed based on the concept of degree of freedom. For a set of m equations that includes n variables, in which n_1 variables are measured, and p parameters, the unmeasured variables and parameters are observable if the number of measured variables n_1 is larger than or equal to the number of degree of freedom for this set of equations. The number of degree of freedom for a set of equations is the number of variables and parameters subtracted by the number of equation, i.e., n+p-m. For a set of m equations that includes n variables, in which n_1 variables are measured, and p parameters, the measurements have redundancy if the number of measured variables n_1 is larger

than the number of degree freedom of this set of equations, n+p-m. Also, the number of redundancy of measurements is equal to n_1-(n+p-m).

The examination of observability and redundancy can be conducted for each unit or each balance node or for entire process (multiple units). If it is conducted for each unit, then the examination result is called local observability and redundancy. If it is conducted for entire process, then the examination result is called global observability and redundancy.

For a set of constraint equations of a unit, it is said that the unmeasured variables and parameters are local observable, if the number of measured variables is larger than or equal to the degree of freedom of this set of equations, which is the number of variables (measured and unmeasured) and parameters subtracted by the number of equations. In local observability and redundancy examination, the classification of measured variables and unmeasured variables is slightly different from the definition given above. A class of dummy measured variables is intrduced in local examination to represent the unmeasured flow rate variables that can be directly determined by available measured variables at the up or down stream. The number of measured variables equal the sum of the numbers of measured variables and dummy measured variables in the equations, and the number of unmeasured variables equal the number of unmeasured variables subtracted by number of dummy measured variables.

For a set of constraint equations of a unit, it is said that the measured variables have local redundancy if the number of measured variables is larger than the degree of freedom of this set of equations, and the number of local redundancy of measurements equals the number of measured variables subtracted by the number of degree of freedom. For individual measured

variables, it is said that a measured variable is redundant if all unmeasured variables and parameters are observable after the measured variable is changed to a unmeasured variable. Otherwise, the measured variable is not redundant.

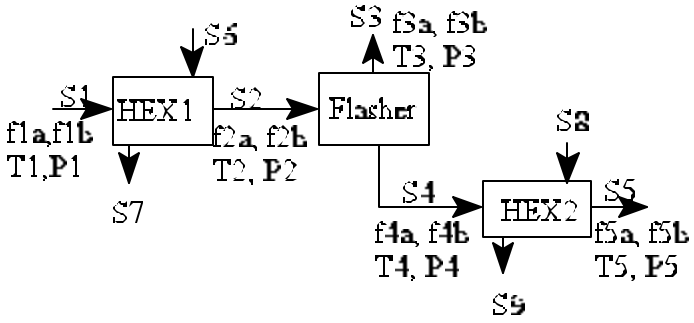

Figure 3.11 A Simple Flowsheet Diagram

Figure 3.11 shows a process flow diagram with three units, and these three units are heat exchanger (HEX1), flasher, and heat exchanger (HEX2). In streams S1, S2, S3, S4, and S5, there are two components A and B. If variables f1a, f1b, T1, P1, f5a, f5b, T5, and P5 are measured variables and other are unmeasured variables, then the unmeasured variables f2a, f2b, f4a, and f4b are dummy measured variables in flasher unit examination. Because f2a, f2b, f4a, and f4b can be directly determined by measured variables f1a, f1b, f5a, and f5b respectively through the component mass balances. Howerver, T2 and T4 are not dummy measured variables because they can not be directly determined by available measured variables.

For a heat exchanger shown in Figure 3.7, this unit has nine equations which involved 13 variables (F1, F2, F3, F4, T1, T2, T3, T4, H1, H2, H3, H4, and ΔT_m) and two parameters (U and Q_{loss}) if both cold and hot streams have single components. The degree of freedom for this set of equations and variables are six. Therefore, six variables must be measured variables or

dummy measured variables to satisfy the observability, and more than six variables must be measured or dummy measured variables to provided redundancy for error rectification.

After the unit by unit examination of observability and redundancy, the global observability and redundancy are examined for entire process based on the number of measured variables and degree of freedom for the entire process. In global observability and redundancy examination, all dummy measured variables belong to unmeasured variables.

If the measured variables are not correctly selected, some of unmeasured variables or parameters may be unobservable even though the number of measurements is larger than the degree of freedom. In order to avoid the incorrect selection of measured variables, a coefficient matrix of linearized constraints is used to further examine the observability for entire process based on Crowe's method. In this step, the nonlinear constraints are linearized using a set of feasible solution of the constraint equations that is close to the normal operating condition. Then this linearized constraints are rearranged as:

$$\mathbf{Ax} + \mathbf{Bz} + \mathbf{E\theta} = 0 \tag{3-40}$$

or

$$(A\ B\ E)\begin{pmatrix} x \\ z \\ \theta \end{pmatrix} \quad 0 \tag{3-41}$$

where **A**, **B**, and **E** are the linearized constraint coefficient matrices with respect to measured variables **x**, unmeasured variables **z** and parameters **θ**. Eq. 3-40 or Eq. 3-41 can be rearranged as:

$$\mathbf{Bz} + \mathbf{E\theta} = -\mathbf{Ax} \tag{3-42}$$

or

$$(B\ E)\begin{pmatrix} z \\ \theta \end{pmatrix} \quad Ax \tag{3-43}$$

A lemma given by Crowe in Chapter II is used to determine the observability. If there exists a nonzero vector **t** such that (**BE**) **t** = 0, then each unmeasured variable or parameter corresponding to a nonzero element of **t** is unobservable. Therefore, the solution of **t** from equation (**BE**) **t** = 0 identifies the unobservable unmeasured variables or parameters. More discussion on this lemma was given in Chapter II.

Based on the discussion above, a general method to examine the observability and redundancy of process models is given as:

1. Examine the local observability and redundancy unit by unit based on the criteria given above, i.e., the number of measured variables must be larger than or equal to the degree of freedom. All unmeasured variables and parameters must be observable for each unit. It is not required that every unit has redundancy in measurements. However, at least one degree of freedom is recommended for the unit with parameters to be estimated.

2 Examine the global observability and redundancy for entire process based on the criteria given above. The number of measured variables must be larger than the degree of freedom of the plant model. The number of redundancy in measurements equal the number of measured variables subtracted by the degree of freedom of the plant model.

3. Linearize the nonlinear constraints in plant model using a set of feasible solution of the constraint equations that is close to the normal operating condition and rearrange the linearized constraints as Eq. 3-43. Solve the equation (**B E**) **t** = 0 for the solution **t**. If the solution of **t** is a zero vector, then all unmeasured variables **z** and parameters **θ** are observable; If some elements of **t** is nonzero, then the variables corresponding to the

nonzero elements are unobservable. This step is to avoid the incorrect selection of measured variables.

This is the general procedure to examine the observability and redundancy of the plant model. In case of unobservability or non-redundancy exists, then plant model must be modified to satisfy the requirement of observability and redundancy. The strategies to improve the observability and to provide more redundancy of plant model is given in the following:

1. Change the unobservable unmeasured variables into measured variables, if it is measurable.
2. Combine the unobservable variable with other observable unmeasured variable, i.e., combining two unmeasured variables into one, if possible; and recheck the observability of the new unmeasured variable.
3. Add additional constraints on the unobservable variables and recheck the observability of the unmeasured variables.
4. Adjust some of parameters as constants, if their values do not vary significantly or their variations do not significantly affect the accuracy of the plant model. Or divide the parameters into two or more subsets and estimate them alternately in the sequence of on-line optimization.
5. Add repeated measurements for the non-redundant measured variables.

To have a better result from the optimization and to ensure the validity of the optimization result when multiple gross errors exist, excessive measured variables in additional to the necessary

measurements are needed. It is recommend to incorporate as many measurements as possible in data reconciliation and parameter estimation of on-line optimization.

C-4-4. Summary on Plant Model Formulation

After the plant model is completely formulated and the process variables are correctly classified into measured variables (**x**), unmeasured variables (**z**), and parameters (**θ**), the accuracy of the plant model must be examined. To assess precision of the plant model, the simulation results predicted by the plant model must be compared with the true data of the plant, such as the consistent and complete plant design data to ensure that the constraint equations are correctly describing the processes. This can be done by designating some of plant design values as measured data. Then this data is used to estimate the values of the unmeasured variables and the plant parameters, and the estimated parameters and process variables are compared with the plant design data. If the predicted results are very close to the design data with a less than 1% relative difference, then it is said that the plant model precisely simulates the plant.

Above is the brief discussion on the development and examination of plant model. The following gives the general procedure to formulate a plant model:

1. Derive the process constraints according to the conservation laws and other knowledge about the process.
2. Select plant parameters (**θ**) to be updated by on-line optimization. Classify the variables in plant model into measured variables (**x**) and unmeasured variables

(**z**) according to the measurability and/or available measurements for variables. Incorporate as much measurement information as possible.

3. Examine the observability of unmeasured variables **z** and parameters **θ** and the redundancy of measured variables **x** by the proposed method. All unmeasured variables and parameters must be observable and excessive degree of redundancy is required to have more accurate estimation.

4. Evaluate the precision of the process model by comparing the plant model with the true information, such as the plant design data.

Above are the necessary steps for formulating an effective and precise plant model for on-line optimization.

D. Summary

On-line optimization involves three steps: eliminating or rectifying gross errors in data sampled from the DCS, estimating parameter values to update the process simulation, and conducting economic optimization to generate a set of optimal set point for the DCS of the plant. Based on the nature of chemical process models, only the combined gross error detection and data reconciliation algorithms are applicable for identifying and rectifying gross errors, and the simultaneous data reconciliation and parameter estimation methods are suitable for estimating process parameters. Therefore, two procedures to conduct on-line optimization are proposed as discussed previously in this chapter.

There are several methods that can be used to reconcile process data for gross error detection and parameter estimation. These methods are measurement test method (or least

squares method) using the normal distribution function, Tjoa-Biegler's method using contaminated Gaussian distribution, and robust method using Lorentzian distribution or Fair function. Based on the comparison of influence function and relative efficiency for these distributions, the theoretical evaluation concluded that both contaminated Gaussian distribution and Lorentzian distribution will have a better performance than the normal distribution in effectively bounding the effect of gross errors and than Fair function in a higher relative efficiency and less sensitive to the presence of gross errors. The normal distribution has the highest estimate accuracy when the measurements contain only random error.

As mentioned above, precise and accurate process simulation model is essential for on-line optimization. The process model serves as constraints in the nonlinear optimization problems for gross error detection, data reconciliation, parameter estimation, and economic optimization. The general procedure to formulate a process model and the method to examine the observability and redundancy of a plant model have been proposed. Also, some consideration has been given to improve the performance of process simulation model based on the computation results and statistics.

In subsequential chapters, the process model for sulfuric acid process will be formulated and its accuracy will be evaluated. The performance of the normal distribution, contaminated Gaussian distribution, and Lorentzian distribution will be evaluated by the numerical study based on the gross error detected rates, number of type I error, and error reduction. Also, both two-step and one-step estimation will be conducted and compared based on the computation efficiency and accuracy. Finally, plant economic optimization will be conducted using a values

added objective function with different economic scenarios and environmental restrictions to study the economic improvements from on-line optimization.

CHAPTER IV PLANT MODEL FORMULATION

The methodology and procedure to perform on-line optimization has been outlined in previous chapter. This chapter deals with the development of process simulation model for the Monsanto's designed sulfuric acid process of IMC Agrico Company. The process will first be described. Then, the detail material and energy balances and reaction rate equation in this model will be established, and the process model will be validated.

A. Description of the Contact Sulfuric Acid Process

The sulfuric acid process used in this study is the IMC Agrico Company's Uncle Sam plant in Convent, Louisiana. Both design and actual plant data was collected for the purpose of model validation and implementation of on-line optimization. The Uncle Sam plant's "E" train is a 3200 TPD 93 mole% sulfuric acid plant designed by the Monsanto Envio-Chem System, Inc. which began to operate in March, 1992. The overall conversion of elemental sulfur to sulfuric acid is about 99.7%. It represents the state-of-art technology of the contact process. The contact process is a three step process that produces sulfuric acid and steam from air, molten sulfur and water. The process flow diagram is shown in Figure 4.1, and the process consists of three sections which are the feed preparation section, the reactor section, and the absorber section.

In the feed preparation section, molten sulfur feed is combusted with dry air in the sulfur burner. The reaction is:

$$S + O_2 \Longrightarrow SO_2 + \text{Heat}$$

The reaction is exothermic and goes to completion. The gas leaving the burner is composed of sulfur dioxide, nitrogen, and unreacted oxygen at approximately 1400^{o}K.

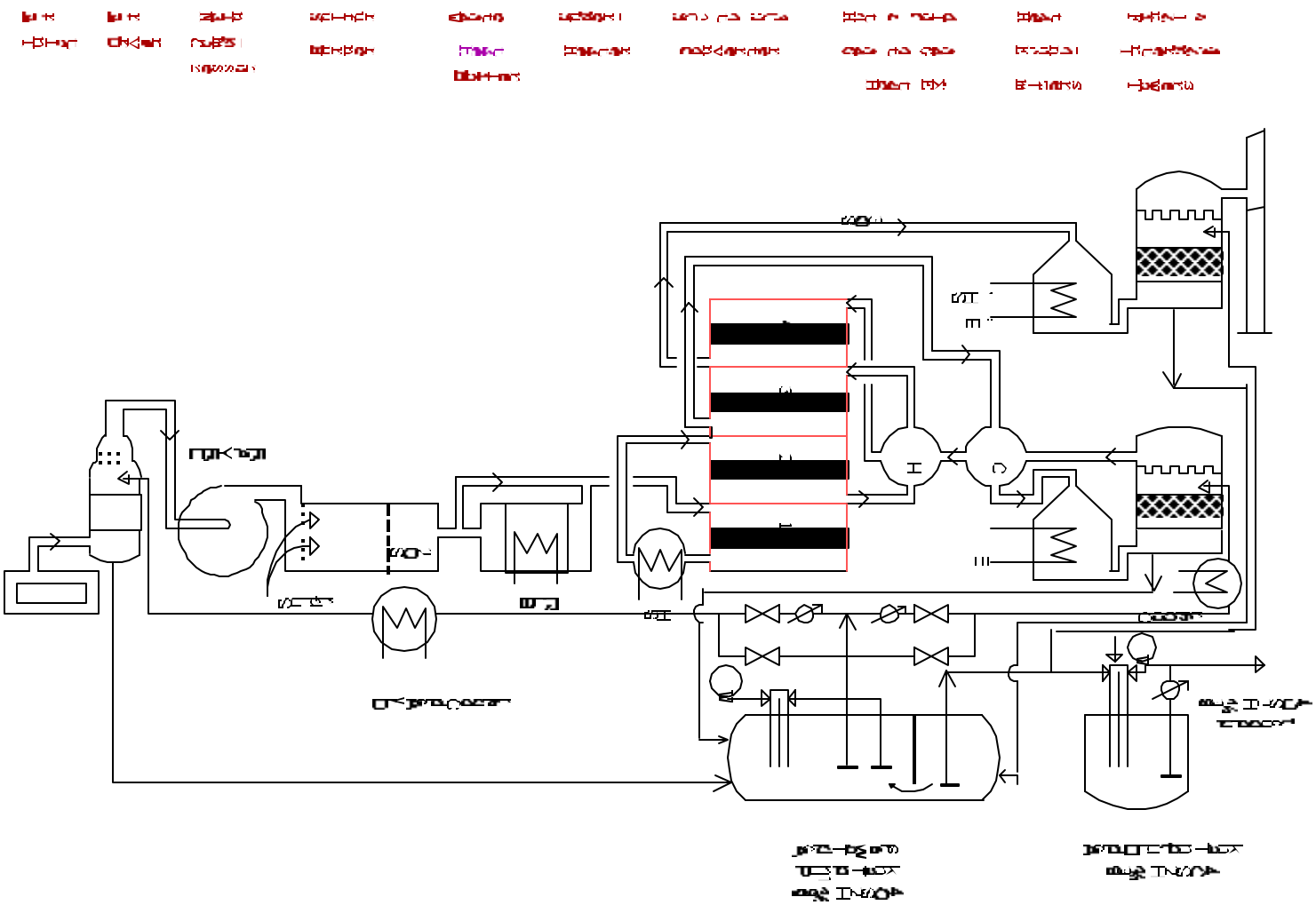

Figure 4.1 The Contact Process for Sulfuric Acid Formation

The equipment used in this section include an air filter, drying tower, a main compressor and a sulfur burner. The compressor is steam driven turbine with an efficiency of about 65%. It is a five stage, polytropic turbine on steam side and a centrifugal blower on the gas side. The pump takes in approximately 150,000 cfm of ambient air at -3 inches water and discharges it at about 160 inches of water and 230°F under normal operation. The compressor turbine speed is adjusted to change the production rate for each train. The drying tower removes ambient moisture from the intake air with 98 wt% sulfuric acid flowing at a rate of about 3600 gpm.

In the sulfur burner, the dry compressed air discharged from the turbine is reacted with molten sulfur to produce sulfur dioxide. The sulfur dioxide, along with nitrogen and unreacted oxygen enters waste heat boiler. The waste heat boiler is equipped with a hot gas bypass so that the temperature of the gases entering the first catalyst bed can be controlled to 788°F. This boiler is a shell and tube type supplied with water from the economizers. The boiler produces saturated steam at about 500°F and 670 psig and utilizes about 9% blowdown. The rest of the steam is passed to superheater to produce superheated steam at about 750°F.

The second section of the contact process plant is the reactor or converter section. The reactor consists of four beds packed with two different types of vanadium pentoxide catalyst. In this part the gas mixture from the feed preparation section is further reacted in the fixed catalyst beds to produce sulfur trioxide and heat according to the reaction:

$$2SO_2 + O_2 \rightleftharpoons 2SO_3 + \text{Heat}$$

The reaction is exothermic and the equilibrium conversion decreases with the increase in reaction temperature. For this reason, the process uses four packed beds, and heat exchangers between each bed remove the produced energy to reduce the temperature. As shown in Figure 4.2, the equilibrium conversion of sulfur dioxide decreases with the increase in operating temperature. Removing reaction heat from each reactor increases the conversion of sulfur dioxide to sulfur trioxide and this removed heat is used to produce steam. Also, the equilibrium conversion increases by decreasing the concentration of sulfur

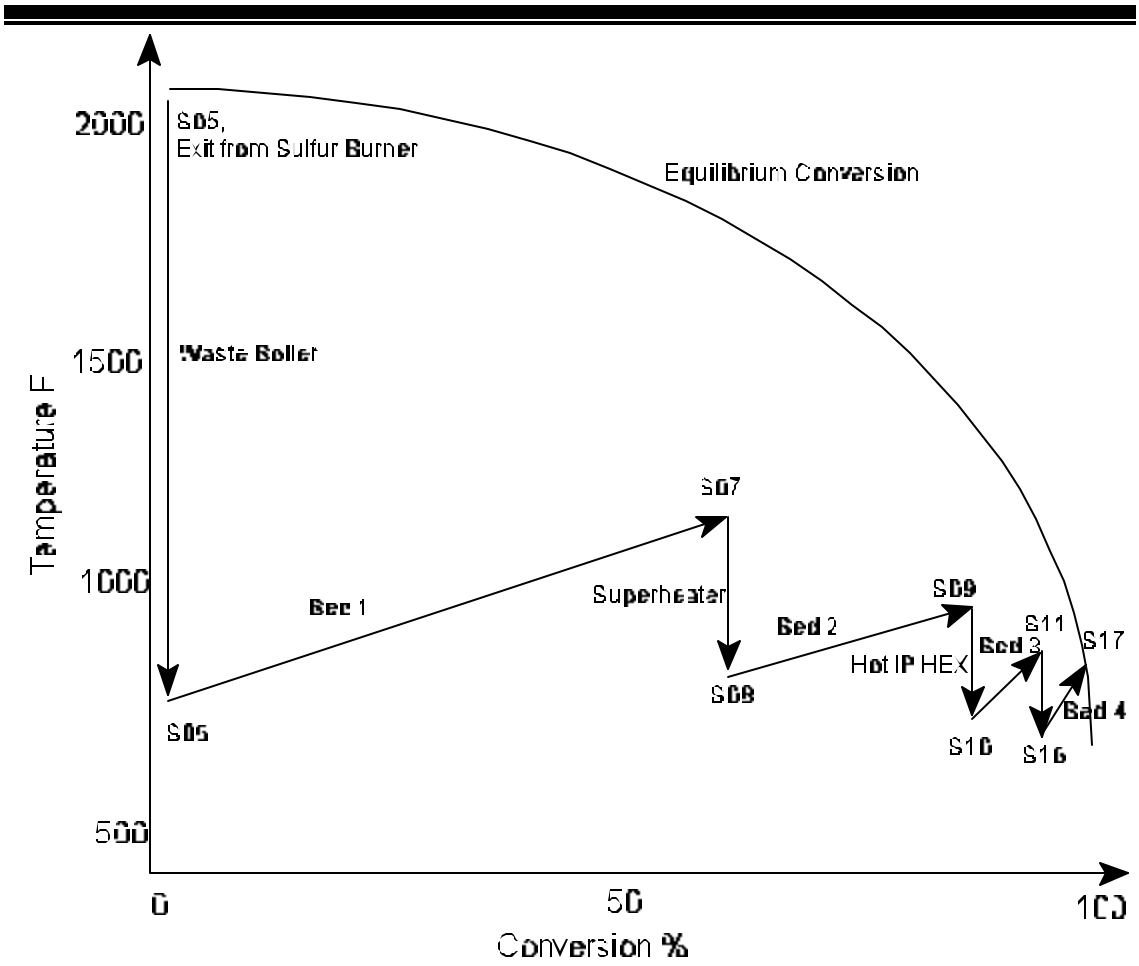

Figure 4.2 Temperature-Conversion of SO2 for Sulfuric Acid Plant

trioxide, and an inter-pass tower is used to absorb and remove sulfur trioxide from the gas stream between the third and the fourth catalyst beds. This design ensures the high conversion.

As shown in Figure 4.1, the superheater (SH) is used to cool the exit gas from the first bed by the saturated steam from waste heat boiler (BLR). It produces superheated steam at about 750°F and 630 psig. The hot inter-pass heat exchanger (H) is used to cool the gases from the second catalyst bed. The cold inter-pass heat exchanger (C) and economizer (E) are used to cool the gases from the third catalyst bed before these gases pass to the inter-pass tower. The hot and cold inter-pass heat exchangers are used also to heat the unabsorbed gases from the inter-pass tower while cooling the gases from the second and the third bed respectively. The gases from the fourth bed consist of sulfur trioxide, nitrogen, oxygen and a small amount of sulfur dioxide, and they are cooled by the superheater (SH') and economizers (E') before passing to the final tower for absorption of sulfur trioxide. The superheated steam is used to drive the compressor turbine, and the excess steam is one of the plant products.

The final section of the contact process plant is the absorber section. In this section the SO_3 is absorbed from the reaction gas mixture into 98 wt% sulfuric acid to produce a more concentrated acid. Also, heat is produced according to the equation:

$$SO_3 + H_2O \Rightarrow H_2SO_4 + \text{Heat}$$

As shown in Figure 4.1, the equipments in this section include the final acid absorption tower, inter-pass absorption tower, acid pump tank, dilution acid tank and three heat exchangers. These two absorption towers use 98 wt% acid to produce more concentrated acid. Water is added to the two tanks to keep the sulfuric acid strength at 93 wt% in acid dilution tank and

98 wt% in acid tower pump tank. The exit gases from the final absorption tower are discharged to the air with less than 4 lb of SO_2 per ton of sulfuric acid produced.

The boiler feed water is pre-heated to 500°F at 670 psig by the economizers (E and E'). It then passes to the waste heat boiler (BLR) to produce steam. Then, superheated steam is generated in the superheater (SH). The superheated steam is used to drive the turbine and the excess steam is one of the products, which is used in an adjacent plant.

This concludes the brief description of the contact sulfuric acid process. Further process details are given in the discussion of process model that follows.

B. Process Model

As discussed previously, the process model has to be written as the open form equation based model for on-line optimization. Therefore, the process simulation model will be formulated in an open form format; and it is formed based on the conservation laws, rate equations, and equilibrium relations. These equations in the plant model are the constraints of the nonlinear optimization problems in on-line optimization. The optimization problems will be solved using a optimization modeling language, GAMS (general algebraic modeling system). This section discusses the detail plant simulation, i.e., the material and energy balances, the physical and thermodynamic properties, and reaction rate equations, required for on-line optimization.

The open form equation based process model is different from close form sequential modular model developed by the flowsheeting simulation systems. In the open form format, the equations can be written implicitly as $f(x, z) = 0$ or explicitly as $x = g(z)$. The solution for all variables (x and z) are obtained simultaneously. However, in the close form sequential model,

the equations can only be written explicitly as x = g(z). The solution of the close form model is sequential, i.e., the solution of variable x is determined by the value (solution) of z. If the constraints are highly nonlinear and an explicit expression is not available for some of the variables, then an iterative procedure is required to search for the solution for the close form process model.

The plant model expressions for open form model are a set of constraint equations which describe the process behavior and represent the relationship of process variables and parameters. For a chemical process, this set of constraint equations include the material and energy balances, chemical reaction rate equations, heat transfer equations, and vapor-liquid equilibrium equations. The plant model for the sulfuric acid contact processes includes the constraint equations for the sulfur burner, four catalytic convertors, two gas-to-gas heat exchangers, three economizers, a superheater, a waste heat boiler, and final and inter-pass absorption towers. A flowsheet diagram with stream and unit names used in model equations is shown in Figure 4.3, and Table 4-1 gives a description of these streams. The constraint equations are established in following section and they are programmed in GAMS language and used to reconcile plant measurements, estimate plant parameters, optimize the plant profit, and minimize emissions from the plant.

Heat Exchanger Network: As shown in Figure 4.3, the heat exchanger network in sulfuric acid plant includes two gas-to-gas hot and cold inter-pass heat exchangers (HEX066 and HEX065), three gas-to-compressed-water economizers (economizer 3B, 4CD, and 4A),

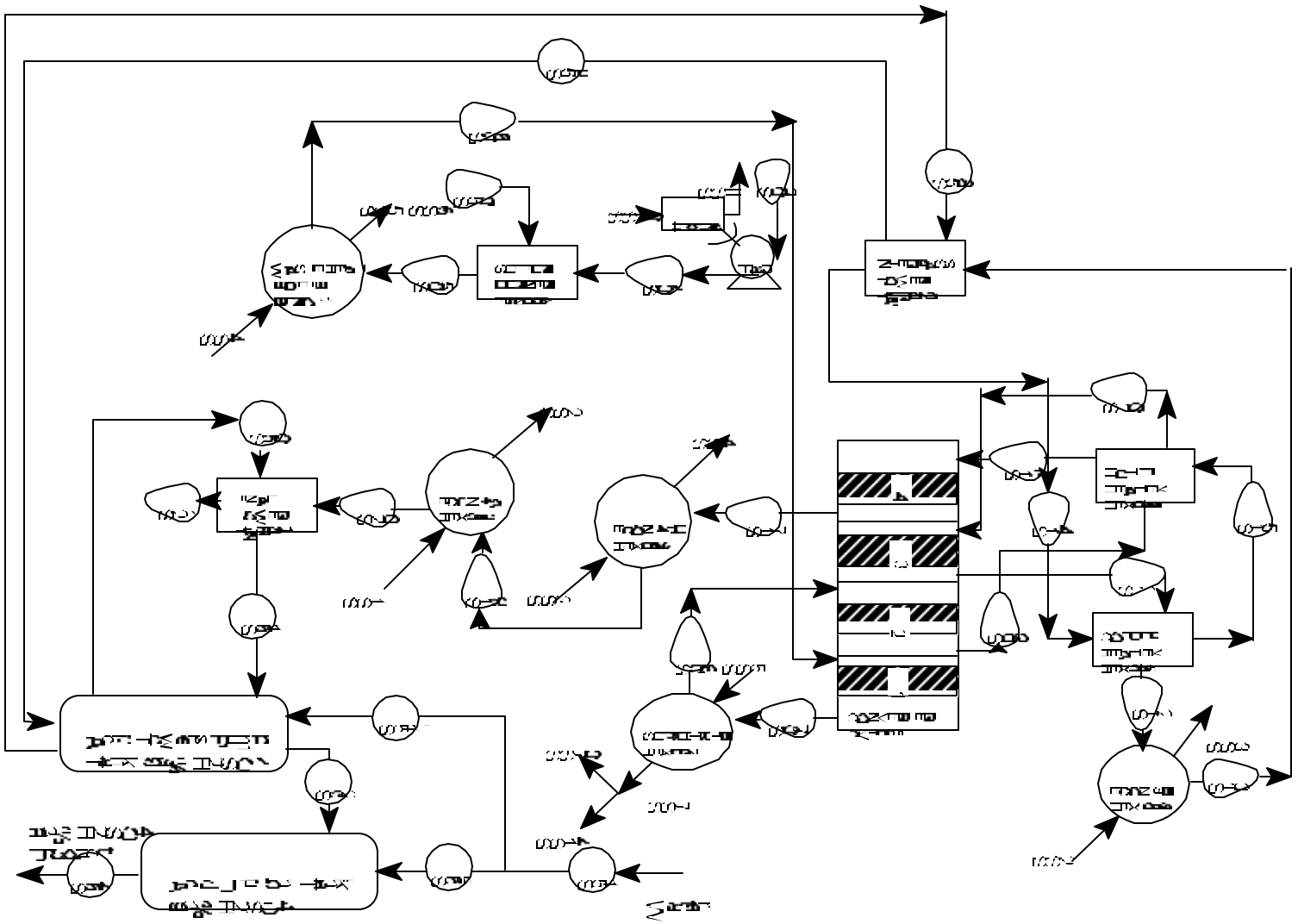

Figure 4.3 Flowsheet Diagram for the Sulfuric Acid Plant

Table 4-1 Description of Process Streams (Refer to Figure 4.3, the Process Flow Diagram for the Sulfuric Acid Process)

Name of Stream	Description

S03	Dry air to compressor (Fan)
S04	Dry air from compressor to sulfur burner
S05	Gas stream exiting from sulfur burner to waster boiler
S06	Gas stream exiting from waste boiler to the first convertor
S07	Gas stream exiting from convertor I to superheater 1B (HEX067)
S08	Gas stream exiting from superheater 1B to the second convertor
S09	Gas stream exiting from the second convertor to hot inter-pass heat exchanger (HEX066)
S10	Gas stream exiting from hot inter-pass heat exchanger to the third convertor
S11	Gas stream exiting from the third convertor to cold inter-pass heat exchanger (HEX065)
S12	Gas stream exiting from cold inter-pass heat exchanger to economizer 3B (HEX068)
S13	Gas stream exiting from economizer 3B to inter-pass absorption tower (TWR040)
S14	Gas stream exiting from inter-pass absorption tower to cold inter-pass heat exchanger
S15	Gas stream exiting from cold inter-pass heat exchanger to hot inter-pass heat exchanger
	Gas stream exiting from hot inter-pass heat exchanger to the fourth convertor
S16	Gas stream exiting from the fourth convertor to economizer 4CD (HEX069)
S17	Gas stream exiting from economizer 4CD to economizer 4A (HEX069)
S19	Gas stream exiting from economizer 4A to final absorption tower
S20	Gas stream exiting from final absorption tower and discharging to atmosphere
S21	Sulfur feed stream to Sulfur Burner
S50	dilution water that is added to acid tower pump tank and acid dilute tank
S51	Compressed water stream to economizer 4A (HEX069)
SS1	Compressed water stream from economizer 4A to economizer 3B (HEX068)
SS2	Compressed water stream from economizer 3B to economizer 4CD (HEX(069)
SS3	Saturated water stream from economizer 4CD to waste boiler (BLR011)
	Steam stream from waste boiler to superheater (HEX067)
SS4	Blowdown stream from waste boiler
SS5	Superheated steam streams from superheater
SS6	High pressure steam to turbine which is split from stream SS7
SS7	Low pressure steam exiting from the turbine of compressor (Fan)
SS70	High pressure steam split from stream SS7
SS8	Sulfuric acid stream to inter-pass absorption tower
SS14	Sulfuric acid stream exiting from inter-pass absorption tower
S58	Sulfuric acid stream to final absorption tower
S59	Sulfuric acid stream exiting from final absorption tower
S60	Sulfuric acid product
S61	
S64	

a gas-to-superheated-steam superheater (superheater 1B), and a gas-to-vapor waste heat boiler (BLR011). In these units, there is no mass transfer or chemical reaction. The inlet component

flow rates are equal to their outlet component flow rates for both sides. The energy balance states that the decrease of the enthalpy in the hot side is equal to the increase of enthalpy in cold side plus the heat loss, i.e., $(H^{inlet} - H^{outlet})_{hot} = (H^{outlet} - H^{inlet})_{cold} + Q_{loss}$. For the hot inter-pass heat exchanger (HEX066), $(H^{inlet} - H^{outlet})_{hot} \sum_i F_9^{(i)} h_9^{(i)} - \sum_i F_{10}^{(i)} h_{10}^{(i)}$ and $(H^{outlet} - H^{inlet})_{cold} \sum_i F_{16}^{(i)} h_{1}$. The heat transferred in an exchanger is proportional to heat transfer area A, overall heat transfer coefficient U, and the mean logarithm temperature difference between two sides ΔT_{lm}, i.e., $Q = UA\Delta T_{lm}$, where Q is the enthalpy change on cold side, i.e., $Q (H^{outlet} - H^{inlet})_{cold} \sum_i$

The material and energy balances as well as heat transfer equations are similar for all units in heat exchanger network. Table 4-2 gives the constraint equations for the hot inter-pass heat exchanger as an example of process constraint equations for all heat exchanger units. They are written in an open form format, and the molar flow rate is used in mass balance equations. The enthalpy equations for gases, compressed water, and superheated steam are developed in Appendix C.

Figure 4.3 shows that the hot IP heat exchanger (HEX066) involves the heat exchange between hot stream S09 from second catalyst bed and cold stream S15 from cold IP heat exchanger. The constraint equations (material and energy balances and heat transfer equation) for this unit are given in Table 4-2. The two rows of the table under material balance give the overall mass balance and all species mass balances. The overall mass balance is the summation of all species mass balances, and this is true for all processe units.

Table 4-2 The Constraint Equations for Hot Inter-Pass Heat Exchanger

Material Balances	
Overall	$(F_{10}^{(SO_2)} \quad F_{10}^{(SO_2)} \quad F_{10}^{(O_2)} \quad F_{10}^{(N_2)}) \quad (F_{09}^{(SO_2)} \quad F_{09}^{(SO_2)} \quad F_{09}^{(O_2)} \quad F_{09}^{(N_2)}) \quad 0$ $(F_{16}^{(SO_2)} \quad F_{16}^{(SO_2)} \quad F_{16}^{(O_2)} \quad F_{16}^{(N_2)}) \quad (F_{15}^{(SO_2)} \quad F_{15}^{(SO_2)} \quad F_{15}^{(O_2)} \quad F_{15}^{(N_2)}) \quad 0$
Species	$O_2: \quad F_{10}^{(O_2)} \quad F_{09}^{(O_2)} \quad 0, \qquad F_{16}^{(O_2)} \quad F_{15}^{(O_2)} \quad 0$ $N_2: \quad F_{10}^{(N_2)} \quad F_{09}^{(N_2)} \quad 0, \qquad F_{16}^{(N_2)} \quad F_{15}^{(N_2)} \quad 0$ $SO_2: \quad F_{10}^{(SO_2)} \quad F_{09}^{(SO_2)} \quad 0, \qquad F_{16}^{(SO_2)} \quad F_{15}^{(SO_2)} \quad 0$ $SO_3: \quad F_{10}^{(SO_3)} \quad F_{09}^{(SO_3)} \quad 0, \qquad F_{16}^{(SO_3)} \quad F_{15}^{(SO_3)} \quad 0$
Energy Balances	
Overall	$\left(\sum_i F_{10}^{(i)} h_{10}^{(i)} \quad \sum_i F_{09}^{(i)} h_{09}^{(i)} \right) \quad \left(\sum_i F_{15}^{(i)} h_{15}^{(i)} \quad \sum_i F_{16}^{(i)} h_{16}^{(i)} \right) \quad Q_{loss} \quad 0$ where $h_k^i(T) \quad R(a_1^i T \quad \frac{1}{2} a_2^i T^2 \quad \frac{1}{3} a_3^i T^3 \quad \frac{1}{4} a_4^i T^4 \quad \frac{1}{5} a_5^i T^5 \quad b_1^i \quad H_{298}^i)$ $i \quad SO_2, SO_3, O_2, N_2; \; k \quad 09, 10, 15, 16 \quad KJ/kmol$
Heat Transfer	$\left(\sum_i F_{16}^{(i)} h_{16}^{(i)} \quad \sum_i F_{15}^{(i)} h_{15}^{(i)} \right) \quad (U_{exch} A_{exch} \Delta T_{lm}) \quad 0$

Therefore, if all species mass balances are used to describe the process, then the overall mass balance does not need to be included. The species mass balances are used to describe the relationship of the input and output flow rate variables. The two rows in Table 4-2 under energy balances give the overall energy balance and heat transfer equation. In addition, each species enthalpy, h(T), is expressed as a polynomial function of the stream temperature given in the table.

In the constraints of Tables 4-2, F denotes the component molar flowrate, kmol/sec, and its superscript i and subscript k denote the component names and stream numbers respectively. h's in the equations represent the species enthalpies of streams, MMJ/kmol, and Q_{loss} is the heat loss from the exchanger. T is the stream temperature, and ΔT_{lm} is the logarithm mean temperature difference between hot and cold sides of the exchanger. In the heat transfer equation, U and A are the overall heat transfer coefficient and heat transfer area respectively. In these equations, the total flow rates, species flow rates (or composition), and temperatures of streams are the measurable variables. Species enthalpies and the mean temperature difference are the unmeasurable variables. The heat transfer coefficient and heat loss are the process parameters to be estimated or constants depending on the character of exchangers and processes. Others such as heat transfer area and coefficients in enthalpy equations are constants.

Reactor System: The reactor system in this plant includes a sulfur burner and four catalytic convertors. The following describes the constraint equations for sulfur burner and the first convertor. The constraint equations for the other convertors are developed in the same way as the first convertor.

When a chemical reaction is involved in the process, it is convenient to use the mole material balance to describe relationship of input and output flow rates of a unit for a component. Also, the overall material balance is obtained from the component material balances, i.e., summation of component material balances gives the overall material balance. The sulfuric acid process involves three reactions, i.e, reaction of sulfur to sulfur dioxide, reaction of sulfur dioxide to sulfur trioxide, and absorption reaction of sulfur trioxide to sulfuric acid. It is decided to use the mole balance to describe the material balances of the units in the process, i.e, all material balance equations for the sulfuric acid process are written with mole balance relations. Moles are conserved when there are no reaction, and the change of the number of molar for a component is determined by the reaction rate and stoichiometric coefficient when there are reactions.

As shown in Figure 4.3, the inputs of sulfur burner are dry air stream, S04 from main compressor, and liquid sulfur stream, S50. The dry air reacts with molten sulfur to produce sulfur dioxide and heat in the burner. The sulfur dioxide, along with nitrogen and unreacted oxygen enters the waste heat boiler. At the design operating temperature of the sulfur burner, all of the sulfur is converted to sulfur dioxide and some sulfur trioxide is formed from sulfur dioxide. Under the design operating conditions, the equilibrium conversion of SO_2 to SO_3 is 3.8% (mol) of the total produced SO_2. However, the plant measurements have shown that 2 % (mol) of the SO_2 is converted into SO_3 in this unit, and this value is incorporated in the mass and energy balances of this unit.

The material and energy balance equations for this unit are given in Table 4-3. The two rows of this table under material balance give the overall mole balance and component mole

balances. The mole balance for each component is established based on the conservation law. The steady state mole balance for a component is written as:

$$Fin(i) - Fout(i) + Fgen(i) = 0 \quad (4\text{-}1)$$

where i represents the names of components. Fin(i), Fout(i), and Fgen(i) are input flow rate F04(i), output flow rate F05(i), and generation rates of components from reaction, r(i). The overall mole balance is the summation of all component mole balance.

Two reactions take place in this unit, i.e., reaction one of sulfur to sulfur dioxide and reaction two of sulfur dioxide to sulfur trioxide. All of the sulfur is completely converted to sulfur dioxide, and 2% (mol) of the produced sulfur dioxide is further converted to sulfur trioxide in this unit. Therefore, the reaction (generation) rate for each component is related to the input flow rate of sulfur F50 and the stoichiometrical coefficient of a component in the reaction. Also, the reaction rate of a product component has a positive value and the reaction rate of a reactant component has a negative value. For example, the component mole balance for sulfur dioxide is:

$$SO_2: \quad F_{04}^{SO_2} \quad F_{05}^{SO_2} \quad 0.98F_{50} \quad 0 \quad (4\text{-}2)$$

where $F04^{SO2}$ and $F05^{SO2}$ are the input and output flow rates of sulfur dioxide, and 0.98F50 is the generation rate of sulfur dioxide. For reaction one (complete conversion of sulfur to sulfur dioxide), sulfur dioxide is a product with stoichiometric coefficient of one. In reaction two, sulfur dioxide is a reactant with stoichiometric coefficient of one. Therefore, the total reaction rate for sulfur dioxide in two reaction is F50-0.02F50 = 0.98F50.

Table 4-3 The Process Constraint Equations for Sulfur Burner

Material Balances	
Overall	$F_{04} \quad F_{05} \quad 0.01F_{50} \quad 0$ *where* $F_{04} \quad F_{04}^{O2} \quad F_{04}^{N2}$ $F_{05} \quad F_{05}^{O2} \quad F_{05}^{N2} \quad F_{05}^{SO2} \quad F_{05}^{SO3}$
Species	$O_2: \quad F_{04}^{(O_2)} \quad F_{05}^{(O_2)} \quad 1.01F_{50} \quad 0$ $N_2: \quad F_{04}^{(N_2)} \quad F_{05}^{(N_2)} \quad 0$ $SO_2: \quad F_{04}^{(SO_2)} \quad F_{05}^{(SO_2)} \quad 0.98F_{50} \quad 0$ $SO_3: \quad F_{04}^{(SO_3)} \quad F_{05}^{(SO_3)} \quad 0.02F_{50} \quad 0$ $S: \quad F_{50} \quad F_{05}^{(S)} \quad F_{05}^{(SO2)} \quad F_{05}^{(SO3)} \quad 0$ *where* $F_{04}^{(SO_3)} \quad 0, \; F_{04}^{(SO_3)} \quad 0, \; F_{05}^{(S)} \quad 0$
Energy Balances	
Overall	$F_{50}h^{(sulfur)} \quad \sum_i F_{04}^{(i)}h_{04}^{(i)} \quad F_{50}\Delta h_{rxn}^{SO_2} \quad 0.02F_{50}\Delta h_{rxn}^{SO_3} \quad \sum_i F_{05}^{(i)}h_{05}^{(i)} \quad Q_{loss} \quad 0$ *where* $\Delta h_{rxn}^{SO_2} \quad h(T)^S \quad h(T)^{O_2} \quad h(T)^{SO_2}$. $\Delta h_{rxn}^{SO_3} \quad 1.827\times(\,24{,}097 \quad 0.26T \quad 1.69\times10^{-3}T^2 \quad 1.5\times10^{5}/T)$, *BTU/lb mol*
Enthalpy Function	$h_k^i(T) \quad R(a_1^iT \quad \frac{1}{2}a_2^iT^2 \quad \frac{1}{3}a_3^iT^3 \quad \frac{1}{4}a_4^iT^4 \quad \frac{1}{5}a_5^iT^5 \quad b_1^i \quad H_{298}^i) \quad KJ/kmol$ $i \quad SO_2, SO_3, O_2, N_2, sulfur(L); \; k \quad 04, 05$

The steady state overall energy balance is established based on the first law of thermodynamics. Neglecting changes in kinetic and potential energy, this equation is (Felder and Roussleu, 1986):

$$- \Delta H + Q - W = 0 \qquad (4\text{-}3)$$

where ΔH is the change in enthalpy between input and output streams, i.e., $\Delta H = H_{out} - H_{in}$, and $\Delta H \sum_{output}$. Here n_{AR} is the number of moles of reactant A that is reacted, and v_A is the stoichiometric coefficient of reactant A in the reaction. Here the reference conditions are the reactant and product species at 298^0K and 1.0 atmosphere as described in Appendix C. Q is the heat added to the system and W is the amount of work done by the system. The energy equation for sulfur burner unit is written as:

$$F_{S0} h^{(sulfur)} \sum_i F_{04}^{(i)} h_{04}^{(i)} F_{S0} \Delta h_{rxn}^{SO_2} 0.02 F_{S0} \Delta h_{rxn}^{SO_3} \sum_i F_{05}^{(i)} h_{05}^{(i)} Q_{loss} 0 \qquad (4\text{-}4)$$

where the first and second terms represent the energy for input streams S50 and S04. The third and fourth terms in this equation denote the generated rates of heat for reaction one and two. The fifth and sixth terms are the energy for output stream S05 and heat loss from this unit.

In Table 4-3, F denotes stream species flow rate, kmol/sec, and h presents species enthalpy, MMJ/kmol. Δh_{rxn}^{SO2} and Δh_{rxn}^{SO3} are the heats of reaction of sulfur oxidation and SO_2 oxidation reactions at the temperature of the burner. Q_{loss} in energy equation denotes the heat loss from sulfur burner. The heat of reaction for sulfur oxidation is calculated from the enthalpies of components at reaction temperature:

$$\Delta h_{rxn}^{SO2} = h(T)_S + h(T)_{O2} - h(T)_{SO2} \qquad (4\text{-}5)$$

where the enthalpies are calculated by the regression equations from NASA Technical Manual 4513C (McBride et al., 1993). The detail enthalpy regression functions for all components are given in Appendix C. The enthalpy function used in Eq. 4-5 is slightly different from enthalpy functions for determining the sensible heat. In the process model, all enthalpy functions for gas streams use sensible enthalpy function except the enthalpy function in Eq. 4-5. The reference state for sensible enthalpy function is 298.15 K and 1Bar for species or elements, and enthalpies for O2, N2, SO2, SO3 at the reference state (298.15 K and 1 Bar) is zero. In Eq. 4-5, the enthalpy functions are not substrated by the enthalpies of the species or elements at 298.15 K. Therefore, the enthalpy for species (e.g., SO_2) at reference sate is the heat of formation for the species, and the enthalpy for elements (e.g., O2, S) at reference state is zero. The heat of reaction for sulfur dioxide oxidation to sulfur trioxide is calculated from an empirical formula, a function of reaction temperature, which is given in the kinetic model section of Appendix D.

The four catalytic reactors are adiabatic, plug flow reactors. In these convertors, sulfur dioxide is converted to sulfur trioxide in an exothermic chemical reaction. The kinetic model for this catalytic reaction was given by Harris and Norman (1972). Harris and Norman developed an empirical function to determine the intrinsic rate for the oxidation reaction of sulfur dioxide which is discussed in Appendix D. The intrinsic reaction rate equation is given in Figure 4.4. The real reaction rate of SO_2 (r_{SO3}) is calculated by intrinsic rate multiplying by the reaction effectiveness factor E_f, i.e., $r_{SO3} = r_{SO2}E_f$. This reaction effectiveness factor is a lump parameter that combines all of the mismatches in the kinetic model, and this includes current bulk density and current activity of the catalyst, variation

$$\text{Reaction:} \qquad SO_2 + \frac{1}{2}O_2 \rightleftharpoons SO_3$$

SO_2 conversion rate equation (instrinstic reaction rate):

$$r_{SO_2} = \frac{P^{\bullet}_{SO_2} P^{\bullet 1/2}_{O_2}}{(A + BP^{\bullet 1/2}_{O_2} + CP^{\bullet}_{SO_3} + DP_{SO_3})^2}\left[1 - \frac{P_{SO_3}}{K_P P_{SO_2} P_{O_2}^{1/2}}\right]$$

r_{SO_2} rate of reaction, $\frac{\text{lb mole of } SO_2 \text{ converted}}{\text{hr lb catalyst}}$

$P_{O_2}, P_{SO_2}, P_{SO_3}$ interfacial partial pressures of O_2, SO_2, SO_3, atm

$P^{\bullet}_{O_2}, P^{\bullet}_{SO_2}$ interfacial partial pressures of O_2 and SO_2 at zero conversion under the total pressure at the point in the reator, atm

K_P thermodynamic equilibrium constant, $atm^{\frac{1}{2}}$

$$\text{Log}_{10} K_P = 5129/T + 4.869, \qquad T \text{ in } {}^{o}K$$

A, B, C, D are function of temperature T:

Catalyst Type LP 110:

$A = e^{-6.80 + 4960/T}$, $B = 0$, $C = e^{-10.32 + 7350/T}$, $D = e^{-7.98 + 6370/T}$

Catalyst Type LP 120:

$A = e^{-5.69 + 4060/T}$, $B = 0$, $C = e^{-6.45 + 4610/T}$, $D = e^{-8.59 + 7020/T}$

Figure 4.4 Rate Equation for the Catalytic Oxidation of SO_2 to SO_3 Using Type LP-110 and LP-120 Vanadium Pentoxide Catalyst

of real wet surface of catalyst. Also, the heat of SO_2 oxidation reaction is determined from an empirical function discussed in Appendix D (Harris and Norman, 1972), which is given with the function (Eq. D-6) to determine the temperature difference between bulk gas and catalyst pellet (in Bulk Gas to Pellet Temperature Gradient section of Appendix D). The empirical function for heat of SO_2 oxidation reaction is:

$$\Delta h_{rxn}^{SO3} = 1.827\times(-24{,}097-0.26T+1.69\times10^{-3}T^2+1.5\times10^5/T), \text{ Btu/lb-mole} \qquad (4\text{-}6)$$

The four reactors are assumed to be perfect plug flow reactor. Therefore, the material and energy balance equations are differential equations for these four packed bed reactors, and they are established based on the conservation laws. The following gives a discussion on the formulation of constraint equations for Convertor I, and the material and energy balance equations for this reactor are given in Table 4-4. The constraints for other three convertors are similar to those for Convertor I.

From Figure 4.3, the input to Convertor I is the gas from the waste heat boiler (S06) and the output goes to superheater 1B (S07). In Table 4-4, the two rows under material balances give overall and species material balances. The two rows under energy balances give the overall energy balance and the enthalpy function for each species. In these equations, r^I_{so2} and r^I_{so3} are the intrinsic reaction rate and the actual rection rate for Convertor I. The intrinsic reaction rate, r^I_{so2}, is determined by an empirical equation given in Figure 4.4, and the actual reaction rate of SO_2 oxidation, r^I_{so3}, is the product of intrinsic reaction rate and the reaction effectiveness factor E^I_f for Convertor I. In Table 4-4, ρ^I_B is the bulk density of catalyst in lb/ft^3, and A is the cross

section area of convertors. Δh_{rxn}^{SO3} is the heat of the reaction, and it is determined by an empirical function and temperature

Table 4-4 The Process Constraint Equations for Convertor I

Material Balances	
Overall	$\frac{dF_1}{dL} = \frac{1}{2} r_{SO_3} A$ $F_1 = F06$, at $L = 0$; $F_1 = F07$, at $L = l_1$ where $r_{SO_3} = r^1_{SO_2} E^1_f \rho_B^1$; $F_1 = \sum_i F_1^{(i)}$ $F_1 = F_1^{SO2} + F_1^{SO3} + F_1^{O2} + F_1^{N2}$
Species	SO_3: $\frac{dF_1^{(SO_3)}}{dL} = r_{SO_3} A$ SO_2: $\frac{dF_1^{(SO_2)}}{dL} = -r_{SO_3} A$ O_2: $\frac{dF_1^{(O_2)}}{dL} = -\frac{1}{2} r_{SO_3} A$ N_2: $F_{07}^{(N_2)} - F_{06}^{(N_2)} = 0$ B. C.: $F_1^{(i)} = F06^{(i)}$, at $L = 0$; $F_1^{(i)} = F07^{(i)}$, at $L = l_1$ where $i = SO_3, SO_2, O_2$
Energy Balances	
Overall	$\frac{dH_1}{dL} = r_{SO_3} \Delta h_{rxn}^{SO_3} A$ $H_1 = H06$, at $L = 0$; $H_1 = H07$, at $L = l_1$ where $H_1 = \sum_i F_1^{(i)} h_1^{(i)}$ $\Delta H_{rxn}^{SO3} = 1.827 \times (-24{,}097 - 0.26T + 1.69 \times 10^{-3} T^2 + 1.5 \times 10^5 / T)$, Btu/lb-mole

Enthalpy Function	$h^i_I(T) \quad R(a_1^i T \ \frac{1}{2} a_2^i T^2 \ \frac{1}{3} a_3^i T^3 \ \frac{1}{4} a_4^i T^4 \ \frac{1}{5} a_5^i T^5 \ b_1^i \ H^i_{298}) \quad KJ/kmol$ $i \quad SO_2, SO_3, O_2, N_2$

given in Eq. 4-6. F_I and H_I are the molar flow rate in kmol/sec and enthalpy in MMJ/sec for Convertor I. Also, the boundary conditions for these differential equations are required to connect the variables in these equations to the variables in the input and output streams. These boundary conditions are given with the equations as shown in Table 4-4.

In the constraint equations for this unit, total flow rates, composition (or species flow rates), and temperatures are measurable variables. The reaction rates and species enthalpies are unmeasurable variables. E_f^I is the process parameter to be estimated. The others, such as cross section area of convertor, bulk density of catalyst, and coefficients in enthalpy equations are constants.

The ordinary differential equations for material and energy balances in this unit are discretized into the algebraic difference equations using improved Euler's method (Carnahan, et al., 1969). These algebraic difference equations are written in GAMS program and solved with the other constraints in the plant model. The boundary conditions of the algebraic difference equations are the input and output conditions of the packed beds.

Absorption Tower Section: This section includes an inter-pass absorption tower and a final absorption tower. These units involve mass transfer of SO_3 from gas phase to liquid phase, i.e., the absorption reaction of sulfur trioxide. For both towers, it is assumed that SO_3 in gas

stream is completely absorbed by sulfuric acid solution, and all other gases are considered as inert gases. Also, the total molar flow rate for sulfuric acid stream is counted as the sum of molar flow rates of SO_3 and water in the acid stream. Based on these assumptions, the mole flow rate of water in acid stream should remain unchanged between input and output at the absorption tower. The difference between output and input for both SO_3 and total molar flow rates in acid stream is equal to the molar flow rate of SO_3 in gas stream. The detail material and energy balance equations for final absorption tower are given in Table 4-5 where sulfuric acid stream (S60) absorbs the SO_3 from the gas stream S20. The constraint equations for inter-pass absorption tower are similar to the equations in Table 4-5.

In Table 4-5, the three rows under material balances give the overall mole balances, relations for stack concentrations of sulfur dioxide and oxygen to relate the emission concentrations of sulfur dioxide and oxygen to species flow rates in this unit, and component mole balances. The first row under energy balances gives the overall energy balance of final absorption. In the overall energy equation, Δh_{rxn} is the heat of reaction for sulfur trioxide absorption. The heat of sulfur trioxide absorption at 298 K is given by (Smith and Van Ness, 1987)

$$SO_3(g) + H_2O(l) \Rightarrow H_2SO_4(l) + 132.4 \text{ MMJ/kmol} \qquad (4\text{-}7)$$

In these two absorption towers, the operating temperature range is 82-118°C. The variation of the heat of reaction in this temperature range is less than 5% of the heat of reaction. Hence, the heat of this reaction was taken as a constant, 132.4 MMJ/kmol. The enthalpy functions for the

gases and sulfuric acid are given in the second row under energy balances, and the derivation of enthalpy equation for sulfuric acid solution is given in Appendix C.

In the constraint equations of Table 4-5, stream flow rates F, temperatures T, and concentrations of O_2 and SO_2 (C_{O2} and C_{SO2}) are measurable variables. Species enthalpies, h, are unmeasurable variables, and the coefficients in enthalpy functions are constants.

Table 4-5 The Process Constraint Equations for Final Absorption Tower

Material Balances	
Overall	$(F_{21}^{(SO_3)}\ F_{21}^{(SO_2)}\ F_{21}^{(O_2)}\ F_{21}^{(N_2)})\ (F_{61}^{SO_3}\ F_{61}^{H_2O})$ $(F_{20}^{(SO_3)}\ F_{20}^{(SO_2)}\ F_{20}^{(O_2)}\ F_{20}^{(N_2)})\ (F_{60}^{SO_3}\ F_{60}^{H_2O})\ 0$
Stack O_2 and SO_2	$F_{21}C_{O_2}\ F_{21}^{(O_2)}$ $F_{21}C_{SO_2}\ F_{21}^{(SO_2)}$
Species	O_2: $F_{21}^{(O_2)}\ F_{20}^{(O_2)}\ 0$ N_2: $F_{21}^{(N_2)}\ F_{20}^{(N_2)}\ 0$ SO_2: $F_{21}^{(SO_2)}\ F_{20}^{(SO_2)}\ 0$ SO_3: $F_{20}^{(SO_3)}\ F_{60}^{SO_3}\ F_{61}^{SO_3}\ 0;\ F_{21}^{(SO_3)}\ 0$ H_2O: $F_{60}^{H_2O}\ F_{61}^{H_2O}$
Energy Balances	
Overall	$\left(\sum_i F_{20}^{(i)}h_{20}^{(i)}\ \sum_i F_{21}^{(i)}h_{21}^{(i)}\right)\ (F_{61}h_{61}\ F_{60}h_{60})\ F_{20}^{(SO_3)}\Delta h_{rxn}\ 0$
Species	$h_k^i(T)\ R(a_1^iT\ \frac{1}{2}a_2^iT^2\ \frac{1}{3}a_3^iT^3\ \frac{1}{4}a_4^iT^4\ \frac{1}{5}a_5^iT^5\ b_1^i\ H_{298}^i)\ KJ/kmol$ $i\quad SO_2, SO_3, O_2, N_2;\ k\quad 20,21$ h_k = - 145.8407C + 9.738664e-3T+ 8.023897e-3TC+ 83.61468C^2 + 60.19207, Kcal/gmol, k=60,61 for sulfuric acid solution

Overall Material Balance: The overall material balance relates the flow rates of raw materials to the production of products and wastes. For the sulfuric acid process, the production rate of sulfuric acid (F_{64}, lb/sec) can be determined by either the use of sulfur feed rate (F_{50}, kmol/sec) or the absorption rates in inter-pass and final towers. These two constraints are:

$$(F_{64}\ C_{64})/2.204/98.02 = F_{50}\ x \tag{4-8}$$

and

$$(F_{64}\ C_{64})/2.204/98.02) = [(\ F_{61} - F_{60}\ ) +\ (\ F_{59} - F_{58}\ )] \tag{4-9}$$

where x is the conversion of sulfur to sulfuric acid and C64 is the mass fraction of sulfuric acid for the product stream F64. The unit of production rate of sulfuric acid (F64) is lb/sec and the other flow rates (F50, F58, F59, F60, and F61) are kmol/sec. The constant, 2.204 is a conversion, 2.204 lb/kg. The constant 98.02 is the molecular weight of sulfuric acid. These two constants are used to converted the unit of F64 from lb/sec to kmol/sec to be consistent with the unit of other flow rates.

The overall conversion rate of sulfur (x) is determined by:

$$F_{50} \quad F_{21}^{(SO_2)} \quad F_{50}x \tag{4-10}$$

where F_{50} and F_{21}^{SO2} are the flow rates of sulfur and the unconverted SO_2 to be discharged.

The dilution water flow rate F_{51} (kmol/sec) is used for both acid tower pump tank and acid dilution tank. It is used to adjust the acid strength. The amount of dilution water is determined by the production rate of sulfuric acid (F64) and product concentration (C64), i.e,

$$F_{51} = F_{64}\ (1\text{-}C_{64})/(2.204\times18.02) + F_{64}\ C_{64}/(2.204\times98.02) \tag{4-11}$$

In Eq. 4-11, F_{64} $(1\text{-}C_{64})/(2.204\times18.02)$ is the amount of water in sulfuric acid solution and F_{64} $C_{64}/(2.204\times98.02)$ is the amount of water that is used to react with sulfur trioxide to produce sulfuric acid. Constants, 18.02 and 98.02, are the molecular weight for water and sulfuric acid. The conversion, 2.204 lb/kg, and molecular weight constants are used to converted the flow rate of F64 from lb/sec to kmol/sec for F51.

The constraint for the ratio of oxygen to nitrogen in the air is:

$$F_{04}^{(N_2)} \quad (79/21)F_{04}^{(O_2)} \quad 0 \tag{4-12}$$

The steam from superheater SS7 is splitted into two streams SS70 and SS14. SS70 is used for the turbine of the compressor (Fan in Figure 4.3) and SS8 is the output of steam from the turbine. The flow rate of SS8 is the same as SS70, and the enthalpy of SS70 is reduced after passing the energy to the turbine. Therefore, SS8 is called lower pressure steam stream, and the stream SS14 is the high pressure steam stream. The flow rates for lower and high pressure steam streams are F_{S8} and F_{S14} in kmol/sec. The production rates of lower and high pressure steams are determined by:

$$F_{S7} = F_{S8} + F_{S14} \tag{4-13}$$

and

$$F_{S8}(h_{S70} - h_{S8}) = W_{turbine} = F_{04}(P_{04} - P_{03})/\rho_{04}/\eta_P /\eta_M \tag{4-14}$$

where the flowrates for steam streams SS70 and SS8 are the same, i.e., $F_{S70} = F_{S8}$ Eq. 4-13 is a mole balance over the split of the stream SS7. Eq. 4-14 is the energy balance on the compressor to determine the amount of steam required by the turbine. In these two equations, F is the flow rates of steam in kmol/sec, and h is the steam enthalpy in MMJ/kmol. P_{03} and P_{04}

is the inlet and discharged pressure of the compressor (Fan in Figure 4.3) for gas streams in kg/m^2, and ρ is the density of gas stream in kg/m^3. η_P and η_M are the compressor efficiency and mechanical efficiency. They are 0.65 and 0.9 respectively (Zhang, 1993).

Inequality Constraints: In plant profit (economic) optimization, a number of inequality constraints are imposed on the optimization based on the equipment capacities, raw material availability, product quality requirements, operation condition restrictions, and environmental concerns. Without these types of restrictions, the optimal operation conditions from economic optimization may be infeasible.

For sulfuric acid process, the inequality constraints that will bound the optimal solution in the feasible operation region are given in Table 4-6. The first restriction is the air flow rate from compressor which affects the gas concentrations in the reactor train, the conversion of sulfur dioxide, the turbine steam usage and the emission of sulfur dioxide. The upper bound represents the maximum capacity of the compressor. The second restriction is the sulfur feed flow rate (F50) which is adjusted to meet the sulfur dioxide emission environmental requirement and is limited by the capacities of sulfur burner and the convertors. The third restriction is that the SO_2 emission must be lower than the maximum allowable discharge rate required from EPA regulation, which is 4.0 pounds of SO_2 per ton of sulfuric acid produced. The remained eight restrictions are the temperatures of the inlet and outlet streams of four convertors. The selection of the lower limit for four packed-bed reactors is the minimum temperature requirement below which there is insufficient energy for autoignition (Doering, 1976 and Richard, 1987). The upper limit imposed on reactor temperatures is to prevent catalyst deactivation.

Table 4-6 Inequality Constraints of Sulfuric Acid Process for Profit Optimization

Descriptions	Inequality Constraints	Design Data
Inlet air flow rate, kmol/sec	$2.0 \le F_{04} \le 4.0$	xxxx
Sulfur Feed, lb/min	$F50 \le 1600$	1460
SO_2 emission, lb SO_2/ ton H_2SO_4	$F21SO_2/F64 \le 4$	4.0
1st bed inlet temperature, F	$780 \le T06 \le 1150$	788
1st bed outlet temperature, F	$780 \le T07 \le 1150$	1143
2nd bed inlet temperature, F	$780 \le T08 \le 1150$	824
2nd bed outlet temperature, F	$780 \le T09 \le 1150$	967
3rd bed inlet temperature, F	$780 \le T10 \le 1150$	824
3rd bed outlet temperature, F	$780 \le T10 \le 1150$	869
4th bed inlet temperature, F	$780 \le T16 \le 1150$	797
4th bed outlet temperature, F	$780 \le T16 \le 1150$	835

Summary: The development of constraint equations for the plant model was discussed above. The physical properties of streams are given in Appendix C. The detail kinetic model for SO_2 oxidation reaction is described in Appendix D. In the following section, this plant model will be validated by comparing the results from the GAMS simulation with plant design data.

C. Validation of Process Model

Based on the method proposed in previous chapter, the process variables are classified as measured variables and unmeasured variables according to the availability of measurements from plant distributed control system, as well as the observability and redundancy of the plant

model. Also, the heat transfer coefficients and reaction effectiveness factors for four convertors are classified as process parameters because they are time varying and do not change with the operation conditions.

The process variables that are classified as measured variables are given in Tables 4-7, and process parameters are given in Tables 4-8. In Table 4-7, the names, brief descriptions, and the design values for the measured variables are given. The process parameters include seven heat transfer coefficients and four reaction effectiveness factor. The names, description, and design values of these parameters are given in Table 4-8. The values of parameters given in Table 4-8 were determined by the simultaneous data reconciliation and parameter estimation using the design data for measured variables given in Table 4-7. In total, the process model for sulfuric acid plant has 43 measured variables, 732 unmeasured variables, and 761 linear and nonlinear equality constraints. The inequality constraints given in Table 4-6 are incorporated as bounds for the corresponding variables in the program.

The accuracy and validity of the process model are examined by comparing the simulation results from the process model with the plant design data for the sulfuric acid plant. First, the process constraint equations for entire plant are examined unit by unit using Fortran programs. The constraint equations for each unit are written in a Fortran program to calculate the parameters and operating conditions in the unit. The predicted results by these Fortran programs are compared with the plant design data to verify the material and energy balance equations for each unit. Then, the constraint equations for the entire plant are written in a GAMS program to conduct simultaneous data reconciliation and parameter

Table 4-7 The Plant Design Data of Measured Variables for the Sulfuric Acid Plant

Measurement	Description	Plant design data

T04	Temperature of gas stream S04, ^{0}K	383.15
T05	Temperature of gas stream S05, ^{0}K	1396.15
T06	Temperature of gas stream S06, ^{0}K	693.15
T07	Temperature of gas stream S07, ^{0}K	890.15
T08	Temperature of gas stream S08, ^{0}K	713.15
T09	Temperature of gas stream S09, ^{0}K	792.15
T10	Temperature of gas stream S10, ^{0}K	714.15
T11	Temperature of gas stream S11, ^{0}K	738.15
T13	Temperature of gas stream S13, ^{0}K	438.15
T14	Temperature of gas stream S14, ^{0}K	355.15
T15	Temperature of gas stream S15, ^{0}K	594.15
T16	Temperature of gas stream S16, ^{0}K	698.15
T17	Temperature of gas stream S17, ^{0}K	719.15
T19	Temperature of gas stream S19, ^{0}K	546.15
T20	Temperature of gas stream S20, ^{0}K	405.15
T21	Temperature of gas stream S21, ^{0}K	355.15
T58	Temperature of sulfuric acid stream S58, ^{0}C	82.00
T59	Temperature of sulfuric acid stream S59, ^{0}C Temperature	118.00
T60	of sulfuric acid stream S60, ^{0}C	82.00
T61	Temperature of sulfuric acid stream S61, ^{0}C	93.00
TS1	Temperature of compressed water stream SS1, F	220.00
TS2	Temperature of compressed water stream SS2, F	310.00
TS3	Temperature of compressed water stream SS3, F	403.00
TS4	Temperature of compressed water stream SS4, F	500.00
TS7	Temperature of superheated steam stream SS7, F	750.00
F04	Total molar flow rate of gas stream S04, kmol/sec	xxxx
F05	Total molar flow rate of gas stream S05, kmol/sec	xxxx
F14	Total molar flow rate of gas stream S14, kmol/sec	xxxx
F20	Total molar flow rate of gas stream S20, kmol/sec	xxxx
F50	Total molar flow rate of sulfur stream S50, kmol/sec	0.3445
F58	Total molar flow rate of H_2SO_4 stream S58, kmol/sec	14.591
F59	Total molar flow rate of H_2SO_4 stream S59, kmol/sec	14.917
F60	Total molar flow rate of H_2SO_4 stream S60, kmol/sec	6.953
F61	Total molar flow rate of H_2SO_4 stream S61, kmol/sec	6.970
FS1	Molar flow rate of steam stream SS1, kmol/sec	xxxx
FS5	Molar flow rate of steam stream SS5, kmol/sec	xxxx
PS5	Pressure of steam stream SS5, psia	684.7
PS7	Pressure of steam stream SS7, psia	654.7
X	Total conversion of SO_2 to SO_3	0.997
C_{SO2}	Molar fraction of SO_2, 100 PPM	4.153
C_{O2}	Molar fraction of O_2	0.045
C58	Concentration of H_2SO_4 (wt. fraction) at steam S58	0.980
C60	Concentration of H_2SO_4 (wt. fraction) at steam S60	0.980

Table 4-8 Process Parameters for the Sulfuric Acid Process Model

Parameters	Descriptions	Values
E_f^I (EFFI)	Reaction effectiveness factor for convertor I	0.241
E_f^{II} (EFFII)	Reaction effectiveness factor for convertor II	0.161
E_f^{III} (EFFIII)	Reaction effectiveness factor for convertor III	0.109
E_f^{IV} (EFFIV)	Reaction effectiveness factor for convertor IV	**0.035**
U_{boiler}(BLRU)	**Heat transfer coefficient of waste boiler**	xxxx
U_{ex65} (EX65U)	**Heat transfer coefficient of cold IP heat exchanger**	xxxx
U_{ex66} (EX66U)	**Heat transfer coefficient of hot IP heat exchanger**	xxxx
U_{ex67} (EX67U)	**Heat transfer coefficient of superheater**	xxxx
U_{ex68} (EX68U)	**Heat transfer coefficient of economizer 3B**	xxxx
U_{ex69} (EX69CDU)	**Heat transfer coefficient of economizer 4CD**	xxxx
U_{ex69A} (EX69AU)	**Heat transfer coefficient of** economizer 4A	xxxx

estimation for evaluating the performance of this plant model using the least squares method as given in Eq. 3-34.

The procedure of the simulation with GAMS is shown in Figure 4.5. First, the plant design data for measured variables listed in Table 4-7 is included in the GAMS program and is treated as measurements for data reconciliation. This plant design data is considered as measurements which are necessary for reconciling process data and estimating process parameters. Solving this data reconciliation problem will simultaneously reconcile the plant design data listed in Table 4-7 for measured variables and estimate the process parameters in Table 4-8 and all unmeasured variables in the plant model. The reconciled plant design data and estimated

parameter from GAMS simulation are compared with plant design data. The reconciled data should agree closely with the plant design data since it is accurate and consistent. Also, the parameters estimated by this procedure should essentially the same as those used for the plant design.

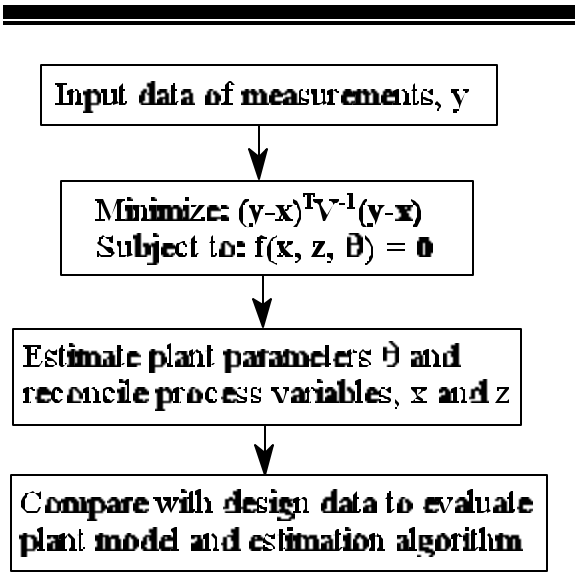

Figure 4.5 Procedure of GAMS Simulation to Evaluate Sulfuric Acid Plant Model

The reconciled values for the measured variables are compared with the original plant design data for the same measured variables shown in Table 4-9. It showed the reconciled measurements are close to the part of design data that was selected to be treated as measured variables, and the largest difference is only 0.991% of the design data. This means that the constraint equations in the plant model are precise and agree with the consistent plant design data. Otherwise, the reconciled data for these measured variables would not be close to the plant design data. Also, this result agrees with the fact that no errors exist in the plant design data. The detail simulation results for the sulfuric acid plant from simultaneous data reconciliation and parameter estimation are compared with the plant design data for evaluating the performance of the plant model in the following paragraphs.

Heat Exchanger Network: The important criteria for evaluating the performance of constraint equations for heat exchangers are the predicted heat duty, heat loss and heat transfer

coefficient. Table 4-10 gives the comparison of heat duties, heat losses, and heat transfer coefficients between plant design data and GAMS simulation for the units in heat

Table 4-9 Comparison of Reconciled Values and Design Data for Measured Variables

Measurement		Design Data	Reconciled Data	Relative Difference
T04	ºK	383.15	383.15	0.000%
T05	ºK	1396.15	1396.17	0.001%
T06	ºK	693.15	692.47	0.098%
T07	ºK	890.15	890.86	0.080%
T08	ºK	713.15	712.49	0.093%
T09	ºK	792.15	792.84	0.087%
T10	ºK	713.15	712.48	0.094%
T11	ºK	738.15	738.82	0.091%
T13	ºK	438.15	438.16	0.002%
T14	ºK	355.15	355.16	0.003%
T15	ºK	594.15	594.15	0.000%
T16	ºK	698.15	697.94	0.030%
T17	ºK	719.15	719.36	0.029%
T19	ºK	546.15	546.15	0.000%
T20	ºK	405.15	405.15	0.000%
T21	ºK	355.15	355.14	0.003%
T58	ºC	82.00	81.36	0.780%
T59	ºC	118.00	119.17	0.991%
T60	ºC	82.00	82.10	0.129%
T61	ºC	93.00	92.90	0.107%
TS1	ºF	220.0	219.99	0.005%
TS2	ºF	310.0	310.00	0.000%
TS3	ºF	403.0	403.00	0.000%
TS4	ºF	500.0	500.01	0.002%
TS7	ºF	750.0	750.01	0.001%
F04	kmol/sec	xxxx	xxxx	0.007%
F05	kmol/sec	xxxx	xxxx	0.017%
F14	kmol/sec	xxxx	xxxx	0.008%
F20	kmol/sec	xxxx	xxxx	0.020%
F50	kmol/sec		0.3445	0.3340.145%
F58	kmol/sec	14.591	14.595	0.027%
F59	kmol/sec	14.917	14.920	0.020%
F60	kmol/sec	6.953	6.953	0.000%
F61	kmol/sec	6.970	6.970	0.000%
FS1	kmol/sec	xxxx	xxxx	0.000%
FS5	kmol/sec	xxxx	xxxx	0.000%
PS5	psia	684.7	684.71	0.001%
PS7	psia	654.7	654.70	0.000%
X		0.997	0.997	0.000%
C_{SO2}	100 ppm	4.153	4.153	0.000%
C_{O2}	mole fraction	0.045	0.045	0.000%
C58	weight fraction	0.98	0.980	0.000%
C60	weight fraction	0.98	0.980	0.000%

Table 4-10 Comparisons of the Model Predictions and Plant Design Data for Heat Exchanger Networks

			Plant Design Data	Model Prediction	Percent Difference
Cold IP Heat Exchanger EX65	Heat Duty,	MMJ/sec.	18.31	18.13	1.0%
	Heat Loss,	MMJ/sec.	0.428	0.296	30.8%
	Trans. Coef.,	J/sec.-ft^2-K	xxxx	xxxx	2.9%
Hot IP Heat Exchanger EX66	Heat Duty,	MMJ/sec.	8.22	8.20	0.2%
	Heat Loss,	MMJ/sec.	0.216	0.217	0.4%
	Trans. Coef.,	J/sec.-ft^2-K	xxxx	xxxx	1.5%
Superheater EX67	Heat Duty,	MMJ/sec.	18.41	18.36	0.3%
	Heat Loss,	MMJ/sec.	0.484	0.33	31.8%
	Trans. Coef.,	J/sec.-ft^2-K	xxxx	xxxx	1.5%
Economizer 3B EX68	Heat Duty,	MMJ/sec.	11.30	11.26	0.4%
	Heat Loss,	MMJ/sec.	0.297	0.296	0.3%
	Trans. Coef.,	J/sec.-ft^2-K	xxxx	xxxx	35.6%
Economizer 4CD EX69CD	Heat Duty,	MMJ/sec.	13.27	13.29	0.2%
	Heat Loss,	MMJ/sec.	0.349	1.047	200.0%
	Trans. Coef.,	J/sec.-ft^2-K	xxxx	xxxx	7.5%
Economizer 4A EX69A	Heat Duty,	MMJ/sec.	10.55	10.52	0.3%
	Heat Loss,	MMJ/sec.	0.277	0.242	12.6%
	Trans. Coef.,	J/sec.-ft^2-K	xxxx	xxxx	1.5%
Waste Boiler BLR001	Heat Duty,	MMJ/sec.	74.31	74.94	0.8%
	Heat Loss,	MMJ/sec.	1.95	1.95	0.0%
	UA*,	J/sec.-K	xxxx	xxxx	1.6%

* The heat transfer coefficient for waste boiler is not available from design data, hence the product of heat transfer coefficient and area is compared here.

exchanger network. In addition, Table 4-11 compares the reconciled input and output temperatures from model prediction with plant design data.

As shown in Table 4-10 , the difference of heat duties between the simulation and plant design data are within 1.0% for all units in the heat exchanger network. The largest difference among all units is 1.0% of the design data for cold inter-pass heat exchanger, and the average difference of heat duties for all units is 0.46% of their design data.

Table 4-10 shows that the difference between the prediction by the simulation and plant design data for heat transfer coefficient is within 3% of plant design data for all units except for Economizer 3B and 4CD. The largest and average differences of heat transfer coefficients excluding for Economizer 3B and 4CD are 2.9% and 1.8% of the plant design data respectively.

However, the predicted heat transfer coefficients for Economizer 3B and 4CD are different from the plant design data, and the differences are 35.6% and 7.5% of design data respectively. The reason for the difference is that the steam stream flow for these two units in the original design is different from that in present operation which is simulated by the present plant model. In the plant now, the steam stream SS2 goes to economizer 3B and then to economizer 4C in serial. In the original design, the steam stream SS2 was splitted into two streams SS2' and SS2", where SS2' went to economizer 3B and SS2" went to economizer 4C. Then, the output steam streams of economizer 3B and 4C were combined together as SS3 and went to economizer 4D. The output temperature of steam stream of economizer 3B and the input

temperature of steam stream of Economizer 4CD in original design were different from that in present simulation shown in Table 4-10, and the predicted

Table 4-11 Comparison of the Reconciled Temperatures from Model Prediction and the Plant Design Data for Heat Exchanger Networks

		Plant Design Data	Model Predictions	Percent Differences
Cold IP Heat Exchanger EX65	Hot Side: Input, F	869.4	870.2	0.09%
	Output, F	541.6	541.6	0.00%
	Cold Side: Input F	180.0	179.6	0.22%
	Output F	609.7	609.7	0.00%
Hot IP Heat Exchanger EX66	Hot Side: Input, F	967.1	967.4	0.03%
	Output, F	824.0	823.0	0.12%
	Cold Side: Input F	609.7	609.8	0.02%
	Output F	797.0	796.6	0.05%
Superheater EX67	Hot Side: Input, F	1142.9	1143.9	0.09%
	Output, F	824.0	822.9	0.13%
	Cold Side: Input F	498.2	500.0	0.36%
	Output F	750.1	750.0	0.13%
Economizer 3B EX68	Hot Side: Input, F	541.6	541.6	0.00%
	Output, F	330.0	329.0	0.30%
	Cold Side: Input F	310.0	310.0	0.00%
	Output F	430.0	403.0	-
Economizer 4CD EX69CD	Hot Side: Input, F	835.2	835.2	0.00%
	Output, F	524.3	523.4	0.17%
	Cold Side: Input F	4C: 310.0 4D: 430.0	403.0	-
	Output F	4C: 430.0 4D: 499.0	500.0	0.20%
Economizer 4A EX69A	Hot Side: Input, F	524.3	523.4	0.17%
	Output, F	270.0	269.6	0.15%

	Cold Side: Input F Output F	220.0 310.0	220.0 310.0	0.00% 0.00%
Waste Boiler BLR001	Hot Side: Input, F Output, F	2054.0 788.41	2054.0 788.0	0.00% 0.05%
	Cold Side: Input F Output F	500.0 500.0	500.0 500.0	0.00% 0.00%

mean temperature differences for these two units do not match plant design data. This mismatch directly affects the values of heat transfer coefficients for these two units. However, this will give an accurate prediction of plant operations when data from the distributed control system is used.

The differences between predicted heat losses from the simulation and the design data vary and are as much as 200 % of design data for Economizer 4CD, 30.8% of the design data for cold IP heat exchanger, and 31.8% of design data for superheater 1B as shown in Table 4-10. The reason for this is that the magnitude of heat loss values is small compared with the heat duties and that they are very sensitive to the variation of stream temperatures. Even 0.5 K difference of a reconciled stream temperatures from design data will significantly change the percent error of estimated heat loss, but does not change much the relative difference of heat duty between its predicted value and the design data. In addition, small amount of water in steam stream SS4 has been vaporized in economizer 4D in actual operating. While stream SS4 is considered as saturated water in present plant model, which makes the simulated heat duty of economizer 4D is slightly less than the actual operation data. This results in larger heat loss in model prediction for economizer 4CD than the plant design data.

Table 4-10 shows that the average difference of reconciled stream temperatures between model prediction and the plant design data is 0.09% excluding the steam streams for Economizer

3B and 4CD for which the data can not be used to compared (the stream configuration of these two units for present plant is different from one for the design). The largest and average differences of temperatures between prediction of model simulation and plant design data are 1.8 ^{o}F and 0.37 ^{o}F respectively, for all of stream temperatures excluding the output stream of steam of Economizer 3B and input stream of steam of Economizer 4CD. The differences of steam stream temperatures for Economizer 3B and 4CD between the reconciled and the plant design data are caused by the different configuration of steam stream flow as discussed above.

In summary, the comparisons show that the predicted heat duties and transfer coefficients for the units in heat exchanger network are close to the plant design data with 0.46% and 1.8% of the average differences of the plant design data respectively. This results indicate the material and energy balance equations in the plant model accurately describe the process operations. The differences for heat losses between model prediction and design data varies for different units. The average difference for all units excluding Economizer 4CD is 12.65% of their design data.

Reactor System: As shown in Figure 4.3, the reactor system in the sulfuric acid plant consists of sulfur burner for the sulfur oxidation reaction and four packed bed chemical reactors for the SO_2 oxidation reaction. The constraint equations for these units include material and energy balance equation as well as reaction rate equations. The comparisons of GAMS simulation and plant design data for these units are given in the following paragraphs.

In sulfur burner, sulfur is completely converted into SO_2, and 2.0% of the produced SO_2 is further converted into SO_3. The model prediction agrees with plant design data as shown in Table 4-12. The reconciled component flow rates of gas streams and sulfur flow rate are the

same as the plant design data, and the stream temperatures from the model and the plant design data are the same. The data for heat loss in sulfur burner was not available from the plant design data. The model predicted 5.272 MMJ/sec. (or 5.1% of the total heat duty) for the heat loss in sulfur burner. The value of heat loss in sulfur burner predicted by the plant model is reasonable compared with the data of heat losses in heat exchangers. The operating temperature in this unit is as high as 1396 K, and a larger amount of heat loss is expected as compared with the heat exchangers.

Table 4-12 The Comparison of Model Prediction and Plant Design Data for Sulfur Burner

	Design Data	Model Prediction
$F04SO_2$-$F05SO_2$, Kmol/sec.	0.0 - xxxx	0.0 - xxxx
$F04SO_3$-$F05O_3$, Kmol/sec	0.0 - xxxx	0.0 - xxxx
$F04O_2$-$F05O_2$, Kmol/sec	xxxx - xxxx	xxxx- xxxx
$F04N_2$-$F05N_2$, Kmol/sec	xxxx - xxxx	xxxx - xxxx
Temp. (S04 -S05), K	383.2 - 1396.2	383.2 - 1396.2
Heat loss, MMJ/sec.	-	5.272

For four packed-bed reactors, the reconciled gas component flow rates and stream temperatures from model prediction are compared with plant design data, and they are shown in Table 4-13 through 4-16. These four tables show that all component flow rates predicted by the plant model are the same as the plant design data and the differences of stream temperatures between the reconciled and plant design data are less than 0.7 K.

The GAMS simulation predicts the effectiveness factors of the SO2 oxidation reaction as 0.241, 0.161, 0.109, 0.035 for convertors I, II, III, and IV. These effectiveness factors are parameters in the plant model. As discussed previously, the effectiveness factors

Table 4-13 The Comparison of Model Prediction and Plant Design Data for Convertor I

	Design Data	Model Prediction
FSO_2 $^{(In-Out)}$, Kmol/sec	xxxx - xxxx	xxxx - xxxx
FSO_3 $^{(In-Out)}$, Kmol/sec	xxxx - xxxx	xxxx - xxxx
FO_2 $^{(In-Out)}$, Kmol/sec	xxxx - xxxx	xxxx - xxxx
FN_2 $^{(In-Out)}$, Kmol/sec	xxxx - xxxx	xxxx - xxxx
Conversion of SO_2	62.5%	62.5%
Temp. (S06 - S07), K	693.2 - 890.2	692.5 - 890.9
Effectiveness factor	-	0.241

Table 4-14 The Comparison of Model Prediction and Plant Design Data for Convertor II

	Design Data	Model Prediction
FSO_2 $^{(In-Out)}$, Kmol/sec	xxxx - xxxx	xxxx - xxxx
FSO_3 $^{(In-Out)}$, Kmol/sec	xxxx - xxxx	xxxx - xxxx
FO_2 $^{(In-Out)}$, Kmol/sec	xxxx - xxxx	xxxx - xxxx
FN_2 $^{(In-Out)}$, Kmol/sec	xxxx - xxxx	xxxx - xxxx
Conversion of SO_2	86.9%	86.9%
Temp. (S08-S09), K	713.2 - 792.2	712.5 - 792.8
Effectiveness factor	-	0.161

Table 4-15 The Comparison of Model Prediction and Plant Design Data for Convertor III

	Design Data	Model Prediction
FSO_2 $^{(In-Out)}$, Kmol/sec	xxxx - xxxx	xxxx - xxxx
FSO_3 $^{(In-Out)}$, Kmol/sec	xxxx - xxxx	xxxx - xxxx
FO_2 $^{(In-Out)}$, Kmol/sec	xxxx - xxxx	xxxx - xxxx
FN_2 $^{(In-Out)}$, Kmol/sec	xxxx - xxxx	xxxx - xxxx
Conversion of SO_2	94.8%	94.8%
Temp. (S10 - S11)	713.2 - 738.2	712.5 - 738.8
Effectiveness factor	-	0.109

Table 4-16 The Comparison of Model Prediction with Plant Design Data for Convertor IV

	Design Data	Model Prediction
FSO_2 $^{(In-Out)}$, Kmol/sec	xxxx - xxxx	xxxx - xxxx
FSO_3 $^{(In-Out)}$, Kmol/sec	xxxx - xxxx	xxxx - xxxx
FO_2 $^{(In-Out)}$, Kmol/sec	xxxx - xxxx	xxxx - xxxx
FN_2 $^{(In-Out)}$, Kmol/sec	xxxx - xxxx	xxxx - xxxx
Conversion of SO_2	99.7%	99.7%
SO_2 emission, PPM	400	400
Temp. (S16-S17), K	698.2 - 719.2	697.9 - 719.4
Effectiveness factor	-	0.035

are lump parameters that combine all of the mismatches in the kinetic model. This includes current bulk density and current activity of the catalyst, variation of real wet surface of catalyst. The definition of these reaction effectiveness factor parameters are slightly different from the original definition in kinetic theory. In kinetic theory, the reaction effectiveness factor is defined as the ratio of intrinsic reaction rate that is measured under no other mass transfer limitation to the real reaction rate that is measured with mass transfer limitation. Therefore, the reaction effectiveness factor under this definition only reflects the effect of mass transfer rates. The reaction effectiveness factor defined in the present model is a lump parameter which incorporates more mismatch information in the process. Although there is no data for reaction effectiveness factors available from plant design data for comparison, agreement between the plant model prediction and plant design data for component flow rates and conversions of sulfur dioxide indicates that the values of these parameters are accurate. The reactor effectiveness factors were originally determined from the empirical formulas with the assumption of pseudo first order reaction. The modification of the reaction effectiveness factors to plant parameters provides better simulations of the plant.

The step size is an important parameter in discretizing the differential equations to have an accurate solution. The differential balance equations for four convertors were discretized as algebraic difference equations using improved Euler's method. A comparison of the solutions for various step sizes is presented in Tables 4-17 and 4-18 for SO_2 flow rate and total flow rate in Convertors I and IV. Tables 4-17 and 4-18 show the total flow rate and SO_2 flow rate as a function of step size through the Convertors I and IV. Step number

Table 4-17 Comparison of Various Step Sizes for Improved Euler's Method for Convertor I

Position Z/L	Total flow rate of gas stream in Convertor I				
	5 steps	10 steps	50 steps	100 steps	200 steps
0.0	2.99700	2.99700	2.99700	2.99700	2.99700
0.2	2.97966	2.97960	2.97963	2.97964	2.97964
0.4	2.95668	2.95629	2.95621	2.95620	2.95620
0.6	2.93018	2.92926	2.92898	2.92897	2.92897
0.8	2.90901	2.90697	2.90642	2.90641	2.90640
1.0	2.89791	2.89479	2.89412	2.89410	2.89410
Position Z/L	SO_2 flow rate of gas stream in Convertor I				
	5 steps	10 steps	50 steps	100 steps	200 step
0.0	.33700	.33700	.33700	.33700	.33700
0.2	.30231	.30220	.30227	.30228	.30228
0.4	.25636	.25557	.25541	.25541	.25541
0.6	.20335	.20152	.20096	.20094	.20094
0.8	.16103	.15695	.15585	.15581	.15580
1.0.0	.13882	.13257	.13124	.13121	.13120

Table 4-18 Comparison of Various Step Sizes for Improved Euler's Method for Convertor IV

Position Z/L	Total flow rate of gas stream				SO_2 flow rate of gas stream			
	5 steps	10 steps	50 steps	100 steps	5 steps	10 steps	50 steps	100 steps
0.0	2.51100	2.51100	2.51100	2.51100	.01800	.01800	.01800	.01800
0.2	2.50942	2.50943	2.50942	2.50940	.01485	.01487	.01485	.01480
0.4	2.50779	2.50780	2.50779	2.50772	.01158	.01161	.01159	.01144
0.6	2.50609	2.50610	2.50609	2.50597	.00818	.00819	.00817	.00795
0.8	2.50434	2.50434	2.50433	2.50419	.00467	.00468	.00466	.00438
1.0	2.50282	2.50271	2.50267	2.50255	.00163	.00143	.00134	.00111

of 5, 10, 50, 100, and 200 were used. Also, the total flow rate and SO_2 flow rate profiles are shown in Figure 4.6 for Convertor IV. Comparison result of Convertor I shows that there was two significant figures of accuracy for the flow rate of sulfur dioxide and four significant figures of accuracy for the total flow rate for step number of 10. For step number of 100, there was six significant figure of accuracy for the total flow rate. The comparison result of Convertor IV shows that there was two significant figures of accuracy for the flow rate of sulfur dioxide and four significant figures of accuracy for the total flow rate for step number of 5. Since concentration of SO_2 is very small in Convertor IV, the reaction rate is very small, and it became zero or a negative value for step number larger than 100. This may be caused by round off and truncation errors. An interval size of five steps was used in this model for Convertors I to IV. Based on the comparison results of step sizes, it is recommended that 50 steps be used for Convertors I and II and 10 steps be used for Convertors III and IV.

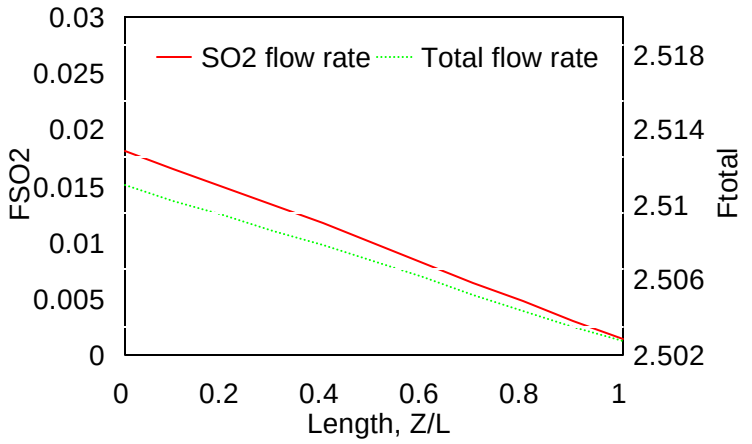

Figure 4.6 Flow Rate Profiles for Convertor IV

Summary: The plant model for the sulfuric acid plant written in GAMS program accurately predicts the conversion from sulfur to sulfuric acid product and the extraction of heat

generated in the processes to produce steam as a by-product. The simulation results agree with plant design data with a overall average difference of 1% from the design data. Particularly, this simulation successfully predicted the steam production, overall sulfur conversion and SO_2 emission which are very important factors in terms of plant's economics and emissions to environment.

CHAPTER V OPTIMAL IMPLEMENTATION OF ON-LINE OPTIMIZATION

A. Introduction

In this chapter, the current operating data for sulfuric acid plant is used to conduct on-line optimization. This includes rectifying gross errors of plant data sampled from distributed control system using combined gross error detection and data reconciliation method, estimating process parameters and reconciling plant data using simultaneous data reconciliation and parameter estimation method, optimizing plant operating set points using the updated process and economic models. Also, a number of cases that can be encountered in plant operations are investigated to demonstrate how on-line optimization improves the plant profit and reduces the emission.

The measurement test method and the methods based on Tjoa-Biegler's contaminated Gaussian distribution and Lorentzian distribution are used to conduct combined gross error detection and data reconciliation; and their performances on various magnitudes of gross errors and multiple gross errors are evaluated based on the numerical results. Also, the proposed modified compensation strategy is incorporated with measurement test method, which is called modified compensation measurement test (MCMT) method. It is to demonstrate how this strategy improves the misrectification of data that occurs in data reconciliation from the presence of large gross errors. This strategy has a significant advantage in terms of the method of solutions and computation efficiency compared with the modified iterative elimination strategy, which was incorporated in measurement test method and known as MIMT method.

Both two-step and one-step methods are used to estimate parameters in the plant model for on-line optimization using the simulated plant data. The results from these two strategies are

evaluated to determine the best way to conduct parameter estimation based on the accuracy and computation efficiency of the methods. For the two-step method, a strategy to construct the new set of measurements from step one has been proposed to avoid the interaction of both data reconciliation in step one (combined gross error detection and data reconciliation) and in step two (simultaneous data reconciliation and parameter estimation) in Chapter III, and it is incorporated in the two-step method. In addition, how process model formulations affects the results of gross error detection, data reconciliation, parameter estimation is discussed based on computation results. This provides guidelines for the best way to formulate process models.

Based on the results of this research, the optimal way to conduct on-line optimization is proposed, and this is tested with the sulfuric acid plant of IMC Agrico Company. Moreover, an interactive on-line optimization system is developed to alleviate engineer's effort of applying on-line optimization. This program incorporates the results of this research. Finally, the main results from this research are summarized, and a comparison with the research of other investigators is given.

B. Results of On-Line Optimization Using Current Plant Data from DCS

As discussed in Chapter III, on-line optimization takes plant data (measurements) from distributed control system and solves three optimization problems in sequence to provide optimal set points for distributed control system. The following paragraphs will discuss results from conducting on-line optimization using data from the distributed control system of the sulfuric acid plant.

The process measurements are taking from the Baily distributed control system of sulfuric acid plant. The distributed control system provides the direct measurements for all of temperatures, pressures, and compositions and some of flow rates required for on-line optimization. However, the direct measurements of flow rates for gas streams (air from compressor F04, gases from sulfur burner F05, gases from inter-pass absorption tower F14, and gases from economizer 4A F20) are not available. Therefore, these measurements are obtained using the discharge pressure and speed of compressor (Fan). The flow rate of stream S04 (F04) is determined by the discharge pressure and speed of the compressor with the compressor performance chart. Then the flow rates of F05, F14, and F20 are determined by the flow rate F04 and assuming 2%, 94.8%, and 99.7% (99.7% is a direct measurement) of SO2 conversion at the corresponding streams. Also, the standard deviations of the measured variables are needed for on-line optimization, and these values are listed in Table 5-1 along with the names, descriptions, and plant design data. The standard deviations were determined from plant data, and they were given by Zhang (Zhang, 1993). In addition, two sets of plant data from DCS are used to conduct on-line optimization, and they are given with the optimal solutions in the subsequent tables.

The three optimization problems of on-line optimization for two-step method are combined gross error detection and data reconciliation (data validation) using Tjoa-Bigeler's contaminated Gaussian distribution given in Eq. 3-33, simultaneous data

Table 5-1 Plant Design Data of Measured Variables for Sulfuric Acid Plant

Measured variables	Definition	Design Data	Standard deviation
T04, K	Temperature of gas stream S04,	383.150	3.6
T05, K	Temperature of gas stream S05,	1396.176	3.6
T06, K	Temperature of gas stream S06,	692.538	3.6
T07, K	Temperature of gas stream S07,	890.787	3.6
T08, K	Temperature of gas stream S08,	712.554	3.6
T09, K	Temperature of gas stream S09,	792.732	3.6
T10, K	Temperature of gas stream S10,	712.585	3.6
T11, K	Temperature of gas stream S11,	738.712	3.6
T13, K	Temperature of gas stream S13,	438.083	3.6
T14, K	Temperature of gas stream S14,	355.202	3.6
T15, K	Temperature of gas stream S15,	594.156	3.6
T16, K	Temperature of gas stream S16,	697.632	3.6
T17, K	Temperature of gas stream S17,	719.628	3.6
T19, K	Temperature of gas stream S19,	546.184	3.6
T20, K	Temperature of gas stream S20,	405.192	3.6
T21, K	Temperature of gas stream S21,	355.136	3.6
T58, C	Temperature of acid stream S58,	80.857	3.6
T59, C	Temperature of acid stream S59,	119.173	3.6
T60, C	Temperature of acid stream S60,	82.095	3.6
T61, C	Temperature of acid stream S61,	92.904	3.6
TS1, F	Temperature of steam stream SS1,	219.957	3.6
TS2, F	Temperature of steam stream SS2,	310.003	3.6
TS3, F	Temperature of steam stream SS3,	402.934	3.6
TS4, F	Temperature of steam stream SS4,	500.128	3.6
TS7, F	Temperature of steam stream SS7,	749.997	3.6
F04, kmol/s	Mole flow rate of gas stream S04,	xxxx	0.04
F05, kmol/s	Mole flow rate of gas stream S05,	xxxx	0.04
F14, kmol/s	Mole flow rate of gas stream S14,	xxxx	0.04
F20, kmol/s	Mole flow rate of gas stream S20,	xxxx	0.04
F50, kmol/s	Mole flow rate of sulfur stream S50,	0.344	0.00557
F58, kmol/s	Mole flow rate of acid stream S58,	14.595	0.1637
F59, kmol/s	Mole flow rate of acid stream S59,	14.920	0.1637
F60, kmol/s	Mole flow rate of acid stream S60,	6.953	0.07385
F61, kmol/s	Mole flow rate of acid stream S61,	6.970	0.07385
FS1, kmol/s	Mole flow rate of steam stream SS1,	xxxx	0.03843
FS5, kmol/s	Mole flow rate of steam stream SS5,	xxxx	0.05438
PS5, psia	Pressure of steam stream SS5,	680.704	10.0
PS7, psia	Pressure of steam stream SS7,	654.701	10.0
X, mol%	Total conversion of SO_2 to SO_3,	0.997	0.001
CSO2,100ppm	Mole fraction of SO_2 in gas stream S21,	4.153	0.1
CO2, mol%	Mole fraction of O_2 in gas stream S21,	0.045	0.001
C58, wt%	Weight concentration of H_2SO_4 in stream S58	0.980	0.001
C60, wt%	Weight concentration of H_2SO_4 in stream S60	0.980	0.001

reconciliation and parameter estimation using least squares method given in Eq. 3-34, and the plant economic optimization given in Eq. 3-37. The objective functions in these three optimization problems are specified in Eq. 3-34, 3-35, and 3-37 respectively. The equality constraints are the same for these optimization problems, and they were given in Chapter IV. In addition, the inequality constraints given in Chapter IV are included in plant economic optimization problem. These three optimization problems were written as three GAMS programs (DataVali.gms, ParaEsti.gms, and EconOpti.gms), and they were solved by GAMS. These three programs are given in Appendix F.

The procedure to conduct on-line optimization and the program communication are shown in Figure 5.1. As shown in Figure 5.1, first the plant data file (pdt6-12p.dat) from the DCS and parameter file (pdt6-10p.pe2) from the last sequent of on-line optimization are included in the data validation program, DataVali.gms. DataVali.gms is executed to construct plant data file, pdt6-12p.dv. This data file is used in parameter estimation program, ParaEsti.gms, to estimate process parameters and variables. Executing ParaEsti.gms generates two data files. One is the estimated process parameters, pdt6-12p.pe2, and this data file is used in plant economic optimization next and in data validation for the next sequent of on-

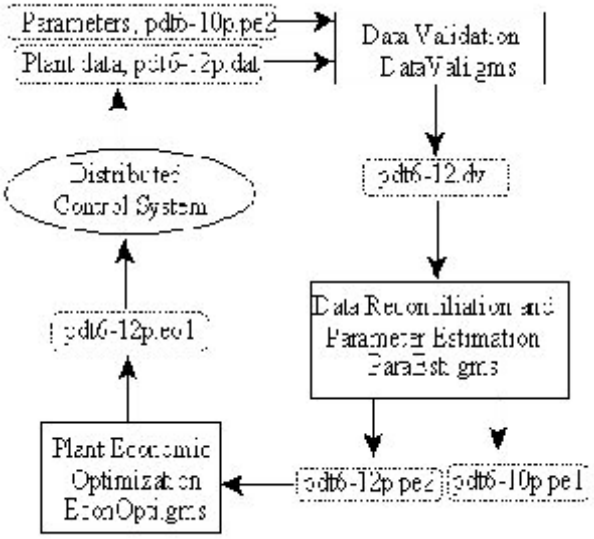

Figure 5.1 Procedure for On-Line Optimization

line optimization. The other data file is the reconciled plant measurements, pdt6-12p.pe1. After parameters are updated, the plant economic optimization program, EconOpti.gms is executed to generate a data file, pdt6-12p.eo1. This data file contains the optimal set points, and it is sent to distributed control system. In addition, GAMS generates a comprehensive corresponding output file for each optimization program, and they are DataVali.lst, ParaEsti.lst, and EconOpti.lst. These files contain detail information about the solutions. All of these files (three GAMS programs, three corresponding output files, and five data files) are given in Appendix F with the same file names.

B-1. On-Line Optimization Cycle

When on-line optimization is conducted at the first time, the parameter values for current operating conditions are not available. However, these values must be given in the plant model for combined gross error detection and data reconciliation if two-step method is used to estimate plant parameters. Therefore, the one-step method (simultaneous gross error detection, data reconciliation, and parameter estimation) is conducted to estimate the values of plant parameters, and these estimated values were used as the parameter values in the plant model for combined gross error detection and data reconciliation in the first sequence of on-line optimization cycle for two-step method. After the first sequence of on-line optimization, the procedure to conduct on-line optimization as well as data generation and exchange among on-line optimization programs are the same as described in Figure 5.1.

The results of on-line optimization given in the following were based on the plant data on June 10, 1997, 3PM (6-10-97) and June 12, 1997, 3PM (6-12-97). The plant data on June

10, 1997 was used to conduct on-line optimization for the first cycle, and plant data on June 12, 1997 was used to conduct on-line optimization for the second cycle. The values of parameters estimated from simultaneous data reconciliation and parameter estimation of the first cycle were used in the plant model for combined gross error detection and data reconciliation of the second cycle. Table 5-2 lists the reconciled operation conditions on 6-10-97, 3PM and 6-12-97, 3PM and the corresponding optimal set points. In this table, the first and second columns list the names and cost coefficients of process variables in the profit function. The third and fourth columns are the current reconciled operating data and the optimal set points from on-line optimization for the plant data on 6-10-97, 3PM, and the fifth and six columns are the current reconciled operating data and the optimal set points from on-line optimization for the plant data on 6-12-97, 3PM. As shown in Table 5-2, on-line optimization gave a 2.3% (or $313,000/year) and 3.1% (or $410,000/year) profit improvement over current operating condition on 6-10-97 and 6-12-97 respectively if the optimal setpoints were sent back to DCS as control targets. This is typical of the improvement on profit obtained from on-line optimization, and it leads to pay back periods of six months to one year according to Ayala (1997).

Table 5-2 The Comparison of Plant Operation and Optimal Solution from Plant Profit Optimization

Variables	Cost coefficients	Plant data 6-10-97, 3PM		Plant data 6-12-97, 3PM		Plant design conditions
		Operating data	Optimal set points	Operating data	Optimal set points	
F50, kmol/sec	$1.70/kmol	0.373	0.379	0.370	0.380	0.345
FS1, kmol/sec	$0.00675/kmol	xxxx	xxxx	xxxx	xxxx	xxxx
F51, lb/sec	$0.00005/lb	20.83	21.15	20.64	21.21	19.15
F64, lb/sec	$0.0097/lb	86.43	87.88	85.67	88.04	79.5
FS8, kmol/sec	$0.0616/kmol	xxxx	xxxx	xxxx	xxxx	xxxx
FS14, kmol/sec	$0.103/kmol	xxxx	xxxx	xxxx	xxxx	xxxx
Emission, lb SO_2/ Ton H_2SO_4		4.2	4.0	4.1	4.0	4.0
Profit, $/second		0.4316	0.4415	0.4281	0.4411	0.3917
Profit Improvements		2.3%,		3.1%, $410,000/year		

The parameters in the plant model include seven heat transfer coefficients and four reaction effectiveness factors for four convertors. Table 5-3 gives the estimated values of parameters using some of plant design data as measurements in column two, the estimated values of parameters with one-step method using plant data on 6-10-97 in column three, and the estimated values of parameters from on-line optimization with two-step method using the plant operating data on 6-10-97 and 6-12-97 in columns four and five respectively. As shown in columns two and three of Table 5-3, the values of parameters estimated by current operating conditions are larger than the design parameter values. The reason is the estimated values of

parameters are determined by the operating conditions, such as flow rates and temperatures. If the plant was running with a production rate that is higher than the plant design production rate, then the current operating flowrates and/or temperature differences between the input and output of heat exchangers may be larger than those from plant design data. As shown in Table 5-2, the sulfur feed rate (F50), steam flow rate (FS1), and sulfuric acid flow rate (F64) of the two sets of current operating data are greater than those of plant design conditions. This gave larger estimated values of the parameters.

Table 5-3 The Estimated Parameters from On-Line Optimization

Parameters Names	Estimated values using plant design data	Estimated values with one-step method using 6-10-97 plant data	Estimated values with two-step method using 6-10-97 plant data	Estimated values with two-step method using 6-12-97 plant data
U_{boiler}, BLRU	xxxx	xxxx	xxxx	xxxx
U_{ex65}, EX65U	xxxx	xxxx	xxxx	xxxx
U_{ex66}, EX66U	xxxx	xxxx	xxxx	xxxx
U_{ex67}, EX67U	xxxx	xxxx	xxxx	xxxx
U_{ex68}, EX68U	xxxx	xxxx	xxxx	xxxx
U_{ex69}, EX69CDU	xxxx	xxxx	xxxx	xxxx
U_{ex69A}, EX69AU	xxxx	xxxx	xxxx	xxxx
E_f^I, EFFI	0.24011	0.2923	0.2881	0.2789
E_f^{II}, EFFII	0.1597	0.1471	0.1372	0.1426
E_f^{III}, EFFIII	0.1071	0.1113	0.1111	0.1044
E_f^{IV}, EFFIV	0.03605	0.0367	0.0396	0.0418

Tables 5-4 and 5-5 list the plant data from DCS, constructed data from data validation, reconciled data from data reconciliation and parameter estimation, and optimal set points from plant optimization using plant data on 6-10-97 and 6-12-97. In Tables 5-4 and 5-5, the measurements that were detected as containing gross errors are shown in underline under reconstructed data column, and the values of these measurements were replaced by the reconciled data from data validation. Six and ten measurements were identified containing gross errors in plant data on 6-10-97 and 6-12-97 respectively. The same six measurements (T07,

T20, TS3, TS7, FS1, and CO2) in two sets of plant data were identified with gross errors. In these six measurements, T07 and T20 are the temperatures

Table 5-4 The Reconciled Data and Optimal Solution from On-Line Optimization Using Plant Data on 6-10-97, 3PM

Measured variables	Plant data	Reconstructed data from DataVali.gms	Reconciled data from ParaEsti.gms	Optimal solution from EconOpti.gms
T04	394.8	394.8	394.4	393.2
T05	1382.0	1382.0	1381.8	1404.1
T06	681.5	681.5	681.1	692.0
T07	873.2	888.8	885.2	895.0
T08	725.4	725.4	728.8	740.0
T09	796.0	796.0	795.0	807.7
T10	709.0	709.0	710.8	731.0
T11	737.0	737.0	736.3	758.4
T13	450.4	450.4	451.8	455.4
T14	355.4	355.4	354.3	397.7
T15	591.5	591.5	591.3	622.4
T16	699.8	699.8	699.4	721.0
T17	722.0	722.0	721.3	747.8
T19	533.2	533.2	536.0	548.4
T20	425.9	412.2	412.3	407.2
T21	356.5	356.5	356.3	378.2
T58	83.3	83.3	80.6	80.9
T59	119.4	119.4	122.2	123.0
T60	85.6	85.6	86.6	82.1
T61	100.6	100.6	99.5	92.9
TS1	233.0	233.0	233.2	219.2
TS2	315.0	315.0	312.7	308.1
TS3	430.0	395.4	393.3	410.0
TS4	500.0	500.0	500.0	520.8
TS7	734.0	709.0	711.8	740.0
F04	xxxx	xxxx	xxxx	xxxx
F05	xxxx	xxxx	xxxx	xxxx
F14	xxxx	xxxx	xxxx	xxxx
F20	xxxx	xxxx	xxxx	xxxx
F50	0.3624	0.3624	0.3732	0.3790
F58	14.99	14.99	14.99	13.90
F59	15.33	15.33	15.34	14.25
F60	7.02	7.02	7.02	6.200
F61	7.04	7.04	7.04	6.224
FS1	xxxx	xxxx	xxxx	xxxx
FS5	xxxx	xxxx	xxxx	xxxx
PS5	689.7	689.7	694.4	675.7
PS7	654.7	654.7	652.9	640.0
X	0.997	0.997	0.9969	0.997
CSO2	4.13	4.13	4.129	4.059
CO2	0.0453	0.0497	0.0509	0.0457
C58	0.986	0.986	0.986	0.98
C60	0.986	0.986	0.986	0.98

Table 5-5 The Reconciled Data and Optimal Solution from On-Line Optimization Using Plant Data on 6-12-97, 3PM

Measured variables	Plant data	Reconstructed data from DataVali.gms	Reconciled data from ParaEsti.gms	Optimal solution from EconOpti.gms
T04	395.9	395.9	396.0	393.2
T05	1382.0	1382.0	1382.2	1402.8
T06	679.3	679.3	679.0	694.6
T07	868.2	883.0	881.2	895.0
T08	723.2	723.2	724.9	739.2
T09	794.8	794.8	793.5	809.1
T10	708.2	708.2	709.5	731.1
T11	735.9	735.9	733.6	757.6
T13	448.7	448.7	450.6	453.1
T14	355.4	355.4	353.9	392.2
T15	589.8	589.8	590.5	619.6
T16	698.2	698.2	698.3	719.8
T17	721.5	721.5	721.3	747.6
T19	533.2	533.2	536.0	549.3
T20	424.3	412.5	411.0	404.3
T21	357.0	357.0	356.8	379.8
T58	82.8	82.8	80.6	80.9
T59	118.9	118.9	121.2	123.2
T60	86.1	86.1	87.4	82.1
T61	101.1	101.1	99.8	92.4
TS1	232.0	232.0	234.6	215.1
TS2	320.0	320.0	314.7	307.1
TS3	440.0	393.0	393.9	408.9
TS4	500.0	500.0	500.2	519.9
TS7	730.0	710.0	712.0	740.0
F04	xxxx	xxxx	xxxx	xxxx
F05	xxxx	xxxx	xxxx	xxxx
F14	xxxx	xxxx	xxxx	xxxx
F20	xxxx	xxxx	xxxx	xxxx
F50	0.3663	0.3663	0.3699	0.3801
F58	15.16	15.16	15.17	13.90
F59	15.51	15.51	15.51	14.25
F60	7.23	7.23	7.23	6.200
F61	7.25	7.25	7.25	6.225
FS1	xxxx	xxxx	xxxx	xxxx
FS5	xxxx	xxxx	xxxx	xxxx
PS5	689.7	689.7	692.1	680.4
PS7	654.7	654.7	655.0	640.0
X	0.997	0.997	0.9970	0.997
CSO2	4.06	4.06	4.06	4.050
CO2	0.046	0.051	0.0511	0.0460
C58	0.986	0.986	0.986	0.98
C60	0.986	0.986	0.986	0.98

of gases exiting from convertor I and exiting from final absorption tower. TS3 and TS7 are the temperatures of steam exiting from Economizer 3B and exiting from superheater. FS1 and CO2 are the flow rate of steam input to Economic 4A and the concentration of O_2 in gas stream exiting final absorption tower. The errors in these measurements are from instrument measuring errors. In addition, four flow rates (F04, F05, F14, and F20) in the plant data on 6-12-97 were detected containing gross errors. The reason that four flow rates were detected as containing gross errors in the same set of plant data was that all four flow rates were calibrated from the same measurement sources, the discharge pressure of compressor and the speed of turbine. Therefore, the measuring error in either/both discharge pressure of the compressor or/and speed of the turbine would cause gross errors in these four flow rates.

B-2. Plant Economic Optimization

In this section, the economic benefit from on-line optimization is studied for plant design data cases and current operating data cases. For plant design data cases, the parameter values estimated by plant design data for measured variables in Table 5-1 were used in the plant model for economic optimization, and the optimal profit from economic optimization is compared with the plant profit under the plant design operation conditions. For current operation data cases, the parameter values estimated by the plant data on 6-12-97 were used in the plant model for economic optimization, and the optimal profit from economic optimization is compared with the plant profit under operating conditions on 6-12-97. Also, a number of cases that can be encountered in plant operation are simulated to show how plant optimization improves the plant profit and reduces the emission.

Plant Optimization for Plant Design Cases: In this section, the parameter values determined by plant design data were used in plant economic optimization. Table 5-6 lists the optimization cases and compares them with plant design data. Table 5-7 lists the operation conditions for the corresponding cases in Table 5-6. In Table 5-6, the first and second columns list the names and cost coefficients of process variables in the profit function. The third through sixth columns list the corresponding optimal values of the process variables, the optimal profits and the improvement over design data for design case and cases 1 to 3. In Table 5-7, the first column lists the names of the important process

Table 5-6 The Basic Economic Cases for the Sulfuric Acid Process

Var.	Cost Coefficients	Design data	Case 1	Case 2	Case 3
F50	\$1.7/kmol	0.3450	0.3456	0.3420	0.3447
FS1	\$0.00675/kmol	xxxx	xxxx	xxxx	xxxx
F51	\$0.00005/lb	19.15	19.29	19.13	19.25
F64	\$0.0097/lb	79.50	80.04	79.41	79.89
FS8	\$0.0616/kmol	xxxx	xxxx	xxxx	xxxx
FS14	\$0.1030/kmol	xxxx	xxxx	xxxx	xxxx
Plant profit, \$/sec		0.3917	0.4032	0.3791	0.4009
Profit improvement		-	2.9%	-3.2% and 80% emission reduction	2.3% and 25% emission reduction
SO2 emission: lb SO_2/ ton H_2SO_4		4.04	4.00	0.742	3.00
Optimization objective		maximize profit	maximize profit	minimize emission	maximize profit with emission less than 3

Table 5-7 Operation Conditions of Basic Economic Cases for the Sulfuric Acid Process

Names of Variables		Design data	Case 1	Case 2	Case 3	Lower bound	Upper bound
T04,	K	383.2	393.0	373.0	393.0	373	393
T05,	K	1396.2	1428.8	1318.3	1417.7	1296	1496
T06,	K	693.2	696.2	704.3	696.8	688	895
T07,	K	890.2	895.0	895.0	895.0	688	895
T08,	K	713.2	713.9	727.3	714.9	688	895
T09,	K	792.2	796.4	801.1	796.6	688	895
T10,	K	713.2	725.3	713.3	723.6	688	895
T11,	K	738.2	752.6	735.5	750.3	688	895
T12,	K	556.2	584.3	550.9	580.0	500	650
T13,	K	438.2	431.5	443.0	432.6	388	488
T14,	K	355.2	400.8	337.2	393.3	305	405
T15,	K	594.2	621.8	575.5	616.6	534	654
T16,	K	698.2	713.5	688.0	710.7	688	895
T17,	K	719.2	739.9	702.8	735.4	688	895
T19,	K	546.2	552.6	552.0	552.1	496	596
T20,	K	405.2	394.4	406.4	395.5	355	455
TS1,	Fº	220.0	200.0	200.0	200.0	200	220
TS2,	Fº	310.0	296.2	309.0	297.1	260	360
TS3,	Fº	403.0	411.5	406.5	410.3	352	452
TS4,	Fº	500.0	510.7	504.0	509.2	450	550
TS7,	Fº	750.0	751.1	772.5	752.2	740	800
F04,	kmol/s	xxxx	xxxx	xxxx	xxxx	0.0	4.0
F05,	kmol/s	xxxx	xxxx	xxxx	xxxx	0.0	4.0
F14,	kmol/s	xxxx	xxxx	xxxx	xxxx	0.7	3.3
F20,	kmol/s	xxxx	xxxx	xxxx	xxxx	0.7	3.3
F50,	kmol/s	0.345	0.3456	0.3420	0.3447	0.0	0.354
F05SO3,	kmol/s	xxxx	xxxx	xxxx	xxxx	0.0	1.0
F07SO3,	kmol/s	xxxx	xxxx	xxxx	xxxx	0.001	4.0
F09SO3,	kmol/s	xxxx	xxxx	xxxx	xxxx	0.001	4.0
F11S03,	kmol/s	xxxx	xxxx	xxxx	xxxx	0.01	4.0
F17SO3,	kmol/s	xxxx	xxxx	xxxx	xxxx	0.0001	4.0
F20SO2,	kmol/s	xxxx	xxxx	xxxx	xxxx	0.00005	1.0

x	0.9970	0.9970	0.9995	0.9978	0.0	1.0

variables, and the second through fifth columns give the corresponding values of these variables for design and case 1 to case 3. The sixth and seventh columns list the lower and upper bounds of these variables which were imposed in the GAMS program for economic optimization.

Case 1 was to maximize the profit of the sulfuric acid plant with the profit function given in Figure 3.6. The emission restriction is that the amount of SO_2 emission should be less than four lb when a ton of sulfuric acid is produced, and it was added to the economic optimization problem. As shown in Table 5-6, the plant profit of case 1 was a 2.9% improvement in profit over the design case. It can be seen from Table 5-7, the operating of gas streams for sulfur burner and four convertors (T04 to T11 and T16 to T17) given by economic optimization were higher than the design temperatures, which were an average of 10 degree higher. This higher operating temperatures gave higher reaction rates, and therefore, it allowed a 0.0006 kmol/second higher sulfur feed rate from case 1 than design data. Hence, case 1 gave a 2.9% profit improvement over design data, which is $370,000/year of profit improvement.

Case 2 was to investigate the limitation of reducing SO_2 emission. The objective in this case was to minimize the amount of SO_2 discharge for per ton of sulfuric acid, i.e., $F21SO_2/F64$. In this objective function, $F21SO_2$ is the component flow rate of SO_2 in the stack and F64 is the rate of sulfuric acid product. The optimization solution showed the minimum emission for sulfuric acid plant was 0.74 lb SO_2/ton H_2SO_4. In this optimization, minimizing $F21SO_2/F64$ was the main driving force for determining the operation conditions. To achieve this, the optimization solution

reduced 0.005 kmol/sec. sulfur feed rate (F50), increased 0.231 kmol/sec. air feed rate (F04), and reduced operating temperature at convertor four to the lower limit, 688 K. These changes gave a lower equilibrium concentration of SO_2 and higher sulfur conversion. The optimal solution from case 2 showed that the sulfuric acid process is able to reduce the emission to 0.74 lb SO_2/ton H_2SO_4 and achieved a 99.95% sulfur conversion.

Case 3 was to maximize the plant profit at a lower SO_2 emission restriction, i.e., F21SO_2/F64 < 3 lb SO_2/ton H_2SO_4. The optimization solution gave a 2.3% of profit improvement over design data and 25% lower SO_2 emission. Under the optimal operating condition, the sulfur conversion was increased about 0.08% compared with design data and this resulted in a lower emission rate and 2.3% higher profit.

This section is to investigate the effect of the product prices on the optimal operation conditions of the plant and to show the improvement of plant profit under optimal operation conditions over the design profit of the sulfuric acid plant. Table 5-8 summarizes the optimal operation conditions under various prices of products and the corresponding plant profits. In Table 5-8, the first and second columns list the names and the units of cost coefficients of the process variables in the profit function, and the third column lists the plant design conditions with respect to the raw materials and products. Table 5-8 shows four different economic cases and the respective optimal operation conditions from plant economic optimization.

In Table 5-8, cases 4 and 5 were to show the effect of change in steam or sulfuric acid prices on the optimal profit. The objective of case 4 is to maximize the plant profit function

Table 5-8 Impacts of Parameters in the Economic Model on Plant Profits for the Sulfuric Acid Process

Name of variables (see Table 4-1 for description)	Unit of cost coef.	Plant design data	Case 4		Case 5		Case 6		Case 7	
			Cost coef.	Optimal values	Cost coef.	Optimal values	Cost coef.	Optimal values	Cost coef.	Optimal values
F50, kmol/sec	$/kmol	0.345	1.70	0.3453	1.70	0.3466		0.3414		0.3492
FS1, kmol/sec	$/kmol	xxxx	0.00675	xxxx	0.00675	xxxx		xxxx		xxxx
F51, lb/sec	$/lb	19.15	0.00005	19.27	0.00005	19.34		19.05		19.49
F64, lb/sec	$/lb	79.5	0.0097	79.97	0.01358	80.27		79.07	0.0097	80.87
FS8, kmol/sec	$/kmol	xxxx	0.0862	xxxx	0.0616	xxxx	0.0616	xxxx		xxxx
FS14,kmol/sec	$/kmol	xxxx	0.144	xxxx	0.103	xxxx	0.103	xxxx		xxxx
Optimal profit			$0.4963/sec		$0.7142/sec		$0.2346/sec		$0.7844/sec	
Plant design profit			$0.4817/sec.		$0.7001/sec		$0.2261/sec		$0.7712/sec	
Profit improvement over current Plant operation conditions			3.3%		2.0%		3.8%		1.7%	

given in Figure 3.6 with a 40% of price increase for both high and low pressure steams. Under this objective, the economic optimization gave the optimal operating conditions that could achieved 3.3% profit improvement over the plant design conditions. The objective of case 5 is to maximize the plant profit function given in Figure 3.6 with a 40% of price increase for sulfuric acid. Under this objective, the economic optimization gave optimal operating conditions that could achieved 2.0% profit improvement over the plant design conditions.

Cases 6 and 7 were to investigate how plant optimization improves the plant economics for some special cases, such as plant must run under reduced rate for certain products. Case 6 assumed that the production rate of the sulfuric acid was more than the market demand; and therefore, the operating objective was to produce more steams only, i.e., P = FS8 S_{FS8} + FS14 S_{FS14}. The objective of case 6 was to maximize the profit from steam only. Under this objective, the economic optimization gave the optimal operating conditions that could achieved 3.8% profit improvement on steam products over the plant design conditions. Case 7 assumed that the production rate of steam was more than the market demand; and therefore, the operating objective was to produce more sulfuric acid only, i.e, P = F64 S_{F64}. The objective of case 7 was to maximize the profit of sulfuric acid only. Under this objective, the economic optimization gave the optimal operating conditions that could achieved 1.7% profit improvement on sulfuric acid product over the plant design conditions.

Profit Sensitivity to Parameters: The impact of the variations of plant parameters on the optimal profit was studied using the plant design data. Table 5-9 shows the impacts of these parameters on the plant profits for cases 8 through 10. In case 8, it was assumed that the catalyst

in convertor III was replaced with other shape of catalyst; and therefore, the reaction effectiveness factors in this convertor increases from 0.11 to 0.13. In case 9, it was assumed that the catalyst in convertor IV was replaced with other shape of catalyst; and therefore, the reaction effectiveness factors in this convertor increases from 0.036 to 0.055. Under these new conditions for the plant, the optimization for both cases adjusted the optimal operation conditions to have a higher sulfur feed rate, and this resulted in a higher sulfuric acid and steam production rates and high optimal plant profit. The profit improvement under the optimal operation conditions over the design profit was 4.4% for case 8 and 5.2% for case 9.

Table 5-9 Impacts of Parameters in the Plant Model on Plant Profits for the Sulfuric Acid Process

Name of Var.	Cost coef.	Plant design data	Case 8	Case 9	Case 10
F50, kmol/sec	$1.7/kmol	0.345	0.3504	0.354	0.356
FS1, kmol/sec	$0.00675/kmol	xxxx	xxxx	xxxx	xxxx
F51, lb/sec	$0.00005/lb	19.15	19.56	19.76	19.87
F64, lb/sec	$0.0097/lb	79.50	81.16	81.99	82.45
FS8, kmol/sec	$0.616/kmol	xxxx	xxxx	xxxx	xxxx
FS14, kmol/sec	$0.103/kmol	xxxx	xxxx	xxxx	xxxx
Plant parameter change			Increase capacity in Convertor III	Increase capacity in Convertor IV	Increase capacity in Convertor IV and sulfur feed
Profit, $/sec		0.3917	0.4089	0.4121	0.4137
Profit improvement over current plant operation conditions			4.4%	5.2%	5.6%

In case 10, the conditions of the plant was the same as case 9. The additional change in this case was that the sulfur feed rate limit was increased. Under this condition, the optimal optimization solution increases the sulfur feed rate by 0.002kmol/sec. compared with case 9. The profit improvement of case 10 over plant design profit was 5.6% or $727,000/year.

Plant Optimization for Current Operation: In this section, the parameters in the plant model were estimated using plant data on 6-12-97, 3PM. These parameters values were used in the plant model for plant economic optimization. Also, the reconciled values of plant data on 6-12-97, 3PM were used to determine the plant operating profit for various profit functions and to compared with the results of plant economic optimization.

Table 5-10 lists the optimal solutions from plant economic optimization for four special operation cases, case 11 to case 14. In Table 5-10, the first to third columns list the names of variables in the profit function, the cost coefficients, and the reconciled operation conditions of plant data on 6-12-97, 3PM. The fourth to seventh columns list the optimal solutions from economic optimization for four special operation cases.

Cases 11 and 12 assumed that the plant must run under a reduced rate for steam production. Therefore, the objective function of the plant economic optimization was changed to maximize the sulfuric acid profit with a lower cost for case 11 and to maximize the production of sulfuric acid only for case 12. Cases 11 and 12 showed that plant

Table 5-10 The Optimal Solutions from Plant Economic Optimization for the Special Operation Cases

Variables	Cost coefficient	Operating data	Case 11 - cut steam production rate	Case 12 - cut steam production rate	Case 13 - cut H2SO4 production rate	Case 14 - reduce 10% of SO2 emission
F50, kmol/sec	\$1.70/kmol	0.370	0.484	0.385	0.377	0.3790
FS1, kmol/sec	\$0.00675/kmol	xxxx	xxxx	xxxx	xxxx	xxxx
F51, lb/sec	\$0.00005/lb	20.64	21.44	21.47	21.04	21.16
F64, lb/sec	\$0.0097/lb	85.67	89.00	89.09	87.31	87.80
FS8, kmol/sec	\$0.0616/kmol	xxxx	xxxx	xxxx	xxxx	xxxx
FS14, kmol/sec	\$0.103/kmol	xxxx	xxxx	xxxx	xxxx	xxxx
Profit function			= S_{F64} F64-C_{F50} F50 -C_{FS1}FS1-C_{F51} F51	= S_{F64} F64	=S_{FS8} FS8 + S_{FS14} FS14 - C_{F50} F50- C_{FS1} FS1 - C_{F51} F51	= S_{F64} F64 + S_{FS8} FS8 +S_{FS14} FS14 -C_{F50} F50 - C_{FS1} FS1 -C_{F51} F51
Current plant profit, \$/second			0.1809	0.8310	0.2472	0.4281
Optimal profit, \$/second			0.1899	0.8642	\$0.2554/sec	\$0.4397/sec
Profit Improvements			5.0%	4.0%	3.3%,	2.7%
SO_2 Emission, lb SO2/ Ton sulfuric acid			4.0	4.0	4.0	3.6

optimization gave 5.0% and 4.0% profit improvements over the operating conditions on 6-12-97, 3PM respectively. Case 13 assumed that plant must run under a reduced rate of sulfuric acid product. Therefore, the objective function of plant economic optimization was changed to maximize the production rate of steam only. The plant optimization for case 13 gave 3.3% profit improvement over the current operation condition if the plant must run under a reduced rate of sulfuric acid product. Case 14 was to optimize the plant operation conditions with a 10% lower emission restriction, 3.6 lb SO2 emission for per ton of produced sulfuric acid. The plant optimization for case 14 adjusted the operation conditions to have 2.7 profit improvement and 10% emission reduction compared with current operation conditions.

Summary: Plant economic optimization demonstrated a potential in improving the plant profits and reducing pollutant emission. The plant economic optimization showed 3% profit improvement or 2.3% profit improvement and 25% emission reduction over the design conditions for the sulfuric acid process at IMC Agrico Company's plant. On-line optimization using current operating data demonstrated that plant economic optimization gave 2.3% ($313,000/year) and 3.1% ($410,000/year) profit improvement over the plant operation conditions on 6-10-97 and 6-12-97. Also, plant economic optimization was able to achieve up to 5% profit improvements over the current plant operation conditions for some special operating cases, such as plant must run under cut rate of certain product. Moreover, plant optimization could assign the operation set points that reduced the SO_2 emission and still achieved 2.7% profit improvement over current operation condition.

B-3. Gross Error Detection and Data Reconciliation for Current Plant Operating Data

In this section, the current plant operating data given in Table 5-4 and 5-5 are used to conduct combined gross error detection and data reconciliation using three methods. These three methods are Tjoa-Biegler's contaminated Gaussian distribution method, measurement test method, and robust method using Lorentzian distribution function. The mathematical statement for these three methods were given in Eq.3-4 for measurement test method, Eq. 3-10 for contaminated Gaussian distribution method, and Eq. 3-14 for Lorentzian distribution method respectively. These three optimization problems were written in GAMS programs, and they were solved by GAMS. These three GAMS programs are given in Appendix F. The gross error detection results from these three methods are summarized in Table 5-11 and 5-12 for the plant data on 6-10-97 and 6-12-97.

Table 5-11 lists the plant data on 6-10-97 and the constructed plant data from Tjoa-Biegler's method, measurement test method, and robust method. In the table, the measurements that were identified with gross errors are showed underline. As shown in Table 5-11, Tjoa-Biegler's method detected six gross errors (T07, T20, TS3, TS7, FS1, and CO2), measurement test method detected three gross errors (T07, TS3, FS1), and robust method detected fourteen gross errors (T04, T07, T14, T15, T16, T17, T20, TS3, TS4, TS7, F58, F59, FS1, and CO2) among 43 measurements.

Table 5-12 lists the plant data on 6-12-97 and the reconstructed plant data from Tjoa-Biegler's method, measurement test method, and robust method. In this table, measurements that were identified with gross errors were marked underline. As shown in Table 5-12, Tjoa-

Biegler's method detected ten gross errors (T07, T20, TS3, TS7, F04, F05, F14, F20, FS1, and CO2), measurement test method detected three gross errors (T07,

Table 5-11 Comparison of the Reconstructed Data from Plant Data on 6-10-97, 3PM for the Three Methods

Measured variables	Plant data	T-B method	Measurement test method	Robust method
T04	394.8	394.8	394.8	417.8
T05	1382.0	1382.0	1382.0	1382.0
T06	681.5	681.5	681.5	681.5
T07	873.2	888.8	890.2	888.4
T08	725.4	725.4	725.4	725.4
T09	796.0	796.0	796.0	796.0
T10	709.0	709.0	709.0	709.0
T11	737.0	737.0	737.0	737.0
T13	450.4	450.4	450.4	450.4
T14	355.4	355.4	355.4	336.7
T15	591.5	591.5	591.5	572.4
T16	699.8	699.8	699.8	688.2
T17	722.0	722.0	722.0	705.0
T19	533.2	533.2	533.2	533.2
T20	425.9	412.2	425.9	413.9
T21	356.5	356.5	356.5	356.5
T58	83.3	83.3	83.3	83.3
T59	119.4	119.4	119.4	119.4
T60	85.6	85.6	85.6	85.6
T61	100.6	100.6	100.6	100.6
TS1	233.0	233.0	233.0	233.0
TS2	315.0	315.0	315.0	315.0
TS3	430.0	395.4	401.8	388.7
TS4	500.0	500.0	500.0	488.4
TS7	734.0	709.0	734.0	698.9
F04	xxxx	xxxx	xxxx	xxxx
F05	xxxx	xxxx	xxxx	xxxx
F14	xxxx	xxxx	xxxx	xxxx
F20	xxxx	xxxx	xxxx	xxxx
F50	0.3624	0.3624	0.3624	0.3624
F58	14.99	14.99	14.99	17.73
F59	15.33	15.33	15.33	18.08
F60	7.02	7.02	7.02	7.02
F61	7.04	7.04	7.04	7.04
FS1	xxxx	xxxx	xxxx	xxxx
FS5	xxxx	xxxx	xxxx	xxxx
PS5	689.7	689.7	689.7	689.7
PS7	654.7	654.7	654.7	654.7
X	0.997	0.997	0.997	0.997
CSO2	4.13	4.13	4.13	4.13
CO2	0.0453	0.0497	0.0453	0.0547
C58	0.986	0.986	0.986	0.986

C60	0.986	0.986	0.986	0.986

Table 5-12 Comparison of the Reconstructed Data from Plant Data on 6-12-97, 3PM for the Three Methods

Measured Var.	Plant data	T-B method	Measurement test method	Robust method
T04	395.9	395.9	395.9	447.7
T05	1382.0	1382.0	1382.0	1382.0
T06	679.3	679.3	679.3	692.7
T07	868.2	883.0	889.4	890.5
T08	723.2	723.2	723.2	723.2
T09	794.8	794.8	794.8	794.8
T10	708.2	708.2	708.2	708.2
T11	735.9	735.9	735.9	735.9
T13	448.7	448.7	448.7	448.7
T14	355.4	355.4	355.4	320.7
T15	589.8	589.8	589.8	564.0
T16	698.2	698.2	698.2	681.0
T17	721.5	721.5	721.5	695.0
T19	533.2	533.2	533.2	533.2
T20	424.3	412.5	424.3	424.3
T21	357.0	357.0	357.0	357.0
T58	82.8	82.8	82.8	82.8
T59	118.9	118.9	118.9	118.9
T60	86.1	86.1	86.1	86.1
T61	101.1	101.1	101.1	101.1
TS1	232.0	232.0	232.0	244.4
TS2	320.0	320.0	320.0	320.0
TS3	440.0	393.0	399.5	389.7
TS4	500.0	500.0	500.0	484.6
TS7	730.0	710.0	730.0	696.5
F04	xxxx	xxxx	xxxx	xxxx
F05	xxxx	xxxx	xxxx	xxxx
F14	xxxx	xxxx	xxxx	xxxx
F20	xxxx	xxxx	xxxx	xxxx
F50	0.3663	0.3663	0.3663	0.3663
F58	15.16	15.16	15.16	18.53
F59	15.51	15.51	15.51	18.88
F60	7.23	7.23	7.23	7.23
F61	7.25	7.25	7.25	7.25
FS1	xxxx	xxxx	xxxx	xxxx
FS5	xxxx	xxxx	xxxx	xxxx
PS5	689.7	689.7	689.7	689.7
PS7	654.7	654.7	654.7	654.7
X	0.997	0.997	0.997	0.997
CSO2	4.06	4.06	4.06	4.06
CO2	0.046	0.051	0.046	0.060

C58	0.986	0.986	0.986	0.986
C60	0.986	0.986	0.986	0.986

F14, FS1), and robust method detected fifteen gross errors (T04, T07, T08, T14, T15, T16, T17, TS1, TS3, TS4, TS7, F58, F59, FS1, and CO2) among 43 measurements.

The results from these three methods for gross error detection and data reconciliation showed that Tjoa-Biegler's method and measurement test method gave better result than robust method. Although the true gross error information was not available for comparison, a 10% to 20% gross errors in measurements is the common case in the plant sampled data. Tjoa-Biegler's method identified that 18% of measurements contain gross errors, measurement test method identified that 7% of measurements contain gross errors, and robust method identified that 34% of measurements contain gross errors.

As discussed in Chapter III for the comparison of relative efficiencies of distributions, variation of Lorentzian distribution is larger than the contaminated Gaussian distribution and normal distribution; and therefore it has a lower relative efficiency (or low accuracy) when measurements do no have very larger gross errors. The numerical studies of gross error detection, which will be discussed in Section D of this chapter, showed that Lorentzian committed a larger number of type I errors (i.e., misidentify a normal measurement as one with a gross error) than Tjoa-Biegler's method and measurement test method when the gross errors in measurements are less than 20F (as shown in Figure 5.5 and Figure 5.6). Therefore, it is reasonable to conclude that robust method using Lorentzian distribution function committed some type I errors in identifying gross errors for the plant data on 6-10-97 and 6-12-97, and some of measurements that did not have gross errors were misidentified with gross errors.

B-4. Sensitivity of Results for Combined Gross Error Detection and Data Reconciliation to Parameter Values in the Plant Model

In this section, the effect of parameter values in the plant model on the result of combined gross error detection and data reconciliation is given. In Chapter III, it was proposed that parameter values from previous parameter estimation be used in the plant model for combined gross error detection and data reconciliation to construct a set of measurements from the data sampled by DCS for estimating current plant parameters. In this section, two sets of parameter values were used in the plant model for combined gross error detection and data reconciliation to construct a set of measurements in the first sequent of on-line optimization. These two sets of starting parameters are plant design parameters and one-step estimated parameters using current plant data. Then the constructed measurements were used to estimate current values of parameters. The estimated current values of parameters were compared for these two sets of starting parameters to show how sensitive the results of the on-line parameter estimation is to the starting parameter values in the plant model for combined gross error detection and data reconciliation.

Table 5-13 lists the estimated parameter values using plant operating data for two different cases. For case of plant design parameters, the plant parameters estimated by plant design data, which are listed in column two (Set A), were used in plant model for data validation at the first sequence of on-line optimization. The parameters estimated sequence

Table 5-13 Estimated Parameters Using Measurements Reconstructed from Plant Operating Data for Cases of Plant Design Data and One-Step Estimated Data

Parameters Names	Plant design parameter case			One-step estimated parameter case		
	Set A: Design parameters	Set B: Estimated values using 6-10-97 plant data	Set C: Estimated values using 6-12-97 plant data	Set D: One-step estimated Parameters using 6-10-97 plant data	Set E: Estimated values using 6-10-97 plant data	Set F: Estimated values using 6-12-97 plant data
BLRU	xxxx	xxxx	xxxx	xxxx	xxxx	xxxx
EX65U	xxxx	xxxx	xxxx	xxxx	xxxx	xxxx
EX66U	xxxx	xxxx	xxxx	xxxx	xxxx	xxxx
EX67U	xxxx	xxxx	xxxx	xxxx	xxxx	xxxx
EX68U	xxxx	xxxx	xxxx	xxxx	xxxx	xxxx
EX69CDU	xxxx	xxxx	xxxx	xxxx	xxxx	xxxx
EX69AU	xxxx	xxxx	xxxx	xxxx	xxxx	xxxx
EFFI	0.24011	0.2591	0.2627	0.2923	0.2881	0.2789
EFFII	0.1597	0.1400	0.1369	0.1471	0.1372	0.1426
EFFIII	0.1071	0.1208	0.1123	0.1113	0.1111	0.1044
EFFIV	0.03605	0.03520	0.0390	0.0367	0.0396	0.0418

was that first the plant design parameters shown in column two (Set A) were used in the data validation of plant data on 6-10-97. Then the reconstructed plant measurements were used to estimated plant parameters, and the estimated values are shown in column three (Set B). The parameters in set B were used in the data validation of plant data on 6-12-97. Then the reconstructed plant measurements were used to estimated plant parameters, and the estimated values are given in column four (Set C). For the case of one-step estimated parameters, first the plant data on 6-10-97 was used to estimate plant parameters using one step method (simultaneous gross error detection, data reconciliation, and parameter estimation), and the estimated parameter values were given in column five (Set D). These parameters (Set D) were used in data validation of plant data on 6-10-97 (step one of two-step method) to construct the plant measurements for next step of parameter estimation. The constructed plant data was used to estimate plant parameters in step two of two-step method, and the values of the estimated parameters are shown in column six (Set E). Then, the parameters in set E were used in data validation of plant data on 6-12-97, and the reconstructed plant data on 6-12-97 was used to estimate plant parameters as shown in column seven (Set F).

As shown in Table 5-13, the values of parameters in Set B and Set C are closer to those in Set A than to Set D, and the values of parameters in Set E and Set F are closer to those in Set D than to Set A. This means that the estimated values of parameters in step two are sensitive to the values of parameters used in the plant model of step one (combined gross error detection and data reconciliation). This also can be seen by the comparison of the estimated parameters using

plant design parameters and one-step estimated parameters in the plant model of the first sequent data validation for plant data on 6-10-97 and on 6-12-97.

Table 5-14 shows the difference of estimated parameters between plant design parameter case and one-step method case. In Table 5-14, fractional differences of estimated parameters between plant design case (Set B) and one-step estimated case (Set E) for plant data on 6-10-97 are listed in column two, and fractional differences of estimated parameters between plant design case (Set C) and one-step estimated case (Set F) for plant data on 6-12-97 are listed in column three. The average percentage differences are 9.6% for plant data on 6-10-97 and 10.4% for plant data on 6-12-97. Table 5-14 shows

Table 5-14 The Fractional Difference of Estimated Parameters Using Plant Design Data and One-Step Estimated Data in the Reconstruction of Plant Measurements

Parameters Names	| Set E - Set B| / Set B Using plant data on 6-10-97	| Set F - Set C| / Set C Using plant data on 6-12-97
BLRU	0.118	0.134
EX65U	0.102	0.102
EX66U	0.047	0.049
EX67U	0.090	0.071
EX68U	0.115	0.075
EX69CDU	0.178	0.234
EX69AU	0.087	0.231
EFFI	0.101	0.062
EFFII	0.020	0.042
EFFIII	0.087	0.070
EFFIV	0.111	0.072
Average	0.096	0.104

that the accuracy of the estimated parameters from simultaneous data reconciliation and parameter estimation is sensitive to parameter values in plant model for data validation.

The parameters used for the data validation should be close to the current operating parameter values. The proposed strategy that using the parameter values estimated from the last sequent on-line optimization in the plant model for combined gross error detection and data reconciliation is appropriate. The reasons are that these values are the most current values of parameters available, and that they are close to the true values.

C. Theoretical Evaluation Results

The performance of algorithms and plant models for on-line optimization have been theoretically evaluated in Chapter III. It was determined that measurement test method, Tjoa-Biegler's method, and robust distribution method are applicable for conducting the combined gross error detection and data reconciliation and the simultaneous data reconciliation and parameter estimation.

In Chapter III, the comparison of influence function and relative efficience showed theoretically that Tjoa-Biegler's contaminated Gaussian distribution and Lorentzian distribution (robust function) methods have better performance in terms of less sensitive to the presence of gross errors and higher relative efficiency when measurements contain both random and gross errors. Tjoa-Biegler's method is more effective for moderate size of gross errors, while Lorentzian distribution method is more effective when a gross error is extremely large. Normal distribution of measurement test method has the highest relative efficiency (estimation accuracy) when measurements only contain random errors.

In general, two separate steps are required to estimate process parameters, i.e., step one to conduct gross error detection and data reconciliation to generate a set of measurements that only contains random errors; and step two to conduct simultaneous data reconciliation and parameter estimation using the set of measurements generated in step one. This is the two-step estimation. Based on the fact that both contaminated Gaussian distribution and Lorentzian distribution methods have the ability to automatically rectify both random and gross errors in measurements, it was proposed in Chapter III that gross error detection, data reconciliation, and parameter estimation can be conducted simultaneously using the plant data from distributed control system. This is the one-step estimation.

As discussed in Chapter III, precise and accurate process model is essential for on-line optimization. The process model serves as constraints in the nonlinear optimization problems for data reconciliation, parameter estimation, and economic optimization. In addition, the process model used for data reconciliation optimization problems must satisfy the observability and redundancy. The general procedure to formulate a process model and the method to examine the observability and redundancy of a plant model have been proposed in Chapter III, and it was applied to sulfuric acid process which will be described in later section.

In Chapter IV, the plant model for the sulfuric acid plant was formulated as a set of open form equations based on the conservation laws and the engineering knowledge. The parameters in the plant model were selected, and they include seven heat transfer coefficients for seven heat exchangers and four reaction effectiveness factors for four packed-bed reactors given in Table 4-8. The plant required 43 measured variables to satisfy the observability and redundancy, and

these measured variables were given in Table 5-1 with the plant design values for these variables. In total, the sulfuric acid plant model has 775 process variables, among which 43 variables are measured variables and 732 are unmeasured variables, 761 linear and nonlinear equality constraints, and 11 parameters.

D. Numerical Evaluation of Combined Gross Error Detection and Data Reconciliation Methods Using Sulfuric Acid Plant

In this section, the measurements test, contaminated Gaussian distribution, and Lorentzian distribution methods are used to conduct the combined gross error detection and data reconciliation using simulated plant data. The nonlinear optimization problem statements for these methods were given in Eq. 3-4 for measurement test (or least squares) method, Eq. 3-10 for contaminated Gaussian distribution method, and Eq. 3-14 for Lorentzian distribution method respectively. For the contaminated Gaussian distribution, the equal prior probability for random and gross errors is assumed, which is $0 = 0.5$ in the distribution function. Also, two values (10 and 20) are used for parameter b in the distribution function to evaluate how the shapes of the contaminated distribution affect the performance of the algorithm. Parameter b is the ratio of the standard deviation for gross error to the one for random error in the distribution. The terms TB10 and TB20 will be used to represent the contaminated Gaussian distribution with parameter b equal to 10 and 20 respectively.

Although the objective functions are different for these three methods, the constraints of the plant model in Eq. 3-4, 3-10, and 3-14 for these methods are the same. These constraints were described in the plant model formulation chapter. The detail plant model includes 761 linear

and nonlinear constraints and 775 process variables of which 43 variables are measured. The true values and standard deviations of these measured variables are given in Tables 5-1 previously. The plant design data for the measured variables was used as the true values and the standard deviations were determined by the plant operation data from distributed control system which were provided by IMC Agrico Company and reported in Zhang' thesis (Zhang, 1993).

In order to compare and evaluate the performance of combined gross error detection and data reconciliation algorithms, the true measurement errors must be known and the same measurements must be used for these methods. Therefore, a number of sets of measurements with known random and gross errors were constructed and used to conduct combined gross error detection and data reconciliation. Each set of measurements was constructed by adding random errors **e** and gross errors a^* to the true values of measured variables, **x**, i.e.,

$$\mathbf{y} = \mathbf{x} + \mathbf{e} + a^* \tag{5-1}$$

where **y** represents the simulated plant measurements and **x** denotes the true values of measured variables. a^* represents the gross errors added to true values of measured variables. The elements in vector * will be one for the measured variables with gross errors and will be zero for other measurements. "a" represents the magnitude of a gross error.

The random errors **e** were generated by pseudo random generator in GAMS with a function NORMAL, i.e.,

$$e(i) = \text{NORMAL}(0, F(i)) \tag{5-2}$$

The random errors generated by Eq. 5-2 will possess the normal distribution character with zero mean and σ^2 variance, and these random errors are added to the true values of all measured variables.

The generation of simulated plant data was incorporated in the GAMS program. For each run, the seed number for random errors and the location and magnitude of gross errors were specified; and a set of new measurements was automatically generated to conduct data reconciliation.

The performances of these algorithms were evaluated based on the correct gross error detection rate, type I error, type II error, and the error reductions of measurements from the results. The gross error detection rate is the ratio of number of gross errors that are correctly detected to the number of total gross errors simulated in measurements. It was called overall power by Narasimhan and Mah (1987). This criterion indicates how successful an algorithm detects gross errors and qualitatively reflects the accuracy of the rectification from an algorithm. Higher gross error detection rate means better performance by the algorithm. Type I and II errors reflect faulty decision by the test statistic. If the null hypothesis is true for a measurement (i.e., a measurement does not contain gross error) and the test rejects the null hypothesis (i.e., the test misidentifies the measurement as having a gross error), then this is called a type I error. The number of type I errors indicates qualitatively the degree of the misrectification by an algorithm. If the null hypothesis is not true for a measurement (i.e., a measurement contains gross error) and the test accepts the null hypothesis (i.e., the test misidentifies the measurement as not having a

gross error), then this is called a type II error. The number of type II error represents the number of gross errors that are not detected.

The both random and gross error reductions of a set of measurements after data reconciliation are important criteria to evaluate the performance of a data reconciliation algorithm. They quantitatively indicate the accuracy of error rectification from the data reconciliation. The relative error reduction after data reconciliation for each measurement, γ_i, is determined by:

$$\gamma_i = (e_{mi} - e_{ri}) / e_{mi} \tag{5-3}$$

where e_{mi} is the true measurement error and is the absolute difference between a measurement y_i and its true value x_i, i.e.,

$$e_{mi} = |y_i - x_i| \tag{5-4}$$

e_{ri} is the remaining error of the reconciled value for a measured variable after data reconciliation and it is the absolute difference between the reconciled value $\tilde{x}_i$ and the true value x_i for a measured variable, i.e.,

$$e_{ri} = |\tilde{x}_i - x_i| \tag{5-5}$$

The optimization problem of Eq. 3-4 for measurement test, Eq. 3-10 for Tjoa-Biegler's contaminated Gaussian distribution method, or Eq. 3-14 for Lorentzian distribution method was written as a GAMS input code and solved by GAMS. The procedure is shown in Figure 5.2. First, the simulated plant data is generated with

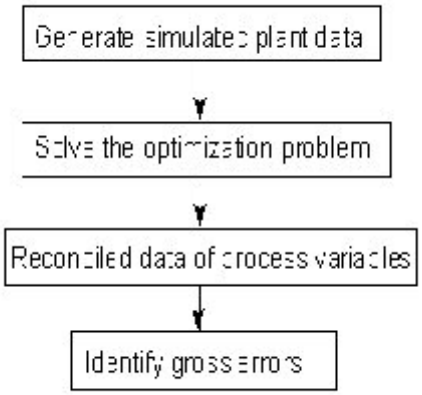

Figure 5.2 Procedure of GAMS Implementation

Eq.5-1, and then this set of measurements is used in the optimization problem to reconcile the process variables by solving the optimization problem. Based on the reconciled data, measurement errors are determined and compared with the test statistic to determine if a measurement contains gross error.

The results from the optimization solution of combined gross error detection and data reconciliation algorithms were compared with the true information to determine the evaluation criteria: gross error detection rate, number of type I errors, and relative error reductions, which are the indication of algorithm performance in rectifying random and gross errors and are a function of the magnitudes and numbers of gross errors in a set of measurements. Then, the performance of these algorithms was evaluated based on these criteria. First, the cases of the single gross error with various error magnitudes were conducted to investigate the ability of detecting gross error and rectifying the errors by these algorithms. Then, the cases of multiple gross errors were examined to see how multiple gross errors affected the rectification results. Also, the proposed modified compensation strategy was incorporated with measurement test to demonstrate the improvements in the misrectification from the presence of larger gross errors.

D-1. Comparison of Algorithm Performances for the Single Gross Error Cases

The objective of this section is to compare the performance for data reconciliation by these methods and to show how the distribution functions affect the results. For this purpose, each set of the simulated plant data was generated by adding one gross error to one of the measured variables and random errors to the true values of all measured variables as stated in Eq. 5-1 with one element in $\clubsuit$ being one and others being zero. The magnitude of a gross error was

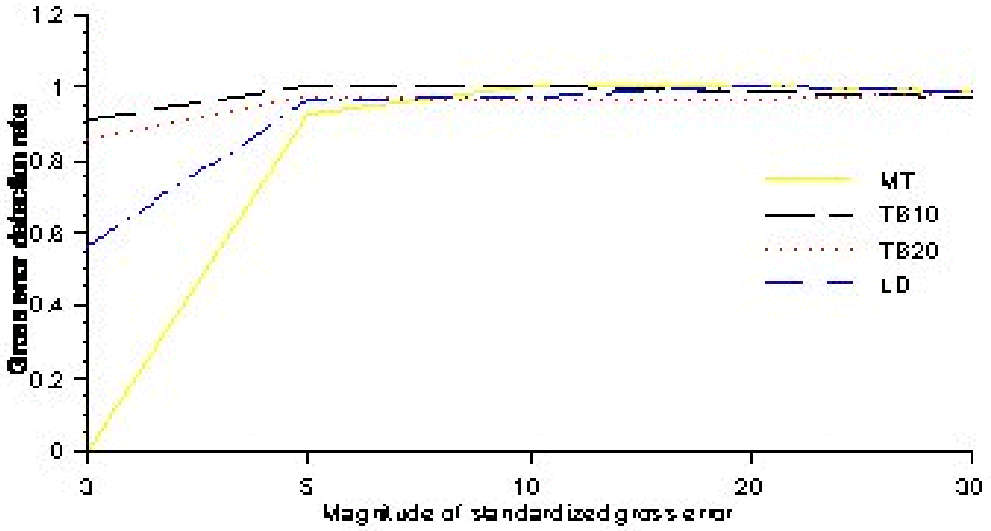

Figure5.3 Comparison of Detection Rates for one Gross Error Added to one Measurement in the Intermediate Streams

set from 3F to 30F. Then the normal distribution for measurement test, contaminated Gaussian distribution for Tjoa-Biegler's method, and Lorentzian distribution for robust method were used to reconcile the data using the simulated plant data. The performance of these algorithms was compared based on the data reconciliation and gross error detection results. The same 645 sets of simulated plant data were used for each algorithm. Each set of simulated plant data contained only one gross error. In these 645 sets of data, each 45 sets of data had the gross error in the same measured variable (one of 43 measurements)with gross error magnitudes in 3F, 5F, 10F, 20F, and 30F and three different random seed numbers.

The statistical results from 2580 runs for the gross error detection rate, number of type I errors, and error reductions of these algorithms were summarized as functions of gross error magnitudes, and they are shown in the following figures. In these figures, the legends, MT, TB, and LD are for measurement test method, Tjoa-Biegler's method and Lorentzian distribution methods respectively.

Gross Error Detection Rate and Number of Type I Errors: Figures 5.3 and 5.4 compare the gross error detection rates for the cases that one gross error was added to one measured variable in the intermediate streams of the process and for the cases that one gross error was added to one measured variable in any streams of the process. Figure 5.3 is to show how well the algorithms rectify the gross error when this gross error exists in the measured variable in an intermediate stream of the process. In the plant model, these types

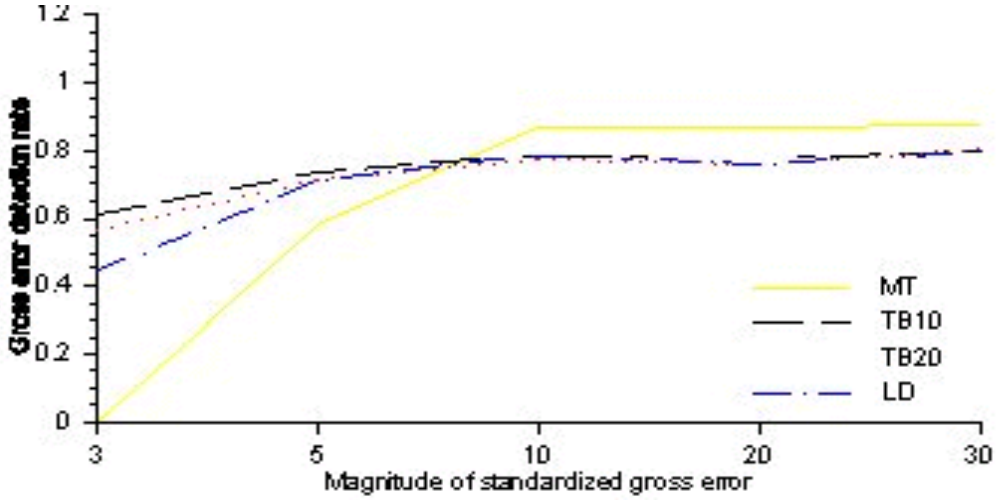

Figure5 .4 Comparison of Detection Rates for One Gross Error Added to one measurement in any stream in the Process

of measured variables are in constraint equations for a process unit as defined in Chapter IV, and the reconciled values of these types of measured variables must satiafy more balance equations than those of measured variables in the input or output stream of the process.

For all algorithms, Figure 5.3 shows that the gross error detection rate increases with the increase in the size of gross errors. All methods have essentially the same detection rates of 95% for the gross error magnitude larger than 5F. Summarized over 645 runs' results, all of three algorithms are able to correctly detect over 95% of the gross error that was added to the measured variables in the intermediate streams and whose size was larger than 5F. For gross error size from 3F to 5F, Tjoa-Biegler's method (TB) has better performance than measurement test (MT) method and Lorentzian distribution (LB). For gross error size at 3F, the measurement test method was not able to detect the gross error at all. The reason is that the critical value determined by Eq. 2-23 (Mah and Tamhane, 1982) for normal distribution with 95% confidential level is about 3.2, which is larger than the simulated gross error size , 3. As discussed in literature

review, it has been reported that the criterion to determine the individual significant level proposed by Mah and the coworkers is too conservative, and this results in larger numbers of type II errors for small gross errors.

In Figure 5.4, gross error detection rates of the algorithms are compared for the cases that one gross error was added to a measured variable in either intermediate streams or in the beginning or ending streams. The figure shows that the patterns of detection rates versus gross error size are similar to ones in Figure 5.3 for the case that one gross error was added to the measured variable in the intermediate streams. The detection rates increase with the increase in size of a gross error for the error less than 5σ, and they remain at the uniform and higher level for a gross error above 5σ. However, the detection rates for all ranges of a gross error are about 25% less than the case where a gross error was added only to the measured variables in the intermediate streams. The pattern of gross error detection rates versus error size for TB and LD is the same as the cases that a gross error was added to the measured variable in the intermediate streams with 20%-30% lower error detection rates. The measurement test method has higher gross error detection rates than TB and LD method for a standardized error greater than 10.

Figures 5.5 and 5.6 show the dependency of numbers of type I errors on the size of the gross error. The patterns of curves in the figures show that measurement test method is very sensitive to the magnitude of the gross error; the number of type I errors increases exponentially with the increase of magnitudes. Tjoa-Biegler's method has a very small number of type I errors for standardized errors less than 20. However, the number of type I errors committed by TB

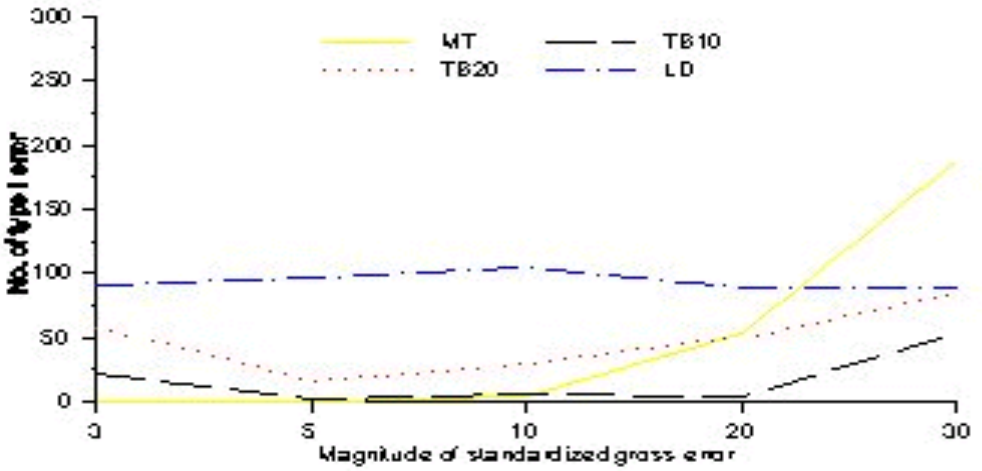

Figure5.5 Comparison of TYPE I Errors for One Gross Error Added to one measurement in the Intermediate Streams over 390 runs

increases with a pattern similar to MT for a larger gross error. This agrees with the prediction from theoretical evaluation as discussed in Chapter III. The contaminated Gaussian distribution has the functional form of the normal distribution and it is not able to bound the effect of a extremely large gross error. Lorentzian distribution method has a very uniform number of type I errors for all ranges of a gross error size. It is able to bound the effect of a larger or even infinite gross error as discussed in theoretical evaluation of Chapter III. It is not sensitive to the magnitude of a gross error.

As shown in Figures 5.3 to 5.6, the gross error detection rates and numbers of type I errors from TB10 and TB20 are similar. TB10 and TB20 do not have significantly different performance. It is concluded that small variation of parameter b in contaminated Gaussian distribution does not have significant impact on the performance of this algorithm. However, it

is expect that the increase of parameter b shifts the performance of this algorithm from normal distribution to robust function.

Random and Gross Error Reductions: The relative random error reduction and relative gross error reduction after data reconciliation are given as a function of gross error size in Figure 5.7 and 5.8 respectively for the algorithms. Figure 5.7 compares the results for relative random error reductions defined in Eq. 5-3 after data reconciliation averaged over 645 runs' results for each algorithm. Tjoa-Biegler's method with b=10 has the highest relative random error reduction among the three algorithms, which is 66.1% reduction of the original measurement errors in average. Measurement test method has the lowest random error reduction, 44.0% reduction of the original measurement errors. Also, the relative random error reduction for the measurement test method is reduced with the increase in size of gross errors. As discussed in theoretical evaluation, the normal distribution function is not able to bound the effect of gross errors and larger gross error will cause larger biased estimation. The decrease of the average error reduction from MT was caused by the misrectification from the presence of larger gross errors. Also, the figures show that the random error reductions from TB and LD are less sensitive to the variations of error sizes than one from MT.

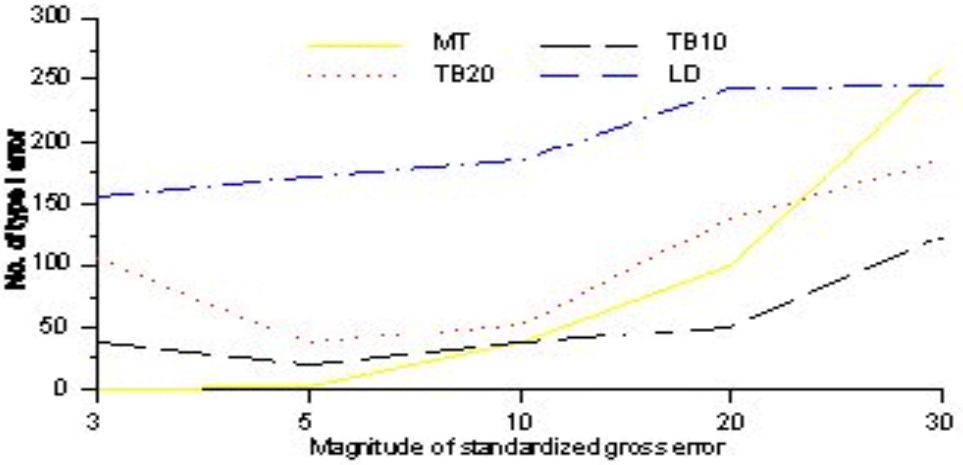

Figure5.6 Comparison Type I Errors for one Gross Error Added one Measurement in any stream Over 645 runs

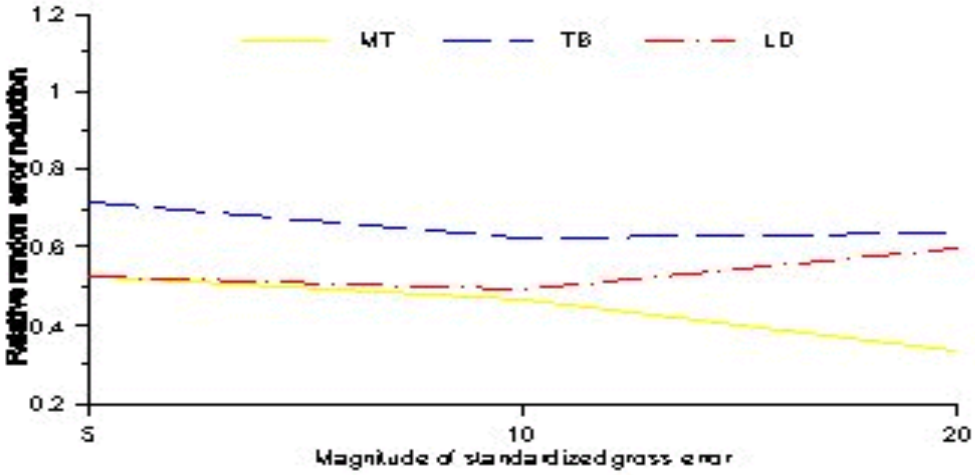

Figure 5.7 Comparison Relative Random Error Reductions for One Gross Error in simulated Plant Data Over 645 runs

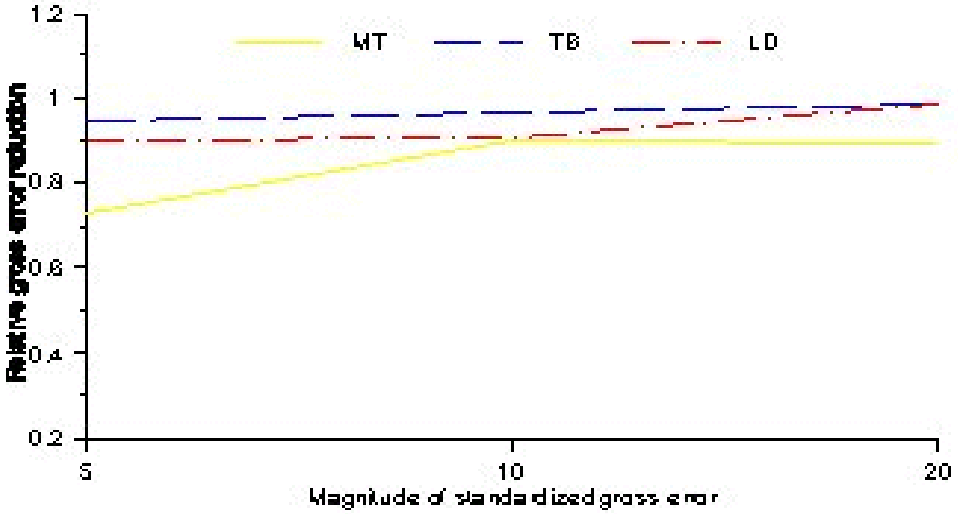

Figure 5.8 Comparison of Relative Gross Error Reduction for One Gross Error in Simulated Plant Data over 645 runs

Figure 5.8 compares the relative gross error reduction after data reconciliation averaged over 645 runs' results for each algorithm. The gross error reduction is determined by Eq. 5-3 as the random error reduction. However, this reduction was summarized only on the measurements with gross errors. The gross error reductions from TB and LD increase with the increase of error sizes. TB and LD have the comparable performance in gross error reduction. Tjoa-Biegler's method has the highest average gross error reduction as 97% of the original gross errors. Measurement test method has the lowest gross error reduction as 84.2% of the original gross errors. Measurement test method has higher gross error reduction at $10F$ of gross error size, and then the gross error reduction decreases with the increase in size of gross errors. The reason for this probably is the method is based on the normal distribution function where gross errors are not allowed, and it is not able to rectify larger gross errors. This method is not effective in rectify the gross errors larger than $10F$, and this may cause the reduced gross error reduction.

Summary: Figures 5.3 and 5.4 show that Tjoa-Biegler's method has highest gross error detection rates for the gross errors ranging in $3F$ to $30F$. As mentioned earlier, the test statistic of measurement test is too conservative (the critical value is $3.2F$ for the model of sulfuric acid process if 95% confidential level is used). Therefore, it was unable to detect the gross errors at $3F$ and the smaller. For size of gross errors larger than $5F$, all algorithms have almost perfect error detection rates for the case that a gross error was added to the measured variable in the intermediate streams.

The patterns of number of type I errors, relative random and gross error reductions versus gross error sizes shown in Figures 5.6, 5.7, and 5.8 indicate that the performance of measurement test method is sensitive to the magnitudes of gross errors and its performance decays with the increase of error sizes. Both Tjoa-Biegler's method and Lorentzian distribution have more uniform performances over a wide range of gross error magnitudes compared with measurement test method. The number of type I errors for gross error size from 3σ to 30σ increased 259 for measurement test method, 86 for Tjoa-Biegler's method, and 90 for Lorentzian distribution method. The relative random error reduction for gross error size from 5σ to 20σ reduced 18.9% for measurement test method that had an averaged 44.0% reduction and 7.2% for Tjoa-Biegler's method that had an averaged 66.1% reduction. The relative random reduction increased 7.2% for Lorentzian distribution method that had an averaged 53.7% reduction. The relative gross error reduction for gross error size from 5σ to 20σ reduced 16.3% for measurement test method that had an averaged 84.2% reduction. The relative gross error reduction increased 3.8% for Tjoa-Biegler's method that had an averaged 96.7% reduction and 8.1% for Lorentzian distribution method that had an averaged 93.3% reduction.

In average, Tjoa-Biegler's method gave highest gross error detection rate, smallest number of type I errors, highest random and gross error reduction for the gross error size from 3σ to 30σ. Tjoa-Biegler's method has the best performance for these gross error sizes. The results in Figures 5.7 and 5.8 also showed that Lorentzian demonstrated an better performance improvement than Tjoa-Biegler's method when the size of gross error goes to larger. This indicates a trend that Lorentzian distribution will perform better than contaminated Gaussian

distribution when the gross error is larger than 30 times the standard deviation. It agrees with the conclusion from the theoretical evaluation that Lorentzian distribution is more effective for larger gross errors.

The overall performance of the algorithms is summarized in Table 5-15. The second row in the table lists the average gross error detection rates over the gross error sizes from 3σ to 30σ. The detection rates are 78.2% for measurements test, 97.4% for Tjoa-Biegler's method, and 89.7% for Lorentzian distribution. The third row in Table 5-2 gives the average relative random error reductions, which are 44.0% for measurement test method, 66.1% for Tjoa-Biegler's method, and 53.7% for Lorentzian distribution respectively. The fourth row of the table shows the average relative gross error reductions that are 84.2% for measurement test, 96.7% for Tjoa-Biegler's method, and 93.3% for Lorentzian distribution. The comparison for single gross error cases concluded that Tjoa-Biegler's method has the best performance in error reductions and gross error identification for the errors ranging from 3σ to 30σ.

Table 5-15 Summary of the Overall Performances of Algorithms for One Gross Error

	Measurement Test Method	Tjoa-Biegler's Method	Lorentzian Distribution
Average gross error detection rate	78.2%	97.4%	89.7%
Relative random error reduction, >	44.0%	66.1%	53.7%
Relative gross error reduction,>	84.2%	96.7%	93.3%

D-2. Comparison of Performance of Algorithms for Multiple Gross Errors

The objective of this section is to investigate the effects of multiple gross errors on the reconciliation results for the algorithms. Therefore, a set of simulated plant data is generated by adding one, two, three, or four gross errors to the measured variables and random noises to all measured variables. Then, the normal distribution, contaminated Gaussian distribution, and Lorentzian distribution were used to reconcile the process variables using the same simulated data with one, two, three, or four gross errors ranging from $5F$ to $20F$. In this section, the gross error size of $3F$ and $30F$ was not conducted. The reason was that the results from the one gross error case for the gross error ranges from $5F$ to $20F$ was able to demonstrate the important characters of gross error detection results. In addition, the modified compensation strategy was incorporated with measurement test, i.e., modified compensation measurement test (MCMT), to demonstrate how it improves the misrectification.

The statistical results for gross error detection rates and numbers of type I errors were summarized based on the 640 runs for each algorithm and they are listed in Tables 5-16 and 5-17. As shown in these two tables, the gross error detection rates decrease and numbers of type I errors increase when the number of gross errors in a set of measurements increases for all algorithms. The reason is that the algorithms are more difficult to judge if measurements contain gross errors or not when more gross errors are present in a close neighborhood (e.g., two or more gross errors are present in one unit or two adjacent units). Therefore, the rectification accuracy reduces. However, if two abnormal measurements located in two non-adjacent units, these two gross errors will act like individual gross errors, and they will not interact.

Table 5-16 The Comparison of Gross Error Detection Rates for Multiple Gross Errors

Algorithms	Gross error detection rate				
	Sizes of gross error	One gross error	Two gross errors	Three gross errors	Four gross errors
Tjoa - Biegler's method	5F	1.0	0.878	0.867	0.789
	10F	1.0	0.956	0.845	0.778
	20F	0.987	0.922	0.867	0.867
Lorentzian distribution	5F	0.962	0.922	0.830	0.817
	10F	0.974	0.933	0.859	0.806
	20F	1.0	0.933	0.852	0.872
Measurement test method	5F	0.923	0.878	0.733	0.739
	10F	1.0	0.989	0.918	0.944
	20F	1.0	1.0	0.948	0.967
Modified compensation measurement test method	5F	0.923	0.856	0.726	0.733
	10F	0.987	0.989	0.889	0.917
	20F	1.0	0.989	0.933	0.950

Table 5-17 The Comparison of Numbers of Type I Errors for Multiple Gross Errors

Algorithms	Number of type I errors				
	Sizes of gross error	One gross error	Two gross errors	Three gross errors	Four gross errors
Tjoa - Biegler's method	5F	2	13	18	41
	10F	5	12	41	79
	20F	3	54	47	79
Lorentzian distribution	5F	65	58	70	74
	10F	74	70	80	155
	20F	78	107	164	167
Measurement test method	5F	0	0	4	2
	10F	3	13	57	85
	20F	53	145	258	396
Modified compensation measurement test method	5F	0	0	1	1
	10F	0	1	9	9
	20F	0	0	33	39

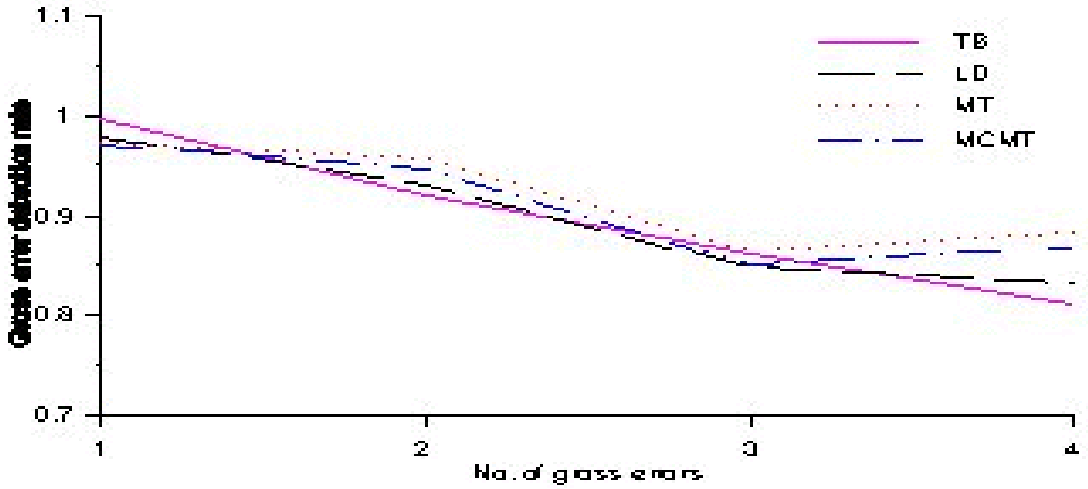

Figure 5.9 Effects of Numbers of Gross Errors on Gross Error Detection Rates of Algorithms for Errors Ranging form 5F to 20F

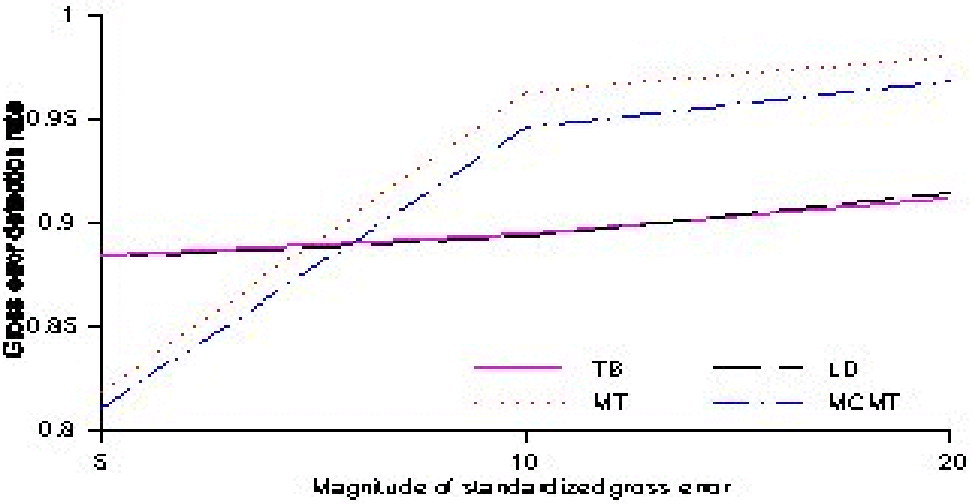

Figure 5.10 Effects of Errors on Magnitudes of Gross Error Detection Rates of Algorithms for Multiple Gross Errors

Figure 5.9 compares the effects of numbers of gross errors on gross error detection rates, and Figure 5.10 shows the effects of gross error magnitudes on the gross error detection rates for multiple gross error cases. As shown in Figure 5.9, the patterns of gross error detection rate versus number of gross errors are similar for four algorithms. The gross error detection rates reduce with the increase of number of gross errors. The reduced gross error detection rates are probably caused by the increase possibility of multiple gross errors existing in a close neighborhood (e.g., more than two gross errors exist in one unit or two adjacent units) when number of gross errors in a set of measurements increases. As seen in Figure 5.10, the pattern of gross error detection rate versus gross error sizes for multiple gross errors is similar to those for single gross error cases shown in Figure 5.4. In general, gross error detection rates increase with the increase of gross error sizes. However, the variations of the detection rates for Tjoa-Biegler's method and Lorentzian distribution are insignificant. These two algorithms are not sensitive to the variation of gross error sizes.

Figures 5.11 and 5.12 compare the effect of number of gross errors and gross error magnitude on number of type I errors for four algorithms. It is seen from these two figures that the increase of gross error numbers and magnitudes tends to cause larger numbers of type I errors which indicates a higher misrectification. This situation is particularly serious for measurement test method. The increase of numbers of type I error from one gross error to four gross errors is 427 for measurement test, 49 for MCMT, 189 for Tjoa-Biegler's method, and 179 for Lorentzian distribution. The increase of numbers of type I error from 5F to 20F for

multiple gross errors is 846 for maturement test, 70 for MCMT, 320 for Tjoa-Biegler's method, and 249 for Lorentzian distribution.

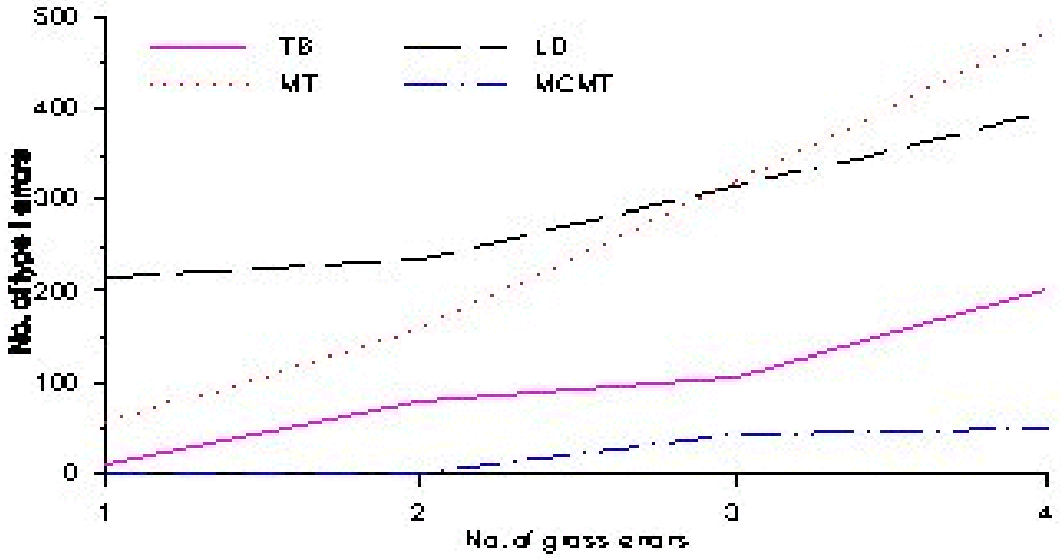

Figure 5.11 Effects of Numbers of Gross Errors on Type I Errors of Algorithms for Multiple Gross Errors

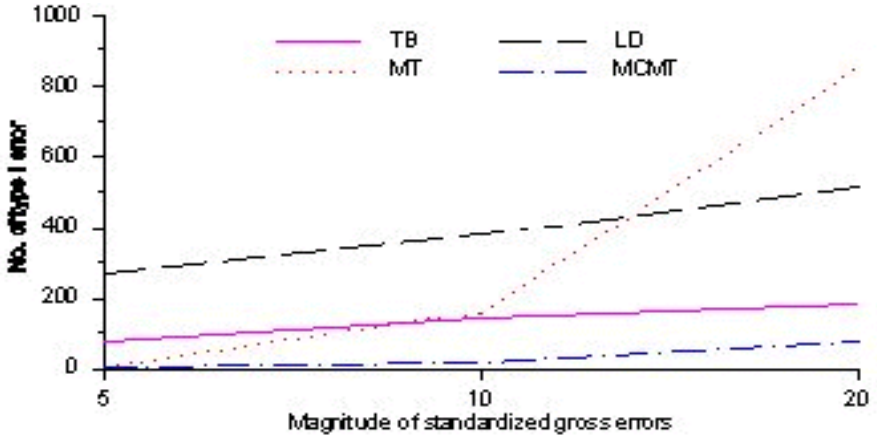

Figure 5.12 Effects of Error Magnitudes of Type I Errors of Algorithms for Multiple Gross Errors

The comparisons in Figures 5.11 and 5.12 show that the modified compensation strategy significantly reduces the misrectification in measurement test method for the cases of multiple gross errors and larger size of gross errors. In the four algorithms, the modified compensation measurement test has the best performance, and measurement test method has the worst performance. Also, the numerical results for both single and multiple gross error cases show that Tjoa-Biegler's method and Lorentzian distribution committed small number of type I errors. This suggests that this modified compensation strategy be incorporated with Tjoa-Biegler's method and robust method to further improve their performance. This strategy is easy to implement without requiring the modification of main program of the optimization problem. It only requires replacing the input plant data with the reconstructed plant data from the last run's solution as discussed in the previous chapter. It can be automatically conducted by the computer program. Based on the location of detected gross errors, the built-in program determines which measurements need to be compensated with the reconciled data and updates the values of these measurements for next data reconciliation automatically. This strategy is easy to incorporated in on-line optimization implementation.

D-3. Summary

The numerical study for both single and multiple gross errors concluded that Tjoa-Biegler's method has the best performance for moderate gross error size (3σ - 30σ) in simultaneously rectifying both random and gross errors. Lorentzian distribution demonstrates the tendency to exceed the performance of Tjoa-Biegler's method when gross errors are larger than 30 times the standard deviation. The measurement test method results in significant biased

estimation in reconciling measurements containing both random and gross errors. Also, the results showed that Lorentzian distribution is the least sensitive to the variations of the gross error size, and measurement test method is the most sensitive to the variations of the gross error size.

The numerical results from modified compensation measurement test demonstrated that the modified compensation strategy significantly reduced the biased estimation in measurement test method. This was observed by significantly reduced number of type I errors committed by MCMT compared with measurement test method. Also, a small number of type I errors from Tjoa-Biegler's method and Lorentzian distribution method were observed from the numerical results. It is expected that this modified compensation strategy can further improve the performance of Tjoa-Biegler's method and Lorentzian distribution method. In addition, this strategy is easy to conduct without requiring modification of main program of the optimization problem. It can be automatically conducted by computer program, and it is appropriate for use with on-line optimization.

The gross error detection results using the actual plant operating data (plant data on 6-10-97 and 6-12-97) given in Table 5-11 and 5-12 are in agreement with the theoretical and numerical evaluation results for gross error detection using simulated plant data. For the two sets of current plant data on 6-10-97 and 6-12-97, measurement test method detected six gross errors, Tjoa-Biegler's method detected 16 gross errors, and Lorentzian distribution method detected 29 gross errors. All of the detected gross errors were smaller than $20F$, and most of them were smaller than $10F$. As shown in Figures 5.3 and 5.4 for gross error detection rate and Figures 5.5 and 5.6 for number of type I errors, measurement test method had the smallest gross

error detection rate and committed the smallest number of type one errors in three methods for gross errors less than 20F. Lorentzian distribution function of robust method committed the largest number of type I errors in three methods for gross errors less than 20F. Also, the relative efficiency of Lorentzian distribution of the robust method is lower than the normal distribution function of measurement test method and contaminated Gaussian distribution function of Tjoa-Biegler's method. This means than Lorentzian distribution has a lower accuracy when the gross errors in measurements are smaller (e.g., less than 20F). The detected gross errors for current operating data are smaller than 20F, and the numbers of gross error detected by three methods for plant data on 6-10-97 and 6-12-97 agreed with results from the theoretical and numerical evaluation results given above.

E. Results for Parameter Estimation

In this section, the one-step and two-step estimation strategies are used to conduct parameter estimation. In one-step estimation, the gross error detection, data reconciliation and parameter estimation are conducted simultaneously using an algorithm that is able to rectify both random and gross errors. One-step estimation combines gross error detection, data reconciliation, and parameter estimation into one optimization problem. The mathematical statement for one step estimation is given in Eq. 3-36 using Tjoa-Biegler's method. One step estimation eliminates the interaction between two data reconciliation associated with gross error detection and with parameter estimation. However, the estimation accuracy may be reduced due to the reduced data quality. In one-step estimation, the plant data sampled from distributed control system is directly used in the one-step optimization to estimate the parameter values, and

this data may contain both gross errors and random errors. In two-step estimation, the measurements with gross errors are rectified in combined gross error detection and data reconciliation, and the data used to estimate plant parameters in step two only contains random error.

The two-step estimation requires a separated gross error detection and data reconciliation step to detect and rectify the gross errors in plant data and a data reconciliation and parameter estimation step to update the parameter values using the data from gross error detection and data reconciliation. As discussed in previous chapter, these two steps use the same plant model and only the difference is that parameters in a plant model are constants for gross error detection step and variables for parameter estimation step. The data reconciliation in combined gross error detection and data reconciliation should use the current values of the process parameters, but these values come from the subsequent parameter estimation step. Therefore, a strategy is proposed to avoid this dilemma. It uses the old parameter data estimated from the last on-line optimization cycle for gross error detection and data reconciliation to reconcile process variables and detect gross errors. Then a new set of measurements, which contains only random errors, is constructed using part of the original data that contains only random errors combined with the reconciled values of the plant data that contains gross errors. This set of constructed measurements is used to simultaneously estimate process parameters and variables. The mathematical statement for step one and step two are given in Eq. 3-34 using Tjoa-Biegler's method for combines gross error detection and data reconciliation and Eq. 3-35 using the least squares method for simultaneous data reconciliation and parameter estimation.

The procedure to solve optimization problems in Eq. 3-34 for step one of two-step estimation and Eq. 3-36 for one-step estimation is the same as described in Figure 5.2 for combined gross error detection and data reconciliation. The only difference in Eq. 3-36 for one-step estimation is that the parameters in the plant model are variables rather than constants for step one (combined gross error detection and data reconciliation) of two-step estimation in Eq. 3-34. The optimization problem (Eq. 3-35) of step two for two-step estimation is essentially the same as Eq. 3-36 for one-step estimation. The only difference is that the measurements contain only random errors for Eq. 3-35, but they contain both random and gross errors for Eq. 3-36. The parameters are variables in Eqs. 3-35 and 3-36, and they are to be estimated with the process variables.

The plant model for conducting parameter estimation is given in Chapter IV for the sulfuric acid process, and it is the same as used in the combined gross error detection and data reconciliation of last section. The same 110 sets of simulated plant data were generated by GAMS using Eq. 5-1 and were used to conduct one-step and two-step estimation. These 110 sets of simulated plant data contain 110 gross errors with a 10F of magnitude. In each set of data, one measured variable was added with a gross error, and all measured variables were added with random errors.

When GAMS solved the optimization problem of simultaneous data reconciliation and parameter estimation in Eq. 3-35 (step two of two-step method) or simultaneous gross error detection, data reconciliation, and parameter estimation in Eq. 3-36 (one-step method), it was encountered that about 50% of cases failed to converge to the optimal solution, if all the seven

heat transfer coefficients and four reaction effectiveness factors listed in Table 4-7 were considered as parameters in the plant model. While searching for the optimal solution, the optimization algorithm failed to bring the searching points back to the feasible region. This is a problem associated with the optimization algorithm or the bound setting for some important variables.

The solver, CONOPT, was used in GAMS to solve the optimization problems in on-line optimization primarily. Also, the solver, CONOPT2, has been used to solve the simultaneous data reconciliation and parameter estimation optimization problems to see if other algorithm can improve the solution. The result was that both CONOPT and CONOPT2 had similar performance. However, CONOPT could find the optimal solution of some problems for which CONOPT2 could not, and CONOPT2 could find the optimal solution of some problems for which CONOPT could not. The reason of solution failure was that the step search brought searching points to an infeasible region, and then it was not able to get back to feasible region and then failed to reach the optimal solution. Therefore, a tighter upper bound on sulfur feed (F50) in the optimization problem was given to improve the solution, and it was successful for some simulated plant data sets.

Using different solver or changing bounds on some variables can improve the solution of the simultaneous data reconciliation and parameter estimation problem or simultaneous gross error detection, data reconciliation, and parameter estimation problem. However, one set of simulated plant data required using CONOPT to successfully solve the optimization problem, and the other set of simulated plant data required CONOPT2 or changing bound on F50 to

successfully solve the optimization problem. This is not appropriate for the comparison and evaluation of different algorithms and strategies, which requires that the same information be used for different algorithms or strategies.

The number of parameters was reduced by dividing the eleven parameters into two sets of parameters, i.e., one set of parameters includes seven heat transfer coefficients and the other set of parameters includes four reaction effectiveness factors. These two sets of parameters can be updated alternately in the sequence of on-line optimization. Then, the plant model is modified to include only seven heat transfer coefficients as plant parameters. After the modification, the solution of the optimization problem for simultaneous data reconciliation and parameter estimation or simultaneous gross error detection, data reconciliation, and parameter estimation was significantly improved, and about 95% of the cases were able to reach the optimal solution with this procedure.

The computation results of the reconciled data for one-step estimation are summarized in Table 5-18 using the 110 sets of simulated plant data. The table lists the gross error detection rates, numbers of type I errors, remaining standardized errors, relative standard deviation reduction, and relative error reduction after data reconciliation for key measurements. The key measurements are the measured variables that are directly related to the determination of parameters in plant models. It is required that the key measurements must be directly related with other measured variables through at least three independent equality constraints.

In Table 5-18, the first column gives the names of the measurements. The second column lists the gross error detection rates for each measurement when gross errors were added to this measurement. The third column lists the numbers of type I errors committed

Table 5-18 Statistical Results of Reconciled Data for One-Step Estimation

Variable Name	Gross error detection rates	No. Of type I errors	Remaining error after reconciled	Relative S.D. reduction after reconciled	Relative error reduction after reconciled
T06	100%	5	0.5097	0.718	0.541
T07	100%	4	0.4115	0.763	0.708
T08	100%	4	0.3396	0.8	0.685
T09	100%	1	0.3734	0.785	0.704
T10	100%	2	0.6001	0.683	0.547
T11	100%	1	0.6002	0.711	0.575
T15	100%	4	0.6255	0.656	0.503
T16	100%	3	0.2731	0.841	0.749
T17	100%	1	0.3543	0.803	0.68
T19	40%	9	0.9038	0.0076	0.221
TS2	40%	11	1.0803	0.169	0.376
TS3	60%	13	0.9726	0.266	0.354
TS4	100%	3	0.6329	0.483	0.263
F04	100%	1	0.321	0.816	0.582
F05	100%	2	0.3256	0.825	0.73
F14	100%	3	0.2999	0.84	0.742
F20	100%	1	0.2925	0.835	0.723
F50	100%	0	0.1746	0.904	0.824
FS1	100%	0	0.2976	0.808	0.817
FS5	100%	1	0.1904	0.856	0.837
X	100%	1	0.0649	0.895	0.883
CO2	100%	0	0.4457	0.731	0.625
Average	92.7%	70	0.459	0.691	0.621

by one step estimation for each measurement when gross errors were added to this measurement. The fourth column gives the average of remaining errors in key measurements after data reconciliation over 110 runs' result. The remaining error is the absolute difference between the reconciled and the true value as defined in Eq.5-5. The average remaining error over key measurements is about 0.459σ, where σ is the standard deviation of measurements given in Table 5-1. The fifth column indicates the relative standard deviation reduction after data reconciliation for key measurements over 110 runs' result. The relative standard deviation reduction is the ratio of the standard deviations of the 110 sets of reconciled data to those of 110 sets of measurements. There is an average 69.1% of standard deviation reduction for key measured variables. The sixth column gives the relative error reduction after data reconciliation. The relative error reduction is defined in Eq.5-3, i.e., the ratio of the remaining errors after data reconciliation to the absolute measurement errors.

Table 5-18 summarizes the computation results from one-step estimation. It shows that one-step estimation achieved a 92.7% of average gross error detection rate and committed 70 type I of errors over the 110 runs. The average remaining error, relative standard deviation reduction, and relative error reduction after data reconciliation were 0.459σ, 69.1% reduction of the measurement variations, and 62.1% reduction of the original errors over 110 runs' result.

Table 5-19 summarizes the computation results from two-step estimation. The two-step estimation used the same 110 sets of simulated plant data as one-step estimation to conduct combined gross error detection and data reconciliation of step one. At this step,

Table 5-19 Statistical Results of the Reconciled Data for Two-Step Estimation

Variable Name	Gross error detection rates	No. Of type I errors	Remaining error after reconciled	Relative S.D. reduction after reconciled	Relative error reduction after reconciled
T06	100%	2	0.465	0.741	0.525
T07	100%	2	0.3558	0.805	0.73
T08	100%	0	0.2806	0.856	0.721
T09	100%	1	0.3097	0.851	0.775
T10	100%	2	0.4985	0.752	0.624
T11	100%	1	0.4986	0.779	0.674
T15	100%	0	0.6475	0.643	0.471
T16	100%	0	0.2577	0.855	0.751
T17	100%	2	0.3376	0.826	0.717
T19	100%	1	0.522	0.732	0.551
TS2	100%	1	0.6262	0.723	0.64
TS3	100%	2	0.675	0.669	0.575
TS4	100%	4	0.4799	0.719	0.435
F04	100%	2	0.3315	0.8	0.568
F05	100%	4	0.3268	0.817	0.735
F14	100%	2	0.307	0.837	0.755
F20	100%	3	0.2992	0.833	0.731
F50	100%	2	0.1511	0.91	0.853
FS1	100%	2	0.1655	0.914	0.898
FS5	100%	1	0.1054	0.934	0.91
X	100%	0	0.0651	0.898	0.882
CO2	100%	1	0.475	0.725	0.564
Average	100%	35	0.3718	0.797	0.686

the gross errors are detected and rectified, and a set of plant data was constructed from this step using the proposed strategy. Then this set of constructed plant data was used to conduct simultaneous data reconciliation and parameter estimation of step two.

In Table 5-19, the results for gross error detection rate and number of type I errors were obtained from step one. While the remaining error, relative standard deviation reduction, and relative error reduction were obtained from step two. Table 5-19 shows that two-step estimation achieved a 100% of average gross error detection rate and committed 35 type I of errors over the 110 runs. The average remaining error, relative standard deviation reduction, and relative error reduction after data reconciliation were 0.37F, 79.7% reduction of the measurement variations, and 68.6% reduction of the original errors.

Table 5-20 compares the parameter estimation results from two strategies. In this table, the first and second columns list the names and plant design values of parameters in the process model, where the plant design values of parameters was determined by the plant design data for measured variables given in Table 5-1. The third, fourth, and fifth columns give estimated means of parameters, ratios of estimated parameter standard deviations to estimated means, and the relative difference between estimated means and true values from one-step estimation. The sixth, seventh, and eighth columns give the estimated means of

Table 5-20 Comparison of Estimated Parameter Data from Two Strategies

Parameter Names	Plant design values	One-step estimation			Two-step estimation		
		Estimated means	Estimated S.D./mean	(mean-true) /true	Estimated means	Estimated S.D./mean	(mean-true) /true
BlrU	xxxx	xxxx	0.73%	0.21%	xxxx	0.31%	0.17%
Ex65U	xxxx	xxxx	3.37%	0.65%	xxxx	2.40%	0.54%
Ex66U	xxxx	xxxx	3.42%	0.98%	xxxx	2.96%	0.61%
Ex67U	xxxx	xxxx	1.83%	0.60%	xxxx	1.48%	0.52%
Ex68U	xxxx	xxxx	16.8%	0.99%	xxxx	4.11%	1.85%
Ex69cdU	xxxx	xxxx	6.98%	0.15%	xxxx	1.99%	0.62%
EX69aU	xxxx	xxxx	12.0%	0.93%	xxxx	3.54%	1.53%
Average			6.44%	0.64%		2.40%	0.83%

parameters, the ratios of estimated parameter standard deviations to estimated means, and the relative differences between estimated means and true values from two-step estimation. For one-step estimation, the largest and average estimated standard deviations were 16.8% and 6.4% of the mean values; and the largest and average relative differences between the estimated and the true were 0.99% and 0.64% of the true values. For two-step estimation,the largest and average estimated standard deviations were 4.1% and 2.4% of the mean values; and the largest and average relative differences between the estimated means and the true values were 1.8% and 0.8% of the true values.

The result in Table 5-20 showed that the estimation variation (standard deviation of estimated parameters) from one-step estimation was larger than one from two-step estimation. The reason is the redundancy condition in two-step estimation is better than one in one-step estimation. This provides more restriction for two-step estimation when the optimization solution adjusts the variable values and makes the solution have a smaller variation. The difference between the estimated means and the true is comparable for these two strategies.

In Table 5-21, the overall performance is compared for these two strategies on parameter estimation accuracy, data reconciliation accuracy, gross error identification, and computation effort. As shown in Table 5-21, two-step estimation demonstrated 4% lower variation on estimated parameter values, 6.5% higher error reduction, and 10.6% higher relative standard deviation reduction on reconciled data than one-step estimation. Also, two step estimation had 6.3% higher gross error detection rate and committed 50% less of type I errors than one-step estimation. Both two-step and one-step estimation had comparable estimation accuracy on the plant parameters. However, two-step estimation required 82% more computation time than one-step estimation did. It is concluded that two-step estimation strategy is recommended for the sulfuric acid plant model.

Table 5-21 Comparison of the Overall Performances of Two Strategies

		One-step estimation	Two-step estimation
Overall parameter estimation accuracy	Variation of estimation: S.D./mean	6.44%	2.40%
	Relative difference of estimated parameters from true	0.64%	0.83%
Overall reconciled data accuracy	Relative error reduction after reconciled	62.13%	68.57%
	Relative S.D. reduction after reconciled	69.06%	79.72%
Gross error detection	Average gross error detection rate	0.927	1
	Number of type I errors	70	35
Computation time		4.16 Second	7.62 Second Step one: 3.88 Sec. Step two: 3.74 Sec.

In summary, the comparisons in Tables 5-7 and 5-8 for these two strategies showed that both one-step and two-step were able to accurately estimate the plant parameters and process variables for the sulfuric acid process. Two-step estimation demonstrated a better performance in estimation accuracy than one-step estimation, while one-step estimation required less computation time as discussed in above paragraph. Also, one-step estimation eliminates the interaction between two data reconciliations for gross error detection and for parameter

estimation. For the sulfuric acid process, the two-step estimation is recommended to be used in on-line optimization based on the numerical results.

F. Evaluation of Plant Model Formulations

The constraint equations for all units of sulfuric acid contact process have been developed in Chapter IV. In this section, the objective is to examine the observability and redundancy of sulfuric acid plant model and to investigate how the plant model formulation affects the accuracy of the optimization problems in on-line optimization.

F-1. Examination of Observability and Redundancy for Sulfuric Acid Plant Model

The process measurements are taking from the Baily distributed control system of sulfuric acid plant. The distributed control system provides the direct measurements for all required temperatures, pressures, steam flow rates, and acid flow rates for on-line optimization. However, the direct measurements of flow rates for gas streams are not available at all. Some of measurements of gas steams are required to satisfy the observability in data reconciliation. The examination of observability and redundancy determines that four flow rates for gas streams (air from compressor F04, gases from sulfur burner F05, gases from inter-pass absorption tower F14, and gases from economizer 4A F20) must be measured to satisfy the observability of variables, which are associated with gas streams, for detail plant model. How the observability and redundancy was determined will be described in the following using waste heat boiler unit as an example. Therefore, these required gas flow rate measurements are obtained using the discharge pressure and speed of compressor (or turbine). The flow rate of stream S04 (F04) is determined by the discharge pressure and speed of the compressor with the compressor

performance chart. Then the flow rates of F05, F14, and F20 are determined by the flow rate F04 and assuming 2%, 94.8%, and 99.7% (99.7% is a direct measurement) of SO_2 conversion at the corresponding streams.

The open form equation based plant model for sulfuric acid plant has been established in Chapter IV, and the measured variables and parameters for this plant were listed in Table 4-7 and 4-8. How the observability of unmeasured variables and parameters was examined is discussed using the waste heat boiler unit in the following.

For the waste heat boiler, the constraint equations are shown in Table 5-22. This unit has 20 constraint equations in total, and they are four species material balances for four components in gas stream, one material balance for steam stream, and material relationship on the blowdown between streams SS4 and SS6, one overall energy balance, one heat transfer equation, eight enthalpy equations for four components of two gas streams (S05 and S06), three enthalpy equations for three steam streams (SS4, SS5, and SS6), and one logarithm mean temperature equation. All these equations contains 29 variables. Among these variables, FS5, TS4, TS5, TS6, PS5, T05, T06, are measured variables where the temperature for steam streams SS4, SS5, and SS6 are the same, i.e., TS4= TS5= TS6. F05O2, F05N2, F05SO2, F05SO3 are dummy measured variables, and they are determined

by measured variables (F04 and F05), concentration relation of components in stream S04, and molar balances of the burner. FS4 is a dummy measured variable, and it equal measured variable FS1 in the up stream. The heat loss Q_{loss} and heat tansfer area A_{boiler} are constant. Therefore,

this unit has 12 measured variables and 17 unmeasured variables ( ) t_{lm}, F06O2, F06SO2, F06SO3, F06N2, FS6, h05O2, h05SO2, h05SO3, h05N2, h06SO3, h06SO2,

Table 5-22 The Constraint Equations for Waste Heat Boiler

Description	Waste boiler extracts the heat generated in sulfur burner.
	Inlet: S05, SS4 Outlet:S06, SS5, SS6
Species material balances	O_2: $F_{05}^{(O_2)} - F_{06}^{(O_2)} = 0$ N_2: $F_{05}^{(N_2)} - F_{06}^{(N_2)} = 0$ SO_2: $F_{05}^{(SO_2)} - F_{06}^{(SO_2)} = 0$ SO_3: $F_{05}^{(SO_3)} - F_{06}^{(SO_3)} = 0$ *Steam*: $F_{S4} = F_{S5} + F_{S6}$ $0.09F_{S4} = F_{S6}$

Overall energy balances	$\left(\sum_i F_{06}^{(i)} h_{06}^{(i)} - \sum_i F_{05}^{(i)} h_{05}^{(i)}\right) - (F_{s4} h_{s4} - F_{s5} h_{s5} - F_{s6} h_{s6}) + Q_{loss} = 0$ where $h^i_k(T) = R(a_1 T + \frac{1}{2} a_2 T^2 + \frac{1}{3} a_3 T^3 + \frac{1}{4} a_4 T^4 + \frac{1}{5} a_5 T^5 + b_1 - H_{298})$ KJ/kmol $i = SO_2, SO_3, O_2, N_2$; $k = 05, 06$ $h_n = 1.08617707T - 5.63134\times10^{-4}T^2 + 8.34491\times10^{-7}T^3 - \frac{1.14266\times10^4}{T} + \frac{1.01824\times10^6}{T^2}$, BTU/lb $n = S4, S6$ $h_n = 5.32661T - 0.2839015P - 7.352389\times10^{-3}T^2 + 3.581547\times10^{-6}T^3 - 7.289244\times10^{-5}P^2 + 4.595405\times10^{-4}TP$ $n = S5$, BTU/lb
Heat transfer	$\left(\sum_i F_{05}^{(i)} h_{05}^{(i)} - \sum_i F_{06}^{(i)} h_{06}^{(i)}\right) - Q_{loss} - (U_{boiler} A_{boiler} \Delta T_{lm}) = 0$ $\Delta T_{lm} = \frac{(T05 - TS5) - (T06 - TS4)}{\ln\{(T05 - TS5)/(T06 - TS4)\}}$

h06O2, h06N2, hS4, hS5, hS6). Also, the heat transfer coefficient U_{boiler} is a parameter to be estimated. Hence, the degree of freedom of this unit is (29 variables + 1 parameters - 20 equations) = 10, and this unit has 12 measured variables. The number of measured variables is larger than the degree of freedom, and this unit satisfies the local observability.

If the flow rate variables F04 and F05 for gas streams S04 and S05 are not measured variables, then the component flow rates F05O2, F05SO2, F05SO3, and F05N2 can not be considered as dummy measured variables. Therefore, the waste heat boiler has only eight

measured variables which is less than the degree of freedom (10 degree of freedom) for this unit. If the four gas stream flow rates (F04, F05, F14, and F20) are not measured variables, then all variables associated with gas streams in the sulfuric acid process are unobservable.

The local observability and redundancy was examined for 14 units in sulfuric acid process similar to the waste heat boiler unit as discussed here. After local observability was examined, the global observability and redundancy was determined by the number of measurements and the degree of freedom for entire process. The detail process model of sulfuric acid plant has 761 equations, 775 variables among which 43 are measured variables, and 11 parameters. The degree of freedom for this plant model is 25, and the number of measured variables for this process is 43, which is larger than the degree of freedom. Therefore, the plant satifies the global observability and redundancy.

F-2. Comparison of Detail and Simple Plant Models

In general, a detail plant model includes material and energy balances, reaction rate equations, heat transfer equations, and others. It will represent the process behavior more accurately than a simple plant model that includes only material and energy balances, where reactor conversions and column separation are specified. The following compares the performance of the simple and detail plant models for sulfuric acid contact process. The same 215 sets of simulated plant data generated with Eq. 5-1 were used to conduct combined gross error detection and data reconciliation with Tjoa-Biegler's method. The procedure is the same as discussed in combined gross error detection and data reconciliation section.

The detail plant model for sulfuric acid process includes the species mass and energy balances and heat transfer equations for seven heat exchangers, species mass and energy balances, kinetic model (reaction rate equations) for four sulfur dioxide convertors, species mass and energy balances for two absorption towers and one sulfur burner. These fourteen units are linked together by the species mass balances, energy balances, reaction rate equations, and heat transfer equations. The simple plant model includes only the species mass and energy balances for all fourteen units in the sulfuric acid plant. The species mass balances for four convertors are established based on the conversion of SO_2 and the stoichiometric coefficients of the reaction. The numbers of equations, variables, and measurements are given in Table 5-23 for these two plant models. The simple plant model

Table 5-23 The Configuration of Simple and Detail Plant Models

	Simple Plant Model	Detail Plant Model
Total number of variables	221	775
Number of measured variables	61	43
Number of unmeasured variables	160	732
Number of constraint equations	197	761

has 221 process variables and 197 constraint equations. Among the process variables, 61 variables must be measured variables to satisfy the observability and redundancy of the simple plant model. The detail plant model has 775 process variables and 761 constraint equations. Among the process variables, 43 variables must be measured variables to satisfy observability and redundancy of the detail plant model.

Both simple and detail plant models were used as constraint equations for gross error detection and data reconciliation. In Table 5-24, the overall performance is summarized for the simple and detail plant models averaging over the results of 215 runs for each plant model. These 215 runs used 215 sets of simulated plant data that were generated with Eq. 5-1. As shown in Table 5-24, the detail plant model has 29.3% higher gross error detection rate, 76 less type I errors, 32.1% higher random error reduction and 25.7% higher gross error reduction than simple plant model. It requires 2.3 times longer computation time than the simple plant model. The comparisons in Table 5-24 concluded that the detail simulation plant model is recommended for the use in on-line optimization.

Table 5-24 Comparisons of Overall Performance for Two Plant Models

	Simple plant model	Detail plant model
Gross error detection rate	67.1%	96.4%
Number of type I errors	102	26
Relative random error reduction	38.2%	64.3%
Relative gross error reduction	66.1%	91.9%
Computation time	1.65 Sec.	3.84 Sec.

The detail plant model has higher gross error detection rate, more accurate estimation results, and required fewer measured variables.

G. Optimal Solution of On-Line Optimization

As discussed in previous chapters, on-line optimization involves solving three nonlinear optimizations as well as the communication of data between the optimization problems and between on-line optimization system and plant distributed control system. It is necessary to have a coordination program to integrate them. An interactive interface program is developed to alleviate the effort of engineers in applying on-line optimization and to coordinate the solution of optimization problems in on-line optimization. The three-step procedure (combined gross error detection and data reconciliation, simultaneous data reconciliation and parameter estimation, and economic optimization) is incorporated in the interface program (Interactive On-Line Optimization System) to conduct on-line optimization.

G-1. Program Structure of Three Nonlinear Optimization Problems

For on-line optimization, the three nonlinear optimization problems use the same process model as constraints, and they are solved by the same optimization algorithm with GAMS, the General Algebraic Modeling System. These three optimization problems have a similar program content as shown in Figure 5.13. The optimization problems for the combined gross error detection and data reconciliation and the simultaneous data reconciliation and parameter estimation require the information listed in Figure 5.13, except the inequality constraints. While the economic optimization problem requires the information listed in Figure 5.13, except the plant measurements and the standard deviations. Also, the plant parameters are constants in the combined gross error detection and data reconciliation and in economic optimization, and they

are variables in simultaneous data reconciliation and parameter estimation. The values of parameters are updated in parameter estimation step for the use in economic optimization and next data validation. In addition, the objective function in each optimization problem can be different dependent on the goal to be achieved. The GAMS source codes to conduct the three nonlinear optimization problems for sulfuric acid process are given in Appendix F.

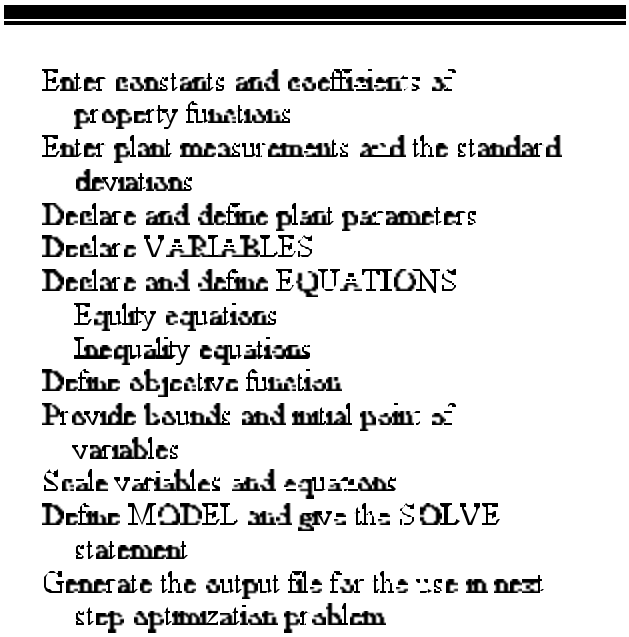

Figure 5.13 Steps in the GAMS Program for Optimization Problems

The initial points of variables and scaling of the variables and equations are optional in the optimization programs. However, successful optimization solutions strongly rely on the appropriate initial point to start searching for the optimal solution. Because the model is highly nonlinear and multiple optimal solutions exist, the optimization algorithm may not be able to find the correct optimal solution or reach the optimal point if the appropriate initial point information is not provided. Also, scaling of all variables and coefficient matrix of the linearized constraint equations is important in reducing the computation error and improving the solution of the optimization problem. In addition to the consideration of algorithms and the plant model formulation as discussed previously, the knowledge about the process, appropriate initial point

assignment, and scaling for the process model are the essential conditions for the success of the optimization solutions.

G-2. Coordination of Optimization Problems and Data Exchange

Based on the investigation results and computation experience, the best procedure to conduct the on-line optimization system is proposed as shown in Figure 5.14. This includes solving the three optimization problems in sequence, the data exchange between the three optimization problems, the communication of on-line optimization system and the distributed control system, as well as the examination of steady state of the process operation and the optimization solutions. It is necessary to have a coordination program to integrate individual step in on-line optimization. The interactive on-line

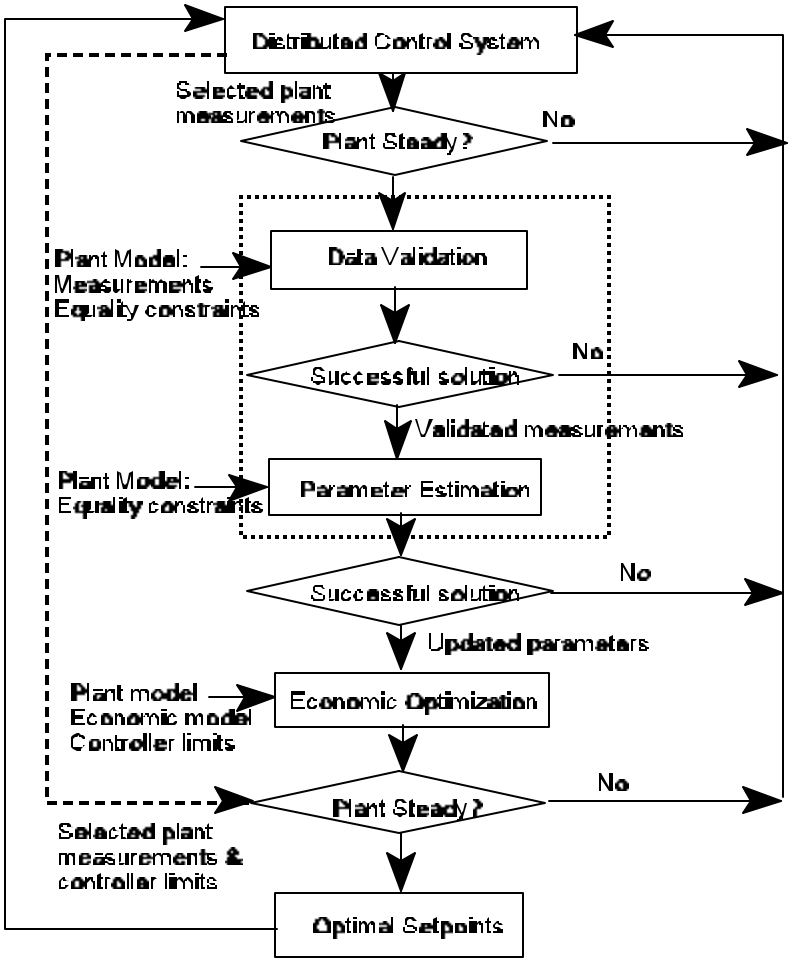

Figure 5.14 The Procedure for On-Line Optimization

optimization system has been developed to perform this work and to alleviate the effort for engineers to apply the on-line optimization.

As shown in Figure 5.14, the procedure to conduct on-line optimization is first the plant data is extracted from distributed control system to detect if the process is in steady state condition. If it is in steady state , then the plant sampled data is incorporated in the program of gross error detection and data reconciliation and the system has GAMS solve the optimization problem. After solving this optimization problem and reconciling the process data, the GAMS program detects the gross error in measurements based on the estimated errors of measurements and the built-in test statistic. Also, this step generates a data file that includes a set of plant measurements with only random errors which is constructed from the result of data validation using the proposed strategy discussed in previous chapter. Then the solution is examined to see if the solution is successful. It is suggested that the success of solution be based on the number and location of the detected gross errors. If it is found that more than five measurements in a close neighborhood contain gross errors, then this usually is an indication of the failure of an algorithm in reconciling process data. If this is the case, then the result from data validation should be discarded, and the on-line optimization procedure is restarted.

Once the solution of data validation is successful, then the generated plant data file from data validation step is incorporated in the simultaneous data reconciliation and parameter estimation program. The system has GAMS execute this program and solve the optimization problem. After the optimal solution is found, the GAMS program automatically generates a plant parameter data file that includes the names and estimated values of the parameters. Then, the

optimization solution is examined to see if the estimated parameter values are reasonable. Each estimated parameter value is compared with the pre-specified ranges of the parameter. If it is out of the pre-specified range, then this value can not be used in economic optimization. The parameter data from the optimal solution is discarded, and the on-line optimization procedure is restarted.

Once the solution of parameter estimation is successful, then the generated plant parameter data file is incorporated in the economic optimization program to update the plant model. Also, the new economic data and controller limits are incorporated in this program. Then interactive on-line optimization system has GAMS execute this program and solve the economic optimization problem. When the optimal solution is found, the program generates a optimal set point data file that includes the optimal objective values and the optimal operation conditions. Then, the status of the process is reexamined to see if the process still operates under the same steady state conditions as the plant sampled data was taken to updated plant parameters. Also the controller limits are examined to see if the optimal set points violate the controller limits. If the process still operates in the original steady state conditions and no violation with controller limits is found in the optimal set points, then the optimal set points are sent to the distributed control system to adjust the set points for controllers.

When the distributed control system implements the new optimal set points, the plant moves from the old operating conditions to new optimal conditions. The plant remains operating in these optimal conditions for a time period, and then the on-line optimization procedure is repeated again to search for the new optimal set points.

Above is the optimal procedure to conduct on-line optimization and it can be applied to any process. In addition, two optimization problems for combined gross error detection and data reconciliation and for simultaneous data reconciliation and parameter estimation may be combined into one optimization problem as discussed in the previous chapter. In this case, the two boxes in Figure 5.14 for combined gross error detection and data reconciliation (data validation) and for parameter estimation become one step to identify the gross error in measurements and estimate process parameters and variables.

G-3. Development of Interactive On-Line Optimization Interface Program

The interactive on-line optimization system provides a mechanism where all of the information needed to build the three nonlinear programming problems is provided by the process engineer through interface windows, and the three optimization problems share and transfer information as shown in Figure 5.15. The engineer provides the process simulation and economic models, raw material availability and product demand data through the interface windows for the on-line optimization system to develop the optimization programs. The system then extracts plant data from the distributed control system,

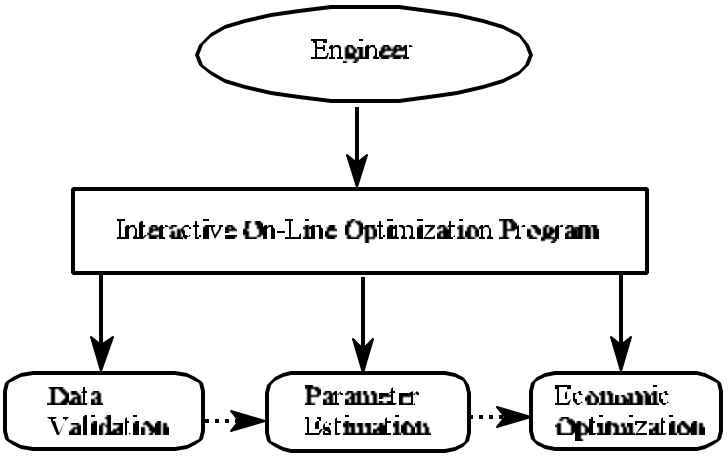

Figure 5.15 Structure of the Interactive On-Line Optimization System

performs data validation, parameter estimation and economic optimization to generate the optimal set points for the distributed control system. The interactive on-line optimization system guides the engineer to enter the necessary information, and the engineer does not need to understand the details of methodology of on-line optimization. Also, the system ensures that a complete set of information is obtained.

Microsoft's Visual Basic 5.0 was used for development of interactive on-line optimization program, which is shown diagrammatically in Figure 5.16. Visual Basic 5.0 provides an efficient way to create User Access Windows as an interface to enter information (data and equations) which can be used to generate programs to be run by applications such as the optimization language GAMS. The Visual Basic program is used to create an interface program (interactive on-line optimization system) that provides user access friendly windows for engineers to enter plant information, generates GAMS programs for three optimization problems based on the built-in methodology of on-line optimization and entered plant information, has GAMS compile and execute the programs of the optimization problems, and presents the optimal solution for engineers. This only requires that the process engineer provide the plant model, economic model, and plant data from the distributed control system. The process engineer does not have to know the methodology of on-line optimization and write GAMS programs for the three optimization problems because the interactive on-line optimization system writes these programs. Also,

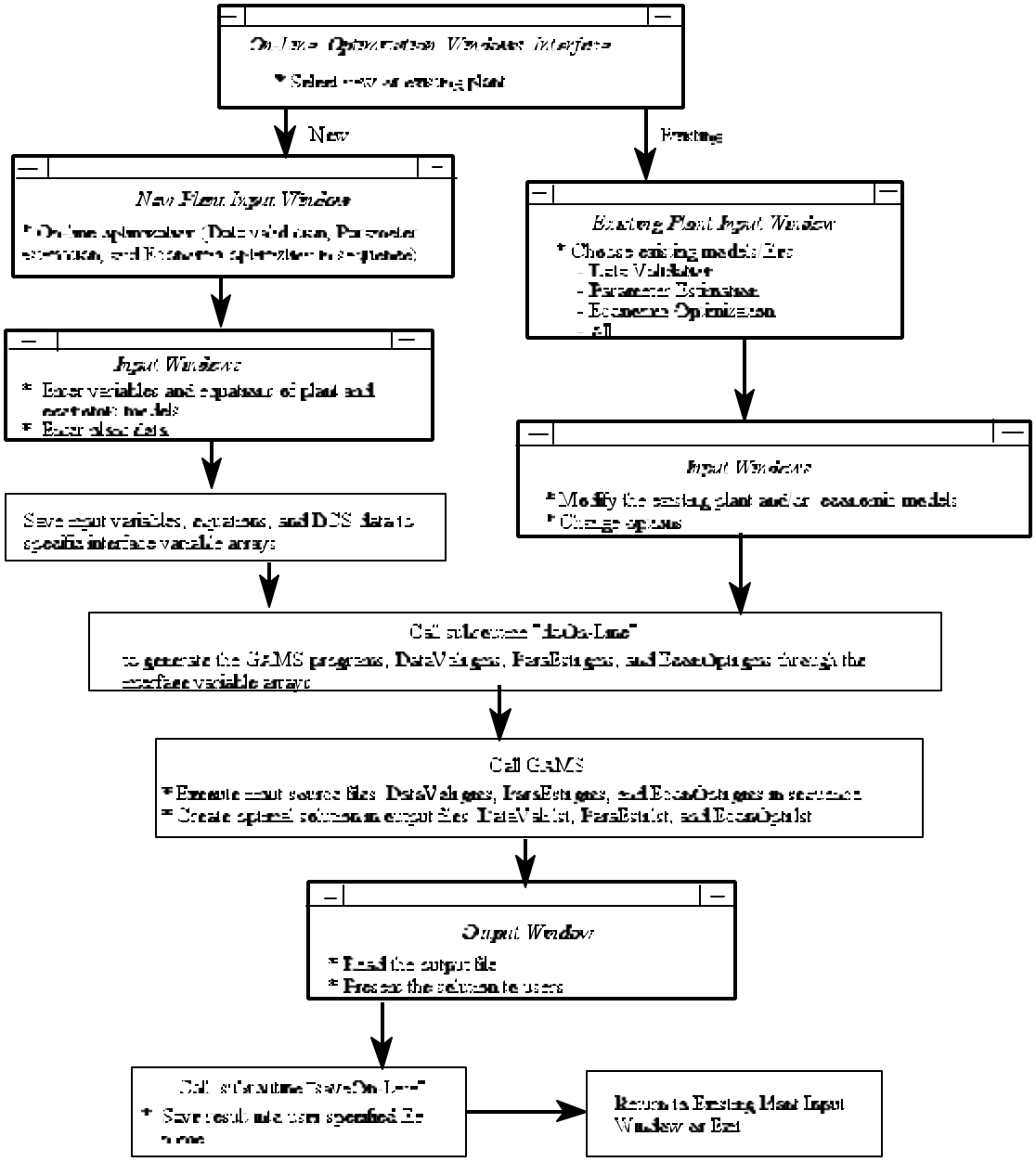

Figure 5.16 Diagram for Interactive On-Line Optimization System Using Visual Basic

a friendly and easy access on-line HELP is available to guide the engineer entering the plant information.

Above is the general information about the interactive on-line optimization interface program. The detail description and example demonstration about this program have been given in the manual and tutorial of the interactive on-line optimization system which is included in Appendix G.

H. Comparison with Other Investigations

The objective of this research project was to systematically investigate the optimal structure of on-line optimization and to theoretically and numerically evaluate the applicable algorithms for conducting on-line optimization. Also, an actual chemical process, sulfuric acid plant from IMC Agrico Company was used to conduct this investigation. The following compares the contribution from this research project with other investigations.

Investigation of Optimal Structure: Previous research on on-line optimization was reported by two groups: industrial applications and academic studies, all of which focused on the study of individual components of on-line optimization. There was no detail description about the whole structure of on-line optimization as this research project does which includes the study of algorithms for individual component and the integration of these components. The industrial applications (Bailey, et al., 1993; Bayles, M., 1996; Culter and Ayala, 1993; Fatora, et al., 1992; Gott, et al., 1991; Hardin, et al., 1995; Kelly, et al., 1996; Mudt, et al., 1995; Mullick, 1993; and Scott, et al., 1994) focused on the implementation of economic optimization, and they did not give the detail information of the methodology used. Also, most of the industrial on-line

optimization applications did not have gross error detection step or just used a simple time series screening method to filter out the abnormal measurements, which is not effective in detecting the persistent gross errors. The academic studies (Albuquerque and Biegler, 1993 and 1995; Tjoa and Biegler, 1991; Britt and Luecke, 1973; Crowe, C. M., 1986, 1989, 1992, and 1994; Johnston and Kramer, 1995; Leibman, et al., 1992; Mah and Tamhane, 1982; Mah, et al., 1976; Mah, 1990; Narasimhan and Mah, 1987 and 1988; Rollins, D.K., and J.F. Davis, 1992 and 1993) focused on the study of the algorithms for individual components, such as gross error detection, data reconciliation, and parameter estimation individually. Most of them used a simple hypothetical process model with all variables measured and linear constraints to test the developed algorithms. These process models do not represent the real, complicated chemical and refinery processes in which constraints are highly nonlinear and large portion of process variables are unmeasured.

This research project systematically investigated the structure and the methodology of on-line optimization using an actual chemical process, the sulfuric acid process from IMC Agrico Company at Convent, Louisiana. It covered the methodology and implementation for all components required in on-line optimization, i.e., theoretical and numerical evaluation of the algorithms for gross error detection, data reconciliation, and parameter estimation, study of economic potential from on-line optimization for chemical processes and the impact of plant model formulation on the performance of on-line optimization, as well as the integration of individual components of on-line optimization. The research results should provide a better

understanding about the individual components of on-line optimization and how these components work together and communicate with one another.

Application of Industrial Process: Using an actual chemical process rather than a hypothetical process to test the methodology of on-line optimization provides better insight about true behavior of on-line optimization. It is more valuable for examining the methodology and more convincing to practicing engineers. It is very difficult for academic researchers to get plant information because companies usually do not want to share their proprietary information with others. It was fortunate that IMC Agrico and Monsanto agreed to share their companies' proprietary data. This provided us with the opportunity to test the available theoretical algorithms with a real industrial chemical process and made our research results much more valuable. Also, using an actual chemical process in our investigation provided first hand experience on how the plant model formulation affects the performance of on-line optimization. The basic considerations in better formulating plant model were given based on our study results.

Theoretical and Numerical Evaluation of Algorithms: The present work theoretically and numerically evaluated the available algorithms and distribution functions used in the algorithms. These algorithms are applicable to gross error detection, data reconciliation, and parameter estimation for complicated and nonlinear process models; and they are measurement test method using the normal distribution (Mah and Tamhane 1982), Tjoa-Biegler's method using contaminated Gaussian distribution (Tjoa and Biegler, 1991), and robust methods using Lorentzian distribution (Huber, 1981 and Johnston and Kramer 1995) or Fair function (Albuquerque and Biegler, 1995). In addition to the works of Tjoa and Biegler (1991) and

Albuquerque and Biegler (1995 and 1996), which tested their algorithms using a simple hypothetical process model, and Johnston and Kramer (1995) that just briefly mentioned the Lorentzian distribution, our work first applied these algorithms to the industrial process, sulfuric acid plant, and compared their performance based on the results for sulfuric acid plant. The results indicated that the contaminated Gaussian distribution and Lorentzian distribution are more effective in automatically rectifying random and gross errors than normal distribution (measurement test or least squares method) that has been widely studied and applied.

Albuquerque and Biegler (1996) and Johnston and Kramer (1995) briefly discussed the theoretical evaluation of algorithm using influence function. The present work systematically evaluated and compared the performances of all applicable distributions in reconciling process data using the combination performance of influence function and relative efficiency.

Serth and Heenan (1986 and 1987) have numerically compared the performance of measurement test (MT), iterative measurement test (IMT), modified iterative measurement test (MIMT), method of pseudonodes (MP), and screened combinatorial (SC) method using a simple linear steam-metering system. It was concluded that MIMT represents the best combination of computation speed and efficiency (accuracy). Kim, et al., (1997) reported that performance of MIMT was enhanced by using nonlinear program (NLP) technique and they demonstrated the enhancement using a simple adiabatic CSTR process that has six variables and three constraints. The advantage of NLP technique over the successive linearization used by Serth and Heenan's MIMT is that it explicitly handles nonlinear constraints and the bounds of variables are automatically incorporated in the optimal solution. It was found that the linearization-based

technique does not successfully treat the large measurement errors for highly nonlinear system as NLP does. The present work used NLP technique to solve the nonlinear data reconciliation problems as Kim, et al., did for the complicated and highly nonlinear chemical process. Also, a modified compensation strategy was proposed to improve the data reconciliation accuracy. The proposed strategy is more effective and requires smaller number of iterations than modified iterative strategy in MIMT.

Integration of On-Line Optimization: Based on the results of this research, the optimal procedure and best algorithms to conduct on-line optimization have been proposed as discussed previously. Also, the integration of components in on-line optimization was studied and the strategy to construct data from the result of previous step to use in following step was proposed. Based on the results, an interactive on-line optimization interface program has been developed to alleviate the effort for engineers to apply on-line optimization. This program incorporates the detail algorithms for on-line optimization and the detail procedure for data exchange. It provides user friendly interface windows to guide engineers to enter required plant information, and it automatically generates and executes the programs of optimization problems involved in on-line optimization.

In summary, this research work provided a detail and systematical investigation on the methodology of on-line optimization. It should help understand the on-line optimization technology and provide the basis for continuing study in the integration of process economics, design, operations, simulation, optimization, and control, which represents the Postmodern Era of Process Control as mentioned in Edgar's award lecture (Edgar, 1997).

I. Summary

On-line optimization is an effective approach for economic improvement and source reduction in chemical plants and refinery processes. On-line optimization involves several steps and these are gross error detection to identify and rectify the gross errors in plant data from distributed control system, parameter estimation to update the values of process parameters in the plant simulation model, and economic optimization to generate a set of optimal set points that will optimize the plant economic objective and satisfy the constraints in the plant simulation model.

Optimal Procedure of On-Line Optimization: The optimal procedure to conduct on-line optimization has been proposed based on the results from this research. For a chemical plant or refinery process, the best procedure for on-line optimization is shown diagrammatically in Figure 5.14. It involves solving three nonlinear optimization problems of Data Validation (gross error detection and data reconciliation), Parameter Estimation (simultaneous data reconciliation and parameter estimation) and Economic Optimization. It first conducts combined gross error detection and data reconciliation to detect and rectify gross errors in plant data sampled from distributed control system using the Tjoa-Biegler's method (the contaminated Gaussian distribution) or robust method (Lorentzian distribution). This step generates a set of measurements containing only random errors for parameter estimation. Then, this set of measurements is used for simultaneous parameter estimation and data reconciliation using the least squares method. This step provides the updated parameter values in the plant model for economic optimization. Finally, optimal set points are generated for the distributed control system

from the economic optimization using the updated plant and economic models. This optimal procedure can be used for any process to conduct on-line optimization.

In addition, the gross error detection, data reconciliation, and parameter estimation can be combined into one optimization problem and conducted simultaneously. For this case, the Data Validation and Parameter Estimation in Figure 5.14 can be combined into one step, and the best procedure is first to conduct the simultaneous gross error detection, data reconciliation, and parameter estimation using Tjoa-Biegler's contaminated Gaussian distribution or Lorentzian distribution with plant data from distributed control system. Then, the updated plant model and current economic model are used to conduct economic optimization to generate the optimal set points for distributed control system to control.

Economic Optimization: Plant economic optimization demonstrated a potential in improving the plant profits and reducing pollutant emission. The plant economic optimization showed 3% profit improvement or 2.3% profit improvement and 25% emission reduction over the design conditions for the sulfuric acid process at IMC Agrico Company's plant. On-line optimization using current operating data demonstrated that plant economic optimization gave 2.3% ($313,000/year) and 3.1% ($410,000/year) profit improvement over the plant operation conditions on 6-10-97 and 6-12-97. Also, plant economic optimization was able to achieve up to 5% profit improvements over the current plant operation conditions for some special operating cases, such as plant must run under a reduced rate of products. Moreover, plant optimization could determine set points that reduced the SO2 emission and still achieved 2.1% profit improvement over current operation condition.

Data Validation: The performance of algorithms was theoretically evaluated using the influence function and the relative efficiency of the distribution used by the algorithm. The comparison of influence functions for the distributions showed that both contaminated Gaussian and Lorentzian distributions are effective in rejecting the contribution of gross errors in measurements on the estimation. They are able to rectify the measurements containing gross errors through other measurements that do not contain gross errors. While measurement test method which is based on a normal distribution has a significantly biased estimation in reconciling process data for measurements containing both random and gross errors; and the degree of bias increases unboundedly with the increase in the error magnitude. Therefore, an iterative elimination strategy was necessary for the normal distribution to avoid the bias whenever a gross error was detected. The comparison of relative efficiency shows that normal distribution has the highest efficiency when measurements are normal (no gross error). The relative efficiency decreases in order as: the contaminated Gaussian distribution, Lorentzian distribution, and Fair function. It was concluded that the contaminated Gaussian distribution has the best performance for the moderate gross error size, Lorentzian is more effective for extremely large gross errors or infinite gross errors, and normal distribution has the highest estimation accuracy when measurements do not contain gross errors.

The numerical study for combined gross error detection and data reconciliation concluded that Tjoa-Biegler's method has the best performance for moderate gross error size in simultaneously rectifying both random and gross errors. It achieved the highest gross error detection rate, highest random and gross error reduction, and committed the lowest number of

type I errors in the three distributions (normal, contaminated Gaussian, and Lorentzian distributions) for the gross error range in 3σ - 30σ. Lorentzian distribution demonstrated a tendency to exceed the performance of Tjoa-Biegler's method when gross errors are larger than 30 times the standard deviation. Measurement test resulted in significant biased estimation (misrectification) in reconciling measurements containing both random and gross errors; and this was observed by lower error reduction and large number of type I errors committed by measurement test method. Also, the numerical results showed that Lorentzian distribution is the least sensitive to the variations of gross error sizes, and measurement test is the most sensitive to the variations of gross error sizes.

A modified compensation strategy has been proposed and incorporated with measurement test method to avoid the biased estimation due to the presence of gross errors. The improvement on estimation accuracy from this strategy is the same as the modified iterative strategy proposed in literature. However, the modified compensation strategy requires much smaller number of iterations and is more straight forward to conduct without requiring modification of the program of the optimization problem. It can be automatically conducted by computer program, and it can be included in on-line optimization. The numerical results from modified compensation measurement test (MCMT) demonstrated that the modified compensation strategy significantly reduces the biased estimation of measurement test. This was observed by significantly reduced number of type I errors committed by the algorithm. Also, a small number of type I errors from Tjoa-Biegler's method and Lorentzian distribution was observed from

numerical results. It is recommended that this modified compensation strategy be incorporated with Tjoa-Biegler's method and Lorentzian distribution to further improve their performance.

Parameter Estimation: The methodology (mathematical statement of optimization problem) for parameter estimation in on-line optimization is similar to one for combined gross error detection and data reconciliation. The only difference is that the process parameters are variables in simultaneous data reconciliation and parameter estimation step rather than constants in combined gross error detection and data reconciliation. Therefore the algorithm used to reconcile data in simultaneous data reconciliation and parameter estimation step should have the same performance as it does in combined gross error detection and data reconciliation. Based on the algorithm and characteristic of measurement data used for parameter estimation, two alternative estimation strategies have been proposed for conducting parameter estimation, two-step estimation and one-step estimation, as described previously. Two-step estimation is corresponding to the procedure of three optimization problems for on-line optimization, i.e., combined gross error detection and data reconciliation, simultaneous data reconciliation and parameter estimation, and economic optimization. One-step estimation is corresponding to the procedure of two optimization problems for on-line optimization, i.e., the simultaneous gross error detection, data reconciliation, and parameter estimation, and the economic optimization.

The overall performance of both one-step and two-step estimation was compared based on parameter estimation accuracy, data reconciliation accuracy, gross error identification, and computation effort. Two-step estimation demonstrated 4% lower variation on estimated parameter values, 6.5% higher error reduction, and 10.6% higher relative standard deviation

reduction on reconciled data than one-step estimation. Also, two step estimation had 6.3% higher gross error detection rate and committed 50% less of type I errors than one-step estimation. Both two-step and one-step estimation had comparable estimation accuracy on the plant parameters. However, two-step estimation required 82% more computation time than one-step estimation did.

In summary, two-step estimation demonstrated a better performance in estimation accuracy than one-step estimation for sulfuric acid process, while one-step estimation required less computation time as discussed in above paragraph. Also, the one-step estimation eliminates the interaction between two data reconciliations for gross error detection and for parameter estimation. For the sulfuric acid process, the two-step estimation is recommended to be used in on-line optimization based on the numerical results.

CHAPTER VI CONCLUSIONS AND RECOMMENDATIONS

A. Conclusions

Based on the results of this research for on-line optimization of chemical plants and petroleum refineries, it is concluded as following:

1. For a chemical process or refinery, the optimal procedure to conduct on-line optimization includes solving three nonlinear optimization problems of combined gross error detection and data reconciliation, simultaneous data reconciliation and parameter estimation, and economic optimization in sequence, as well as the data exchange as shown in Figure 5.14. Also, the gross error detection, data reconciliation, and parameter estimation can be combined into one optimization problem. Then, the optimal procedure includes solving two nonlinear optimization problems for simultaneous gross error detection, data reconciliation, and parameter estimation and for economic optimization.

2. On-line optimization using current operating data demonstrated that plant economic optimization gave 2.3% ($313,000/year) and 3.1% ($410,000/year) profit improvement over the plant operation conditions on 6-10-97 and 6-12-97. Plant economic optimization demonstrated a potential in improving the plant profits and reducing pollutant emission. The plant economic optimization showed 3% profit improvement or 2. 3% profit improvement and 25% emission reduction over the design conditions for the sulfuric acid process at IMC Agrico Company's plant.

3. Theoretical studies of algorithms used for data reconciliation were based on the influence function and relative efficiency of the distribution functions used by the algorithms. The

comparison of influent functions of the distribution functions showed that the sensitivity of the distribution functions to the presence of gross errors decreases in an order as: normal distribution of measurement test method, Fair function of robust method, contaminated Gaussian distribution of Tjoa-Biegler's method, and Lorentzian distribution of robust method. The comparison of relative efficiencies of the distribution functions used by the algorithms showed that the estimation accuracy from a distribution function increased in order as: Fair function, Lorentzian distribution, contaminated Gaussian distribution, and normal distribution. It was concluded that the Tjoa-Biegler's contaminated Gaussian distribution has the best performance for moderate gross error size; Lorentzian distribution is more effective for extremely large gross errors or infinite gross errors; and normal distribution has the highest estimation accuracy when measurements do not contain gross errors based on the theoretical studies.

4. Numerical studies were evaluated based on the results of gross error detection rate, number of type I errors, relative random and gross error reductions from three algorithms summarized on the simulation results from 4000 runs. The three algorithms are measurement test method using the normal distribution, Tjoa-Biegler's method using contaminated Gaussian distribution, and robust method using Lorentzian distribution for combined gross error detection and data reconciliation. The numerical evaluation concluded that Tjoa-Biegler's method has the best performance for moderate gross error size in simultaneously rectifying both random and gross errors. It achieved the highest gross error detection rate (97.4%), highest random and gross error reductions (66.1%

and 96.7% respectively), and committed the lowest number of type I errors in three distributions for the gross error range (3σ - 30σ). The method based on Lorentzian distribution demonstrated the tendency to exceed the performance of Tjoa-Biegler's method when gross errors were large (larger than 30σ). Measurement test method had results with a significant biased estimation (misrectification) in reconciling measurements containing both random and gross errors.

5. A modified compensation strategy has been proposed to avoid the biased estimation due to the presence of large gross errors for the data reconciliation algorithms. The improvement on estimation accuracy from proposed strategy is the same as the modified iterative strategy proposed in literature. However, the modified compensation strategy requires fewer number of iterations and is more straight forward to incorporate without requiring modification of the program of the optimization problem. The numerical results from modified compensation measurement test (MCMT) method demonstrated that the modified compensation strategy significantly reduces the biased estimation in measurement test. This was observed by significantly reduced number of type I errors committed by the algorithm.

6. The parameters in a plant model can be estimated by two-step estimation method or one-step estimation. The numerical results on parameter estimation showed that both one-step and two-step estimation strategies can accurately estimate process parameters and variables for the sulfuric acid plant. Two-step estimation demonstrated 4% lower variation on estimated parameter values, 6.5% higher error reduction, and 10.6% higher

relative standard deviation reduction on reconciled data than one-step estimation. Also, two step estimation had 6.3% higher gross error detection rate and committed 50% less of type I errors than one-step estimation. However, two-step estimation required 82% more computation time than one-step estimation did. For the sulfuric acid process, the two-step estimation is recommended to be used in on-line optimization based on the numerical results.

7. The Monsanto designed sulfuric acid process of IMC Agrico Company at Convent, Louisiana, was used to test the methodology of on-line optimization and to study the effect of plant model formulation on the results. Based on the results, the open form equation based plant model improves the performance of plant models and the solutions of the nonlinear optimization problems in on-line optimization.

8. A general procedure to examine the observability and redundancy of open form equation based model has been proposed, and it was applied to sulfuric acid contact process model.

9. An interactive, window interface program, Interactive On-Line Optimization System, has been developed to alleviate the effort of engineer to apply on-line optimization. This program incorporated the detail methodology of on-line optimization developed in this research project and automatically links with optimization software (GAMS) for solving the optimization problems of on-line optimization.

B. Recommendations

The following recommendations are made for future investigation in this area:

1. Although the methodology of on-line optimization is general and applicable for all chemical processes, the plant model formulation is specific for different types of chemical processes. The plant model formulation requires extensive knowledge of the process for developing the plant simulation and examining the observability and redundancy of the simulation model. Additional work can be focused on the software development for establishing the open form equation based plant model. This will significantly reduce the effort of engineers in applying on-line optimization and avoid the errors that are possibly committed in the plant simulation.

2. The knowledge of error structures of the plant data is important for effectively verifying and adjusting the data. Better understanding about the distribution behavior pattern of measurement errors is very important in improving the gross error identification and estimation accuracy in reconciling process data. Therefore, the further study of the instrument errors is essential to provide more accurate distribution function and to have the algorithm perform better.

3. Although steady state process simulation models represent the behavior of continuous processes, the study of the modeling of dynamic response of these processes is important in describing the unsteady state behavior of processes and investigating the transient behavior of the process from set point change.

APPENDIX A. TERMINOLOGY

Bounds - define the allowable range of process variables. The low and up bounds represent the allowable minimum and maximum operating conditions of the process variables and the raw material availability and product quality requirements.

Closed form sequent modular plant model - follows the traditional design rules, using the information for the input streams of a unit to determine the values of the output variables. Changes of variables in input streams can affect variables in output streams, but the changes of variables in output streams can not affect the determination of process variables in the input streams.

Control variables - are the variables whose values must be satisfied by adjusting the manipulated variables.

Data reconciliation - Data reconciliation is a procedure to adjust or reconcile process data obtained from distributed control system and obtain more accurate values by adjusting the data to be consistent with material and energy balances.

Distribution function - is used to describe the behavior pattern of measurement errors.

Economic model - is the objective function for economic optimization. It is a function that is used to maximize the plant profit; minimize the operation cost, emission or energy consumption; for example.

Economic optimization - is to determine the plant operation conditions that will optimize the economic objective (model) and satisfy the constraints of the plant model.

Equality constraint equations - are mass and energy balances, heat transfer equations, reaction rate equations (kinetic model), thermodynamic equilibrium equations, physical property functions, and others.

GAMS, General Algebraic Modeling System - was developed at the World Bank to solve large and complex mathematical programming models by using a programming language that makes concise algebraic statements of the models and was easily read by both the modeler and the computer (Brook et al., 1988).

Gross error detection - is a statistical procedure to detect and rectify gross errors in plant sample data sampled from distributed control system.

Gross error detection rate - is the ratio of number of gross errors that are correctly detected by the algorithm to the actual number of gross errors in measurements.

Inequality constraint equations - provide additional restrictions for the economic optimization. The inequality constraint equations for a chemical process are the demand for main and by products, availability of raw materials, maximum capacities of the equipment, restriction on the waste/pollutant emission, and others.

Influent function - is proportional to the derivative of the distribution function. It reflects the influence of contaminated measurements on the estimation.

Initial point - the starting values of variables in a optimization problem for the optimization algorithm to search for optimal solution. The default initial point of GAMS is zero or the bound whichever is closer to zero if the bounds are specified to be different from default values.

Key measured variables - are the variables that are directly related to the determination of plant parameters

Measurable variables - are the variables that can be measured by instruments, such as flow rate, temperature, pressure, composition, or other.

Measured variables - are the variables that have been sampled from plant's distributed control system.

Manipulated variables - are the variables that are adjusted to satisfy the requirement on control variables.

Open form equation based plant model - is written as a set of algebraic and/or differential equations in the form $\mathbf{f}(\mathbf{x}) = 0$. The equations are solved simultaneously for the values of variables, rather than sequentially.

Observability - An unmeasured variable in steady state model is observable if and only if it can be uniquely determined from a set of values for the measured variables, which are consistent with all of the given constraints. Any unmeasured variable which is not so determinable is unobservable (Crowe, 1989).

Optimization algorithm - is a mathematical method to solve an optimization problem, such as simplex method for linear optimization problems and successive linear programming, successive quadratic programming and the generalized reduced gradient method for nonlinear optimization problems.

Parameter estimation - is a statistical procedure to update the values of parameters in the plant model using the plant data reconstructed from the combined gross error detection and data reconciliation.

Plant (simulation) model - is consist of a set of equations that represent the relationship among process variables and describe the process behavior. These include the equality equations (material and energy balances, etc.) and inequality equations (availability of raw materials, demand of products, capacity of equipment, etc.).

Plant parameters - are parameters in plant model that are unmeasurable and whose values change slowly with time and are not affected by the changes of operation conditions., e.g., heat exchanger fouling factors, catalyst effectiveness factors, or tray efficiency. These parameters usually describe the condition of process equipment.

Redundancy - A measured quantity is redundant if and only if it would be observable if that quantity was not measured. Otherwise, the measured quantity is non-redundant (Crowe, 1989).

Relative efficiency - represents the asymptotic efficiency of a distribution to normality. It indicates the estimation accuracy for normal measurements.

Relative error reduction - is the ratio of the remaining error after data reconciliation to the original measurement error.

Set points - are the operating points of the controllers in the distributed control system that are adjusted by n-line optimization.

Type I error - is the event that the algorithm has incorrectly identified a normal measurement (no gross error) as an abnormal measurement (measurement containing gross error).

Type II error - is the event that the algorithm has incorrectly identified an abnormal measurement (measurement containing gross error) as normal measurement.

Unmeasured variables - are the variables that are not sampled from plant distributed control system. Their values will be determined by the measured variables through constraint equations.

APPENDIX B STATISTICAL BACKGROUND INFORMATION

The application of the methods of probability to the analysis and interpretation of empirical data is known as statistical inference. The basic idea is to develop a probability distribution function based on the data sampled from a population and to use this distribution function to test other data that is from the same population. The statistical theory of data reconciliation in on-line optimization is based on the same idea, i.e., assume the data is subject to a certain type of distribution. Then, this distribution is used to reconcile the data for process variables sampled from distributed control system.

The distribution functions for data reconciliation of on-line optimization have been discussed in Chapters II and III. They are the normal distribution function which is used by the least squares method, the contaminated Gaussian distribution function, robust functions (Lorentzian distribution and Fair function). These distribution functions are used to construct the likelihood function (maximum likelihood method) or posterior density functions (Bayesian method). Data reconciliation is conducted by maximizing the likelihood function or the posterior density function subject to process constraints.

The statistical method of data reconciliation can generally be stated as:

$$\begin{aligned} &\underset{\mathbf{x},\,\mathbf{z}}{\textit{Maximize}}: && P(\mathbf{x}, \mathbf{y}) \\ &\textit{Subject to}: && \mathbf{f}(\mathbf{x}, \mathbf{z}) = 0 \\ & && \mathbf{x}^L \le \mathbf{x} \le \mathbf{x}^U,\ \mathbf{z}^L \le \mathbf{z} \le \mathbf{z}^U \end{aligned} \tag{B-1}$$

where $P(\mathbf{x}, \mathbf{y})$ is the likelihood function or posterior density function. $\mathbf{f}(\mathbf{x}, \mathbf{z}) = 0$ is the process constraints such as mass and energy balances. $\mathbf{y}$ is the vector of measurements (sample data) for

the measured variables and **x** is the vector of true values for the same variables as **y**. **z** is the vector of unmeasured variables in the constraints. $\mathbf{x}^L \le \mathbf{x} \le \mathbf{x}^U$ and $\mathbf{z}^L \le \mathbf{z} \le \mathbf{z}^U$ are the bounds on the process variables. Solving this optimization problem gives a set of values for process variables (**x** and **z**) that will maximize the objective function P(**x**, **y**) and satisfy the process constraints **f**(**x**, **z**) = 0. This objective function is used to reconcile the sample data, and the constraint equations are necessary to describe the process. The following will briefly discuss the relation of a distribution function, likelihood function, and posterior density distribution.

I. Relationship of Distribution, Likelihood Function, and Posterior Density Function

A distribution is the sum of all the probabilities of a random variable associated with outcomes in sample set S. Conceptually, it describes the probability structure of the random variable (Larsen and Marx, 1986). It is empirical function regressed from the sampled data. As discussed in Chapters II and III, the distribution functions that are applicable to reconciling the sampled data from distributed control system for on-line optimization are the normal distribution, the contaminated Gaussian distribution, and robust functions.

If the measured data are independent of each other, then the probability for a particular set of data $\{y_1, y_2, .., y_n\}$ is the product of individual probabilities $p(y_i)$, i = 1, 2, .., n. This product is called likelihood function (Barlow, 1989). The likelihood function is expressed as :

$$P(y,x) = P(y_1)P(y_2)\cdots P(y_n) = \prod_i^n P(y_i) \qquad \text{(B-2)}$$

where $P(y_i)$ is the probability distribution function for measurement error i. This distribution function can be different depending on the distribution structure of sampled data, and it can be

the normal distribution function, the contaminated Gaussian distribution function, or robust function.

The concept of conditional probability is used in Bayesian theorem. The probability that an event F occurs if it is known or given that an event E has occurred is denoted by P(F|E) and it is called a conditional probability of F given E. Probability P(F|E) is obtained by letting E be the new reduced sample space. Then fractional probability on E which lies on E∩F (the intersection of E and F, i.e., the sample space consists of the elements contained in the set where E and F overlap) is given by (Guttman, et al., 1982):

$$P(F|E) = \frac{P(E \cap F)}{P(E)} \tag{B-3}$$

An interpretation of Eq. B-3 is that posterior to observing that measurements **y** have been made, the probability of **x** changes from the prior probability, P(**x**), to posterior probability P(**x** |**y**) (Guttman, et al., 1982).

According to Bayesian theorem, the posterior density function P(**x**| **y**) can be written in terms of the conditional probability P(**y**|**x**) of an event that has measurements **y** and is given the true values of the variables as **x**, the prior probability that the variables have the true values as **x** in P(**x**), and the prior probability that the variables have measurements **y** in P(**y**). The Bayesian theorem is (Bretthorst, G. L., 1989):

$$P(\mathbf{x} \mid \mathbf{y}) = P(\mathbf{y} \mid \mathbf{x})\, P(\mathbf{x})/P(\mathbf{y}) \tag{B-4}$$

The prior probability P(**y**) is a normalized constant and independent of **x**. It does not affect the optimization and can be excluded. The conditional probability P(**y** | **x**) is the product of conditional probability for individual measurement P(y|x), i.e.,

$$P(\mathbf{y} \mid \mathbf{x}) = P(y_1 \mid x_1)\, P(y_2 \mid x_2) \cdots P(y_n \mid x_n) = \prod P(y_i \mid x_i) \qquad \text{(B-5)}$$

This probability function P(**y** | **x**) is a likelihood function.

The prior probability of the true values of the variables **x**, P(**x**), can be constructed by the principle of maximum entropy based on the prior qualitative knowledge about the true values of process variables. The detail methodology about maximum entropy is given in Shannon (Shannon, 1948).

For a discrete probability distribution P(i# **I**), i stands for some proposition and **I** represents the information on which the probability distribution is based. The principle of maximum entropy states that if one has some testable information **I**, one can assign a probability distribution to a proposition i such that P(i# **I**) contains only information **I**. This assignment is done by maximizing Shannon's H function (Shannon, 1948),

$$H = -\sum_{i=1}^{n} P(i \mid I) \log P(i \mid I) \qquad \text{(B-6)}$$

subject to the constraints represented by the prior information **I**, where H is referred as entropy by Shannon.

The information could be the normalization, i.e., the summation of probabilities is equal to 1, or knowing mean and variance of the proposition i. If nothing is known about the proposition i, the objective function, i.e., H function, is only subject to normalization constraint

$\sum P_i = 1$. Then, the resultant probability function is a uniform function whose value depends on the range of proposition i. If it is known that only the variance exists and it has zero mean, the constraints of H function are the normalization, first moment, and the second moment. The resultant probability distribution is a normal distribution function with zero mean. If more information is known, then more constraints are considered. Therefore, the resultant distribution function will more complicated and more accurate. However, if the fault information is added to the constraints, it will mislead the distribution function.

For the event of throwing a die with six faces, its probability can be constructed by the principle of maximum entropy. It is to maximize the entropy function H subject to the constraints. If nothing is known about the die except that the sum of probabilities for all possibles outcomes of throwing a die is 1, then the constraint is only the nomalization, i.e.,

$$\sum_{i=1}^{6} P(i|I) = 1 \qquad \text{(B-7)}$$

The possible outcomes of throwing a die will be on six different faces, and 6 in Eq. B-7 represents total number of the possible outcomes of throwing a die. Therefore, this maximization is expressed as:

$$\begin{aligned} &\text{Maximize:} \quad H = -\sum_{i=1}^{6} P(i|I)\log P(i|I) \\ &\text{Subject to:} \quad \sum_{i=1}^{6} P(i|I) = 1 \end{aligned} \qquad \text{(B-8)}$$

Eq. B-8 can be solved by Lagrange multiplier method. Solving Eq. B-8 gives the probability for the event of throwing a die as:

$$P(i \mid \mathbf{I}) = 1/6 \qquad \text{(B-9)}$$

If no information is known about the true values of process variables, then a uniform prior probability (a constant) will be assigned to their distribution, P(**x**), based on the principle of maximum entropy. Therefore, the posterior density function is proportional to the likelihood function, i.e.,

$$P(\mathbf{x} \mid \mathbf{y}) = P(\mathbf{y} \mid \mathbf{x})\, P(\mathbf{x})/P(\mathbf{y}) \propto P(\mathbf{y} \mid \mathbf{x}) \tag{B-10}$$

where P(**x**) and P(**y**) are constants. The Bayesian method is reduced to maximum likelihood method.

The relationship among these distribution functions is summarized in Figure B.1. As shown in Figure B.1, posterior density function from Bayesian method is the most general approach. It is the product of the likelihood function and prior probability P(**x**) of the true values of variables **x** as shown in Eq. B-4. This method incorporates more information in the distribution function than the maximum likelihood method. If the prior probability P(**x**) is a uniform distribution (a constant), then the posterior density function is proportional to likelihood function, and the Bayesian method is converted to maximum likelihood method. The maximum likelihood method is a special case of the Bayesian approach.

If some qualitative distribution information about the true values of variables **x** is available and P(**x**) can be constructed as a function of **x**, then the variances of **x** are incorporated in the posterior density function. Using this posterior density function to reconcile process data can not only provide the point estimation (the estimated values of **x**) as the maximum likelihood method does, but also it can predict the possible variation ranges around the estimated values of **x**, which is indicated by the variances of **x**.

The likelihood function is the product of the distribution function for individual measurement errors as defined in Eq. B-2, i.e, it is constructed from the distribution function for individual measurement errors. Based on the error structure of sampled data, the distribution function can be the normal distribution, the contaminated Gaussian distribution, gamma distribution, robust functions, or others. If the distribution function of measurement errors follows

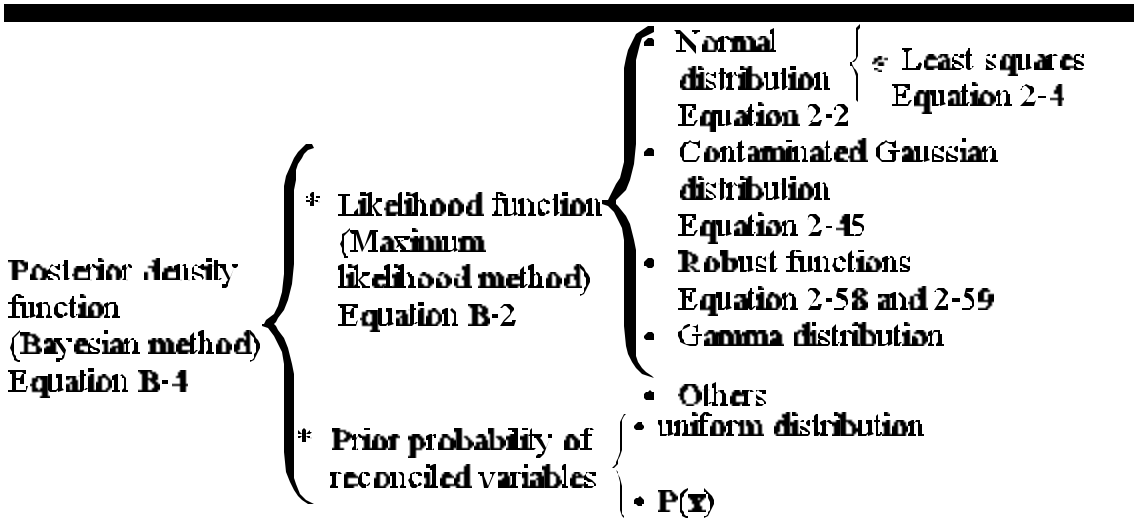

Figure B.1 The Relationship among Probability Distribution Functions for Data Reconciliation

a normal distribution, then the likelihood function is the product of the normal distributions for all measurement errors. The maximization of this likelihood function is equivalent to the minimization of the sum of squared errors weighted by the variance. Therefore, the maximum likelihood method is converted to the least squares method. The least squares method is a special case of maximum likelihood estimation.

II. Comparison of Unconstrained and Constrained Optimization

The methodology of data reconciliation in on-line optimization is similar to the traditional mean estimation of unconstrained optimization. The relations among process variables and parameters (constraints of the plant model) are the necessary conditions for the data reconciliation in on-line optimization. These equations relate the individual measurements obtained from distributed control system and provide the resolution for reconciling data. The following gives simple examples to illustrate the difference and similarity between traditional mean estimation and data reconciliation in on-line optimization.

Traditional estimation uses m repeated data to estimate the mean of one random variable (or n variables for multivariate with m×n data). If all m measurements are randomly measured and normally distributed, whose variance is σ^2. Then the mean of a random variable can be estimated by maximum likelihood method, i.e., maximizing the likelihood function which is a joint normal distribution for all sample data or minimizing the sum of squared differences between the sample data y_i and estimated mean μ. This is expressed mathematically as:

$$\textit{Minimize:}_{\mu} \quad \sum_i (y_i - \mu)^2 / \sigma^2 \tag{B-11}$$

where ∶ and y_i are the estimated sample mean and the sample data of the random variable. Setting the first derivative of Eq. B-11 with respect to ∶ equal to zero gives the global minimization of Eq B-11. The solution for ∶ of Eq B-11 is obtained by:

$$\mu = \frac{1}{m}\sum_{i=1}^{m} y_i \tag{B-12}$$

Eq. B-12 is a function to determine the sample mean of repeated experimental data and it is given in a number of statistical text books (Johnson and Wichern, 1992). The accuracy of the mean depends on the m, number of repeated measurements. In general, the larger m is, the more accurate estimation of ∶ will be.

For data reconciliation of on-line optimization, the values of n measured variables are estimated using one set of n measurements y_i, i = 1, 2, .., n, where y_i represents the measured values of n measured variable x_i. The maximum likelihood method can used to estimate the reconciled values of the measured variables. If all measurements are randomly measured and normally distributed with variances σ_i^2's, then the maximum likelihood estimation method for the data reconciliation can be expressed as:

$$\textit{Maximize: } \frac{1}{(2\pi)^{n/2}|\Sigma|^{1/2}}\exp\left[-\frac{(y-x)^T\Sigma^{-1}(y-x)}{2}\right] \tag{B-13}$$

where **y** represent the measured values of the n measured variables **x**. $\boldsymbol{\Sigma}$ is the variance matrix of the measured variables. Eq. B-13 can be rewritten as:

$$\textit{Minimize: } (y-x)^T\Sigma^{-1}(y-x) = \sum_{i=1}^{n}(y_i - x_i)^2/\sigma_i^2 \tag{B-14}$$

Maximizing the likelihood function in Eq. B-13 is equivalent to the minimizing the least squares function in Eq. B-14. The measured variables **x** are related by the constraints from the plant model. Thus, Eq. B-14 used with plant model is a constrained optimization problem.

Eq. B-11 and Eq. B-14 for traditional mean estimation and data reconciliation have the similarities and differences. Both use maximum likelihood method. However, the traditional mean estimation uses m repeated data to estimate one unknown mean. Data reconciliation uses a set of n measurements and constraint equations to estimate the values of n measured variables. The constraint equations are essential to relate the process variables for data reconciliation, and the variables in a chemical process are variables in the process model. These constraint equations imposed on the process variables make data reconciliation possible.

APPENDIX C PHYSICAL PROPERTIES OF PROCESS STREAMS

In the sulfuric acid contact plant, there are four streams in the whole process. These are the low pressure gases (SO_2, SO_3, O_2, and N_2), liquid sulfur, steam (compressed water and superheated vapor), and sulfuric acid liquid. Since the pressure of the gases is lower (range in 1 atm. to 1.4 atm.) throughout the whole process, they are considered as ideal gases. Their enthalpy and heat capacities are calculated by the regression equations from NASA Technical Memorandum 4513 (Mcbride et al., 1993). Also, the enthalpy for liquid sulfur is determined from the regression equation in the condensed state from NASA Technical Memorandum 4513 (Mcbride et al., 1993). However, the pressure of steam stream is as high as 640-730 psi, and the computation formulas of the enthalpy for steam are obtained by mean of a least square fit of the data from the ASME Steam Table (1977). The enthalpy for sulfuric acid liquid is obtained from a two variables (concentration and temperature) polynomial formula fit to the enthalpy-concentration chart (Ross, 1952).

I. The Physical Properties of Gases and Sulfur

For the ideal gases (O_2, N_2, SO_2, SO_3) and liquid sulfur, the data to calculate the heat capacity and sensible enthalpy is taken from NASA Technical Memorandum 4513 (Mcbride, et al., 1993). Tables C-1 and C-2 list the heat capacity coefficients for gases used in the balance equations as shown below. The heat capacity coefficients for liquid sulfur is given in Table C-3. The reference state for heat capacities and sensible enthalpies of the species is pressure at 1 Bar and temperature at 298.15 ^{0}K.

Table C-1. The Coefficients of Heat Capacity and Enthalpy for Ideal Gases at the Temperature Range of 1000-5000 K

	SO2	SO3	O2	N2
a1	5.2451364	7.0757376	3.6609608	2.9525763
a2	1.97042e-3	3.17634e-3	6.56366e-4	1.39690e-3
a3	-8.03758e-7	-1.35358e-6	-1.41149e-7	-4.92632e-7
a4	1.51500e-10	2.56309e-10	2.05798e-11	7.86010e-11
a5	1.05580e-14	-1.79360e-14	-1.29913e-15	-4.60755e-15
b1	-3.75582e4	-5.02114e4	-1.21598e3	-9.23949e2
b2	-1.074049	-11.187518	3.4153618	5.8718925

Table C-2. The Coefficients of Heat Capacity and Enthalpy for Ideal Gases at the Temperature Range of 300-1000 K

	SO2	SO3	O2	N2
a1	3.2665338	2.5780385	3.7824564	3.5310053
a2	5.32379e-3	1.45563e-2	-2.99673e-3	-1.23661e-4
a3	6.84376e-7	-9.17642e-6	9.84740e-6	-5.02999e-7
a4	-5.28100e-9	-7.92030e-10	-9.68130e-9	2.43531e-9
a5	2.55905e-12	1.97095e-12	3.24373e-12	-1.40881e-12
b1	-3.69081e4	-4.89318e4	-1.06394e3	-1.04698e3
b2	9.6646511	12.265138	3.6576757	2.9674747
H_{298}/R	-3.57008e4	-4.75978e4	0.0	0.0

Table C-3. The Coefficients of Heat Capacity and Enthalpy for Liquid Sulfur

	T > 1000 K	T ≤ 1000 K
a1	3.500784	-7.27406e1
a2	3.81662e-4	4.81223e-1
a3	-1.55570e-7	-1.07842e-3
a4	2.72784e-11	1.03258e-6
a5	-1.72813e-15	-3.58884e-10
b1	-5.90873e2	8.29135e3
b2	-1.52117e1	3.15270e2
H_{298}/R	0.0	0.0

The empirical equations for heat capacity $C_P^i(T)$ and sensible enthalpy $h^i(T)$ for each species are:

$$\frac{C_p(T)}{R} = a_1 + a_2 T + a_3 T^2 + a_4 T^3 + a \quad \text{(C-1)}$$

$$= SO_2, SO_3, O_2, N_2; \quad KJ/kmol-^{\circ}$$

and

$$\frac{H(T)}{RT} = -\frac{H_{298}}{RT} + a_1 + \frac{1}{2}a_2 T + \frac{1}{3}a_3 T^2 + \frac{1}{4}a_4 T^3 + \frac{1}{5}a_5 T^4 \quad \text{(C-2)}$$

$$= SO_2, SO_3, O_2, N_2, S(L); \quad KJ/kn$$

where R is molar gas constant, 8.3145 KJ/kmol-^{0}K. T is the temperature in K. The reference state for enthalpy equation is the standard state, 298.15^{0}K and 1 bar. H_{298} is the absolute enthalpy at the standard state for each species given in NASA Technical Memorandum. It is zero for elements and the heat of formation for the species. Eq. C-2 is used to calculate the sensible enthalpy of a species with reference state as temperature 298.15 K and pressure at 1 Bar. The units of enthalpy and heat capacity are dependent on the units of the constant R.

II. The Physical Properties of Steam

The steam properties are divided into two groups, compressed water from stream SS1 to SS4 and superheated vapor in stream SS5 and SS7. For the compressed water, the variation of enthalpy in the operating pressure range is not significant. It is assumed that its enthalpy is only a function of temperature. The polynomial function of enthalpy for compressed water is regressed from ASME Steam Table data (Meyer, et al., 1977) shown as following:

$$707T - 5.63134\times 10^{-4}T^2 + 8.34\cdot$$

$$\frac{66\times 10^4}{T} + \frac{1.01824\times 10^6}{T^2}, \quad BTU/ \qquad \text{(C-3)}$$

where the unit of temperature T is ^{o}F, and the reference state of the enthalpy is 298.15 K and 1 atm. The regression ranges are 200-500 ^{o}F and 600-750 psi. The comparison of prediction and tabulated data is shown in Figure C-1. The symbol and solid line in the figure represent the tabulated data and formula prediction respectively. The largest relative difference between prediction value and tabulated data is 0.01%.

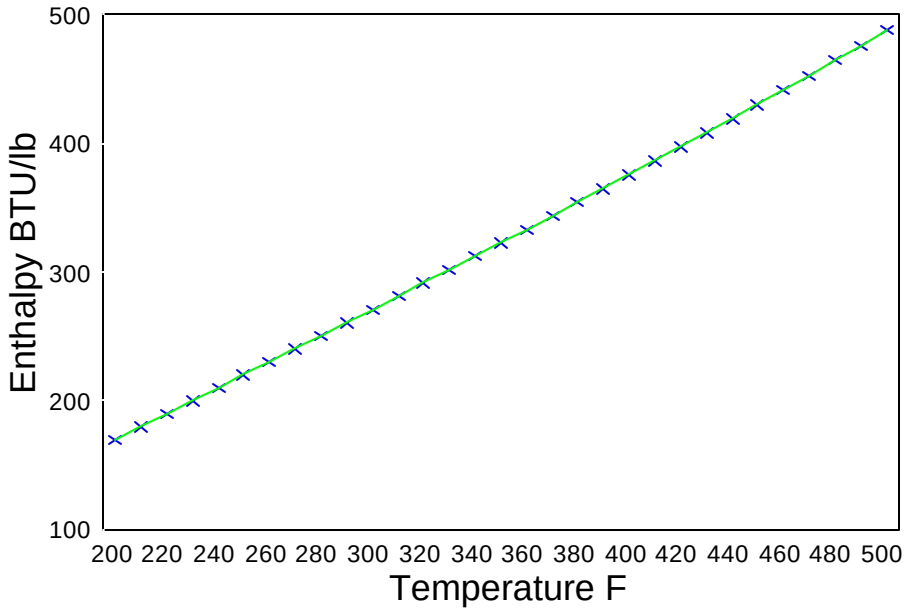

Figure C.1 The Comparison of Prediction and Tabulated Data
for the Enthalpy of Compressed Water

The superheated vapor is fit to a third order polynomial in temperature and second order polynomial in pressure with ASME steam table data (Meyer et al., 1977). The regression function is:

$$\begin{aligned} h = \; & 5.32661T - 0.2839015P - 7.352389\times 10^{-3}T^2 \\ & + 3.581547\times 10^{-6}T^3 - 7.289244\times 10^{-5}P^2 \\ & + 4.595405\times 10^{-4}TP, \; BTU/lb \end{aligned} \tag{C-4}$$

where the unit of temperature is ^{o}F and unit of pressure is psia. The reference state of the enthalpy is 298.15 K and 1 atm. The regression ranges are 200-500 F for temperature and 600-

750 psia for pressure. The comparison of prediction and tabulated data is shown in Figure C-2. The symbol and solid line in the figure represent the tabulated data and formula prediction respectively. The largest relative error between prediction and tabulated data is 0.15%.

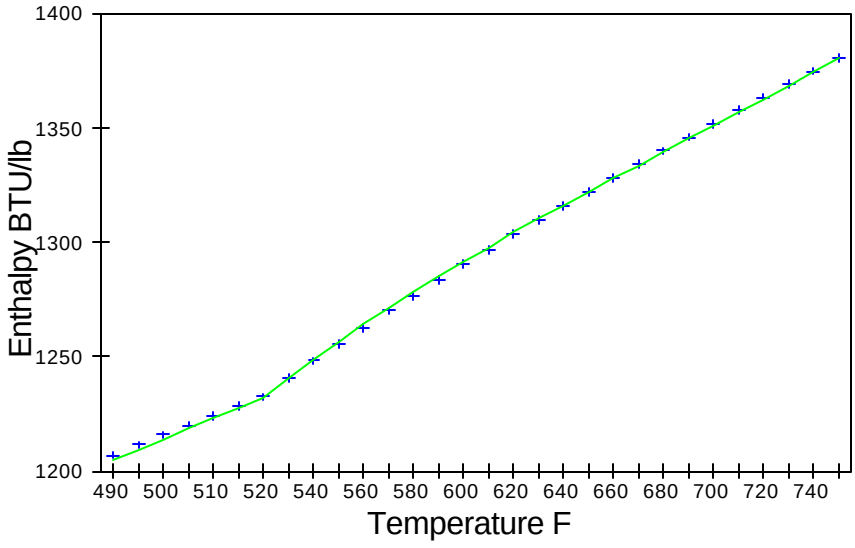

Figure C.2 The Comparison of Prediction and Tabulated Data for Enthalpy of Superheated Vapor at 600 psi

III. The Physical Properties of Sulfuric Acid

For the sulfuric acid stream, one of the difficulties in writing the energy equations is using the right thermodynamic model to calculate the enthalpy of the sulfuric acid system. One possible approach which was used by Crowe (1971), Doering (1976) and Richard (1987) is using RENON activity equation, which leads to relatively complicated equations. Also, the temperatures predicted by this method did not agree with the design data well (Zhang, 1993). Besides, the variations in temperature and concentration of the sulfuric acid system is very small in comparison to the range of application of the thermodynamic equation. Therefore, it was decided that the enthalpy of sulfuric acid system could be regressed directly from enthalpy-concentration chart given by Ross (1952). By inspecting the data of the chart, it was found that the enthalpy at the same concentrations are almost a linear function of temperature. Therefore, the enthalpy data was regressed into a two-variable function, linear in temperature and second order in concentration. The regression result is:

$$h = -145.8407C + 9.738664e\text{-}3T + 8.023897e\text{-}3TC + 83.61468C^2 + 60.19207 \qquad \text{(C-5)}$$

For $60^oC \le T \le 120^oC$; $0.90 \le C \le 1.00$

where the unit of T is ^oC, and C is the weight fraction of sulfuric acid. The unit of enthalpy, h, is kilogram calorie per gram mole, where one gram mole of solution is defined as:

$$80.06x+18.02(1-x)\ g$$

and x is mole fraction of SO_3 defined as:

$$x = \frac{\frac{C}{98.08}}{\frac{2C}{98.08} + \frac{1-C}{18.02}} \qquad \text{(C-6)}$$

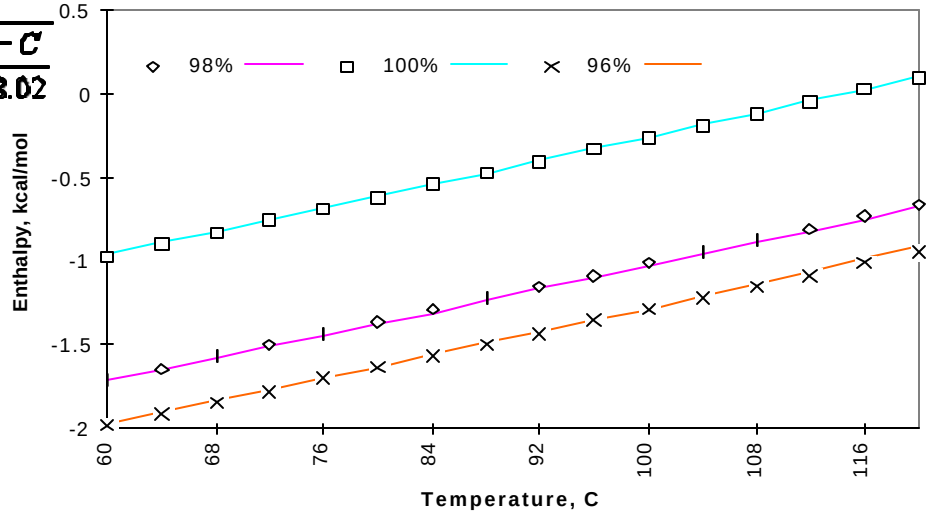

Figure C.3 The Comparison of the Prediction and Tabulated Data for Enthalpy of Sulfuric Acid Solution

The standard states were chosen as h_{H2O}=0.0 kcal/gmol and $h_{100\%H2SO4}$=-1.70kcal/gmol at T=16°C. The enthalpy calculated in Eq. C-5 is referenced to this standard state. The regressed prediction is compared with the chart data as shown in Figure C-3. The largest relative predicted error for this enthalpy is 3%.

APPENDIX D. KINETIC MODEL FOR THE CATALYTIC OXIDATION OF SO_2 TO SO_3

Doering (1976) developed a kinetic model for the catalytic oxidation of sulfur dioxide to sulfur trioxide over vanadium pentoxide catalyst. This model was modified for the contact sulfuric acid plant design by Monsanto Envio-Chem System, Inc. and is discussed below. The oxidation of SO_2 to SO_3,

$$SO_2 + \frac{1}{2}O_2 \rightleftharpoons SO_3 \qquad \text{(D-1)}$$

is carried out over a vanadium pentoxide catalyst promoted by potassium salts. Extensive efforts have been directed at correlating the reaction rate data for this reaction. Doering used Harris and Norman's rate equation for this reaction with Monsanto Type 11 and 210 catalysts. Also, this rate equation was applied to the new LP-110 and LP-120 vanadium pentoxide catalysts which are being used by IMCAgrico's Uncle Sam plants (Richard, 1987). The difference between the old and new catalysts is only their shapes, and the former had a cylindrical shape, while the latter utilizes the Rasching ring form. The difference in shape does not affect the intrinsic reaction rate equation; it only changes the diffusional effect. The new catalysts have 45% to 50% lower pressure drops with the same conversion performance as the old catalysts. The intrinsic rate equation given by Harris and Norman (1972) is:

$$r_{SO_2} = \frac{P^{\circ}_{SO_2} P^{\circ}_{O_2}{}^{1/2}}{(A + BP^{\circ}_{O_2}{}^{1/2} + CP^{\circ}_{SO_2} + DP_{SO_3})^2} \left[1 - \frac{P_{SO_3}}{K_p P_{SO_2} P_{O_2}{}^{1/2}} \right] \qquad \text{(D-2)}$$

where r_{SO2} is the intrinsic reaction rate with units of lb-mol of SO_2 converted per hour per lb catalyst, and K_p is the thermodynamic equilibrium constant with units of $atm^{-1/2}$. P_{O2}, P_{SO2}, and P_{SO3} are interfacial partial pressure of O_2, SO_2, and SO_3 in units of atm; and P^0_{O2} and P^0_{SO2} are interfacial partial pressures of oxygen and sulfur dioxide at zero conversion under the total pressure of reactor, in units of atm. The thermodynamic equilibrium constant can be calculated by:

$$\text{Log}_{10}K_P = 5129/T - 4.869, \quad T \text{ in } {}^oK \tag{D-3}$$

The parameters A, B, C and D in the rate equation, Eq. D-2, were derived from least square regression of the rate data by Harris and Norman(1972). They are the function of temperature in K as following:

Catalyst Type LP-110	Catalyst Type LP-120	
A = exp (-6.80 + 4960/T)	A = exp (-5.69 + 4060/T)	
B = 0	B = 0	(D-4)
C = exp (10.32 - 7350/T)	C = exp (6.45 - 4610/T)	
D = exp (-7.38 + 6370/T)	D = exp (-8.59 + 7020/T)	

The intrinsic rate equation is the rate under the conditions on the catalyst surface. To determine the real reaction rate from the conditions of bulk-gas stream, the following four transport phenomena need to be considered:

1) Diffusion of reactants and product through the pores within the catalyst.

2) Pellet internal temperature gradient.

3) Bulk-gas to pellet temperature gradient.

4) Bulk-gas to pellet concentration gradients.

Diffusion: The effect of diffusion through the catalyst pores is taken into account by multiplying the intrinsic reaction rate by an effectiveness factor, E_f, to get the actual rate, r_{SO3}, i.e.,

$$r_{SO3} = r_{SO2}\, E_f \qquad \text{(D-5)}$$

In Doering's work (1976), followed by Richard (1987) and Zhang (1993), the effectiveness factor for this reaction was calculated by the empirical formulas. After examining the formulas, some inaccuracy was found. Therefore, the model has been modified; and the effectiveness factor was changed to a process parameter to be estimated by plant data for each convertor.

Pellet Temperature Gradients: The intraparticle heat conduction could cause a temperature gradient within the catalyst pellet if the heat conduction is slow relative to the rate of heat generation due to reaction. Based on the criterion developed by Carberry for determining temperature gradient within a catalyst particle, Doering(1976) concluded that a significant temperature gradient does not exist. Therefore, it is assumed that the temperature gradient within these catalyst particle has an insignificant effect on the reaction rate for this system.

Bulk Gas to Pellet Temperature Gradient: The bulk gas temperatures in the packed bed reactors are measured. The uniform pellet temperature can be determined if the temperature gradient across the external film of the catalyst surface can be calculated. Yoshida et al. (1962) presented a method of estimating the temperature gradient using the following equation:

$$\Delta T = \frac{r_{SO_3}\rho_B \Delta h_{rxn}^{SO_3} Pr^{2/3}}{a_v \phi C_p G j_H} \qquad (D-6)$$

where:

) T = temperature drop from a catalyst surface to the bulk gas, K

r_{SO3} = actual reaction rate of SO_2, lb-mol/hr-lb Cat.

) H_{rxn}^{SO3} = 1.827×(-24,097-0.26T+1.69×$10^{-3}T^2$+1.5×10^5/T)

= heat of reaction of SO_2, Btu/lb-mole

C_p = gas heat capacity, Btu/lb-°K

Pr = Prandtl number = 0.83

D$ = (1- ,)D_{app}, lb/ft^3 = Bulk density

N = shape factor = 0.91

G = mass velocity of gas, lb/hr-ft^2

a_v = Specific surface of pellet = 6(1- ,)/d_p , FT^2/FT^3

j_H = 0.91 $Re^{-0.51}$

Re = G/(a_vN :)

: = gas viscosity, lb/ft-hr

The bulk density and spherical diameters of catalysts are given in Table E-1 (Zhang, 1993).

Table D-1 Catalyst Physical Properties

	L-110	L-120
Bulk Density, lb/ft^3	33.8	38.1
Spherical Diameter, ft	0.0405	0.054

The heat capacities of the gas streams are given in Eq. B-2 of Appendix B. The critical gas viscosity were calculated by the following equations(Bird, et al., 1960):

$$\mu_c = 61.6\frac{(M_w T_c)^{1/2}}{V_c^{2/3}}, \quad \text{Micropoise}$$
$$= 0.0149\frac{(M_w T_c)^{1/2}}{V_c^{2/3}}, \quad lb_m/ft\text{-}hr \qquad \text{(D-7)}$$

where M_w is the molecular weight. T_c and V_c are the critical temperature in K and volume in CC per gram-mol respectively. The viscosity for temperature T can be calculated by (Zhang, 1993):

$$\mu = \sum \mu_c^i F_{Tr}^i y_i \qquad \text{(D-8)}$$

where y_i's are molar fractions of gas components, i= SO_2, SO_3, O_2, N_2. F_{tr}^{i}'s are temperature factors for gases which can be calculated by (Zhang, 1993):

$$\text{ix}Tr_i^{0.645} - \frac{0.2}{(1.9Tr_i)^{0.}} \qquad \text{(D-9)}$$

where T_r^{i}'s are the relative temperature of gas components i.

Bulk-gas to pellet concentration gradients: Based on the work of Yoshida, et al. (1962), Doering(1976) concluded that the partial pressure gradients from the bulk gas to the pellet was sufficiently small to be neglected.

Summary: The kinetic model for the oxidation of SO2 to SO3 is given in this appendix. The equations required to determine the reaction rate are summarized in Figure D-1, and they are incorporated in GAMS program. This kinetic model precisely describes

$$\text{Reaction:} \qquad SO_2 + \frac{1}{2}O_2 \rightleftharpoons SO_3$$

SO_2 conversion rate equation:

$$r_{SO_2} = \frac{P_{SO_2}^{\bullet} \, P_{O_2}^{\bullet\,1/2}}{(A + BP_{O_2}^{\bullet\,1/2} + CP_{SO_2}^{\bullet} + DP_{SO_3})^2} \left[1 - \frac{P_{SO_3}}{K_P P_{SO_2} P_{O_2}^{1/2}} \right]$$

r_{SO_2} = rate of reaction, $\frac{\text{lb mole of } SO_2 \text{ converted}}{\text{hr-lb catalyst}}$

$P_{O_2}, P_{SO_2}, P_{SO_3}$ = interfacial partial pressures of O_2, SO_2, SO_3, atm

$P_{O_2}^{\bullet}, P_{SO_2}^{\bullet}$ = interfacial partial pressures of O_2 and SO_2 at zero conversion under the total pressure at the point in the reator, atm

K_P = thermodynamic equilibrium constant, $atm^{-\frac{1}{2}}$

$$\text{Log}_{10} K_P = 5129/T - 4.869, \qquad T \text{ in } {}^{\circ}K$$

A, B, C, D are function of temperature T:

Catalyst Type LP-110:

$$A = e^{-6.80+4960/T}, \quad B = 0, \quad C = e^{10.32-7350/T}, \quad D = e^{-7.38+6370/T}$$

Catalyst Type LP-120:

$$A = e^{-5.69+4060/T}, \quad B = 0, \quad C = e^{6.45-4610/T}, \quad D = e^{-8.59+7020/T}$$

Figure D.1 Rate Equation for the Catalytic Oxidation of SO_2 to SO_3 Using Type LP-110 and LP-120 Vanadium Pentoxide Catalyst

the relation of the reaction operation conditions, such as temperature, pressure, concentrations of gas components. In addition, the modification of reaction effectiveness factors determined from empirical formulas with the assumption of pseudo first order reaction to plant parameters improves the performance of the kinetic model in GAMS program. The simulation with present kinetic model predicted conversion and energy transport in the packed bed reactors as described in Chapter IV.